CRANFIELD UNIVERSITY

ADAM MICHAEL JOESBURY

NEW APPROACHES TO COMPOSITE METAL JOINING

SCHOOL OF AEROSPACE, TRANSPORT AND MANUFACTURING

PhD
Academic Year: 2015 - 2016

Supervisor: Dr. Paul Colegrove and Dr. David Ayre
November 2015

CRANFIELD UNIVERSITY

SCHOOL OF AEROSPACE, TRANSPORT AND MANUFACTURING

PhD

Academic Year 2015 - 2016

ADAM MICHAEL JOESBURY

NEW APPROACHES TO COMPOSITE METAL JOINING

Supervisor: Dr. Paul Colegrove and Dr. David Ayre
November 2015

ABSTRACT

This thesis explores new methods for achieving load-carrying joints between the dissimilar materials of continuous fibre reinforced polymer matrix composites and structural metals. The new composite-to-metal joining methods investigated in this work exploit the metal-to-metal joining techniques of arc micro-welding, resistance spot welding, and metal filler brazing, to form novel micro-architectured metal adherends that can be used for enhanced composite-to-metal joining.

Through a combination of equipment instrumentation and metallographic inspection of fabricated prototype joints, understanding is gained of how materials respond when processed by manufacturing techniques that have not previously been exploited for dissimilar material joining. Mechanical testing of prototype joints; both to ultimate loading strength and partial failure states, with subsequent inspection of specimens and comparative performances evaluation enabled joining performance characterisation of the new joining methods.

Key results include: the identification of micropin reinforced adhesive joints to exhibit pseudo-ductile failure characteristics, resistance spot weld reinforcement of adhesive joints to boost bonding performance, and the use of a polymer infused metal foam to overcome difficulties of thermoplastic to metal adhesion.

Through this work knowledge of how novel micro-architectures reacted under mechanical loading enabled insights to be gained into how perceived manufacturing defects can benefit joining performance. Such examples include, localised material weakness that lead to global pseudo-ductile failure behaviour, and low-strength secondary joining mechanisms boosting primary load transfer systems.

By comparison of the diverse joining methods investigated in this work, trends were identified that suggest joining performance between the two dissimilar materials is improved by increasing the direct interaction between the composite reinforcement fibres and the metal structure. It is demonstrated that joining improvements are gained by forming mechanical connections between metals and composite precursory material before the final manufacturing process of the composite.

Keywords:

Dissimilar, materials, carbon fibre, steel, aluminium, titanium, epoxy, welding, brazing, micropin, bonding, interlocking, infusion, foam, thermosetting, thermoplastic, resistance-spot, prepreg, infusion, micro-architecture, interleaved, through-thickness, mechanical, structural, reinforcement, failsafe

ACKNOWLEDGEMENTS

I am grateful to have had the opportunity of contributing towards investigations that I feel are of significant importance to the development of lightweight structures. I also consider myself to be very fortunate to have had the opportunity of approaching the problem via multidisciplinary investigations, and the benefit which this has afforded me in terms of knowledge gained in the diverse materials science subject areas of fibre reinforced composites processing and metal fusion welding, together with the potential impact this multidisciplinary approach brings to my work. I am also grateful to have been involved in a collaborative project that included other Cranfield University schools, external research organisations, and industrial partners.

First and foremost my greatest thanks is given to my supervisors Dr Paul Colegrove and Dr David Ayre for their ongoing guidance and support. I would like to extend my thanks to other Cranfield University faculty members who also provided me with significant assistance: Prof Stewart Williams, Prof Ivana Partridge, Dr Supriyo Ganguly, and Dr Xiang Zhang. As novel practical investigative and experimental activities formed a great part of my work I would like to sincerely thank the following staff members for their guidance: Flemming Nielsen, Brian Brooks, Andrew Dyer, and Jim Hurley.

As part of my work I was given the great opportunity to travel abroad to use the excellent facilities of the welding engineering centre at the De Nayer Instituut, which forms part of KU Leuven's Thomas More university college in Belgium. My special thanks go to Dr Patrick Van Rymenant for hosting me during this time and the great support he provided.

I would also like to give my sincere thanks to my parents, extended family, my friends and research colleagues for the immeasurable support given to me during my time working towards my PhD. Extended support has also been given to me by my employers during the time of my writing, and so I would like to offer my gratitude to Mr Gordon Bishop and Dr Joe Carruthers at NetComposites Ltd, and Prof Constantinos Soutis and Prof Prasad Potluri at the University of Manchester.

My ultimate thanks go to the EPSRC funded Cranfield University Innovative Manufacturing Research Centre, together with sponsorship and collaboration from Airbus Germany, BAE Systems, EADS Innovation Works, and Helmholtz-Zentrum Geesthacht research centre, for making the Bridging the Divide project possible.

TABLE OF CONTENTS

LIST OF FIGURES

LIST OF TABLES

LIST OF EQUATIONS

LIST OF ABBREVIATIONS

CCC	Carbon-Carbon Composite
CF	Carbon Fibre
CFRP	Carbon Fibre Reinforced Plastic
CMT	Cold Metal Transfer
CT	Computed Tomography
DCS	Differential Scanning Calorimetry
DIC	Digital Image Correlation
DLS	Double Lap Shear
DOE	Design of Experiments
EDX	Energy-dispersive X-ray spectroscopy
FEA	Finite Element Analysis
FEM	Finite Element Method
FRP	Fibre Reinforced Plastic
FVF	Fibre Volume Fraction
GMAW	Gas Metal Arc Welding
GSM	Grams per Square Meter
HIP	Hot Isostatic Press
IMM	Interleaved Multi Material
LCA	Life Cycle Analysis
MFI	Metal Foam Intermediary
MMC	Metal Matrix Composite
MTM	Metal to Metal
NASA	National Aeronautics and Space Administration
OEM	Original Equipment Manufacturer
PEEK	Polyether ether ketone
PIMF	Polymer Infused Metal Foam
QI	Quasi Isotropic
ROM	Rules of Mixtures
RSW	Resistance Spot Weld
SiC	Silicon Carbide
SLS	Single Lap Shear
SMA	Shape Memory Alloy
SuLS	Super Lap Shear
TWI	The Welding Institute (Ltd)
UK	United Kingdom
US	United States [of America]

1 INTRODUCTION

1.1 Motivation

Fibre reinforced composites and metals are both widely used structural materials. These two materials have significantly different properties, manufacturing processes, and in-service behaviour, but are frequently used together within a single load carrying structure. Joining methods between composites and metals almost exclusively rely on the joining techniques of adhesive bonding, the use of mechanical fasteners, or a combination of the two. Due to the differences between the two materials both adhesive bonding and mechanical fastening result in significant penalties in terms of structural efficiency. This work explores new ideas for joining composites to metals. Through these investigations of novel joining process new understanding is gained on how micro-architecture of the two dissimilar material can be manipulated for the purpose of structural joining and how features of micro-architecture effects the mechanical performance of joints. The overall aim of this work is to produce dissimilar material joints that have improved structural efficiency. This technology development need of joining is recognised at the highest level and is stated in UK governmental industrial strategy (Aerospace Growth Partnership, 2013).

1.2 Novel methods of combining adhesive bonding and mechanical fastening for enhanced composite metal joining

It is well understood that adhesive bonding is a structurally efficient joining method, which is particularly suitable for use with composite materials, due to the relatively low stress concentrations compared to the use of mechanical fasteners. However the limitations of adhesive bonding are sensitivity to out-of-plane peel loads and manufacturers' low confidence in the technique due to stringent bonding procedures and difficulty of bondline inspection. The

combined use of mechanical fasteners and adhesive bonding to form a mechanically reinforced adhesive joint is a widely accepted method to address the deficiencies of the exclusive use of adhesive bonding. Furthermore, traditional methods of mechanical fastening have negative impacts on composite materials and adhesive bondlines; hole drilling and fastener installation operations introduces damage that initiate composite delamination and adhesive disbonding.

Adhesive joining and the use of mechanical fastening are established methods of joining composites to metals. These established methods essentially make use of traditional techniques, but with specific modifications, which are necessitated by the use with composite materials. The choice of adhesive polymer and specific formulation, and design of fastener geometries, materials, and installation methods are such modifications. These modifications are incremental developments of established methods to meet the specific requirements of the application. The investigations reported in this work used novel methods; of both forming an adhesive bond and also incorporating mechanical reinforcement, in an effort to seed a step-change in the way in which composites and metals are structurally joined together.

In this study novel composite-to-metal joining techniques were achieved by the application of joining methods that have only historically been used for metal-to-metal joining. The metal-to-metal joining methods exploited were fusion welding and metal-filler brazing techniques. Such techniques are used to form very strong and highly weight-efficient joints between metal parts. As the temperatures required for these joining processes are above the melting temperatures of metals, the processes cannot be used in direct conjunction with fibre reinforced polymer composites, because of the polymers being thermally degraded. However, it is possible to use welding and brazing methods to form novel metal adhered micro-architecture configurations that have the potential to be advantageous in composite-to-metal joining.

1.3 Joining concepts investigated

1.3.1 Metal surface structured through-composite-thickness reinforcement

This joining concept, as illustrated in Figure 1-1, is an adhesive joint that is reinforced by the mechanical locking features of micropins that are anchored to the metal substrate. The micropins bridge across the adhesive bondline to penetrate into the composite laminate.

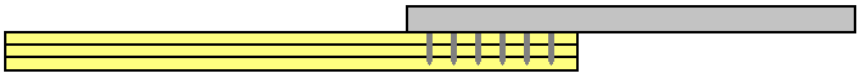

Figure 1-1 – Metal surface structured through-composite-thickness reinforcement

The novelty of this joining concept is the means of providing the mechanical reinforcement by functionalising the metal faying interface by structuring the surface with an array of micropins. The joining concept was originally developed at the Ukrainian National Aerospace University's Kharkov Aviation Institute (Karpov, 2006). The concept was investigated by TWI Ltd using an e-beam processing technique to structure the faying surface of a the metal adherend (Smith, 2005), later a more efficient way of structuring the surface by micro fusion-welding was developed by Fronius GmbH (Fronius International GmbH, 2009) and applied for the purposes of composite joining by the Vienna University of Technology (Ucsnik et al., 2010). Both of these developments of the composite-to-metal joining technique required intricate lay-up of dry carbon fibre fabric followed by a resin infusion process to produce the final joined assemblies. A later development of the TWI Ltd technique was to trial with use of CFRP prepreg (Tu, Guild and Hogg, 2009). The special development of the joining technique reported in this study was to investigate how the joining concept using CMT-Pin welded micropins could be applied to aerospace grade prepreg composites.

1.3.2 Metal to carbon fibre interleaved spot-weld

The joining concept of applying a resistance spot weld to an interleaved stack of metal sheets and carbon fibre fabric, as illustrated in Figure 1-2, is an emergent joining technique and is applied in this work for the purpose of mechanically reinforcing an adhesive joint between metal and a composite laminate.

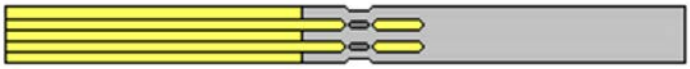

Figure 1-2 – Illustration of the metal to carbon fibre interleaved spot-weld material transition joining

The invention of this joining concept was primarily influenced by two existing joining techniques. The first technique, which was developed by the University of Porto together with the German Aerospace Center, is to locally replace carbon fibre plys with metal sheets to improve the mechanical performance of bolted joints (Camanho et al., 2009). The second technique was developed in a collaborative project by the Automotive Composites Consortium (Shah et al., 2010) and used a variation of the weld-bonding technique for the purposes of composite-to-metal joining. The interleaved spot welding technique utilises electrical resistance generated Joule heating to both melt metal, for the purpose of fusion welding, and to also induce joining interactions directly between the metal and carbon fibre fabric. A subsequent production step is to infuse the carbon fibre with polymer resin to form the composite laminate. The resin infusion also penetrates into the interleaved joint, where the resistance spot weld has been applied; the resin therefore also acts as an adhesive bond between carbon fibre and metal sheets. The joining mechanism is an intimate combination of adhesive bonding between interleaved materials and the interaction of multi-material resistance spot welding.

1.3.3 Thermoplastic infused metal foam as an intermediary material

This joining concept, as illustrated in Figure 1-3, makes use of a novel intermediary material, assembled between the composite and the metal, which can accommodate variations of established joining techniques that have not previously been used for directly joining composites to metals. This joining concept was a combination and extension of two Cranfield University MSc research projects, one project that investigated thermosetting polymer infused metal foam as a new material (Rathi, 2009) and another that investigated methods of joining metal foams (Cashman, Rayani and Nuruddin, 2009).

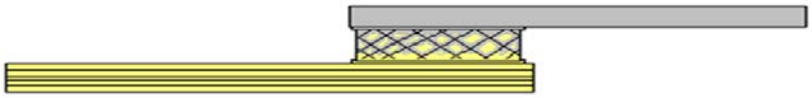

Figure 1-3 – Illustration of the thermoplastic infused metal foam as an intermediary material joining concept

The intermediary material is a porous open-cell metal foam that is infused with a thermoplastic. The infusion of one material into the other creates an integral mechanically interlocking network; between the thermoplastic and the metal foam, which enables transfer of load between the two materials. The metal foam is joined to the metal sheet by a brazing technique, and the infused thermoplastic is welded to the interfacing surface of a FRP composite laminate, a composite which uses the same thermoplastic, as was infused into the metal foam, as a matrix system.

1.4 Investigative approach

The approach taken to investigate and evaluate the joining concepts was to first develop methods of manufacturing prototype specimens and then to evaluate the specimens by both mechanical test and metallographic inspection.

Configurations of prototype joints were first designed that would enable strength and failure mechanisms to be characterised by mechanical testing. Methods were defined that would enable the prototype joint specimens to be manufactured. The manufacturing methods had to take into consideration the necessity for multiple manufacturing stages that were required due to the manufacturing parameters of the dissimilar materials being joined. The clearest example of this is processing temperatures; the temperatures required to form metal-to-metal joints, by welding or brazing methods, are above the degradation temperatures of the polymers used in the composite laminates. Multiple manufacturing trials were required to develop adequate manufacturing methods.

The prototype specimens of the concept joints were evaluated by metallographic inspection as well as by mechanical testing. The metallographic inspection enabled evaluation of both the realised joining concept and also the effectiveness of the manufacturing process. Understanding of the manufacturing process gained by metallographic inspection was used in iterative manufacturing trials in order to improve the manufacturing process. Metallographic inspection of tested, and partially tested specimens, was also used to understand the failure characteristics of the joining methods.

Strength evaluation of the prototype novel joints was by non-standard mechanical testing methods. Therefore to understand the load-strain behaviour of the novel joining concepts, where possible, the joints were baselined against test specimens constructed using traditional joining methods that consisted of part geometries and interfaces that were near identical to the prototype novel joints.

This approach overall enabled the concept joints to be assessed in terms of both joining performance enhancement and also manufacturing feasibility. Further to this, the knowledge gained of the novel joining techniques enabled identification of potential improvements that could be made to the joint geometries and manufacturing methods, and so generated recommendations for possible future investigations depending on real-world requirements of the joining technology.

1.5 Thesis Hypothesis

Adhesive joining is enhanced by the inclusion of mechanical elements; such examples are the use of anti-peel fasteners and the weld-bonding joining technique. Would it therefore be possible to improve the adhesive joining of composite to metals by including mechanical elements in the joint, which provide a graduated transition from composite to metal by methods that avoid the disadvantages to composite structures associated with the use of traditional mechanical fastening techniques?

1.6 Novelty and innovation

- Investigation into the use, and effect of positioning, of sharply tapered CMT-Pin micropins for reinforcing metal to composite adhesive joints
- Fist development of a technique to penetrate carbon fibre fabric with a metallic resistance spot weld and the application of this carbon fibre fabric penetrating resistance spot weld for enhanced structural joining of composites to metals
- Use of laser irradiation to provide indirect heating for the purpose of braze-joining metal foam to metal plate and the first development of a technique to use a thermoplastic infused metal foam intermediary material for structural joining of composites to metal.

1.7 Outline of thesis chapters

1.7.1 Chapter 2 – Literature Review

The literature review discusses the importance of dissimilar material joining; specifically the challenges and traditional solutions of joining composites to metals. The most recent developments of composites to metal joining are explored and opportunities are identified for potential further developments that could be made. The contents of the literature review are applicable to the various joining techniques investigated in individual chapters of this thesis.

1.7.2 Chapter 3 – Surface structured metals as through-composite-thickness reinforcement

Chapter 3 reports investigations into the use of micropins applied to the metallic faying surface for the purpose of mechanically reinforcing an adhesively bonded joint between metal and CFRP, the joining concept that is described in Section 1.3.1.

A method of manufacturing the joining concept is achieved by welding arrays of micropins onto the faying surface; these micropins are then inserted in the through-thickness direction into uncured layups of CFRP. Prepreg is used as a composite precursor. The prepreg cure cycle simultaneously cures the composite and adhesive bond; exploiting the prepreg matrix system as an adhesive.

Optical microscopy of sectioned joints was used to understand the interaction between micropins and composite material micro-architecture. The joint specimens manufactured were designed to enable mechanical characterisation of the joining concept. The micropin reinforced adhesive joints were fundamentally double-lap-shear in arrangement, with various metal substrate thickness and micropin array patters being investigated, so to understand the effect that both the number of micropins, and their positioning within a bondline, have on joining strength. The joints are characterised by quasi-static

mechanical testing using laser extensometry and Digital Image Correlation to measure strain. Partially failed specimens were examined by microsectioning and X-ray Computed Tomography to understand failure mechanisms of the joining concept.

A preliminary study of this joining technique was conducted and the results used to aid in the definition of the main study. The preliminary study is reported in Appendix A.

1.7.3 Chapter 4 – Metal to Carbon Fibre Spot Welding Reinforced Adhesive Joint

Chapter 4 reports investigations of a new concept for reinforcing an adhesively bonded joint, between metal and CFRP, by applying a Resistance Spot Weld through an interleaved stack of metal sheets and dry carbon fibre fabric prior to the composite manufacturing process of resin infusion. The joining concept is described in Section 1.3.2. The resin was exploited as both the composite matrix system and composite to metal adhesive.

Due to the highly novel and previously unexplored process of dissimilar material resistance spot welding, extensive investigations into trialling various metals and interleaved stacking sequences were conducted. Instrumentation of resistance welding equipment enabled characterisation of the dissimilar material welding process, which in turn expedited the identification of optimum welding parameters. Microscopy was used to understand the weld formation processes in this novel mechanical reinforcement method.

Quasi-static mechanical testing was conducted to investigate the strength performance of resistance spot weld reinforced adhesive joints. A range of mechanical tests specimens were designed to enabled characterisation of isolated load-carrying mechanisms that are combined within the reinforced adhesive joint, so to understand how the performance of individual mechanises effect the combined joining performance.

1.7.4 Chapter 5 - Thermoplastic infused metal foam – an intermediary material in a composite to metal joint

Chapter 5 reports an exploration of using a thermoplastic infused metal foam intermediary material, a material which is in itself an interlocking network between metal and polymer, the novel intermediary material accommodate established joining methods between thermoplastics and thermoplastic matrix composites and metal foams and sheet metal. The joining concept is described in Section 1.3.3.

The investigations reported in this chapter focused on manufacturing process developments required to build a prototype of the concept joining method. The three processes being: braze joining of metal foam to metal plate, infusion of metal foam with thermoplastic, and thermoplastic welding between the infused thermoplastic and the matrix system of a carbon fibre reinforced thermoplastic. Heating for the brazing process was provided be laser irradiation of metal plate remote from the braze-joining interface. Infusion of the metal foam with thermoplastic, and thermoplastic welding to composite, were achieved simultaneously by use of an open mould tool placed within a heated platen press. Microsectioning of the materials and joints enabled evaluation of the quality achieved by the processes. Differential Scanning Calorimetry was used to evaluate the condition of the thermoplastic after the infusion process. The prototype joint manufactured was subjected to quasi-static mechanical testing to evaluate the strength of the joining concept and understand failure mechanisms.

1.7.5 Chapter 6 - Overall Discussion and Conclusions

The results of investigations into the three distinct novel joining methods are considered together and discussions made on observed trends and comparisons between them. Topics discussed in this chapter are: residual strength, pseudo-ductility, and increased energy absorption during failure, which are characteristics achieved by use of novel mechanical reinforcement of

adhesive joints. The enhancement of joining performance by increased interaction of metal and composites at the micro-architecture level is discussed, as is how the use of novel mechanical reinforcement of adhesive joints can result in manufacturing process improvements. The final discussion concerns how the investigations in this work could be a step towards elimination of traditional mechanical fastening of composites, which would enable increased structural efficiency through weight saving in dissimilar material joining. Finally in this chapter potential further work is considered and conclusions made for the three individual joining concepts, and also metal to composite joining in general.

2 LITERATURE REVIEW COMPOSITE TO METAL STRUCTURAL JOINING

2.1 Introduction

2.1.1 Materials

The materials considered within the scope of this work are those typically used for load carrying structure in aerospace applications. When composites are referred to, unless otherwise stated, the material can be considered to be a continuous fibre reinforced polymer; with the reinforcement fibres being carbon graphite and the polymer being an epoxy thermoset. The metals considered are predominantly titanium alloys and stainless steels.

2.1.2 Why do we need to join composites to metals

Both metals and composites have desirable mechanical properties for the use in structural applications; these include high specific strength, high specific modulus, and resistant fatigue response. There are however significant differences in these key properties between metals and composites, and these differences can make one material, or the other, more suitable for reacting the specific load being exerted within a structure. Figure 2-1 shows a graphical comparison of the strength of typical metals and CFRP used in aerospace applications.

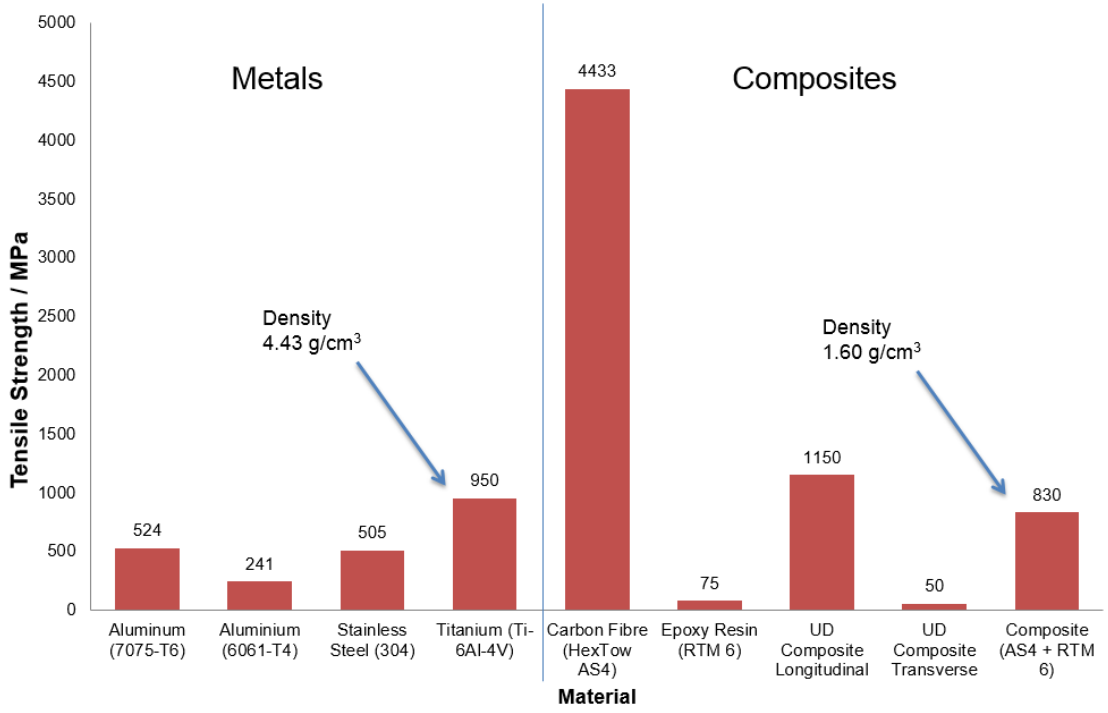

Figure 2-1 - Graphical representation of materials ultimate tensile strength, data from (MatWeb, 2015)

For example, composites typically have greater specific strength than metals, but the strength of composites is highly anisotropic, so when considering an aerospace structure such as a wing, composites are an ideal material choice for reacting the predominantly in-plane loads that occur in the wing skins. Other areas of a wing structure are required to react loading in multiple directions, such as components that function as control surface attachment points, metals have predominantly isotropic strength and so a metal would be a more suitable material choice for such a component of a wing structure. It is common that both metals and composites can have application within a single structure and therefore a structural joint is required between the two materials.

2.1.3 Why established joining processes are not wholly suitable

There is a wide range of established joining techniques available that are suitable for use in aerospace structural applications. In recent history metals have been of predominant use in aerospace and therefore metal joining techniques are of greatest technical maturity. As the aerospace industry is conservative by nature, especially civil aviation, the tendency is to seek to apply the well-understood mature technologies. Which in terms of structural joining is therefore the methods used for forming traditional metal-to-metal joints (Messler, 2004; Niu, 1992).

The differing mechanical properties between composites and metals are due to them being fundamentally different materials. These differences make many of the traditional metal joining techniques either unfeasible, for example the two materials cannot be welded, or they place greater limitations on the joint performance and joining methodology, for example bolting.

2.2 Conventional techniques

2.2.1 Adhesive

2.2.1.1 Kinds of adhesives

When adhesively bonding reinforced polymers, it is necessary to use an adhesive that is compatible with the polymer matrix of the composite. For thermosetting organic polymer matrices, such as epoxies, a similar thermosetting polymer adhesive usually provides good bond performance. Typical organic adhesives for this application include: toughened-epoxies, acrylics, urethanes, and also cyanoacrylates. Likewise, when adhesively bonding metals it is necessary to use an adhesive that is compatible with the surface condition of the metal. Suitable adhesives for bonding titanium are: toughened-epoxies, nitrile-epoxies, polyimides, epoxy-phenolics, and nitrile phenolics (Messler, 2004). For adhesively bonding stainless steels: toughened-

epoxies, acrylics, polyurethane, and cyanoacrylate result in good joint performance (Boyes, 1998).

In order to adhesively bond composites to metals it is necessary to use an adhesive that is compatible with the two different materials being joined. From the above it can be seen that for bonding CFRP (which have an epoxy matrix) to titanium; toughened-epoxies adhesives are suitable, and for bonding CFRP to stainless steel either toughened-epoxies, acrylics, polyurethane, or cyanoacrylates are suitable choices.

2.2.1.2 Advantages and limitations

The advantage of adhesive bonding of composites to metals is primarily the resulting low stress concentration in the parts being joined. A part that is being adhesively bonded is typically referred to as an adherend. Low stress concentration is a significant benefit for composites, as composites are especially sensitive to high stress concentrations. The low stress concentrations also benefit the fatigue performance of a metal adherend. Furthermore, adhesive bonding is a relatively lightweight joining technique, particularly when compared to mechanical fastening.

The significant limitations of adhesive bonding, aside from the limitations that are dictated by the polymeric material properties of the adhesive i.e. bulk strength, modulus, ductility and operating temperature limitations, are the limitations related to the adhesive bonding process. The adhesive bonding process can be significantly time consuming. In addition to being time consuming it can be costly due to use of consumables. The adherend surface requires stringent preparation in order to ensure expected joint strength. Also the process requirement of adherend jigging during adhesive cure, and the time required for cure, add further costs to the process (Baker, Dutton and Kelly, 2004). If an elevated temperature is required for adhesive cure the result can be the introduction of residual stresses in the joint, an effect which is more critical

when materials of differing thermal expansion coefficients are being joined; as is often the case when joining composites to metals (Niu, 1992).

It is stated above that adhesive bonding results in relatively low stresses in the joined adherends, however in order to achieve this effectively, joint geometry considerations have to be made. An adhesive joint works most efficiently when load is transferred between joined parts as shear loading. Some adhesive joint geometries can induce bending moments in the adherend due to load eccentricities. These become more pronounced as adherend thickness increase. Such secondary induced loading states can result in premature failure of an adhesive joint or an adherend. Composite laminates are particularly susceptible due to their relatively low strength in the through-thickness direction. Induced bending moments can also drive bondline failure. Careful design of adhesive joints can minimise induced secondary loading states (Kinlock, 1987). Scarf joints and multiple-stepped-lap joints have been demonstrated to have the greatest strength performance, as presented in Figure 2-2. Shown in Figure 2-3 is an example of a double-lap-shear adhesive joint used in an aerospace structural application, it shows the use of a multiple-stepped-lap joint in the primary structure of an aircraft, the loading conditions of this joint is demanding and the integrity of the joint is flight critical.

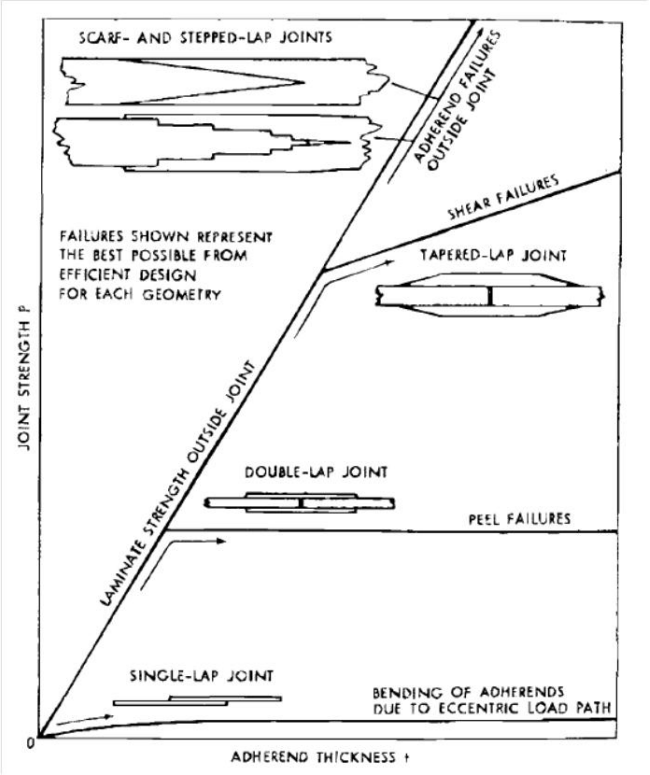

Figure 2-2- Load carrying capacity of adhesive joints. Taken from Hart-Smith (Hart-Smith, 1982).

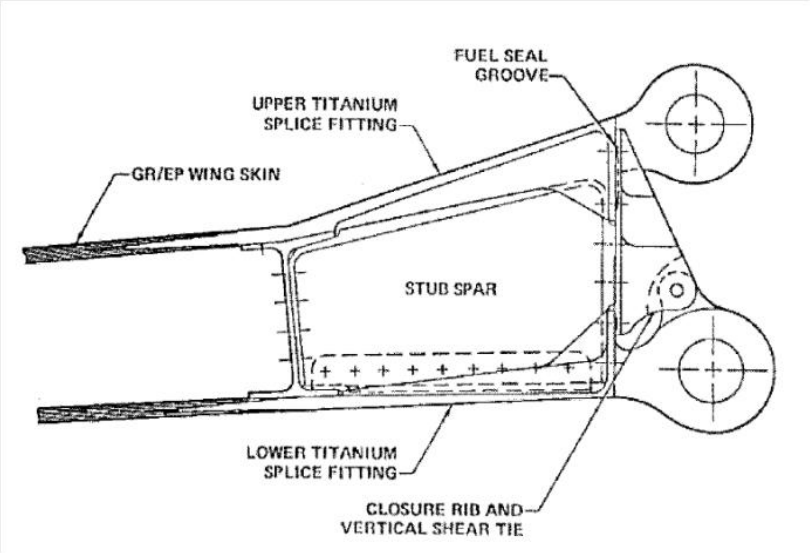

Figure 2-3 - Schematic illustration of the multiple step-lap joint used to attach the carbon/epoxy wing skin to the titanium fuselage attachment lug of the F-18 military aircraft. Taken from Baker (Baker, Dutton and Kelly, 2004).

2.2.2 Mechanical fastening

2.2.2.1 Types of mechanical fastening

When considering joining composites to metals by mechanical fastening it is the sensitivity of composites to mechanical fastening that prescribes: the type of fasteners, fastener arrangement, and installation processes, which can be used. The mechanical fastening of metals is a robust process due to the comparative durability of metals when related to composite. As an example, when mechanical fastening metals, it can be considered that the load will always be proportionally shared by all fastener positions; due to localised yielding of metal at highly loaded fastener positions (which can occur due to low rigor manufacturing practices), this is not the case for a composite, which does not undergo the same type of yielding, and so the mechanical fastening process must be carried out in a more rigorous manner.

When mechanically fastening composites, metallic fasteners are typically used, however the specific type of metal used for the fastener requires careful consideration. Graphite, which constitutes the carbon fibre, has a low electrical potential and this can result in galvanic corrosion between the fibres and some metals. Current density is a good indicator of galvanic compatibility. Figure 2-4 shows a plot of current density for metals coupled with graphite. It can be seen that Ti-6-4 is especially compatible with graphite fibres. Stainless Steels, which includes AISI 304, are also compatible (Messler, 2004).

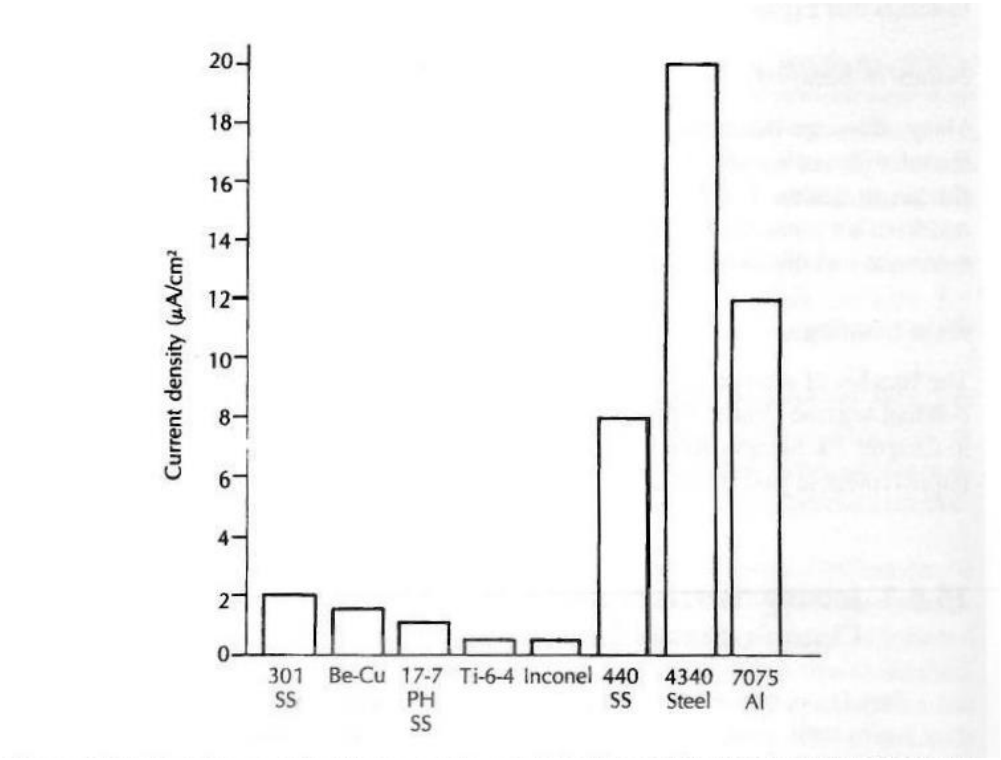

Figure 2-4 - Plot of current density for metals coupled with graphite as an indicator of galvanic corrosion potential, Figure 15.3 (Messler, 1993).

US Military Standard MIL-STD-889B (United States Department of Defence, 1976) provides the galvanic series, and the guidance that in order to minimise galvanic corrosion neighbouring materials in the series should be used together. Titanium alloys and carbon neighbour each other in the galvanic series.

Bolting is the most extensively used method of mechanical joining composites to metals, riveting is also used; the disadvantage of rivets over bolting is that rivet installation processes can damage the composite laminate inside the fastener hole as the rivet shank expands to form an interference fit. Interference fit fastening is generally undesirable for composites due to the likelihood of damage the laminate within the fastener hole (Messler, 2004).

2.2.2.2 Advantages and limitations

The advantages of using mechanical fasteners are that they provide a positive connection with low initial risk. There are also no thickness limitations to the parts that are being fastened. Fasteners also provide through thickness reinforcement; this can be of significant benefit when used with composites (Baker, Dutton and Kelly, 2004).

Limitations to the use of fasteners for joining composites, in addition to galvanic compatibility requirements, are geometric constraints of fasteners and hole sizes. Fasteners and hole size choices are restricted in order to limit stress concentrations within the composite laminate (Messler, 2004).

Fasteners that have larger bearing surfaces have several advantages when used to join composites; they reduce the likelihood of the fastener pulling through the composite laminate. Large bearing surfaces can also help negate the possibility of loss of fastener preload, which can occur due to the visco-elastic nature of the composite polymeric matrix, resulting in stress relaxation, conversely swelling of the polymer matrix due to water absorption can also affect fastener preload, this can increase the clamping force above the compression strength of the laminate. Effects of fastener misalignment, which result in high stress concentrations being applied to the composite laminate due to lack of perpendicularity between exterior surfaces and hole direction, known as fastener cocking, is also reduced by the use of larger bearing surfaced fasteners (Messler, 2004).

Work has been done to improve the performance of bolted composite joints by locally reinforcing the composite laminate by substituting CFRP plys with titanium foils within the laminate, as described in Figure 2-5, to form a hybrid composite (Kolesnikov, Herbeck and Fink, 2008).

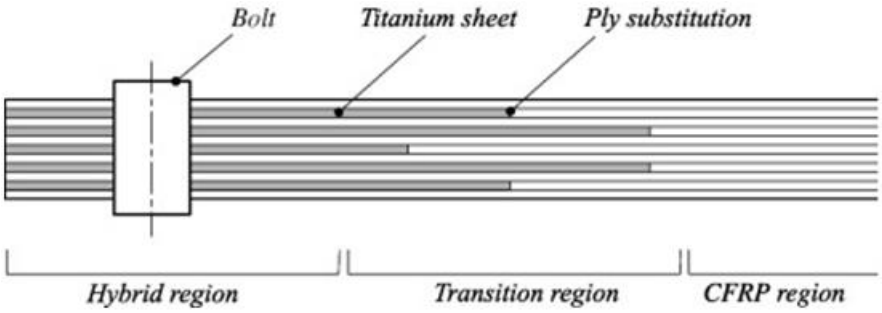

Figure 2-5 - Hybrid composite at bolting location, taken from (Camanho et al., 2009)

The isotropic nature of metals better react the bearing loads resulting from mechanical fastening, in the hybrid composite CFRP, shown in Figure 2-5, plys that are not aligned with the predominate loading direction are replaced with titanium foils, this improves the bearing load resistance while maintaining CFRP plys in the loading direction. The hybrid composite has an improved joining performance compared to an all CFRP laminate. With 20% titanium content the tensile strength of a three-row bolted joint is increased by 91% compared to a CFRP only laminate, and the specific tensile strength is increased by 32% (Fink and Kolesnikov, 2005). The drawbacks to the use of this hybrid composite are the increases in manufacturing time and cost, and also material costs, when compared to CFRP only laminates (Fink et al., 2010).

2.2.3 Fastener reinforced adhesive joints

2.2.3.1 Introduction to fastener reinforced adhesive joints

Adhesive bonding and mechanical fastening can be used in conjunction and result in joining performance that exceeds either of the two joining methods when used in isolation. This is typically achieved by application of adhesive to faying surfaces followed by the installation of fasteners. Time is then required for the adhesive to cure; this may require elevated temperatures. The joint can be designed so that the fasteners provide jigging and interfacial pressure between parts while the adhesive cures, so improving the quality of the adhesive joint. Also, the adhesive can act to seal the joint, preventing solvent ingress that can lead to premature corrosion of the mechanical fastening (Baker, Dutton and Kelly, 2004; Montabone, Nebiolo and Vigada, 1997).

2.2.3.2 Fail-safe feature

When the two methods of adhesive bonding and mechanical fastening are used in conjunction the load is not equally shared between the bonded and fastened regions. In optimally designed bolted-adhered step-lap joints the bolts transmit approximately 1% of the total load (Hart-Smith, 1982). This is due to the adhesively bond having greater stiffness than the mechanical fastening. The joining stiffness is a characteristic of the joining method used, therefore the significant difference in stiffness between adhesive joints and mechanically fastened joints would still be the case if the joining methods were used in isolation. The benefit of using the two joining techniques together is that the fasteners provide an alternative in-plane load path that can contain the spread of a disbond and so provide a fail-safe feature to the joint (Baker, Dutton and Kelly, 2004).

2.2.3.3 Anti-peel fasteners

Mechanical fasteners can be used to provide through-thickness reinforcement of an adhesive joint. Adhesive joints transfer load most efficiently in shear, and are relatively week at withstanding out-of-plane loads, whereas mechanical fasteners perform well at transferring out-of-plane loads. Fasteners can therefore be installed within the bounds of an adhesive joint specifically to react out-of-plane loads, including induced secondary loads, i.e. bending moments that can occur in adhesive joints due to loading eccentricities along the shear load paths. These secondary loads are at a maximum at the adhesive bond extremities, in the loading direction, of lap-joints; this area of an adhesive joint is referred to as the lap-shear ‘run-out’. The secondary induced loads can drive the peeling disbond failure mechanism therefore the fasteners installed at adhesive bond run-outs are termed ‘anti-peel’ fasteners (Baker, Dutton and Kelly, 2004).

2.2.3.4 Advantages and limitations

In addition to the advantage of fasteners as fail-safe features, as explained in Section 2.2.3.2, the use of adhesive bonding and mechanical fasteners together also have structural advantages during normal operational life, the adhesive bonding reduced stress intensity of the joint, compared to a purely fastened joint, which results in an improvement of the fatigue performance of the joint (Messler, 2004). The effect of mechanical joining provided by resistance spot welds in the weld-bonding process provides the same advantages as the use of fasteners with adhesive joining, with the further advantage of the lower weight due to not introducing a fastener, the limitation of this however is that not all metals can be easily welded (Darwish and Al-Samhan, 2004).

The use of anti-peel fasteners has to be carefully designed and installed as the introduction of a fastener hole at the critical location of the bondline run-outs can result in damage that enables premature bondline failure. However, the through-thickness reinforcement provided by fasteners at bondline run-outs also

acts to reinforce the composite laminate, helping to prevent laminate failure (Baker, Dutton and Kelly, 2004).

2.3 New techniques of fastening reinforced adhesive joints

2.3.1 Fit form

Adhesive joining of metal to composite can be achieved as part of the curing cycle. A composite structure is laid-up together with metal components, which can be local reinforcements e.g. bushings (Weber, 2010), then during the composite curing process the composite resin matrix also acts as the adhesive medium. In some situations additional adhesive is added in the form of adhesive films. This method of metal-to-composite joining is referred to as mechanical fit-form.

It has been shown that by designing an adhesive joint to contain geometric features, which introduce an element of mechanical interaction, the strength of the joint is significantly increased. This has been achieved by including grooves in metal parts, into which the end of uncured prepreg composite are then keyed during lay-up (Paulshus et al., 2006).

As with typical adhesive joints, if an elevated composite cure temperature is required stresses can be induced between the interfacing parts as the structure is cooled to the ambient operating temperature, these stresses are then present in the joint even when the joint is not loaded (Adams and Mallick, 1993).

2.3.2 Pre-cure fastener installation

Trials have been conducted by the National Aeronautics and Space Administration (NASA) into the installation of studs and fasteners into uncured composite laminate. In this work holes were formed in a prepreg lay-up for the purpose of installing fasteners prior to composite cure. The test specimens

consisted of an array of screws consolidated within CFRP and fastened into an aluminium plate, as shown in Figure 2-6.

Figure 2-6 - Array of screws joining CFRP laminate to an aluminium plate; connection made prior to laminate cure. This was subsequently subjected to a tensile/bending test. Taken from (Semmes, 2009)

The specimen was loaded to 20.8 kN (the screws were rated to withstand a load of 45.5 kN). Significant deformation resulted in the laminate but the joint did not completely fail (Semmes, 2009).

2.3.3 Weld-bonding

Industry based research has recently been conducted by a consortium of U.S. automotive manufactures into an innovative way of forming structural joints between CFRP and steel for the manufacture of the underbody of a ‘high annual-unit-production’ vehicle. Adhesive bonding is widely used in automotive

manufacturing to join composites and metals, however this is typically only done for vehicles that are produced in relatively low numbers; performance cars being an example. Adhesive bonding is used when production volumes are low; due to the time and cost required for part fit-up and jigging. The investigations by the U.S. consortium were to develop a method of forming such adhesive joints that could be used in the production of high annual-unit-production vehicles (Berger, 2010). The technique is termed weld-bonding and is illustrated in Figure 2-7 and Figure 2-8 below.

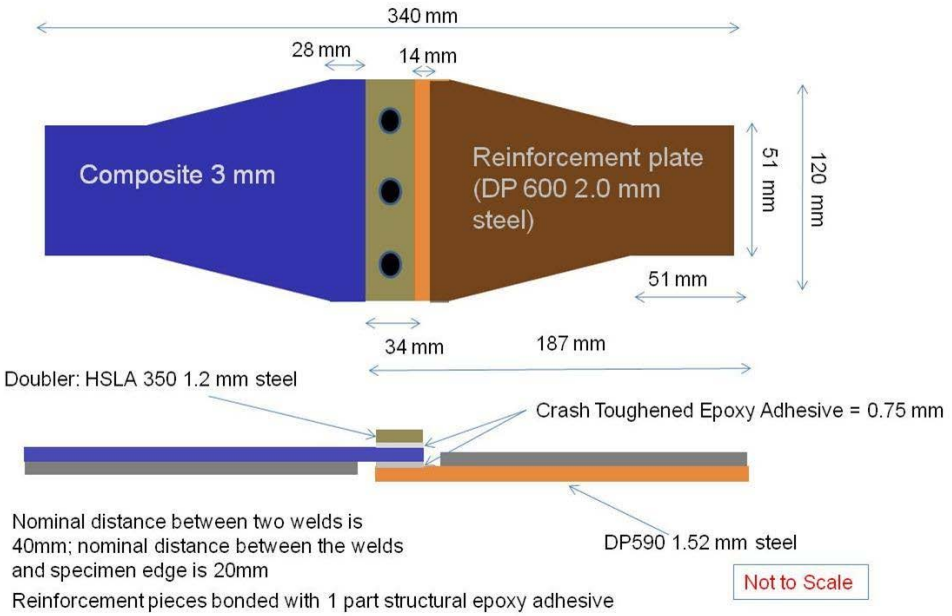

Figure 2-7 - Composite to steel weld-bond joining representative structure, taken from (Berger, 2010).

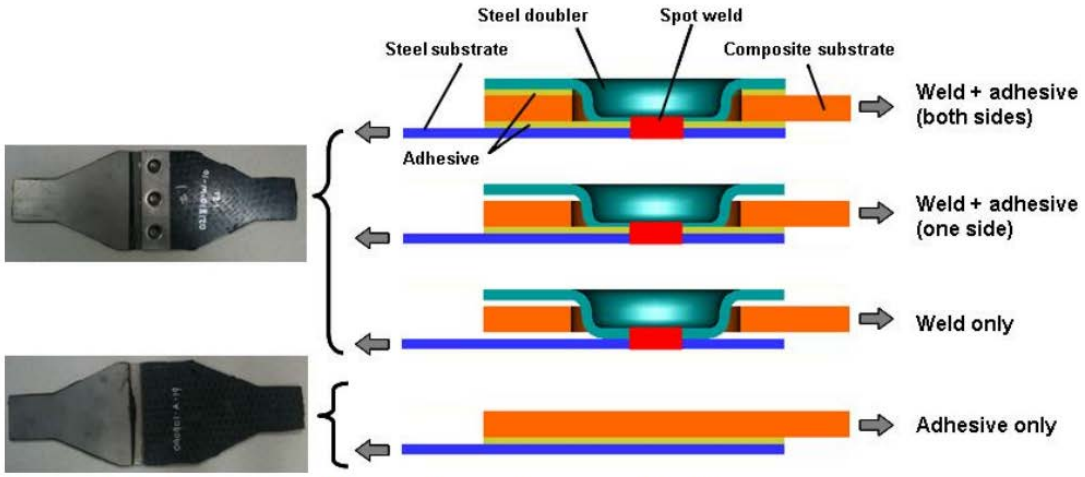

Figure 4. Various types of joint configurations tested in this study

Figure 2-8 - Weld-bond joint used to join composite to steel, taken from (Shah et al., 2010)

The weld-bond joining method uses resistance spot welding to hold steel and composite parts together while the structure undergoes a baking cycle to cure the adhesive. The arrangement of the joint shown in Figure 2-7 and Figure 2-8 is that of the 'super-lap-shear' mechanical tests specimen used in the study. Mechanical testing of this representative structural joint specimen demonstrated that the resistance spot-weld also acts as an alternative load path after adhesive joint failure (which could therefore be described as a fail-safe structural joint) and so extends the performance of the weld-bond joint (Shah et al., 2010). The performance benefits of weld-bonding is well documented in the literature (Darwish and Ghanya, 2000; Santos et al., 2004).

2.3.4 Comeld

TWI has developed the technology 'Comeld' (Smith, 2005). In this technology the metal interface surface of the metal is sculpted by electron beam to form protrusions from the surface (Dance et al., 2004). Dry fibres of a FRP are placed around the protrusions and then infused with resin. In this process the

resin with the dry fibres forms the composite material and the resin also acts as the adhesive between the composite and metal.

In comparisons of Comeld and control joints it has been shown that initial failure occurs at similar loads for each joint, the difference being that the control joint completely fails at a load close to that of the initial failure, whereas after the initial failure of the Comeld joint an alternative load carrying mechanism enables the Comeld joint to continue to carry load up to a complete failure load that is considerably greater than the control. In control joints the final failure has been shown to always be at the adhesive interface whereas in the Comeld joint the failure is shown to be in the composite laminate.

For double-step-lap Comeld joints compared to a control double-step-lap joints the energy absorbed during failure is shown to be 13 times greater for a Comeld joint of titanium and CFRP and five times greater for a joint of stainless steel and GFRP. Comeld technology was also shown to reduce the scatter of failure loads when applied to scarf joints.

2.3.5 Pin-welding

A similar joining technique to Comeld has been developed by Vienna University of Technology; the principle difference from Comeld is the surface structuring method applied to the metal faying surface (Stieglbauer and Kazmaier, 2009; Ucsnik et al., 2010). The geometric features are, as with Comeld, protrusions but are deposited by the CMT-Pin GMAW welding technique developed by Fronius (Fronius International GmbH, 2009). Joints between stainless steel and CFRP were shown to have an improvement in load carrying of +52.3% over control joints with the energy absorption during failure being 27 times greater than the control.

Cold Metal Transfer (CMT) is a development from Dip Transfer GMAW welding; in both Dip Transfer and CMT the deposition of filler metal occurs when the filler wire makes direct contact with the work piece weld pool. The development in

CMT over Dip Transfer is in the method of separating wire from work piece after contact. With Dip Transfer separation of the wire from the work piece is caused by wire fusing-breaking due to the resistance heating resulting from the short circuit high current, but in CMT the current is actively controlled to be reduced to zero at the time of contact and the separation of wire and work piece is achieved by mechanically drawing the wire away from the work piece. By preventing short circuit current flow the associated resistance heating is not present; this makes the CMT welding process cooler than the dip transfer method, and also cooler than most other welding processes. This lower temperature characteristic of CMT welding allows thin gauge plates to be welded. If required the timing of current reduction can be tuned to introduce further heating into the work piece. Additionally: the low, and accurately controllable, temperature characteristics of the CMT technology enable different metal substrates to be joined by a mixed weld/braze technique (Furukawa, 2006).

It is the wire motion and accurate current control features of the CMT technology that enabled the technology to be further developed into the CMT-Pin process. The initial stage of CMT-Pin is the same as CMT, the development is that rather than immediately mechanically drawing the wire away from the work piece, as with CMT, there is a dwell time that allows the weld pool to solidify and so essentially spot weld the wire to the work piece. The second stage in the CMT-Pin process is to use a combination of resistance heating induced by current flow and mechanical pulling of the wire away from the work piece to separates the wire in a manner that leaves geometrically repeatable protrusions of filler wire spot welded to the work piece.

2.3.6 Why these techniques work and what are the advantages and limitations

The new techniques of fastening reinforced adhesive joining that are discussed in this section are structurally effective for the same reasons as those of the established methods discussed in Section 2.3. These reasons are that, firstly, the fastening elements more effectively react the loading conditions that lead to both premature adhesive bondline failure initiation and bondline failure propagation, and secondly, the fastening elements act as a secondary load path once the adhesive bondline has failed.

The development of these new techniques of fastening reinforced joining has occurred for two reasons: the primarily driving force is the structural joining advantage of mechanically reinforcing adhesive joints, and the enabling condition is the new possibilities for construction of such joints that are made possible by the use of composite material manufacturing methods.

A limitation in the manufacture of some of these new techniques is that the processing temperature of metals and polymer composites dictates the order that processes can be carried-out. For example, welding processes have to be done before thermoset polymer curing processes. This is because the welding temperatures are above the degradation temperatures of the polymers. However, this can work towards one of the structural advantages of these joining techniques, which is that the mechanical fastening is made prior to, or at the same time as, the adhesive joint formation. This results in the bondline not being disrupted by the post-process procedures that are typically required to install mechanical fasteners. An example of such a procedure is the hole drilling for the purpose of fastener installation, which can easily generating local damage to an adhesive bondline. Another advantage of mechanical fastening being in place before an adhesive bond has been formed is that an effect of part jigging is provided by the fastening. This can be utilised to both hold parts in the correct position with relation to one another while the adhesive cures and also to maintain a consistent bondline thickness.

2.4 Metal Matrix Composite as a material transition

2.4.1 Motivation for review

The strength of fibre reinforced composite materials is provided, by definition, by the continuous fibres present in the material. The strength of the reinforcement material used in structural [polymer matrix] composites is typically at least one order of magnitude higher than other materials regularly used for load carrying structures (Ashby, 1999). The composite's matrix material consists of ether a polymeric, metallic, or ceramic material. Table 2-1 gives strength values of the various materials for comparison.

Material	**Tensile strength (MPa)**	**Shear strength† (MPa)**
Titanium Ti-6AL4V	950	475
Aluminium 2024-T3	435	218
Stainless steel 304	505	253
Epoxy RTM6	75.0	37.5
Carbon fibre HexForce G1157*	4447	NA

*Constituent fibre: AS4C GP 6K (formerly designated: HS06K)

†Based on stated tensile strength value,

Table 2-1 - Ultimate strength of materials of interest

In a paper by Robert W. Messler, Jr (Messler Jr., 2004) a discussion is made of the importance of considering the joining of parts to be as important as the fabrication of the parts themselves; to consider joining as an 'enabling

technology' rather than a secondary processing step, which is considered after material development for part specific applications. The article further discusses that to achieve high performance joints, the joining process will have to occur at the same time as the material and structure is being manufactured. One method presented to achieve this in the joining of one CFRP part another. The concept involves exposing fibre reinforcements, which can be overlapped or intertwined, before the joining region is infused with a polymer resin. Therefore enabling the principle load carrying structure, the fibre reinforcement, to essentially pass from one part directly into the joining interface, this is show diagrammatically in Figure 2-9.

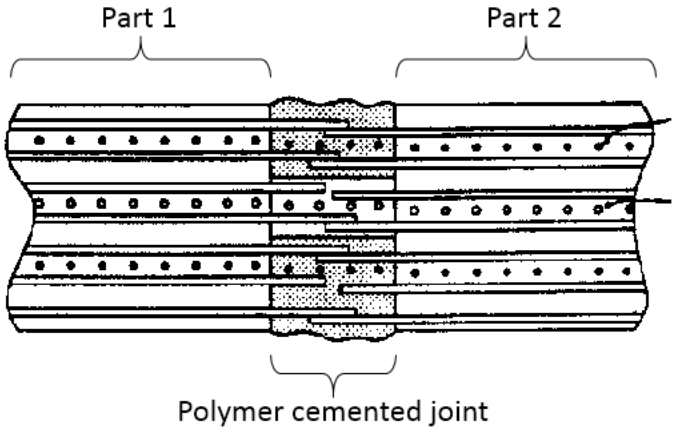

Figure 2-9 - Diagram showing the concept of extending reinforcement fibres of composite parts into a 'polymer cemented joint', taken from (Messler Jr., 2004)

When exploring concepts of how to join CFRP to metals this same idea could be used: to have continuous reinforcement fibres that pass from the polymer matrix of the composite directly into the metal, forming a transition region of Metal Matrix Composite (MMC) within the metal part. Due to the differences in processing temperatures of polymers and metals, with polymers typically being below 150°C and metals typically above 1000°C, it would be necessary to form the MMC before the CFRP.

2.4.2 Overview of attaching fibres into metal while providing protruding fibres that can be connected to plastic

As stated in the previous section, due to processing parameters; specifically temperature, any fibre reinforced material that has regions of both polymer matrix and metal matrix will require the metal region to be fabricated first. Established MMC manufacturing methods produce near net shape components that have the Fibre Volume Fraction (FVF) determined at the beginning of the fabrication process. And the fabrication process almost exclusively includes use of a Hot Isotactic Press (HIP) in the final stages of processing. These two factors prohibit established manufacturing methods from being used to produce a MMC that have protruding dry reinforcement fibres, which can be subsequently formed into a polymer matrix composite. There are however new MMC manufacturing methods that have been developed, principally to avoid the costly HIP process, which could be adapted to provide a MMC that does have regions of dry reinforcement fibres.

2.4.3 Established Metal Matrix Composite manufacturing

The use of reinforcement fibres is applied to metallic materials for much the same purposes as the use of reinforcement fibres with plastics, these being the formation of a composite material that has mechanical properties which are more desirable than the constituent materials in isolation. Reinforced metal composites are termed Metal Matrix Composites (MMC).

As an example: the use of Silicon Carbide (SiC) fibres with titanium produces a MMC, which when compared to bulk titanium, is twice as stiff, one and a half times as strong, and offers a 30% weight saving. There is also a significant improvement in creep behaviour of an MMC over the equivalent bulk metal (Rolls-Royce plc, 1998).

The requirements of high temperatures, high pressures, and long processing dwell times of established MMC manufacturing methods, together with the high

cost of some types of reinforcement fibres and metal matrix systems result in continuous fibre MMCs being relatively expensive materials. Efforts are being made to develop new manufacturing methods that offer significant cost reductions to the final products.

There is ongoing work to further refine established methods of MMC production, which include optimisation of both preform manufacture and consolidation steps, to enable the manufacture of MMC from both lower cost reinforcement fibres and metal matrix systems, for example carbon fibres and aluminium alloys rather than silicon carbide fibres and titanium alloys (Wenzelburger, Silber and Gadow, 2010). Although typically the choice of metal matrix is driven by operational requirements, for example: titanium for high temperature conditions (Hooker and Doorbar, 2004).

2.4.4 New manufacturing techniques

2.4.4.1 Roll-diffusion Bonding

A method has been developed of manufacturing a continuous silicon carbide fibre reinforced titanium alloy MMC by taking advantage of the superplastic flow behaviour of some titanium alloys, this manufacturing process has been termed Roll-diffusion Bonding (Testani and Ferraro, 2010). Figure 2-10 displays a diagram of the Roll-diffusion Bonding process and typical processing parameters are provided in Table 2-2.

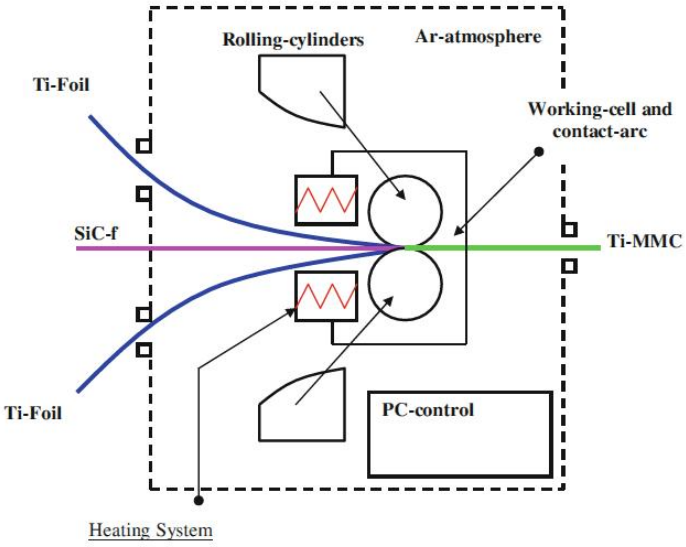

Figure 2-10 - Diagram of the *Roll-diffusion Bonding* method of manufacturing a continuous silicon carbide fibre reinforced titanium alloy MMC (Testani and Ferraro, 2010)

Table 1 Experimental reference parameters adopted for the pilot plant design

Exercise temperature, °C	Mean pressure in the contact arc, MPa	Time, s
900	500	6

Table 2-2 - Typical processing parameters of *Roll-diffusion Bonding* (Testani and Ferraro, 2010).

Roll-diffusion Bonding uses similar processing temperatures and pressures as HIP processes, the differences being that the these conditions are applied locally in a continuous process, as opposed to globally to bulk material in a batch process as with HIP. It is reported that similar MMC material properties can be achieved with Roll-diffusion Bonding as those achieved by HIP processes but with a cost reduction of approximately 40% by using the Roll-diffusion Bonding production method (Testani and Ferraro, 2010).

2.4.4.2 Ultrasonic Consolidation

A low temperature method of manufacturing a MMC has been developed that uses ultrasonic frequency mechanical vibrations to drive a solid-state process (Astashev and Babitsky, 1998), which consolidates a metal matrix around reinforcement fibres, by a combination of plastic deformation and diffusion bonding of the metal matrix (Kong and Soar, 2005). In this process a rolling ultrasonic sonotrode applies pressure and mechanical vibrations to a stack of metal foil and reinforcement fibres; this is illustrated in Figure 2-2.

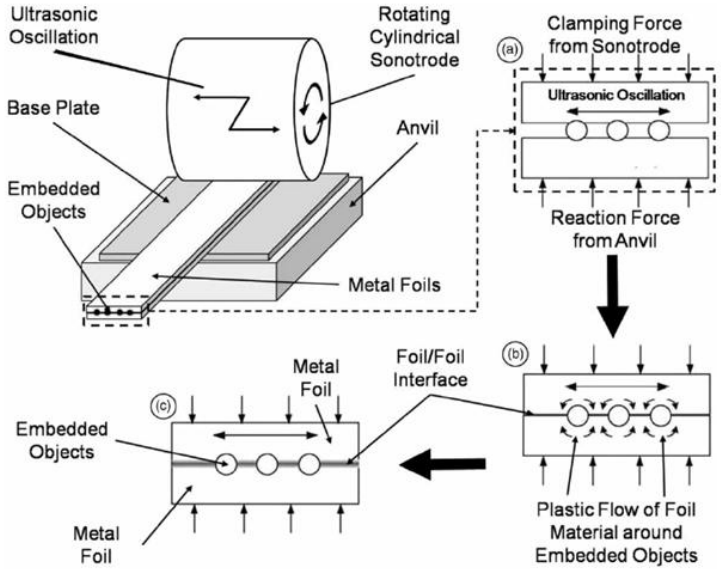

Figure 2-11 - Schematic diagram of the ultrasonic consolidation process for object embedment (Friel and Harris, 2010)

This process has been demonstrated to achieve well consolidated diffusion bonds between foils of aluminium alloy (Kong, Soar and Dickens, 2004), and also shown to not significantly degrade SiC structural reinforcement fibres, or comparatively brittle optical transmission fibres, when used with the same alloy to form a MMC (Kong and Soar, 2005). Work in this area has focused primarily on the manufacture of Shape Memory Alloy (SMA) actuated specimens, and though detailed inspection of the interface between embedded fibres and metal

matrix have been made (Friel and Harris, 2010; Kong and Soar, 2005) no information is currently available on the mechanical properties of SiC reinforced MMC produced by this method.

2.4.5 Braze joining of ceramic matrix composites

An important aspect concerned with MMC is to consider the interfacial joint between the metal and the reinforcement fibre. When suitably compatible reinforcement fibres and metal matrix are chosen strong chemical bonds can be formed due to the affinity between constituent elements of the two materials. This phenomena has been exploited and investigated in detail when developing brazed structural joining techniques between carbon fibre reinforced carbon matrix composites (which are referred to as carbon-carbon composites) and metals.

Carbon-Carbon Composites (CCC) are used for very high temperature applications. It has been found that generally the best joining method between CCC and metals is brazing, which provides good strength performance, allows higher operational temperatures than adhesive bonding, and avoids the significant problems of using metal fasteners with CCC. The problems associated with the use of metal fasteners and CCC are that CCC are very brittle and are also prone to inducing galvanic corrosion of the fasteners. The greatest problem to be overcome with brazing CCC is achieving sufficient wetting of carbon by the braze filler metal (Messler, 1993, 2004).

Achieving sufficient wetting of carbon by a braze filler metal has been achieved by using active metal brazing. Active metal brazes contain small amounts of elements that undergo chemical reactions with the surface of the carbon to produce compounds that are wettable by the bulk of the braze filler metal. It has been observed that good braze wetting of carbon is achieved when chromium, titanium, or silicon are included in braze filler metals (Chen et al., 2010; Singh et al., 2005; Singh, Asthana and Shpargel, 2007).

These findings of braze metal constituents that result in good wettability of the braze metal onto fibres are worth considering when choosing materials to use in the manufacture of a new material that has continuous reinforcement fibres passing between a metal and polymer matrix system. As the use of two matrix systems, and the compatibility between both and the reinforcement fibre, will place further limitations on material choice than if just one matrix system was used.

2.5 Summary

2.5.1 Need for mechanical reinforcement

When considering the joining of dissimilar materials adhesive bonding has the advantages of being lightweight and inducing relatively low stress concentrations in adherends, however some of the disadvantages of adhesive bonding, such as weak out-of-plane load transfer characteristics, brittle failure and complicated joining processes can be mitigated by the use of mechanical fastening in combination with adhesive bonding.

Adhesive bonds are sensitive to out-of-plane loads, both in terms of applied loading conditions and induced loading due to joint geometry and high loading conditions. Out-of-plane loading results in the bondline being locally loaded in through-thickness tension in addition to in-plane shear. Therefore, defects or cracks in the bondline will be exposed to a greater proportion of the Mode I opening condition and so the higher stress concentration factors associated with the condition. This, together with the brittle nature of the polymers used as adhesives leads to rapid crack propagation and bond failure. Using mechanical fastening by the use of fastener elements formed of a more tough material, such as a metal, improves the joint performance. The tougher material of the fastening element can be relied on to more effectively react the out-of-plane loading conditions, therefore protecting the bondline from being exposed to loading conditions that result in ultimate failure of the bond.

If the loading condition pushes the tough mechanical fastening elements beyond there yield limit, or sufficiently into an elastic deformation state, the result is the bondline being exposed to critical loading that results in adhesive bond failure. The mechanical fasting elements can have sufficient residual strength to prevent the ultimate failure of the joint after the bond has failed, therefore behaving in a fail-safe capacity. From this it could be argued that it would be better to simply form the joint by mechanical fastening and not use any adhesive bonding. But when considering typical loading conditions of a structure rather than only the ultimate failure inducing load conditions, fatigue performance of a joint becomes the prime concern. The low stress concentrations induced in adherends, which is inherent of the use of adhesive bonding, benefits the fatigue performance of the joint.

So the overall situation of a mechanical fastening reinforced adhesive joint is that the adhesive joining characteristics protect the structure from negative effects in terms of fatigue and the mechanical reinforcement elements both protect the adhesive bond from being prematurely exposed to failure inducing loading conditions, and when the load conditions exceed this level and failure of the bondline occurs, the fastening elements provide the joint with failsafe residual strength performance.

2.5.2 Need to do this efficiently

In order for a new technology to achieve industrial uptake the efficiency of the manufacturing technique must be considered along with the technological benefit. The traditional method of achieving a mechanically reinforced adhesive joint is a six stage process, as follows:

1. Manufacture metallic part
2. Manufacture composite part
3. Prepare faying surfaces for adhesive bonding
4. Prepare parts for fastener installation
5. Apply adhesive and install fasteners
6. Cure adhesive

Many of the new technologies reviewed here take advantage of composite manufacturing methods to enable installation of mechanical fastening elements before final manufacture of the composite. The processing stages of these new techniques could be listed as follows:

1. Manufacture metallic part
2. Manufacture semi-finished composite part
3. Install mechanical fastening elements
4. Complete manufacture of composite part, which simultaneously forms adhesive bond.

Though this comparison of two manufacturing process is simplistic it illustrates how there is the possibility to reduce the number of manufacturing steps by using novel joining methods. This could save both time and manufacturing costs.

As design methodologies are developed for the novel techniques of achieving mechanically reinforced adhesive joints optimal material use will be identified. Current drawbacks of the isolated use of mechanical fastening and adhesive bonding are that:

- Bondline areas have to be oversized to ensure that stress concentrations are sufficiently limited
- Extra mechanical fasteners have to be installed to accommodate the potential for local fastener position failure

When the two methods of joining are used in conjunction both of the above stated disadvantages can be addressed leading to overall greater structural efficiency; by necessitating a smaller bonded area and installation of fewer fasteners.

2.5.3 Need of finding methods of combining metals and ceramics

As part of this review the concept has been explored of whether a highly effective method of joining composites and metals could be developed by forming a structural joint between the reinforcement fibre of a composite and a metal. This would bypass the polymer matrix of the composite, which is the weakest material when comparing the strength of: reinforcement fibres, polymer matrix, and structural metals. It has been demonstrated in the literature both methods and benefits of active-metal braze joining carbon-carbon composites and metals. This has the potential to be further developed for use in joining metals to polymer composites.

3 SURFACE STRUCTURED METAL AS THROUGH-COMPOSITE-THICKNESS REINFORCEMENT

3.1 Introduction

The ‘metal surface structured through-composite-thickness reinforcement’ joint concept is illustrated in Figure 3-1. This joining concept is fundamentally a mechanically reinforced adhesive joint. The micropins, attached by cold metal transfer welding (CMT), have a sufficiently small diameter such that disruption to the composite reinforcing fibres is significantly reduced when compared with traditional fastening methods (e.g. rivets, bolts). When the micropins are embedded into the composite the joint benefits from through bondline and composite through-thickness reinforcement, by shear loading of metallic surface features at the joining interface.

Realisation of this joining concept is achieved by structuring the bonding interface surface of a 304 stainless steel plate with an array of stainless steel micropins. For the prototype joint specimen a regular array of 35 micropins is welded on both sides of the plate and the plate is embedded into an uncured quasi-isotropic lay-up of M21/T800 prepreg by use of ultrasonic horn, forming a double-lap-shear (DLS) joint. The laminate is then cured in an autoclave, simultaneously forming the adhesive bond as well as the composite laminate.

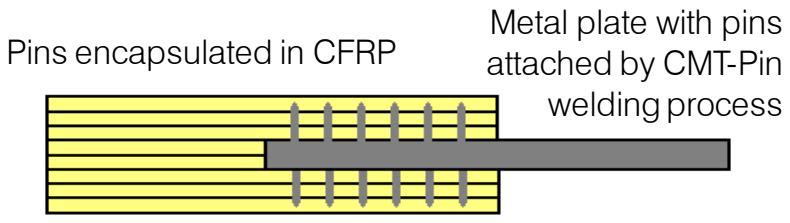

Figure 3-1 - Diagram of the micropin-locking DLS joining concept

A preliminary study of this joining technique was conducted and the results used to aid in the definition of the main study. The preliminary study is reported in Appendix A.

Optical microscopy of sectioned joints is used to understand the interaction between micropins and composite material micro-architecture. The joint specimens manufactured were designed to enable mechanical characterisation of the joining concept. The micropin reinforced adhesive joints are fundamentally double-lap-shear in arrangement, with various metal substrate thicknesses and micropin array patters being investigated, so to understand the effect that both the number of micropins, and their positioning within a bondline, have on joining strength. The joints are characterised by quasi-static mechanical testing using laser extensometry and Digital Image Correlation to measure strain. Partially failed specimens were examined by microsectioning and X-ray Computed Tomography to understand failure mechanisms of the joining concept.

3.2 Methodology

3.2.1 Surface structuring by CMT-Pin welding

The CMT-Pin GMAW derived micro-welding technique is a development of the dip-transfer welding method and was developed by the welding OEM Fronius (Fronius International GmbH, 2009). The materials and consumables used are as required by the optimised process developed by Fronius. The metal substrate used was 304 stainless steel. The surface of the substrate was linished so to remove surface oxidation and any contamination that may have been introduced by the roll manufacturing process of the metal plate. The welding filler metal used was stainless steel 308, and therefore the micropins formed on the surface of the metal plate are stainless steel 308. The shielding gas used in the GMAW process was Corgon 5S2, which is a Linde Gas product, the constituents of which are: 93% argon, 5% carbon dioxide, 2% oxygen.

The CMT-Pin technology allows for active online control of the electric current together with the mechanical feed and retraction of the filler wire. The stages of the of CMT-Pin process stages are as follows: arc ignition, weld pool melting, filler wire to substrate weld, electric current heating of wire, retracting pull of wire, and arc fuse breaking of wire. The process parameters can be set to form various micropin head shapes. In this work a pointed head shape, described by the CMT-Pin process terminology as a ‘pike-head’, was used. Figure 3-2 shows photographs of the CMT-Pin pike forming process.

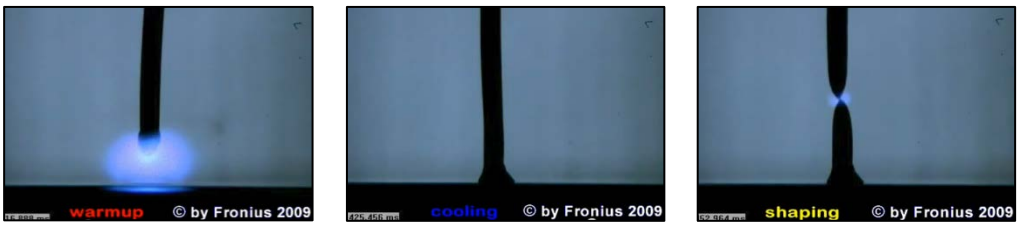

Figure 3-2 – Fronius CMT-Pin pike-head shaped micropin manufacture (Furukawa, 2006)

The pike micropin dimensions are given in Figure 3-3; these are average measured values from a sample size of 10 micropins. In the following work the micropins dimensions will be considered to be 0.8mm diameter and 4.2mm height.

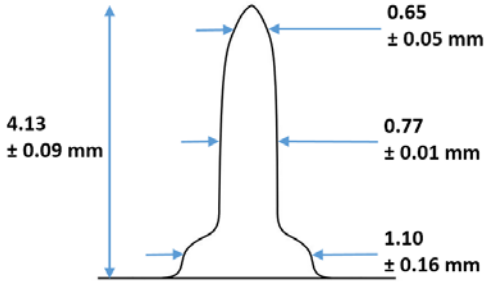

Figure 3-3 - Measured CMT pike-head pin dimensions

In order to form the micropins in the desired pin array patterns a robotic system was used to position the Fronius CMT welding torch in relation to the metal substrate. The micropin formation is achieved entirely by the Fronius CMT Advance welding set, this being the power set and the welding torch, the robotic system is only used to position the welding torch. In this work two robotic systems were used. The choice between which system to use depended simply on equipment availability. The robotic system used had no effect on the micropins or micropins array patterns that were manufactured. The two welding torch positioning systems used were an ABB robotic arm and a Trio Motion three-axis table. These are shown in Figure 3-4.

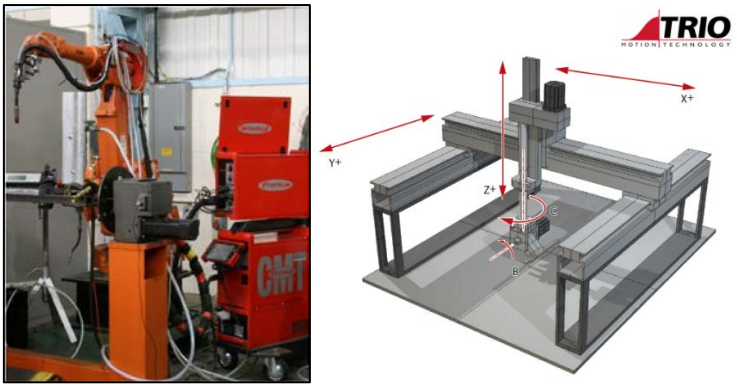

ABB robot Trio Motion

Figure 3-4 - CNC welding torch positioning systems

Figure 3-5 shows examples of micropins arrays that were formed by combined use of the CMT-Pin welding set and the robotic welding torch positioning systems. The micropin array patterns are described in Section 3.2.3.

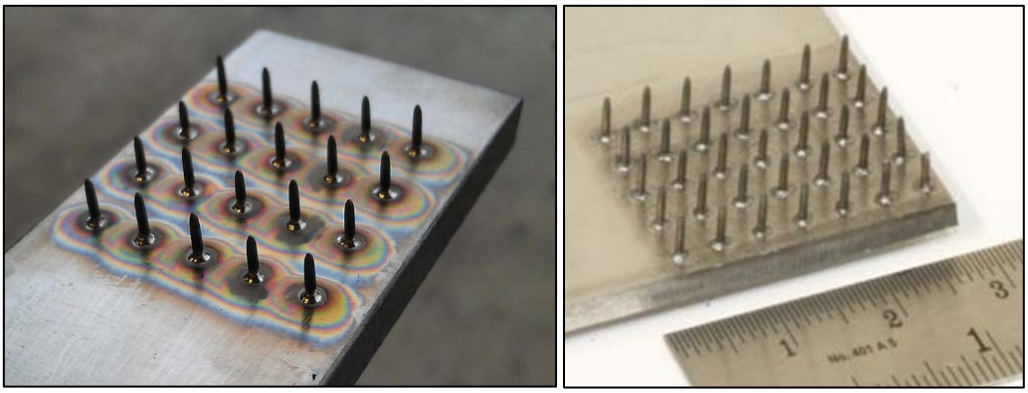

(a) (b)

Figure 3-5 – (a) 5x4 pin-array produced by use of CMT-Pin and Trio Motion three axis table system, showing weld residue and substrate heat-effected zones (b) 5x7 pin-array manufactured by use of CMT-Pin and ABB robot system and cleaned with wire brush for display purposes.

3.2.2 Manufacturing of micropin reinforced composite to metal joint

Following the manufacture of the micropin arrays on to metal substrate they were combined with composite prepreg to form the joint test specimens. The following outlines the joint manufacturing steps.

1. Pin arrays and metal substrate were cleaned to remove welding residue, this was achieved by sand blasting and then submerging in an ultrasonic bath of acetone for 10 minutes.
2. Crack-initiator; 0.17mm thickness PTFE film self-adhesive tape, applied as shown in Figure 3-6. The PTFE tape was applied so to accurately control the dimensions of the faying interface area that would form an adhesive bond. In addition to this the positioning of the tape also controlled where, in relation to the distance between the edge of the

bonded area and the pins, a disbond crack initiated. This ensured that the energy release rate of a crack propagating from the edge of the bondline towards the reinforcement pins was the same for all specimens of each joint type.

3. Laminate CFRP prepreg was prepared for Sections T, M, B, and ply drop-off, as shown in Figure 3-7, with the lay-up as descried in Figure 3-8
4. Pins inserted into CFRP laminate; ultrasonic coupling used to locally soften un-cured thermosetting matrix to allow pins to penetrate laminate, equipment shown in Figure 3-9
5. Thermoset cure cycle in accordance with prepreg manufacture's datasheet (Hexcel Corporation, 2010)

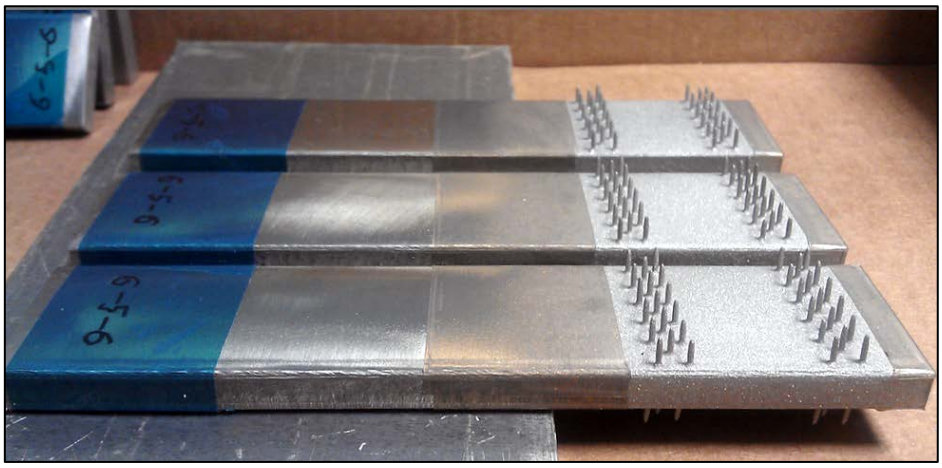

Figure 3-6 – Micropin on substrate metal plates for use in mechanical test specimens, 5-6-5 pin-arrays at bondline edges (runouts), metal interface surfaces prepared by grit blasting and cleaning with acetone in ultrasonic bath, PTFE tape applied as crack initiators at extremities of bonded area.

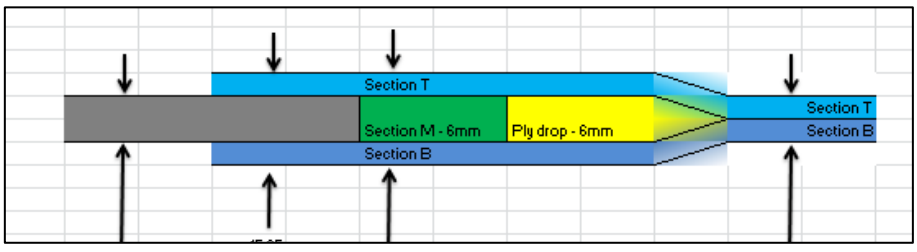

Figure 3-7 – Longitudinal cross-sectional diagram of double-lap-shear joint showing various laminates

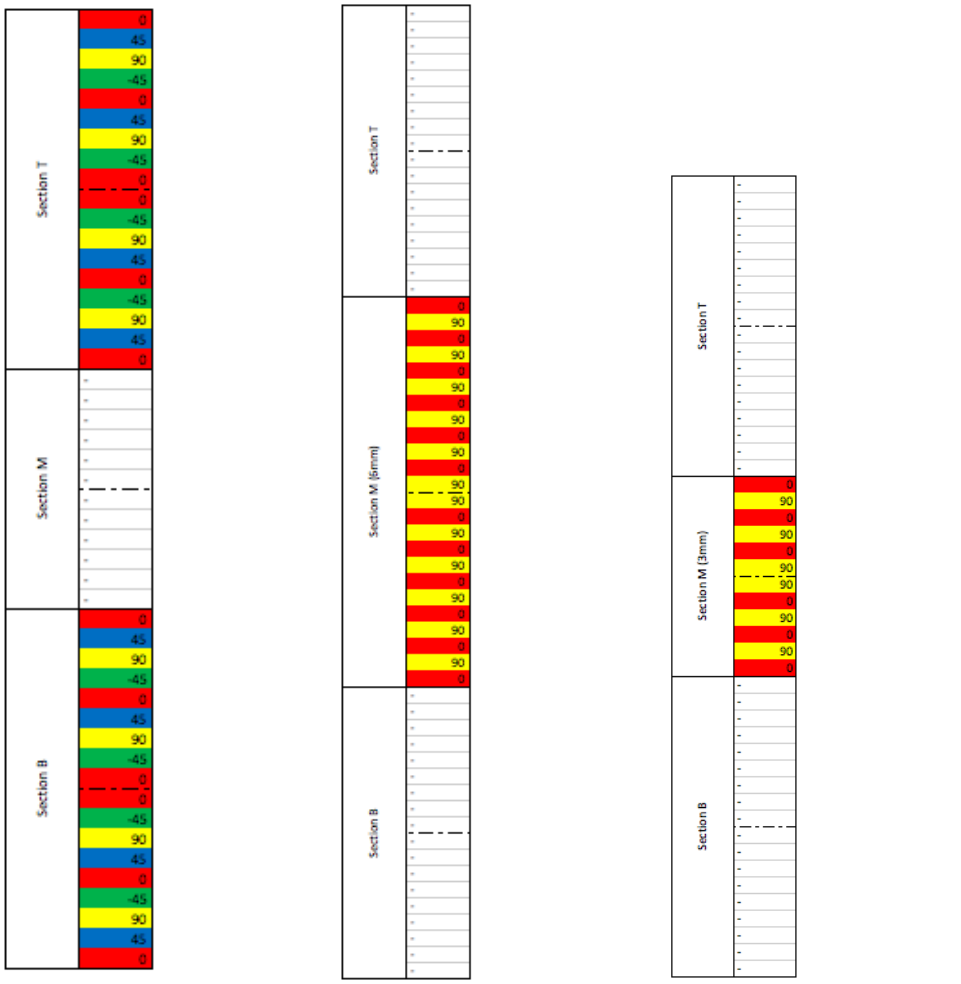

Ply	No. of	% of
0's	12	33.3
90's	8	22.2
+45's	8	22.2
-45's	8	22.2
Tot:	36	100

Ply	No. of	% of
0's	12	50
90's	12	50
+45's	0	0
-45's	0	0
Tot:	24	100

Ply	No. of	% of
0's	6	50
90's	6	50
+45's	0	0
-45's	0	0
Tot:	12	100

Figure 3-8 - Quasi-isotropic laminate lay-up used for sections that have pins inserted, bi-axial laminate lay-up used for 3mm, and 6mm, metal substrate spacing, respectively

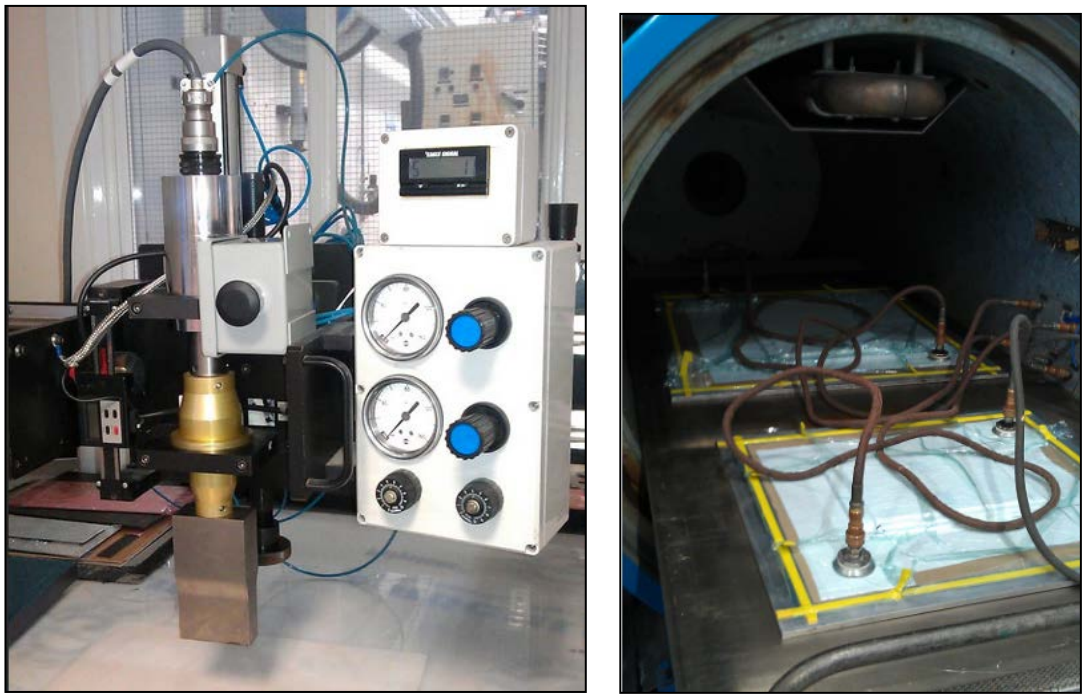

(a) (b)

Figure 3-9 – Photographs of semiautomatic ultrasonic horn (a) and parts being loaded into autoclave for laminate curing (b)

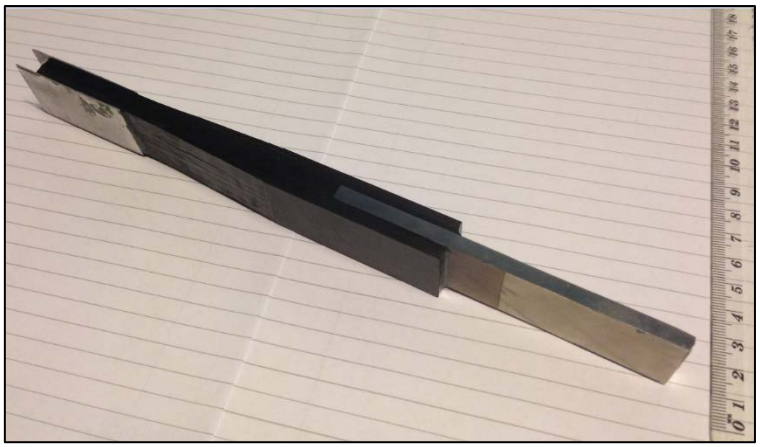

Figure 3-10 – Manufactured mechanical test specimen

3.2.3 Materials and pin-array choice

A preliminary series of mechanical tests were conducted (reported in Appendix A). These were of a DLS joint configuration that had 3mm thick stainless steel 304L with pin arrays on both sides. The pin arrays consisted of 35 micropins in a regular pattern of seven evenly spaced rows with each row consisting of five evenly spaced pins. This was chosen so to be comparable with previous work (Ucsnik et al., 2010). The results of these preliminary mechanical tests were used by a project colleague, Francesco Bianchi, to calibrate a Finite Element Model (FEM) simulation of the joint.

The calibrated FEM was used to conduct a sensitivity study of various geometric parameters. The joint geometries that were varied are as follows: metal adhered thickness, number of micropins, and pin array patterns. The full details of this study are reported in Francesco Bianchi's PhD thesis (Bianchi, 2012). The results of the principle outputs of the FEM study, with respect to choosing key joint configurations that should be mechanically tested, are presented in the following.

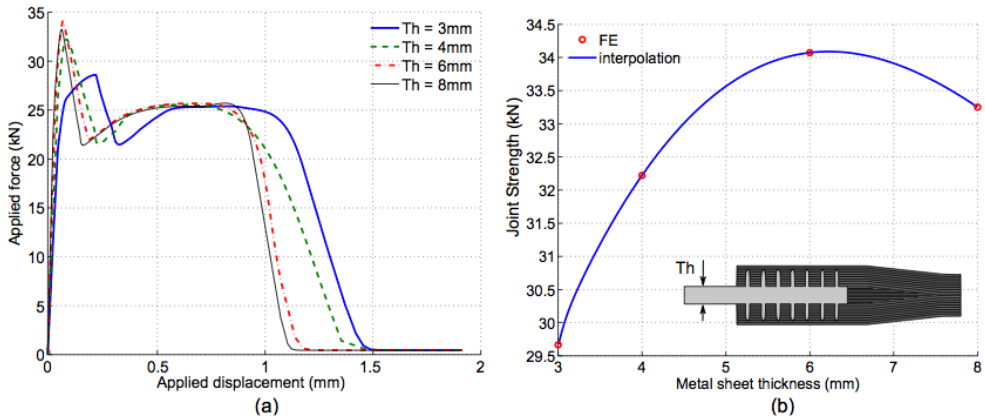

Figure 3-11 - Results of Francesco Bianchi's sensitivity study of metal substrate thickness; 'Effect of the metal substrate thickness on the joint performance: (a) structural response of different thickness joints, (b) strength of the joint – spline interpolation of FE results' (Bianchi, 2012)

The parametric FEM study showed that a maximum strength is predicted when the substrate thickness is 6mm, this peak in load is expected (Kinlock, 1987); the metal substrate stiffness increases as thickness increase, which drives an increase in bondline strength due to reduced metal substrate deformation. However, as the thickness increases the load centroids of the lap-shear planes are further offset from one another, this offset of relative load planes induces a bending moment and associated peel stresses at the laminate edge of the DLS joint. As the magnitude of the induced bending moment increases with increased adherend thickness, it offsets the joint strength increase, which results from increase adherend thickness. Eventually the strength reducing effect of the induced bending moment becomes dominant and the joint strength decreases overall.

The thickness of the composite laminate adherend cannot be reduced, as a minimum thickness of 4.2mm is required in order to fully encapsulate the pins. The 4.5mm laminate adherends used have a stiffness that is an order of magnitude greater than the 6mm thick metal adherend. There is an argument that ideally the stiffness of the composite and metal adherends should be matched in order to maximise adhesive joint performance. However, the thickness required of a stainless steel 304 adherend required to achieve this would have been unfeasible.

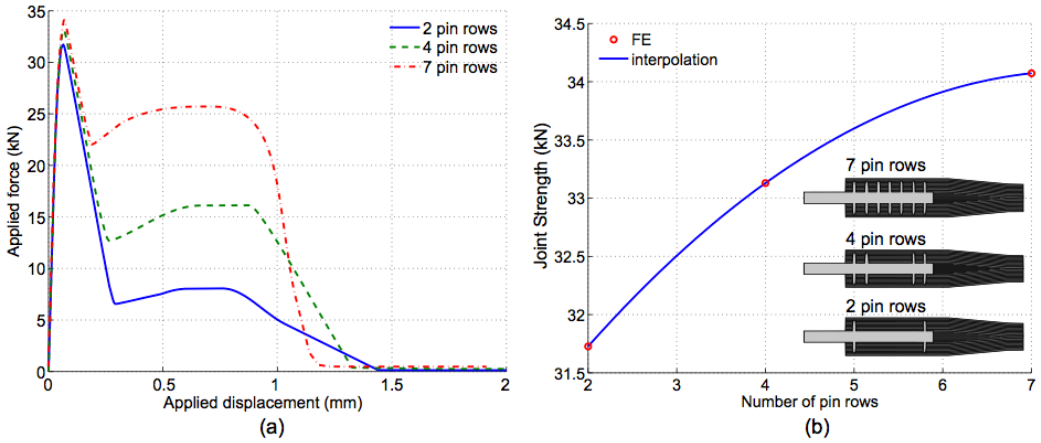

Figure 3-12 - Results of Francesco Bianchi's sensitivity study of number of pin rows; 'Effect of pin row number on the performance of the DLJ: (a) structural response of the joints having different pin row numbers, (b) strength of the joint – spline interpolation of FE results.' (Bianchi, 2012).

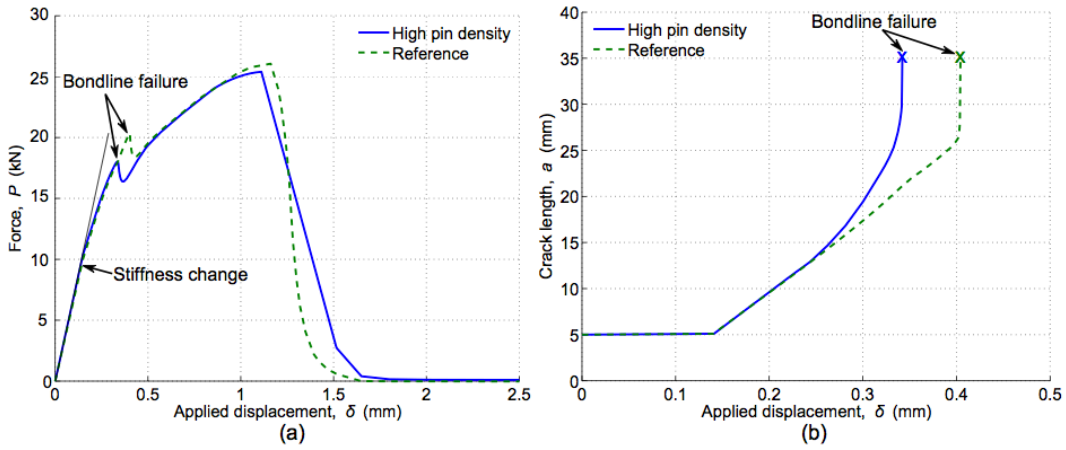

Figure 3-13 - Results of Francesco Bianchi's sensitivity study of arrangement of pin-array pattern; 'Comparison between calculated high pin-density and homogeneous pin arrangement: (a) force vs. applied displacement, (b) Calculated crack extension from its initial size of 5mm vs applied displacement' (Bianchi, 2012)

From Figure 3-12 it is predicted that increasing the number of pins will increases both the maximum load and the residue strength of the joint. It is therefore indicated that in order to increase the strength of the joint, from that

achieved in the preliminary study, the number of pins should be increased. However, for a regular array it is seen from the micrograph in Figure 3-23 that the resin filled eyelets, which are a result of fibre separation during pin insertion, verge on contacting one another with the pin spacing that is used in the 5x7 regular pin array. This minimum distance between pins of the 5x7 regular pin array is 3.75mm.

The effect on increasing the number of pins would therefore result in the minimum separation being reduced, and increase the likelihood of resin rich eyelets merging into one another. This was considered as something to be avoided. A solution to increasing the number of pins is to use a quincunx pin pattern, rather than a regular pattern. A quincunx pattern is formed by adding additional pins diagonally in-between a regular array. The quincunx pattern is described in this work as the '6-5-6 pin array' and is shown in Figure 3-14 and Figure 3-6. In the FEM study the regular pin array was termed 'homogeneous' and the quincunx pattern pin array was termed 'high pin-density'.

It was unexpected that the FEM sensitivity study showed concentrating pins at the edges of the bondline (the edges in the loading direction) had negligible effect in increasing load-carrying capability of the joint. It was expected that the strength should increase due to the increase of reinforcement elements in the region of the bondline subjected to induced peel loads.

Pin arrays chosen, as illustrated in Figure 3-14:

- Reference sample with no pins; to measure the baseline adhesive bond strength between the metal substrate and the composite
- 5x7 regular array; as is directly comparable with previous experimental results
- 6-5-6 quincunx array at bondline edges; uses very similar total number of pins as the 5x7 array while not reducing the pin separation distance from that used in the 5x7 regular array. This

pin arrangement was chosen to confirm the result shown in the FEM study (that pin arrangement is unimportant to joint strength).

- 5x4 regular array; to confirm the joint strength decreases with reduction in total number of pins

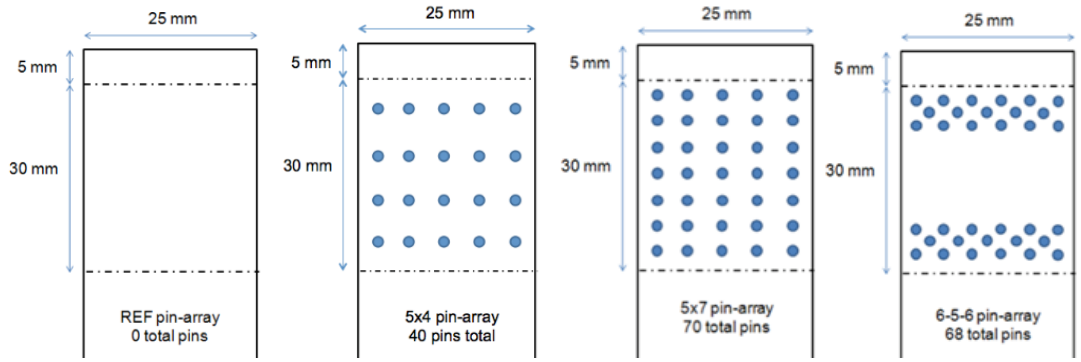

Figure 3-14 – Diagram of pin-array patterns used in the experimental study

The laminate lay-up chosen for use in this study was a near quasi-isotactic (QI) laminate lay-up with greater than 40% of the ply orientation in the +/- 45° direction was chosen to ensure reasonable bearing strength of the composite laminate around the pins (Niu, 1992). As pins of the same height are used throughout this study the same thickness and lay-up stacking sequence was used for all test specimens, so to ensure laminate of the same strength and stiffness was used throughout all test specimens. The same laminate was also used in the reference (without pins) baseline test specimens. Figure 3-8 shows the lay-up stacking sequence used. The 0° ply direction is orientated to be in the direction of DLS joint loading. The laminate design has both a slight bias towards quantity of 0° plys, and the stacking sequence is also arranged so that 0° plys are present at the bonding interface, so to maximise the strength of the adhesive joint (Matthews and Tester, 1985).

3.3 Mechanical testing

3.3.1 Double-lap-shear joint arrangement

A Double-Lap-Shear (DLS) test arrangement was used to minimise peel inducing bending moments on the joining interface, so to enable clear evaluation of the pin reinforced adhesive bond in near complete shear conditions, and which so enable the load carrying capability of the joining concept to be maximised. The pin reinforced DLS adhesive joint is shown diagrammatically in Figure 3-15.

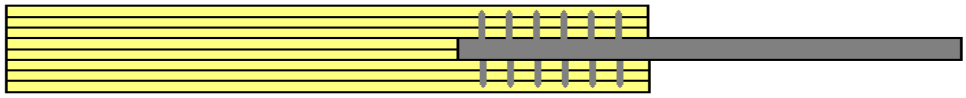

Figure 3-15 - Diagram of longitudinal cross-section through tensile Double-Lap-Shear (DLS) pin-reinforced adhesive joint test specimen

The test specimens were prepared by adhesive bonding aluminium tabs to the composite laminate in the areas that were to be clamped in the testing machine, as can be seen in Figure 3-10. This was to prevent local damage of the laminate at the clamping interface, which could course the sample to slip in the grips. Laser extensometer reflective strips were applied at the boundaries of the joint interface, as described in Figure 3-17. Mechanical testing was performed using an Instron 5500 testing machine, operating with a 100kN load cell, at a cross-head displacement speed of 1mm/min.

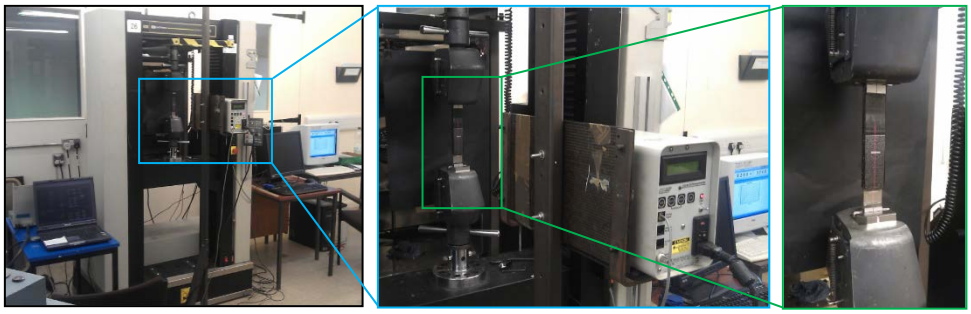

Figure 3-16 - Mechanical test equipment arrangement, using laser extensometer

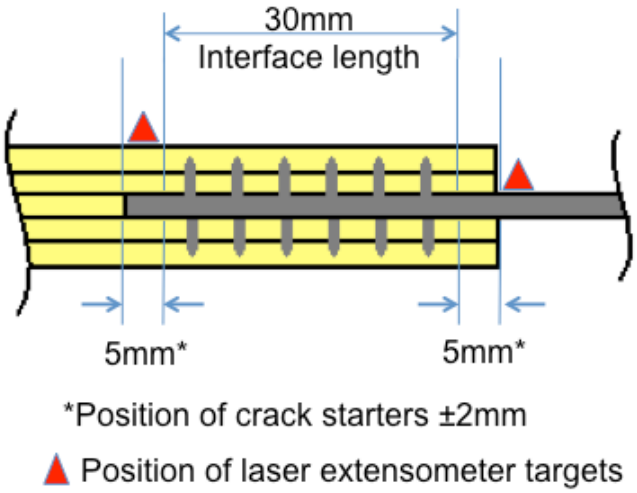

Figure 3-17 - Diagram showing details of the cross-section of the joint interface along the length of tensile DLS pin-reinforced adhesive joint test specimen, with the positions of the laser extensometer reflective targets

3.3.2 Visual Strain Development

Visible strain development of DLS test specimens were observed, and strain measured while undergoing tensile testing, by use of Dantec Dynamics Q-400 Digital Image Correlation (DIC) system and ISTRA 4D software. The side, edge-on, aspect of the sample was observed, as shown in Figure 3-18 below. Viewing this aspect of the samples enabled strain development to be seen simultaneously in both the composite and metal parts of the joint, and crucially also the interface between the two joined materials.

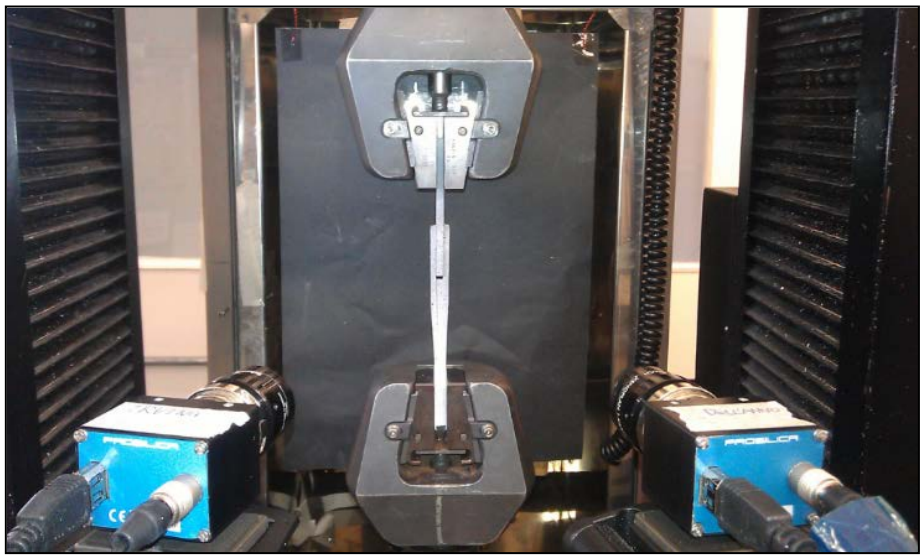

Figure 3-18 – Equipment arrangement for Digital Image Correlation mechanical testing

Special preparation of specimens is required for DIC testing. The DIC test method uses a twin camera arrangement to view surface strain response of a specimen under mechanical test. Requirements of the observed surface are that it is flat, being without noticeable roughness or steps. DIC works by comparing sequential images of a greyscale speckled pattern, therefore a

suitable pattern has to be painted onto the surface that is to be observed, shown in Figure 3-19 is an example of the required greyscale speckled pattern. The patterning is achieved by use of alternating between applications of white and black paint delivered by a spluttered spray achieved by use of a low paint to propellant ratio.

Figure 3-19 - Example of the speckled pattern required for Digital Image Correlation technique of surface strain visualisation

3.4 Metallographic inspection

3.4.1 Pin-fibre interactions

One postulation of this through-thickness joining concept is that when compared to post-cure joining by mechanical fasteners there is comparatively less damage caused to the composite laminate. Sample joints were sectioned and polished by a specific method for exposing details of the composite laminate.

The microsectioning procedure used was a three stage process: trimming and mounting of specimen in epoxy potting resin, followed by rough cutting and coarse grinding to specimen section of interest, and finally fine grinding and polishing of section for microscopy.

Specimens were first trimmed to a sufficiently small size for mounting using a water cooled metallography cut-off saw. The trimmed samples were then encapsulated in either 30mm or 40mm diameter pots, depending on samples size, using an epoxy mounting resin. Once the mounting resin was cured the samples were again trimmed, by the same cut-off saw method, close to the section of interest. Mounted samples were first coarsely ground to accurately reach the section of interest. This coarse grinding was done using a Buehler Metaserv motopol operating in counter-rotation mode and using water lubricated P240 silicon carbide grit paper. All motopol grinding was done at a speed of between 100 and 150rpm and with a pneumatic pressing force of 5lb per specimen being processed.

Once the specimen section of interest was reached the specimen surface was finely ground for 1 to 2 minutes, with the motopol operating in complimentary-rotating mode, using water lubricated P1200 silicon carbide grit paper. This was followed by sample polishing procedures. The same motopol was used, in complimentary-rotating mode, with an increased speed of between 150 and 200rpm and the same pneumatic press force of 5lb per specimen was used for all polishing stages. The first polishing stage was to use a 2µm diamond suspension together with lubricant fluid on a waffle polishing disc for between 2 and 4 minutes. The second polishing stage was to use 0.05µm Linde Alfa alumina suspension in deionised water on a felt polishing disc for between 1 and 2 minutes. The final polishing stage was to use colloidal silica on a damp flock polishing disc, at a reduced speed of 75rpm, for up to 1 minute.

Specimens were then rinsed with water, followed by acetone, and dried under heated blown air before examination using a Nikon Optiphot-66 microscope with a microscope mounted Qimaging Go-3-CLR-10 digital camera and Syncroscopy AcQuis image acquisition software.

The first section of interest was thought the centre of a line of pins along the composite 0º-axis, as illustrated in Figure 3-20 below. The micrographs of this section are shown in Figure 3-21.

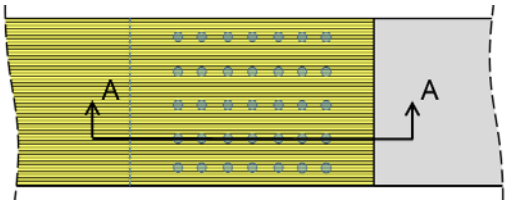

Figure 3-20 – Illustration showing target section of interest, Section A-A, for micrograph shown in Figure 3-21

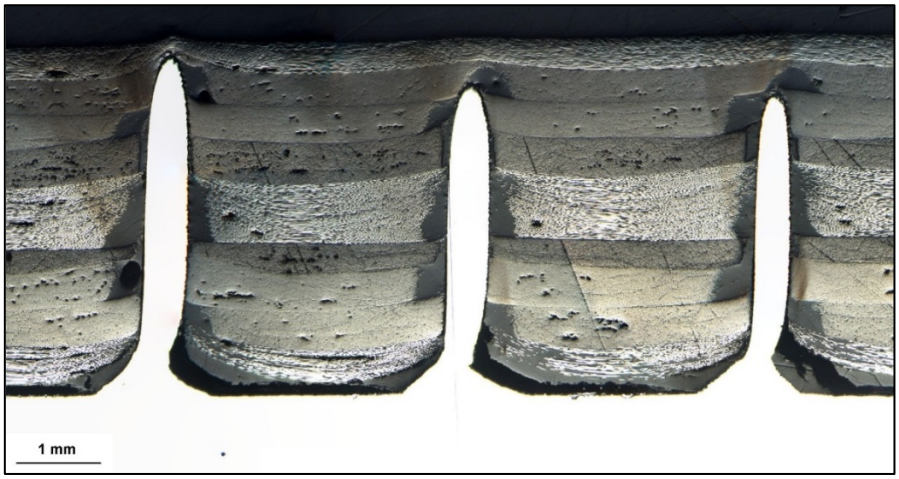

(a)

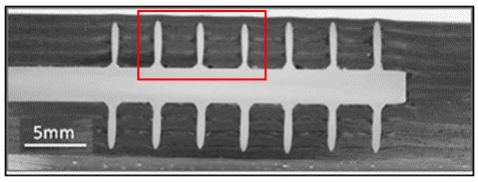

(b)

Figure 3-21 – Optical micrograph showing detail of effect on composite laminate as a result of pin z-direction insertion (a), the sample here has undergone mechanical testing, so allowing observation of mechanical failure. (b) shows the location of the detail view of (a)

A second section of interest was taken though another specimen to understand the nature of the dark zones seen adjacent to pins in Figure 3-21. These microsections were produced using the same grinding and polishing procedure. An illustration of the location of this second section can be seen in Figure 3-22.

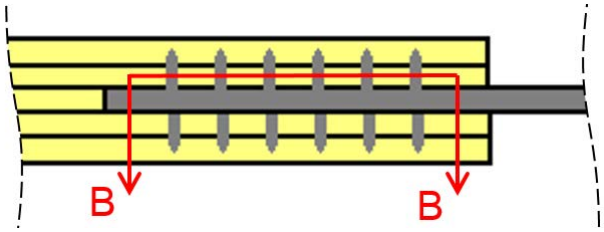

Figure 3-22 – Illustration showing target section of interest, Section B-B, for micrograph shown in Figure 3-23

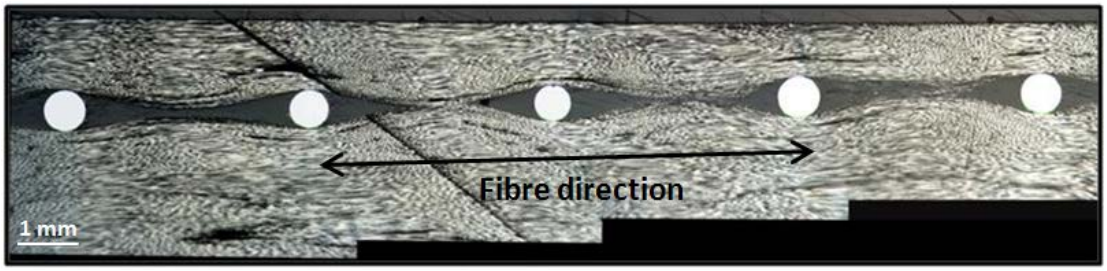

Figure 3-23 – Resin-rich-eyelet merging seen in some cases with a pin separation of 4.3mm (distance between pin centres, 0.8mm diameter pins).

3.4.2 Failure mechanisms

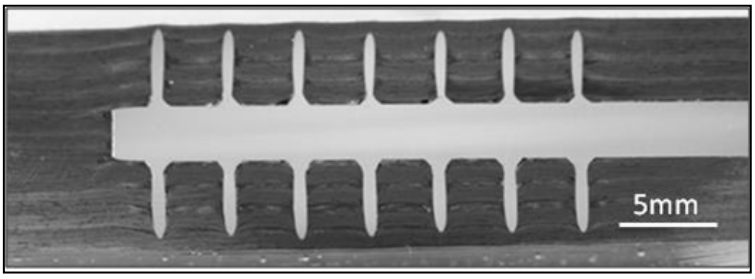

Figure 3-24 – Optical micrograph of sectioned metal surface structured though-composite-thickness reinforcement joint, subjected to approximately 30% of ultimate joint strain

A series of preliminary joint tests (Appendix A), which used the regular 5x7 pin arrays on 3mm substrate showed a sudden, but not complete, failure at approximately 30% of the maximum joint strain maximum joint strain being the strain observed at joint complete failure). The optical microsection along a line of pins in the joint loading direction, shown in Figure 3-24, is of a test specimen that was partially tested up to approximately 30% of expected maximum joint strain; the mechanical test was halted immediately after the sudden but not complete failure, as described above. It can be seen from Figure 3-24 that all pins are connected to the substrate. Therefore the failure at approximately 30% of maximum joint strain is attributed to failure of the adhesive bondline.

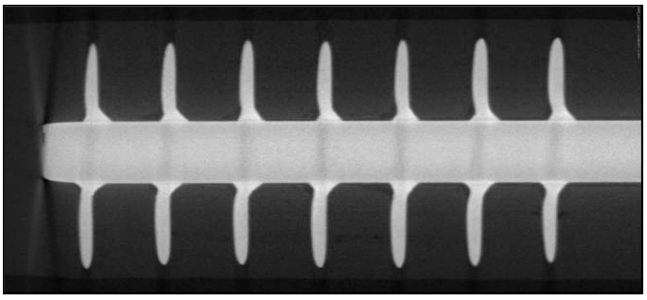

Figure 3-25 – Image produced by x-ray computed tomography of approximately 60% of ultimate joint strain partial test; the metal substrate thickness is 3mm.

Figure 3-25 shows an image that was produced by use of x-ray computed tomography (CT), courtesy of Nikon Metrology UK Ltd. Due to the differences in electromagnetic attenuation of the dissimilar materials of this joint; the x-ray CT equipment has to be calibrated for the material of interest, which results in fine details of all the materials present not being observable. The equipment was tuned to produce detailed images of the metallic component of the joint; therefore details of the carbon fibre and epoxy matrix of the composite cannot be seen. This choice was made as the subject of interest of this examination was the failed state of the metallic component, particularly the pins, as it was known from previous optical microscopy that at the strain levels this joint was subjected to the adhesive bond would have already failed, and therefore the residual load of the joint is being carried by the pins.

Ghosting effects are present in the image shown in Figure 3-25, these effects are due to geometric features of the joint partially obscuring the x-ray propagation through the parts, and so casting shadows artefacts in the reconstructed image.

The test specimen shown in Figure 3-25 was partially tested to a strain that is approximately 60% of the joint maximum strain. It can be clearly seen that the pins have deformed but have not completely failed; no pins have detached. Furthermore, by considering the shape of the deformed pins it can be said that locally the pins are being loaded in a combination of shear and tension, this is illustrated in Figure 3-26.

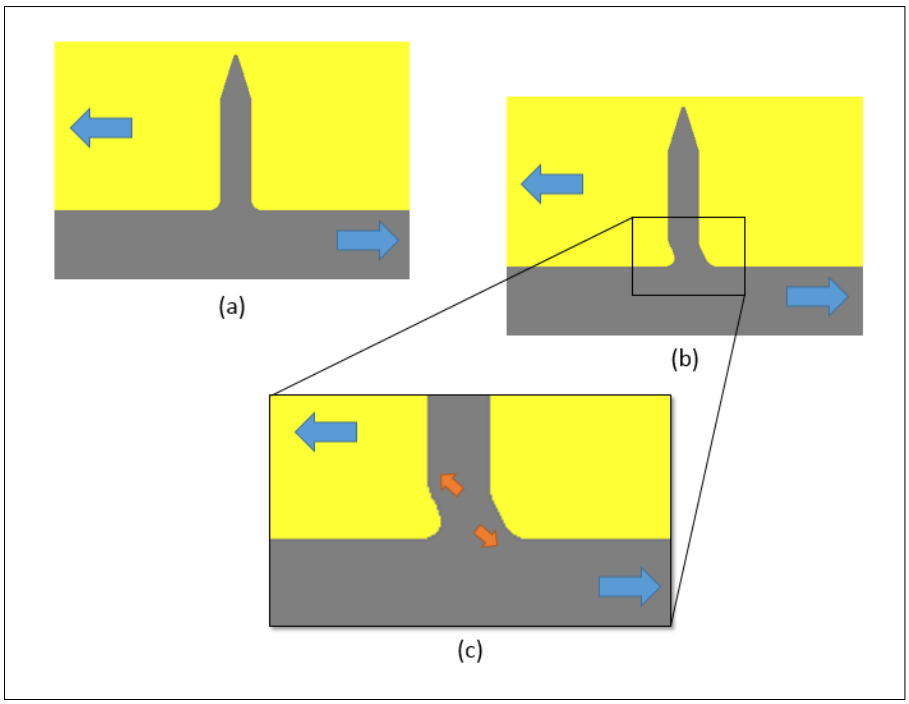

Figure 3-26 - Diagram describing the mixed loading state of deformed micropins, the base of the micropin is loaded in shear (a), local deformation occurs at the base of the micropin (b), loading conditions in the micropin is effected by shape deformation (c).

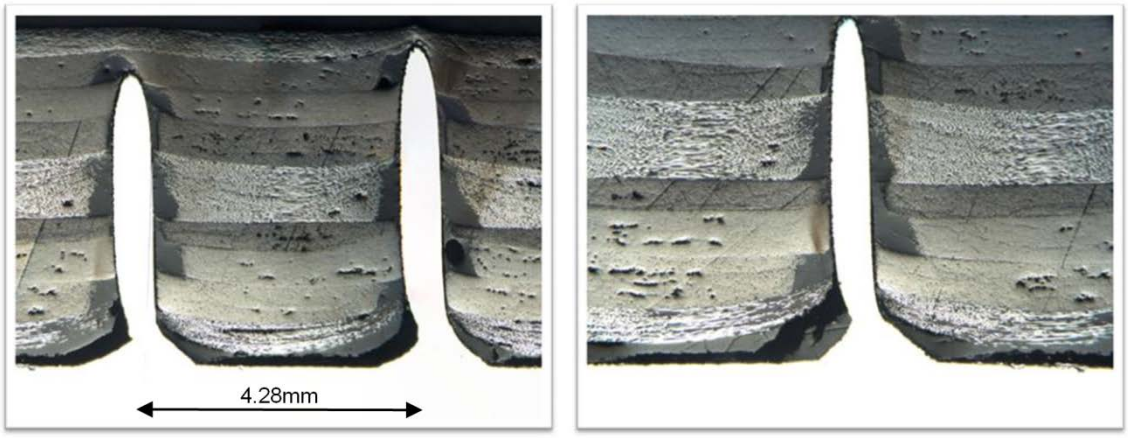

(a) **(b)**

Figure 3-27 – (a) showing adhesive failure (b) showing cohesive failure in a resin rich zone at the base of the pin, partial failure test subject to near ultimate strain.

Figure 3-27 shows optical microsections of a mechanical test specimen that was loaded to a joint strain that was greater than 60% of the expected maximum joint strain, and so very close to absolute failure. These images confirm that at this strain level the bondline has completely failed and separation has occurred between the laminate and metal substrate. The pins have not completely failed and are therefore providing residual strength to the joint.

3.5 Results and Discussion

3.5.1 Strength estimation of joining method

In a typical adhesive joint the strength of several constituent elements have to be considered. These are the strength of the parts being joined, which are referred to as the adherends, and the strength of the adhesive bond itself. There are several ways in which an adhesive bond can fail, for example either adhesively or cohesively. In this pin reinforced adhesive joint there are additional joint constituent elements compared to a simple adhesive only joint.

A list of all these elements are as follows:

- Metal substrate, stainless steel 304
- Adhesive bond, M21 resin system
- Micropin array, stainless steel 308
- Composite substrate, M21 T800 prepreg

In this section the various constituent elements of the joint are assessed individually and an estimation of the strength of each element made. The comparison of the strength of the various elements gives insight into how the joint behaves during mechanical testing, and so aid in understanding the measured results and the observed failure characteristics. This simplified calculation study can only be used as a guide as no element within the joining system is loaded independently, there are interaction between the various elements; some elements cannot be fully loaded until other elements have failed, and this transfer of loading happens progressively, one element is gradually loaded as another element gradually fails. Figure 3-28 describes the various elements in the joining system.

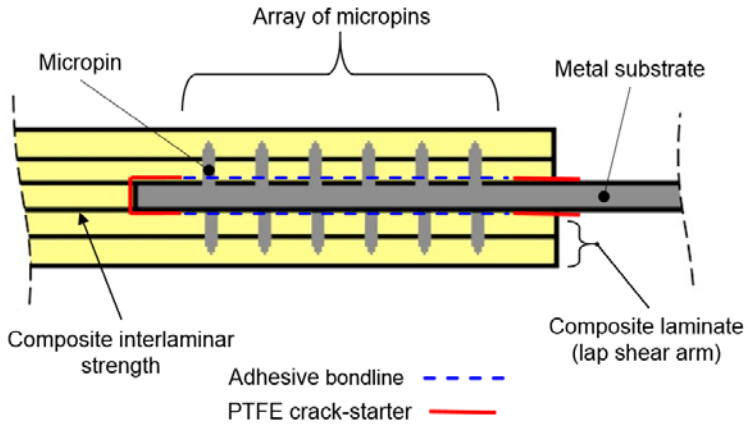

Figure 3-28 – Illustration of joining system elements

The properties of the materials used in the joining system are provided in Table 3-1 for reference.

Material	Yield	Ultimate
Stainless steel, 304L	210 MPa	564 MPa
Stainless steel, 308	Note[1]	Note[1]
Carbon fibre, T800	NA[3]	5880 MPa
Epoxy adhesive bond[2], M21 with 3mm metal adhered	NA[3]	19.7 MPa
Epoxy adhesive bond[2], M21 with 6mm metal adhered	NA[3]	27.2 MPa

[1] In this work the strength of stainless steel 308 is estimated to be equivalent to that of 304; however this will not be true, due to the use of a welding process the material properties will be affected from those of the as-received 308
[2] The values of the composite to metal adhesive bond shear strength was measured experimentally by testing reference sample with no pins; as described in Section 3.2.3
[3] These materials are brittle and so show negligible ductile yield characteristics

Table 3-1 – Properties of the materials used in the pin-reinforced joint

The strength of the specific elements in the joining system have been calculated using the material properties stated in Table 3-1 and the geometries described in Figure 3-3 and Figure 3-14.

	Yield strength / kN			Ultimate strength / kN		
	Bending	Shear	Tension	Bending	Shear	Tension
Single Pin	0.003	0.061	0.106	NA	0.213	0.283
Pin row (10 pins)	0.034	0.610	1.06	NA	2.13	2.83
Pin array (70 pins)	0.236	4.29	7.39	NA	14.9	19.8
Pin array (40 pins)	0.135	2.45	4.22	NA	8.50	11.3
3 x 25mm metal substrate	NA[1]	NA[1]	15.8	NA[1]	NA[1]	42.3
6 x 25mm metal substrate	NA[1]	NA[1]	31.5	NA[1]	NA[1]	84.6
Adhesive; DLS with 3mm metal	NA	TBD[3]	NA	NA	29.6[3]	NA
Adhesive; DLS with 6mm metal	NA	NA	NA	NA	40.8[3]	NA
Composite T, and B, laminate	NA[1]	NA[2]	NA[2]	NA[1]	NA[1]	169

[1] DLS configuration used to eliminate bending of substrate
[2] CFRP materials do not exhibit yield behaviour
[3] This value was measured experimentally in the reference sample tests

Table 3-2 – Strength of the various joining elements in the 'surface structured though-composite-thickness reinforcement' joint concept

3.5.2 Calculation of induced peel stresses

The maximum joint strength of an adhesive joint does not reach the magnitude of the shear strength of an adhesive due to joint geometry inducing out of plane peel loads at the joint edges. Double lap shear (DLS) adhesive joints have an advantage over single lap shear (SLS) joints due to the characteristic that the geometry of the joint induces smaller peel loads. Induced peel loads are not completely eliminated in a DLS joint. The induced peel stress, resulting from the applied sheer stress, of a DLS adhesive joint can be calculated using

Equation 1 (Hart-Smith, 1973, 1983). Table 3-3 describes the nomenclature of the equation, and quotes values that are obtained from the 6mm metal adherend reference joint specimen, as provided in Figure 3-28.

$$\sigma_z \cong \tau\left(\frac{3E_z'(1-\upsilon^2)t}{E_x\eta}\right)^{\frac{1}{4}}$$

Equation 1 - Induced peel stress of DLS adhesive joint

Symbol	Description	Value
σ_z	Induced peel stress in DLS adhesive joint	Calculated
τ	Adhesive shear stress [1]	27.2 MPa
E_x	Young's modulus of adherend [2]	193 GPa
E'_z	Young's modulus of adhesive in peel direction [3]	23 GPa
ν	Poisson's ratio [2]	0.29
t	Thickness of adherend	6 mm
η	Thickness of adhesive layer	0.127 mm

[1] measured maximum in 6mm metal adherend reference DLS tests
[2] Value for 304 stainless steel (MatWeb, 2015)
[3] Value of M21 epoxy tension modulus (Hexcel Corporation, 2010)

Table 3-3 - Nomenclature and values used in Equation 1 to estimate critical peel stress of DLS joint

The calculation estimates the induced peel stress, as a result of the load at which the reference adhesive joint fails, to be 54.0 MPa. The tensile strength of the adhesive bond was not measured in this study. However, the calculated peel stress is almost twice the measured adhesive shear strength (27.2 MPa) and it is unlikely that the tensile strength of the adhesive bond will be twice the shear strength. The yield strength of the pins (210 MPa) is significantly greater than the calculated induced peel stress. Although, geometry of the various elements in the joint will introduce stress intensifying effects, and so these values provided here can only be considered as indicative.

3.5.3 Load-strain response of joints

This section presents the results of mechanical testing of the various joint configurations that are described in Section 3.2.3. A minimum of five specimens of each joint configuration were tested. The columns displayed in the charts of: Figure 3-29, Figure 3-30, Figure 3-31, and Figure 3-32 show the mean average of all specimens measured, and the error bars show the full range of results.

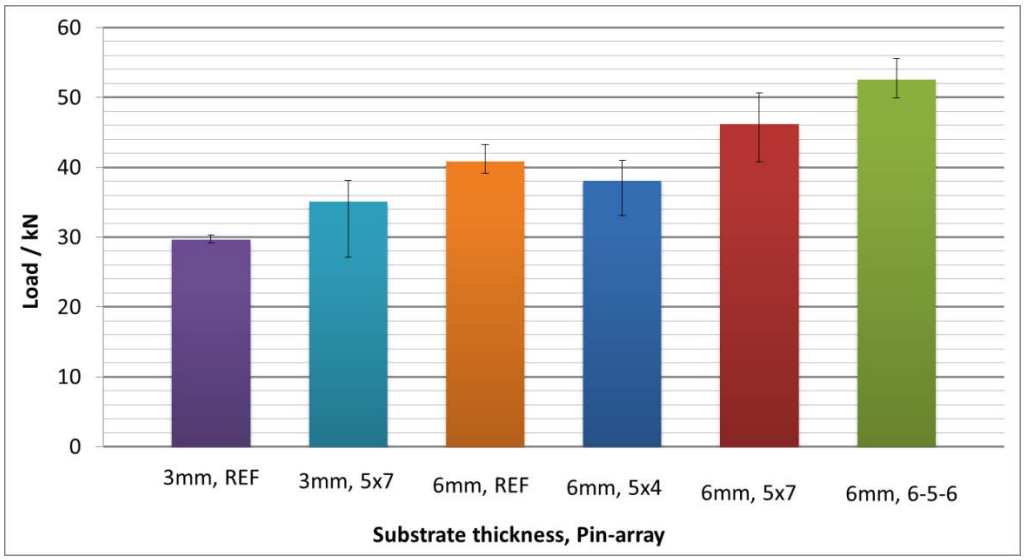

Figure 3-29 – Maximum load for all joint configurations

For the 3mm metal substrate joints, it is not clear that by reinforcing an adhesive joint with micropins results in an improvement of the joint strength; the average maximum strength of the pin-reinforced specimens is higher than the reference adhesive-only specimens, however the range of the pin-reinforced results encompasses the range of the adhesive-only samples.

For the 6mm metal substrate joints, it can be seen that in some cases the use of pins at the interface joint can result in a decrease of maximum joint strength. There appears to be a critical number of pins required before maximum joint strength recovers to the levels of the reference adhesive-only specimens. From the results presented here this would be between 40 and 70 pins required in a regular pin array arrangement.

For the 6mm metal substrate joints a clear improvement in maximum joint strength can be seen when pins are concentrated at run-outs of the bondlines. Even without an increase in total number of pins, compared to arrangement of pins in a regular array. This demonstrates the importance the arrangement pattern of joint reinforcement pins has on the resulting strength of the joint. Therefore it can be said that the loading condition, which the pins are most effective at reacting, occurs at the bondline runouts. This loading case is the secondary induced out-of-plane peel-loads that were discussed in Section 3.5.2.

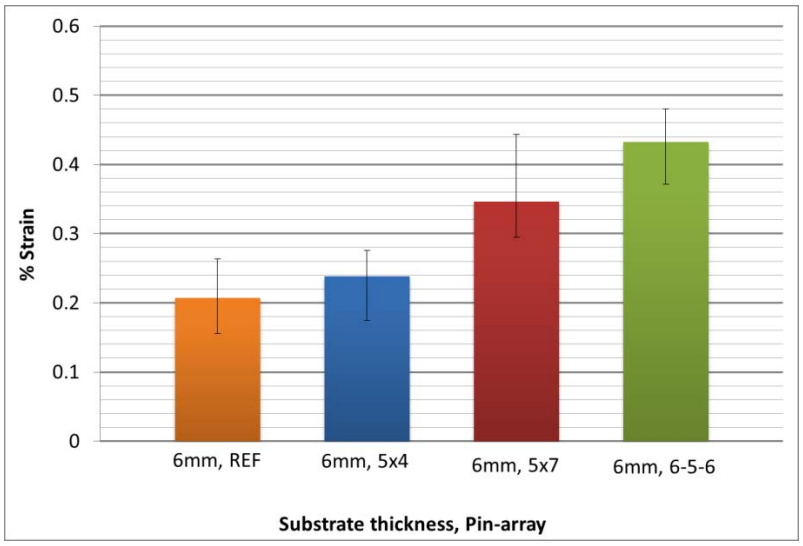

Figure 3-30 – Joint strain at maximum load for joint configurations with 6mm thick metal substrate

For the maximum joint strain of the samples that use 6mm metal substrate, Figure 3-30, it can be seen that the strain at failure is similar for the reference (adhesive-only) joint specimens and the 5x4 regular array pin-reinforced specimens. As the number of pins in the regular array increases, demonstrated by the 5x7 regular array specimens, there is an increase in strain at joint failure. There is a further increase when the pins are concentrated at bondline runouts as opposed to the regular array; as shown by the 6-5-6 specimens. Use of reinforcement pins results in a pseudo-ductile joint failure behaviour, which is a result of a combination of the structural reactions of the various element of the

joint. The pseudo-ductility is a combination effect of elastic deformation and local plastic yielding of the metal substrate and pins, and progressive failure of the bondline, which progressively exposes regions of the joint to loading while relieving other regions.

Use of reinforcement pins results in a joint failure behaviour that has an appearance of ductility. This is a combinative effect of the various deformations, which are both elastic and plastic, and also the discrete failures within the joining system that have been identified by metallographic inspection and are reported in Section 3.4.

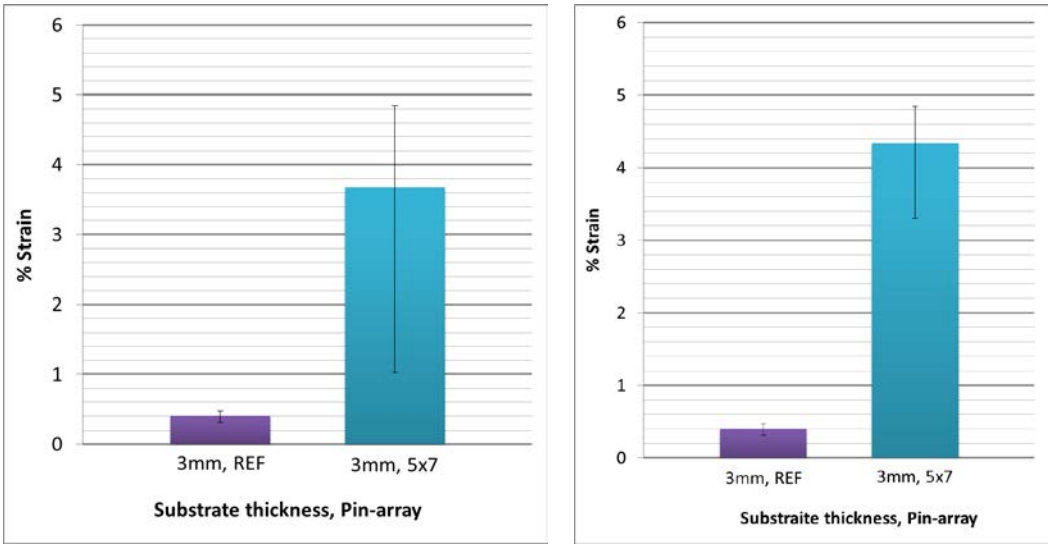

(a) (b)

Figure 3-31 – Joint strain at maximum load for joint configurations with 3mm thick metal substrate: all results (a), possible outlier omitted (b); see Figure 3-33.

When comparing the maximum joint strain, i.e. the strain at ultimate failure, for the joint specimens that use 3mm substrate, as shown in Figure 3-31, there is a comparatively large increase in joint strain, and also a large range of results, seen for the pin-reinforced joints compared with the reference adhesive-only specimens. The reason for this is best described when considering load-strain response of the joints, as seen later in the section in Figure 3-33, the joint is sufficiently strong to permit plastic deformation of the 3mm metal substrate.

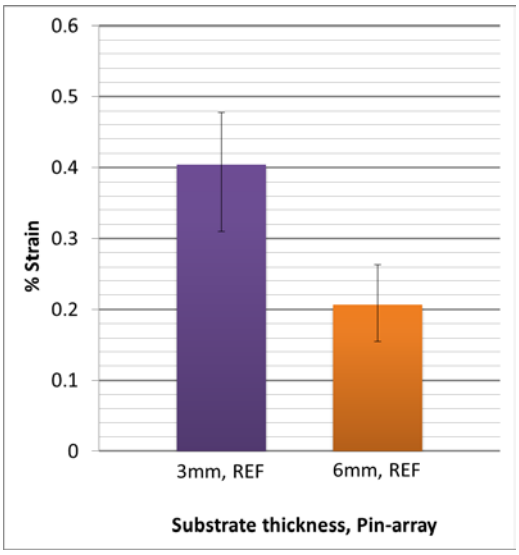

Figure 3-32 – Strain at maximum load for reference, adhesive only, samples

Figure 3-32 shows that the maximum joint strain; the strain at ultimate failure, of the reference joint (adhesive bond only) for the 3mm metal substrate joint is greater than that of the reference joint for the 6mm metal substrate.

The predicted yield load of the 3mm substrate in isolation is 15.8kN, and for the 6mm substrate is 31.5kN, as stated in Table 3-2.

The average adhesive-only reference joint strength of the 3mm metal substrate joint is 29.6kN, and for the 6mm substrate is 40.8kN.

Disproportionally greater strains are seen when the strength of the joint is sufficient for the metal substrates to be loaded beyond their yield point, compared to when the metal substrates are only deforming elastically, due to the reduced tangent modulus associated with yielding behaviour.

The combination of increasing maximum load and increasing maximum strain increases the area under the graph, which is representative of an increase in the energy absorbed as the joint fails.

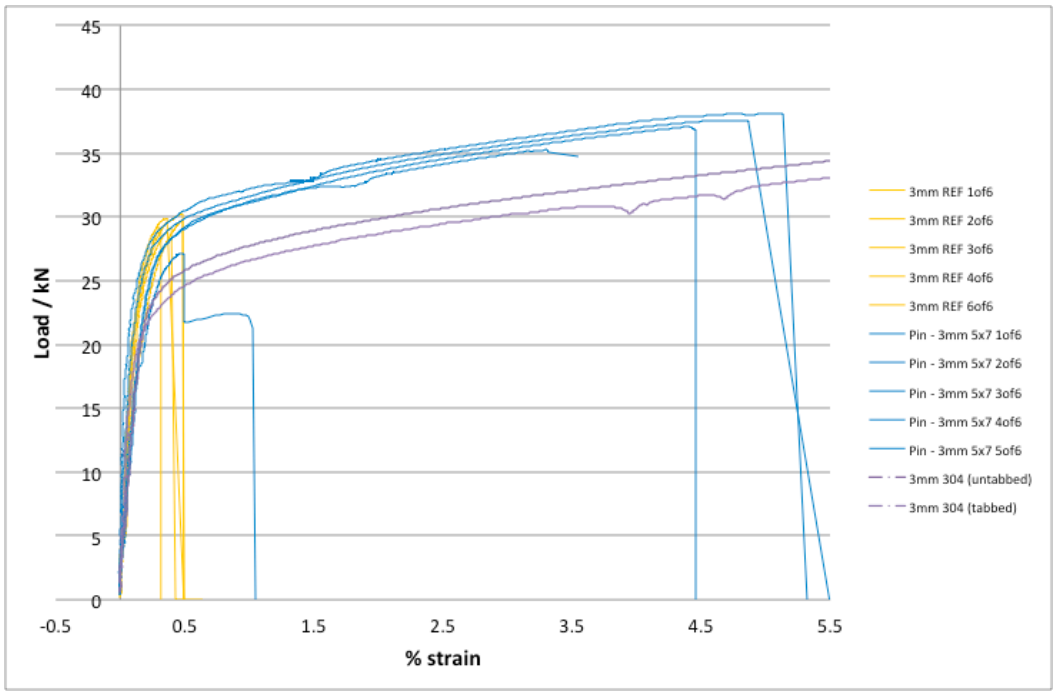

Figure 3-33 – Load-strain response of all joint configurations with 3mm metal substrate

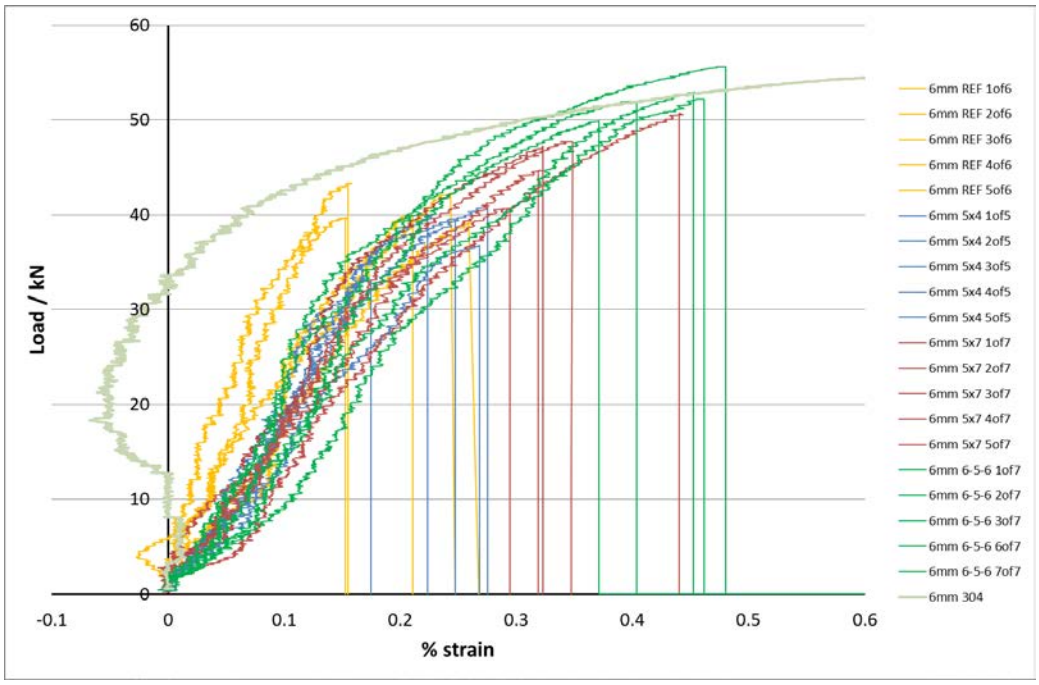

Figure 3-34 – Load-strain response of all joint configurations with 6mm metal substrate

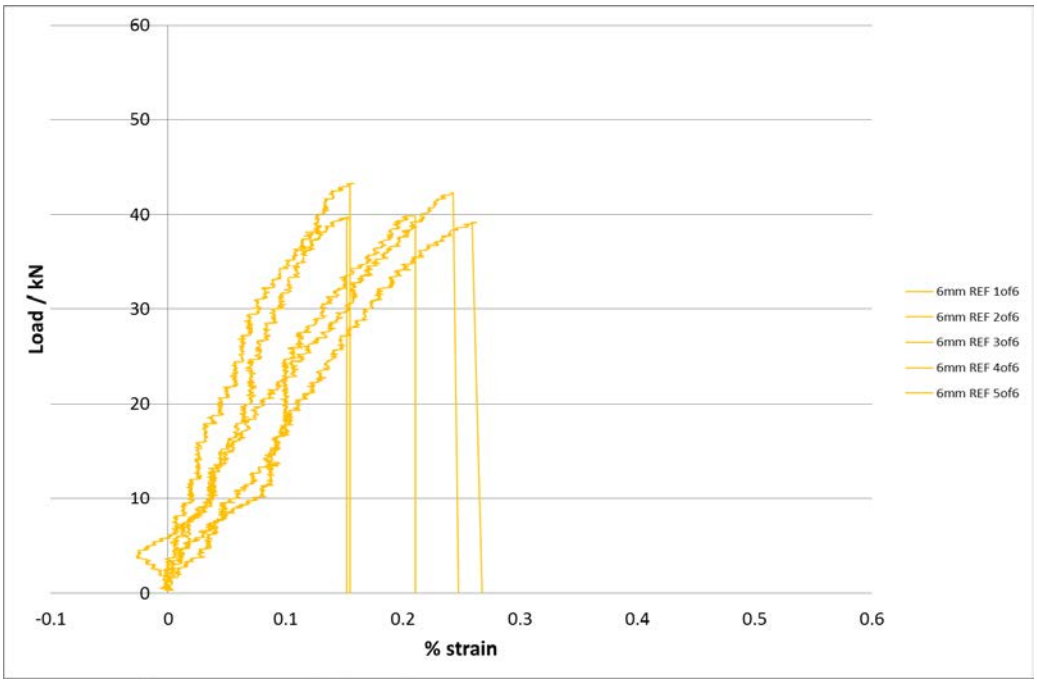

Figure 3-35 - Load-strain response of 6mm metal substrate adhesive reference specimens (matrix adhesion only)

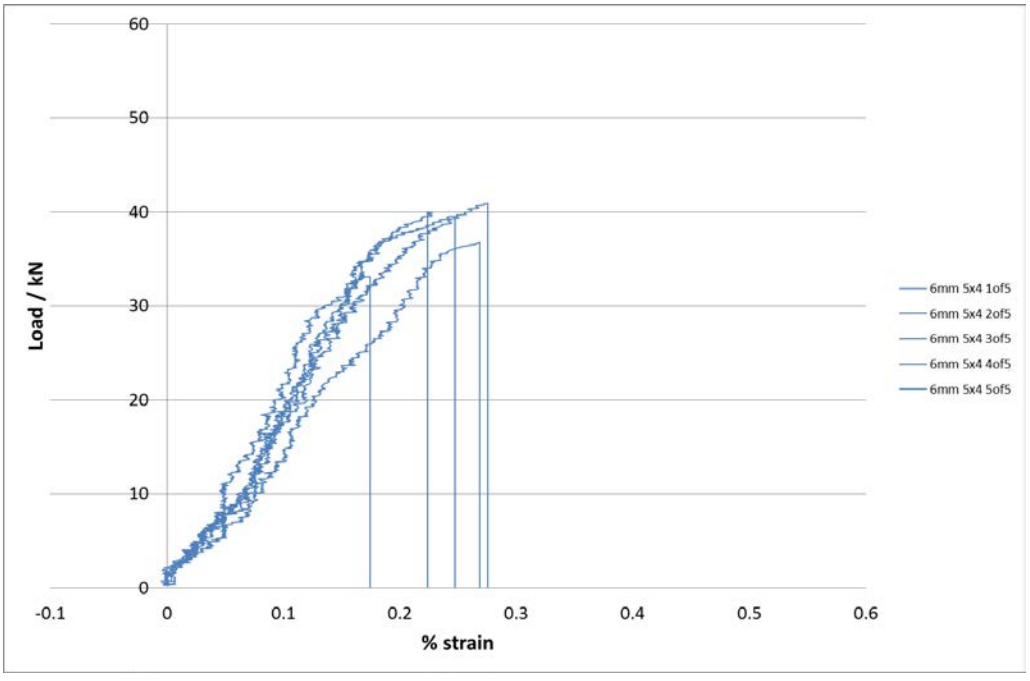

Figure 3-36 - Load-strain response of 6mm metal substrate adhesive joint specimen reinforced with micropins in 5x4 arrays

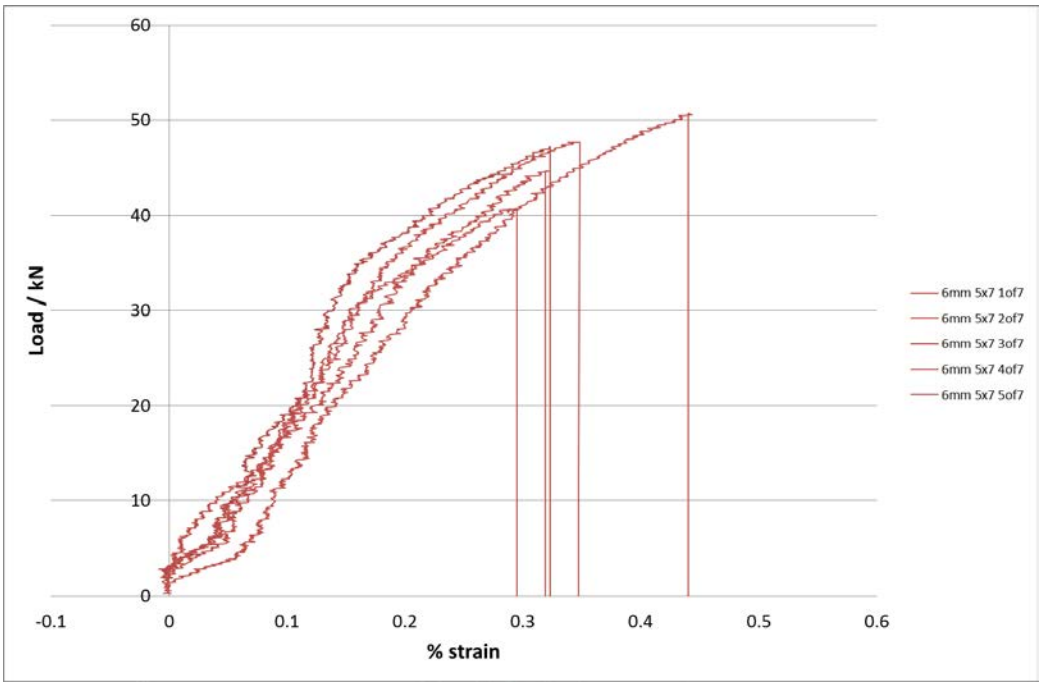

Figure 3-37 - Load-strain response of 6mm metal substrate adhesive joint specimen reinforced with micropins in 5x7 arrays

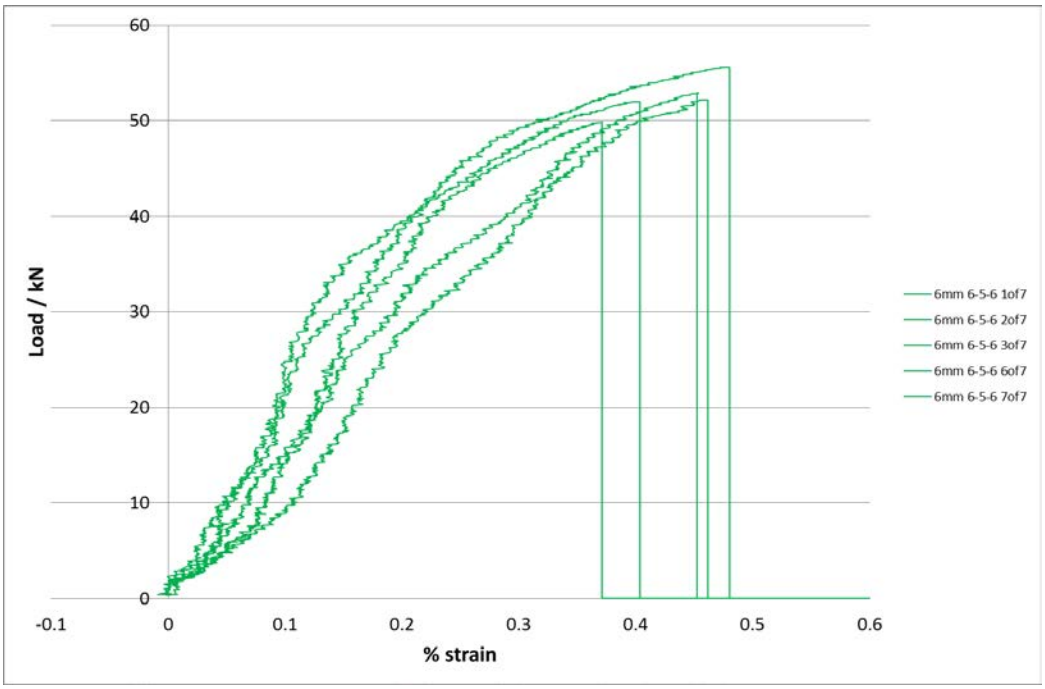

Figure 3-38 - Load-strain response of 6mm metal substrate adhesive joint specimen reinforced with micropins in 6-5-6 arrays

Figure 3-33 shows a comparison between the reference adhesive-only (yellow) and pin-reinforced (blue) joint configurations for specimens that used 3mm metal substrate. Also shown on this chart are results from testing the metal substrate alone (purple). It can be clearly seen, from the substrate only test, the elastic and the plastic deformation regions of the material (stainless steel 304). The identical gradient of the plastic deformation region of the substrate-only and the pin-reinforced joint specimens allows clear identification that the metal substrates of the pin-reinforced specimens undergo the same plastic deformation.

A single test specimen of the pin-reinforced sample shows a different stress-strain response (and is omitted from Figure 3-31(b) as a possible outlier). This specimen shows an intermediate failure. This stress-strain response was seen in all the test specimens of a preliminary study (Appendix A). The intermediate failure was found in the preliminary study to be associated to adhesive bond failure, the second, the ultimate, peak was considered to be residual strength of the joint, which is provided by the pins. The similarities between the yielding region of the substrate-only specimen and the gradient leading up to the second peak of this one test specimen also suggests that it is associated with metal yielding. The predicted ultimate strength of an array of 70 pins, as stated in Table 3-2, is 14.9kN in shear and 19.8kN in tension. The measured value of 22.4kN is comparable but higher than either of these values. The mixed loading state, as described in Figure 3-26, gives an explanation as to why the load is higher than the predicted shear ultimate strength. A reason why the measured load is higher than the predicted tension load could be due to friction between the metal and laminate interface areas.

The discontinuities of the metal-yielding region of the graphs are identifiable as being associated with how the samples were prepared for mechanical testing; it is attributed to slippage of the tabbing material, and is not a characteristic of the joint failure mechanism.

The yielding of the metallic substrate in the 3mm joint specimens was anticipated, and there was concern that it would complicate understanding of the failure mechanism of the pin-reinforced adhesive joint. This was the rationale behind the decision to use 6mm substrate for the series of tests that were devised to understand how variations in the pin array effect the way the joint fails. It can be seen in Figure 3-34, Figure 3-35, Figure 3-36, Figure 3-37, and Figure 3-38 that the joints that use 6mm thickness metal substrate do not exhibit a significant region of substrate yielding.

3.5.4 Visualisation of joint deformation during failure

The results of the Digital Image Correlation (DIC) investigation are presented in Figure 3-39. The results for the reference specimen (matrix adhesion only) are shown in Figure 3-40 and Figure 3-41. The results for the adhesive joint specimen reinforced with micropins in 5x7 arrays are shown in Figure 3-42, Figure 3-43, and Figure 3-44. The results for the adhesive joint specimen reinforced with micropins in 6-5-6 arrays is shown in Figure 3-45, Figure 3-46, Figure 3-47, and Figure 3-48. For this application strains measured by DIC cannot be considered as reliable as results are not calibrated against traditional strain gauges. Also, as these measurements are from viewing the edge of the specimen, tensile strain edge effects will result in a strain that is not representative of the actual strain of the joint interfaces. The usefulness of the DIC technique in this investigation is visualisation of relative displacement of the joined components, and so enabling identification of where a structure is failing. It can be seen, from the images below, how much of the interface area is exposed to strain and how this corresponds to the ultimate failure event for each joint.

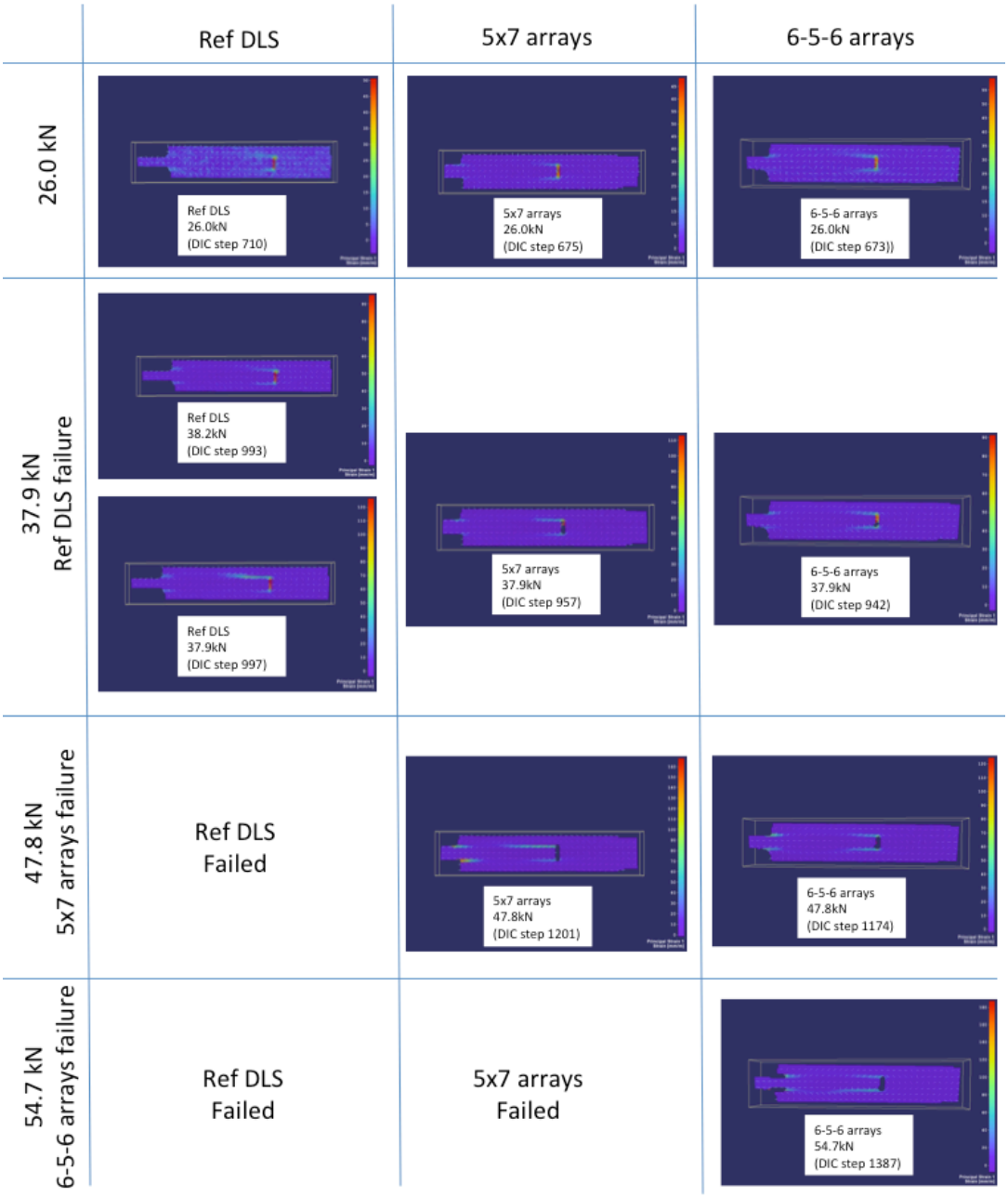

Figure 3-39 – Visual observation of strain by Digital Image Correlation

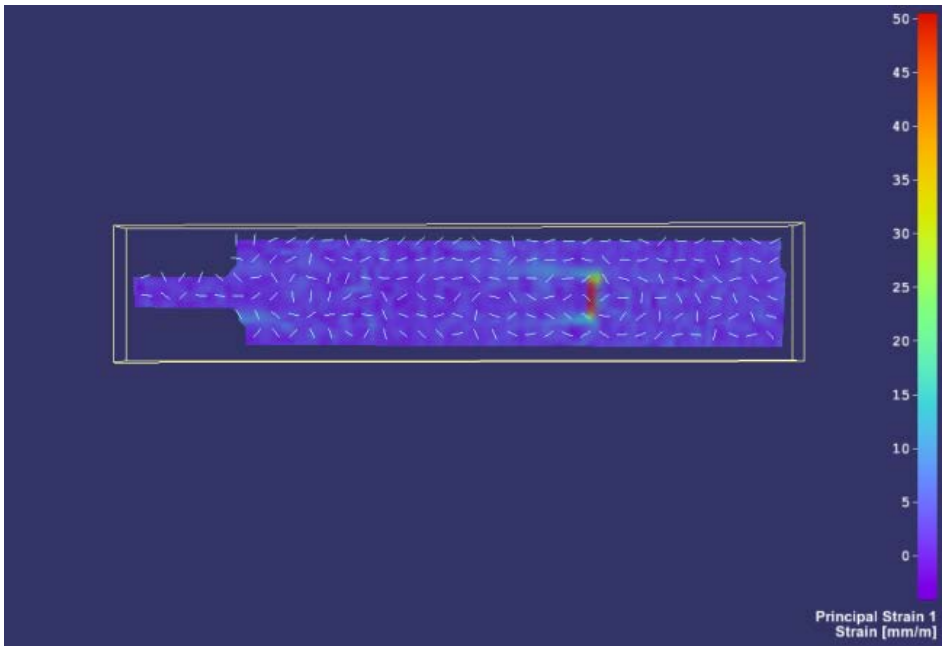

Figure 3-40 - Principle strains (mm/m), measured by DIC, of reference specimen (matrix adhesion only) with an applied load of 26.0kN

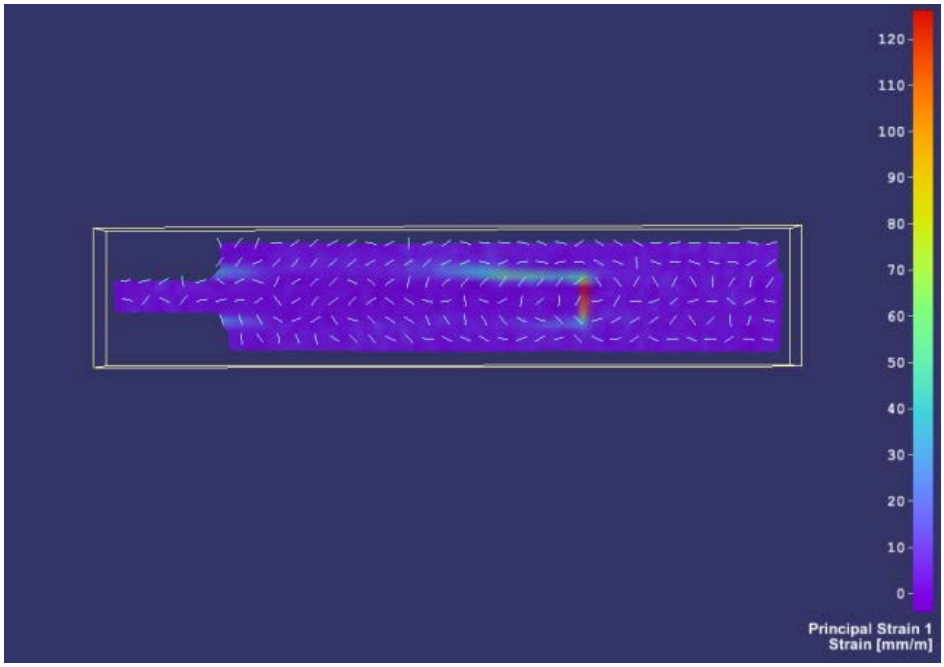

Figure 3-41 - Principle strains (mm/m), measured by DIC, of reference specimen (matrix adhesion only) with an applied load of 37.9kN; which was the load applied imminently before joint ultimate failure

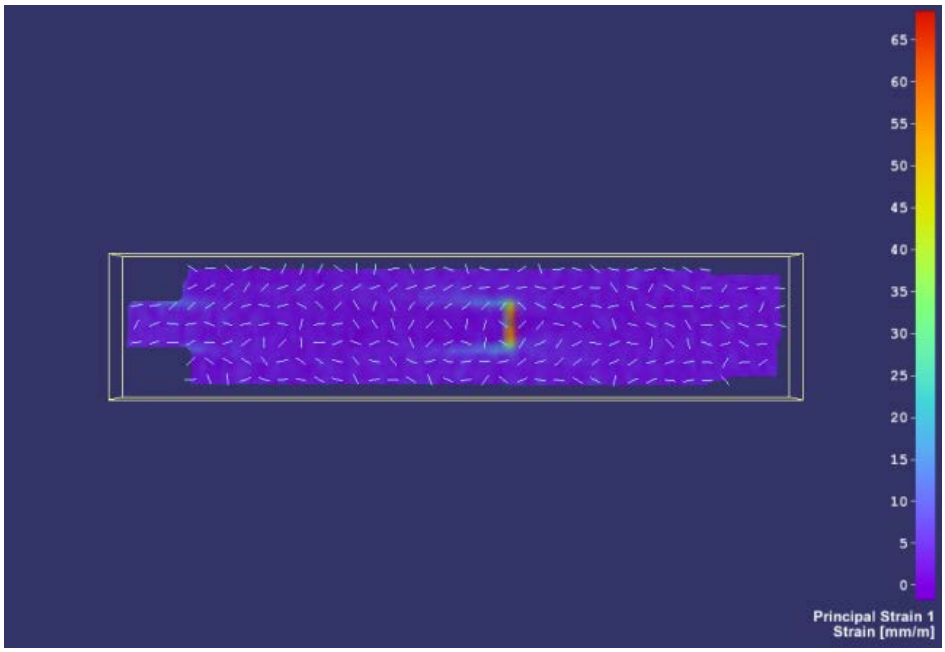

Figure 3-42 - Principle strains (mm/m), measured by DIC, of adhesive joint specimen reinforced with micropins in 5x7 arrays with an applied load of 26.0kN

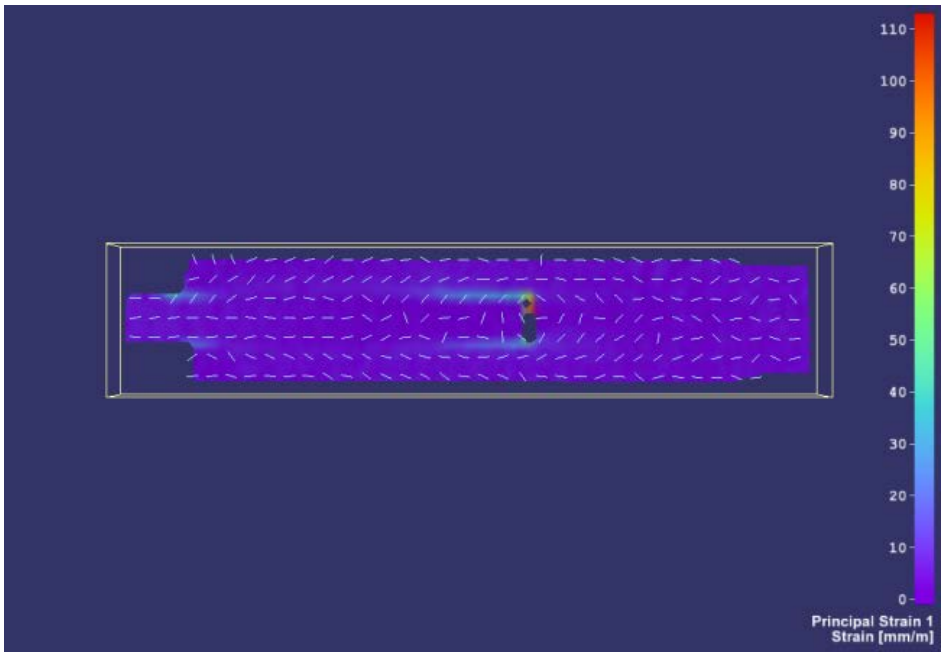

Figure 3-43 - Principle strains (mm/m), measured by DIC, of adhesive joint specimen reinforced with micropins in 5x7 arrays, with an applied load of 37.9kN; which was the load applied imminently before ultimate failure of the reference joint

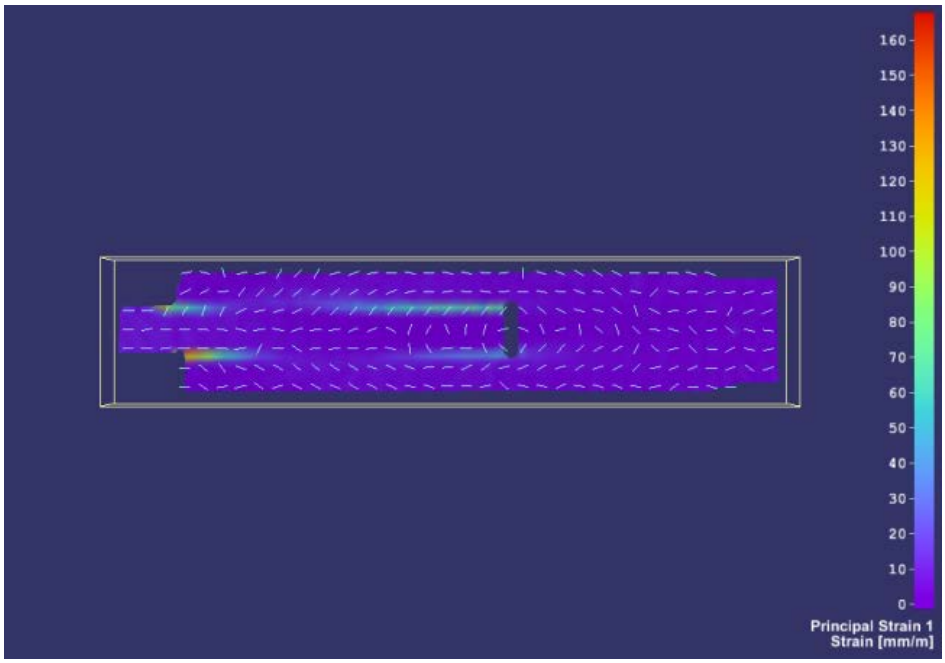

Figure 3-44 - Principle strains (mm/m), measured by DIC, of adhesive joint specimen reinforced with micropins in 5x7 arrays, with an applied load of 47.8kN; which was the load applied imminently before joint ultimate failure

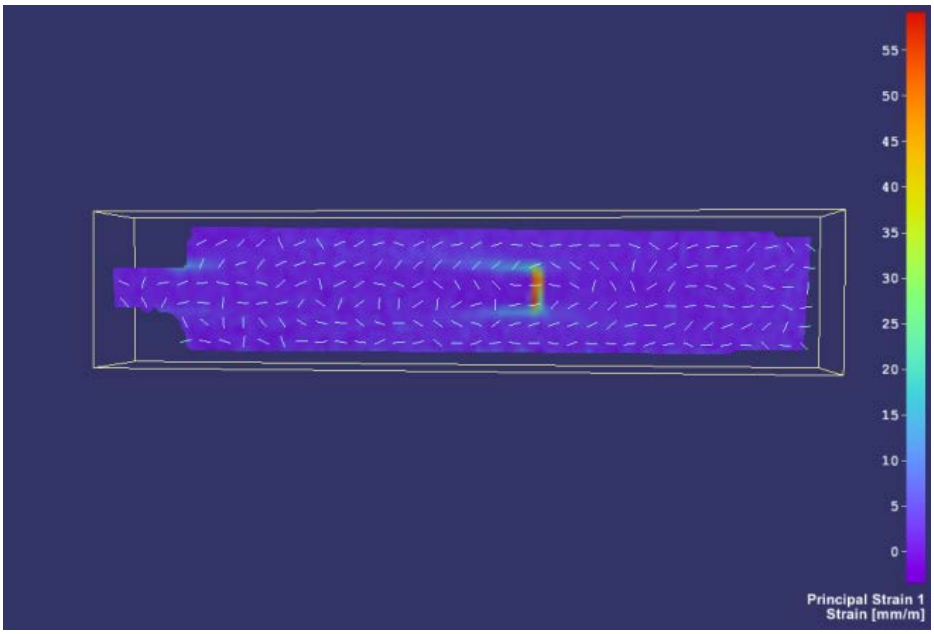

Figure 3-45 - Principle strains (mm/m), measured by DIC, of adhesive joint specimen reinforced with micropins in 6-5-6 arrays with an applied load of 26.0kN

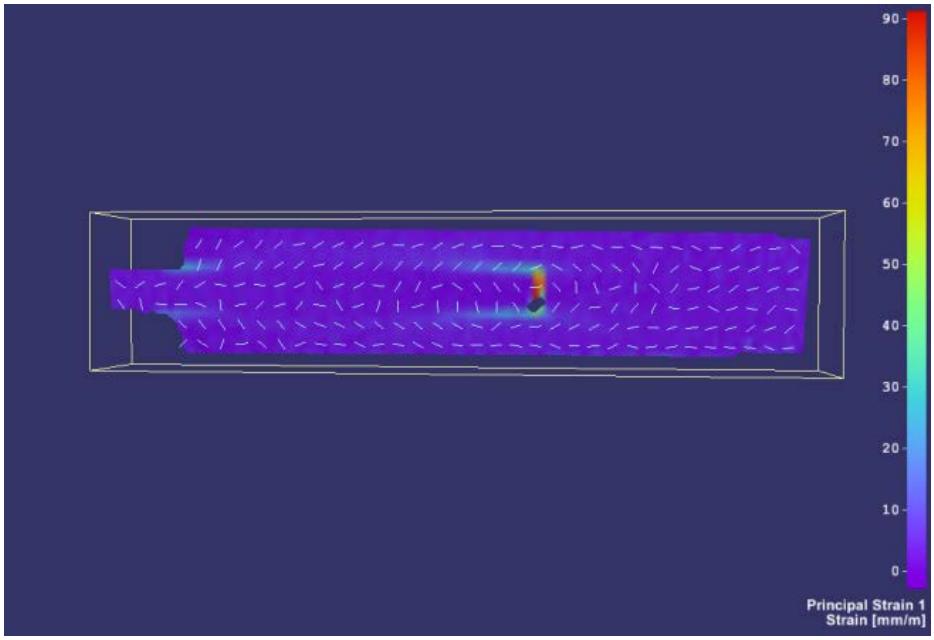

Figure 3-46 - Principle strains (mm/m), measured by DIC, of adhesive joint specimen reinforced with micropins in 6-5-6 arrays, with an applied load of 37.9kN; which was the load applied imminently before ultimate failure of the reference joint

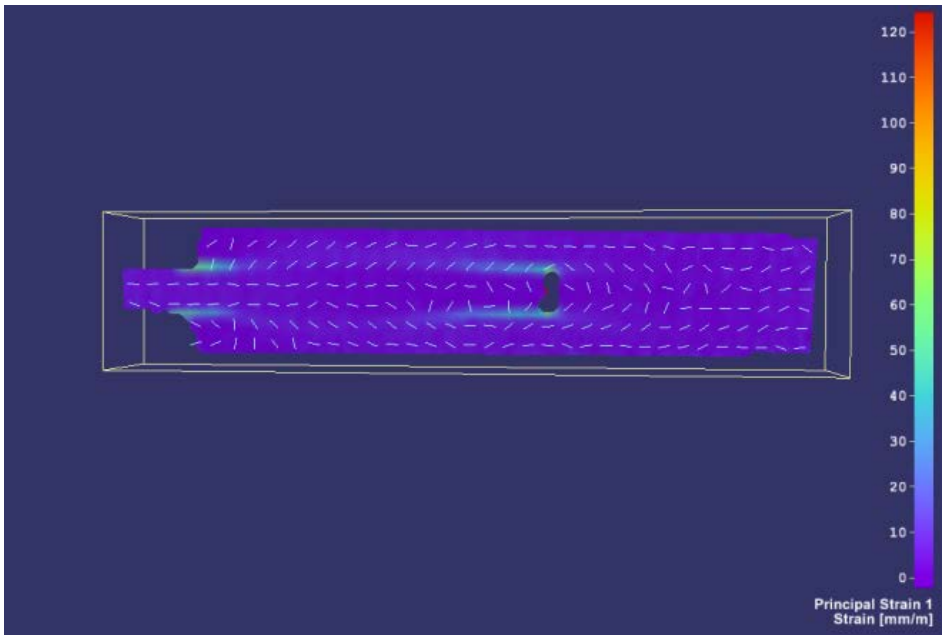

Figure 3-47 - Principle strains (mm/m), measured by DIC, of adhesive joint specimen reinforced with micropins in 6-5-6 arrays, with an applied load of 37.9kN; which was the load applied imminently before ultimate failure of the joint specimen reinforced with micropins in 5x7 arrays

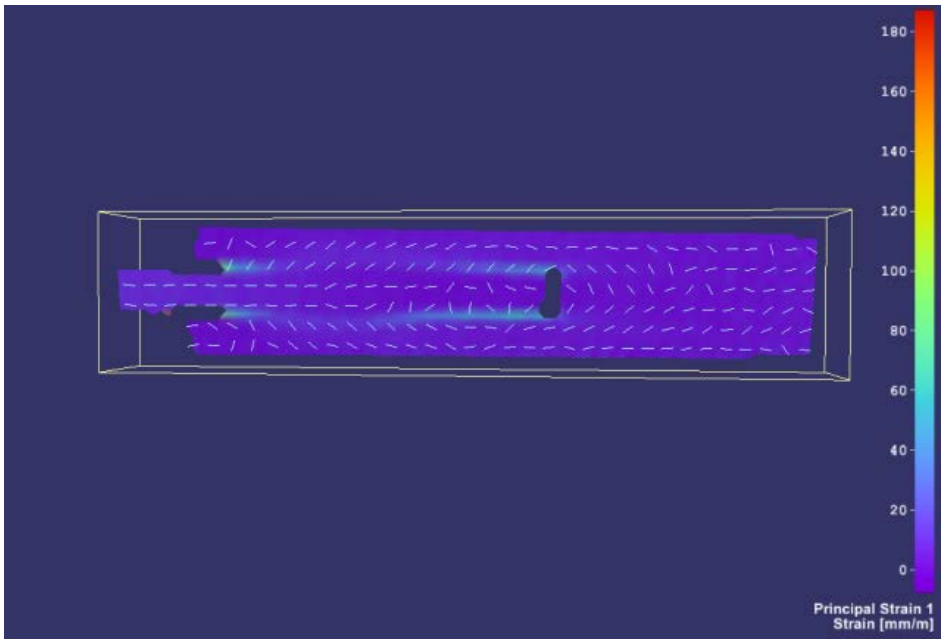

Figure 3-48 - Principle strains (mm/m), measured by DIC, of adhesive joint specimen reinforced with micropins in 6-5-6 arrays, with an applied load of 54.7kN; which was the load applied imminently before joint ultimate failure

How the failure loads of the DIC test specimens compare to previous test sample data:

- The reference specimen failed at a load that is 6.5% lower than the average, and outside the sample range by 0.96kN
- The 5x7 specimen failed at a load that is 3.5% higher than the average, and is within the sample range
- The 6-5-6 specimen failed at a load that is 4.1% higher than the average, and is within the sample range

The failure load of the DIC adhesive-only reference specimen is lower than expected. This could be a result of damage incurred during preparation of the specimen for the DIC test; the edge of the sample had to be ground and polished flat in order to provide a reference surface for analysis.

In all images shown in Figure 3-39, especially the ones at lower loading levels, the high strain seen at the composite end of the DLS joint is the result of unrestrained local displacements due to the presence of crack-starters.

The image resolution of the DIC technique is not sufficiently accurate to identify the crack tip in an adhesive bondline.

It can be seen that the adhesive-only reference sample is intolerant of stress concentrations along the bondline and fails suddenly, this is as expected. Using the average maximum load value for the adhesive-only specimens of 40.8kN, from Figure 3-29, over the total bonded area of 1500mm^2, as described in Figure 3-14, gives a bondline area distributed (average) maximum shear stress of 27.2MPa.

For the joint specimen that has a 5x7 regular array (average failure load from Figure 3-29 of 46.2kN) the bondline distributed (average) stress can similarly be calculated to be 30.8MPa. This can be equivalated to 0.44MPa per pin-bond unit.

The term pin-bond unit being used to distinguish between the load that is being reacted by the pins or the bond in isolation, the term is used to acknowledge

that the pins and bondline react load in unison. The pin-bond unit is described in Figure 3-49. There are 70 pins and therefore 70 pin-bond units in the joint that uses 5x7 regular pin arrays; correspondingly, there are 68 pin-bond units in the joint that uses 6-5-6 arrays.

For the joint that uses 6-5-6 arrays at bondline runouts (average failure load from Figure 3-29 of 52.5kN) the bondline distributed (average) stress can similarly calculated to be 35.0MPa. This can be equivalated to 0.51MPa per pin/bond unit.

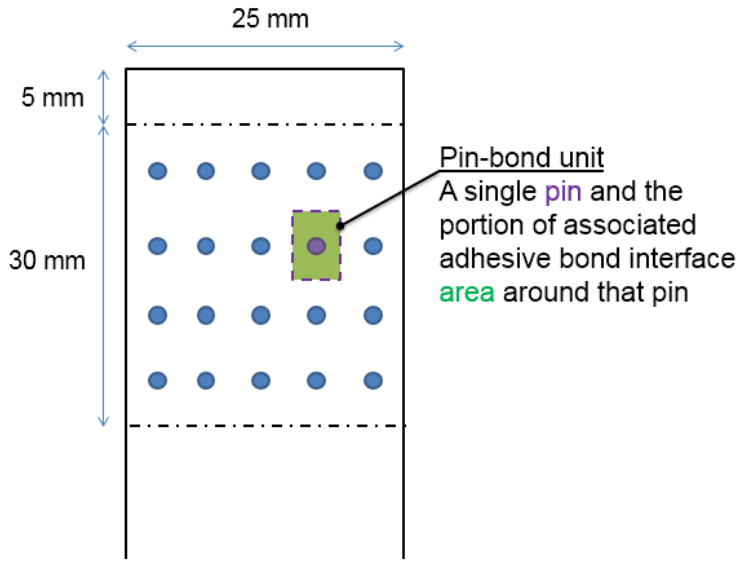

Figure 3-49 - Description of the pin-bond unit. The term 'pin-bond unit' is used as a way to describe how a pin and surrounding bonded area react force in unison

3.5.5 Physicality of joint as a result of manufacturing process

This section describes the physicality of the pin/laminate interactions of the metal surface structured through-composite-thickness joint. The result of inserting the pins into the uncured laminate is observed in Figure 3-23, it is seen that the fibres in the laminae are separated without breakage of the fibres. Resin filled eyelets are formed in the empty discontinuity formed by the presence of the pin. Another result of pin insertion is that fibres are dragged away from the planar interface of the metal adherend. The result is resin rich zones between the fibres and pin fillets (annotated as B in Figure 3-50), this can be considered as regions of thick bond line, which could be detrimental to the effectiveness of the adhesive bond. The region marked as A on Figure 3-50 could be considered as a ‘more optimally bonded region’.

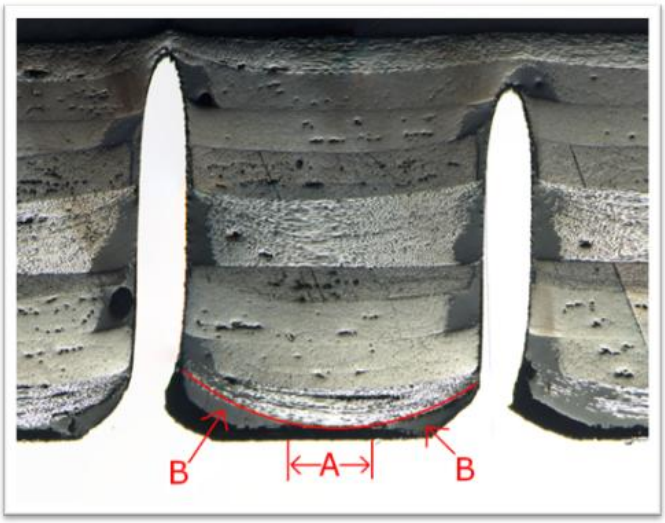

Figure 3-50 - The red line marks the edge of fibres

This observation provides an explanation as to why in some cases the use of reinforcing pins at the adhesive bondline can result in a decrease of joint strength, as described in Section 3.5.3. When too few pins are applied the beneficial reinforcement effect of the pins is not greater than the knockdown effect incurred to the adhesive bondline strength.

The greater strength seen for joints that use 6-5-6 arrays could therefore also be due to having a reduced percentage of the bonding area affected by the presence of pins; there is a considerable area of unaffected bondline in-between the reinforced runout regions.

3.6 Discussion and Conclusions

3.6.1 Concluding message

Structuring the surface of a metal adhered, so to provide through-composite-thickness reinforcement of double-lap-shear adhesive joints, results in increased joining strength. The increased strength is achieved by the reinforcements working to react induced out-of-plane loads and therefore delaying ultimate failure of the joint until greater loading conditions are applied. The micro-welding method used in this work for constructing surface structured metal adherents has significant processing benefits, over other methods demonstrated in the literature, while still enabling an increase in joint strength.

3.6.2 How this chapter supports the message

It is demonstrated that joining strength improvements are the result of the out-of-plane induced loads being reacted by through-composite-thickness structures that are anchored to the metal substrate. This proof was ascertained by identifying that joint strength was increased by arranging the reinforcements in the region of the bondline that is exposed to the greatest out-of-plane loading. This conclusion was further supported by visualisation of strain during specimen testing.

It was also observed that this joining technique has strength capabilities that exceed the yield strength of the metal adhered. In these cases the joint holds while the metal adherend outside of the joining interface undergoes significant yielding. Therefore, demonstrating a pseudo-ductile failure characteristic of this composite to metal adhesive joining technique, the associated benefits are

dependable residual strength of such a joint and increased energy absorption during structural failure.

The processing benefits of the metal surface structuring technique used in this study, which is CMT-Pin welding, is derived from the situation that the technique is both: an additive manufacturing process, and that it is conducted in ambient atmospheric conditions. This study also showed that precursor composite material in the form of prepreg can be used in constructing the joints, which increases the likelihood of the joining technique being suitable for uptake in aerospace applications.

3.6.3 Points that remain open to interpretation

Several failure mechanisms associated with various joint geometries have been identified in this work. The use of too few reinforcing structures resulted in a reduced joint strength compared to a reference adhesive-only joint. The concentration of reinforcements at areas of greatest out-of-plane loading resulted in an increase in joint strength. And the use of a thinner metal substrate resulted in metal substrate yielding prior to joint failure.

Adhesive bonding was achieved by exploiting the M21 matrix system of the CFRP prepreg. No information was available in the literature for the bond shear strength of this epoxy system when used as an adhesive between CFRP and metal. If such information were available, strength values would likely have been measured by a stand mechanical testing method such as ASTM D5868, this test standard uses a single-lap-shear test arrangement with an interface lap area of 25.4 x 25.4mm. Material properties are only truly comparable when they are measured in strict accordance with the same test standard. Therefore, adhesive strength values of M21 measured by a standard such as ASTM D5868 would only be indicative of the strength obtainable in other joint configurations, such as the DLS arrangements used in this work. This situation lead to the decision to measure the adhesive for this specific joint arrangement by testing a baseline reference joint of the same DLS geometry.

These findings indicate that there are joint configuration limits and corresponding failure mode changes that occur as joint geometry and features change. Further testing of elaborated joint configurations, and also the development of a more representative FE model, would enable understanding of when configuration limits occur. This understanding could then be used to generate design guidelines for use in applying this joining technique to real world structural applications.

3.6.4 Further work that could be done

As well as further work to establish joint design guidelines there is also further understanding to be gained of the effect that the various manufacturing processes have on the resulting joining performance. Metallographic inspection enabled observation that the manufacturing process of inserting pins into the composite prepreg induces fibre alignment distortions that are typically considered as defects and are usually associated with reduction of laminate strength. The phenomenon of resin-rich-eyelets around the pins is one such observed feature. Resin rich areas in composite laminates are usually considered to be defects and detrimental to the laminate strength. However some recent studies, influenced by biomimicry concepts (Malkin et al., 2013), have shown that having resin rich areas in a composite laminate increases ductility. Increased ductility is often associated as being beneficial to joining interfaces (de Castro and Keller, 2008). The fact that the potential local-ductility boosting effect of resin rich regions occurs at the interface between the pins and the laminate could be of specific benefit to the joint. One way of quantifying the local change of properties could be by the use of Rules of Mixture (ROM) calculations; comparing the typical composite adherend with that of the locations around the pins, which have lower fibre volume fraction due to the resin-rich-eyelets, also the metal pin itself could be included in the ROM calculation.

It has been established in this work that the loading of the pin shanks is a combination of shear and tension rather than just shear; in order to see the resulting increased strength of this joining technique. It was observed that the pins deform just above where they are anchored to the metal plate. Where the greatest local load concentration is expected (Liu and Hou, 2003; Liu, Raju and You, 1999). This change in local geometry is what is expected to enable the pins to be loaded in tension rather than shear. The pins themselves are spatially restrained by the laminate, they are able to deform due to local interfacial ductility, which is boosted by the local excess of resin provided by the resin-rich-eyelets that are formed by the pin insertion. Therefore it can be considered that this local defect of the resin rich regions has a beneficial effect on the overall joint performance. The joining method could be further optimised by choosing pin geometries that have the shanks of the pins already aligned to carry a significant proportion of the load in tension, this is a further example of biomimicry for improved structural strength (Burns et al., 2012b).

The method of pin insertion relied on heating generated by ultrasonic vibration at the contact interface between the pins and the uncured prepreg. The increased temperature softens the uncured resin matrix system and enables the pins to penetrate the laminate in the through-thickness direction. It is expected that the heating and softening effects will result in a certain degree of uncontrolled resin cure. And that this could impact the fully cured properties of the composite. In this study no investigation was made of the amount of heating induced, or consequently the amount of uncontrolled cure and resulting induced degradation of the matrix system.

The method of inserting the pins used a pneumatically driven gantry that controlled the pressure applied to the work piece by the ultrasonic solenoid. However there was no control of the duration of application. This relied on the operator observing the insertion of the pins and making a decision as to when the pins were sufficiently inserted and the process cycle could be manually halted. A parametric study could be conducted that would investigate the effect

of solenoid pressure and ultrasonic heating duration to determine what effect is made to the joint strength.

Softening of the matrix system also occurs as part of the prepreg cure cycle. Further investigations could be undertaken to understand whether pin insertion could be achieved simultaneously with the cure cycle. Such an approach would require development of a jigging method to hold the laminate and metal substrates in alignment prior to, and during, the curing process as the pins penetrate into the laminate. It would therefore also need to be assessed whether this increased jigging requirement sufficiently offsets the assembly self-jigging benefit of pre-inserting the pins ultrasonically and any reduced mechanical performance that might occur as a result of the ultrasonic heating.

Partial failure tests proved to be highly beneficial in understanding the modes of failure of this joining system. A future study of the fatigue behaviour of these joints could also reveal useful information. Firstly in terms of the effect on fatigue life of DLS adhesively bonded joints by including the pin reinforcements; as the fatigue life of the pins is expected to be considerably lower than that of the adhesive bond. Also joint failure modes, samples with various numbers of fatigue cycles that are less than the ultimate fatigue life of the joints, could be inspected; which could give further understanding of the failure mechanisms in terms of bondline crack propagation and how the pin arrays progressively fail by fatigue.

4 METAL TO CARBON FIBRE SPOT WELDING REINFORCED ADHESIVE JOINT

4.1 Introduction

Adhesive bonding is considered to be the preferential method of structurally joining CFRP components because of the relatively low stress concentrations introduced into the CFRP laminate. It is also understood that reinforcing an adhesive bond with mechanical fastening methods results in improved joining performance of the adhesive bond. The technique of weld-bonding is extensively used in the automotive industry to achieve a combined resistance spot weld (RSW) and adhesively bonded joint between sheets of metal (Darwish and Ghanya, 2000). There are two variations of weld-bonding: weld-through and back-infiltration. In the weld-through process an adhesive is applied to faying surfaces, the surfaces are then brought together and a RSW applied prior to adhesive cure, the RSW penetrates the adhesive layer. In the back-infiltration process metal parts are directly joined by resistance spot welding followed by the application of a low viscosity adhesive to the edge of the overlap, which fills the gap by capillary action (Messler, 2004).

This chapter describes investigations into how the principles of weld-through and back-infiltration RSW weld-bonding can be applied for the purpose of forming structural joints between carbon fibre reinforced plastics and metals. In work by Weiland et al an ultrasonic welding process was used on a fibre preform prior to resin infusion (Weiland, Weimer and Mitschang, 2011). Development of processes for the application of RSW through carbon fibre fabric will first be explored followed by the design and manufacture of proof of concept joints that when mechanically tested give insight into the joining performance of the newly devised technique.

The first stage of this work was to trial resistance spot welding of various metals (titanium, stainless steel, and aluminium) and various interleaved stacking sequences with carbon fibre fabric, so to determine suitable material combinations. Instrumentation of resistance welding equipment (to measure

welding current, electrode pinch force, and electrode movement) enables characterisation of the dissimilar material welding process, which in turn expedites the identification of optimum welding parameters. Microscopy is used to understand the weld formation processes in this novel mechanical reinforcement method.

Following the application of a multi-material RSW the composite manufacturing process of epoxy resin infusion is used to both form the CFRP composite matrix system and form the composite to metal adhesive bond. A range of mechanical tests specimens were designed to enable characterisation of isolated load-carrying mechanisms that are combined within the RSW reinforced adhesive joint, so to understand how the performance of individual mechanises affect the combined joint performance. Quasi-static mechanical testing is conducted to investigate the strength performance of the resistance spot weld reinforced adhesive joints.

4.2 Methodology

This joint concept is achieved by the use of resistance welding and resin infusion techniques in a two stage manufacturing process. In the concept investigated here a resistance welding process is used to generate the temperatures required to achieve melting of the metal. An interleaved stack of metal and dry carbon fibre is assembled, a resistance spot weld is then formed between the exterior metal sheets, the resulting resistance weld penetrated the carbon fibre; forming a welded joint between the metal parts together with an element of braze joining between the metal and the carbon fibre. The second stage is then to resin infuse the carbon fibre. The resin has two functions, it forms the polymer matrix system of the composite laminate and also an adhesive joint between the composite laminate and metal. A diagram of the metal to carbon fibre spot weld-braze reinforced adhesive joint is shown in Figure 4-1.

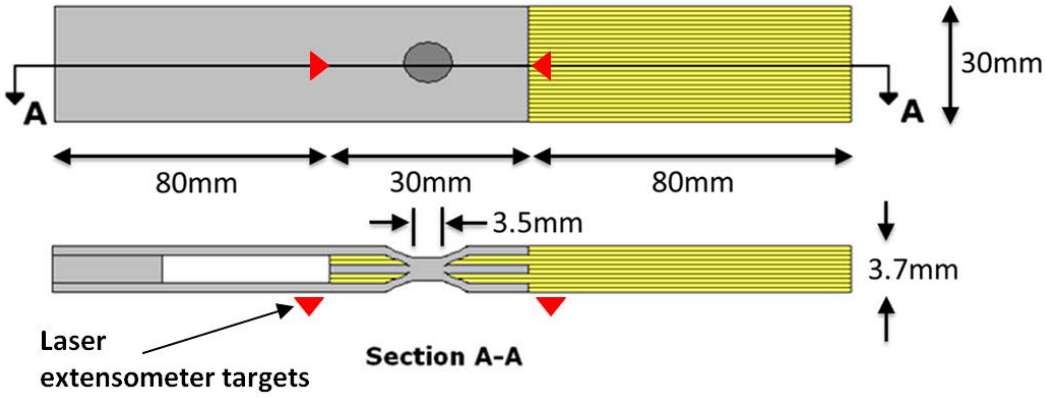

Figure 4-1 – Diagram of the metal to carbon fibre spot weld-braze reinforced adhesive joint. Note: this diagram shows one of the several various interleaved stacking sequences investigated.

Resistance spot welding equipment was used to apply a current through a stack of unidirectional carbon fibre (CF) fabric sandwiched between metal sheets, as shown in Figure 4-2.

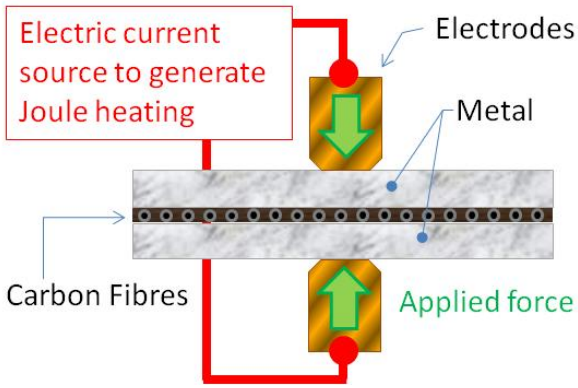

Figure 4-2 - Diagram illustrating the resistance spot welding of a multi-material stack

4.2.1 Development of resistance welding process

There were three study stages to this multi-material RSW investigation. With each stage consisting of parametric studies in which the key RSW parameters are varied so to understand the feasibility of the process. This approach was taken as any change in the material stack affects a change of the through-thickness resistance, as by definition resistance is a key parameter in resistance spot welding, there necessitates a change in the other key parameters (current density, pressure, and time) if successful welding is to be achieved.

The first study (Study 1) was to trial various metals, while keeping the number of carbon fibre fabric plys constant. This first study was to understand metal suitability for use in the process and identify a metal that would be suitable for forming a resistance spot weld-braze through carbon fibre fabric. As the overall aim of the work was to produce structural joints, the metals chosen for investigation are widely used engineering materials. The metals that were trialled are listed in Table 4-1, together with the carbon fibre fabric.

Material	Tensile strength (MPa)	Shear strength† (MPa)
Titanium Ti-6AL4V	950	475
Aluminium 2024-T3	435	218
Stainless steel 304	505	253
Epoxy RTM6	75.0	37.5
Carbon fibre HexForce G1157	833	417

†Based on stated tensile strength value

Table 4-1 - Ultimate strength of joint constituent materials

Material	Resistivity (Ohm-cm)	Thickness (mm)
Titanium Ti-6AL-4V	178×10^{-6}	1.0
Stainless steel AISI 304	72.0×10^{-6}	0.90
Aluminium 2024-T3	5.82×10^{-6}	1.4
Carbon fibre fabric HexForce G1157	$10'000 \times 10^{-6}$	0.25

Table 4-2 – Electrical resistance details of joint constituent materials

The second study (Study 2) was to use the most suitable metal, as identified in Study 1, and vary: the number of CF plys, the number of metal sheets, the thickness of metal sheets, and the interleaved stacking sequence. The purpose of the second study of the investigation was to optimise the interleaved multi-material joint by maximising the number of CF plys that could be incorporated.

The first series of trials of Study 2 was to simply increase the number of HexForce G1157 plys between two 0.9mm thickness sheets of stainless steel 304 (which was the metal identified by Study 1 for use in Study 2). For each increase in number of plys the parametric study was repeated.

Studies 1 and 2 were conducted using a manual pedal operated SIP PL10 column resistance spot welder with standard SIP 03345 straight electrodes, as shown in Figure 4-3. The maximum power output of the device was 10 kVA and the electrode clamp force was measured to be 1314 ± 20 N at activation of current flow, with the peak electrode clamp force measured to be 2305 N when the pedal is fully pressed. The force was measured offline using a Sensy INDI-PSD handheld force transducer with a 9QUAL 10 kN miniature compression load cell. As the SIP PL10 column welder lacked the capability to accurately control electrode pinch force the pinch force was maintained as 1314 ± 20 N (current switch-on trigger) for all welding trials and the parametric studies consisted of systematically varying only the power setting (which affects electric current) and the current application time.

It was also observed that when the pedal of the SIP PL10 spot resistance welder was fully pressed the electrode arms would flex, this deformation resulted in the electrode tips no longer clamping the work piece in a parallel arrangement, the effect of this was to induce an uneven clamping pressure that had a lateral force component. The induced lateral force could cause the electrodes and work piece to slip laterally against one another during the welding operation. This observation supported the decision to press the pedal only to the point at which the current flow initiated.

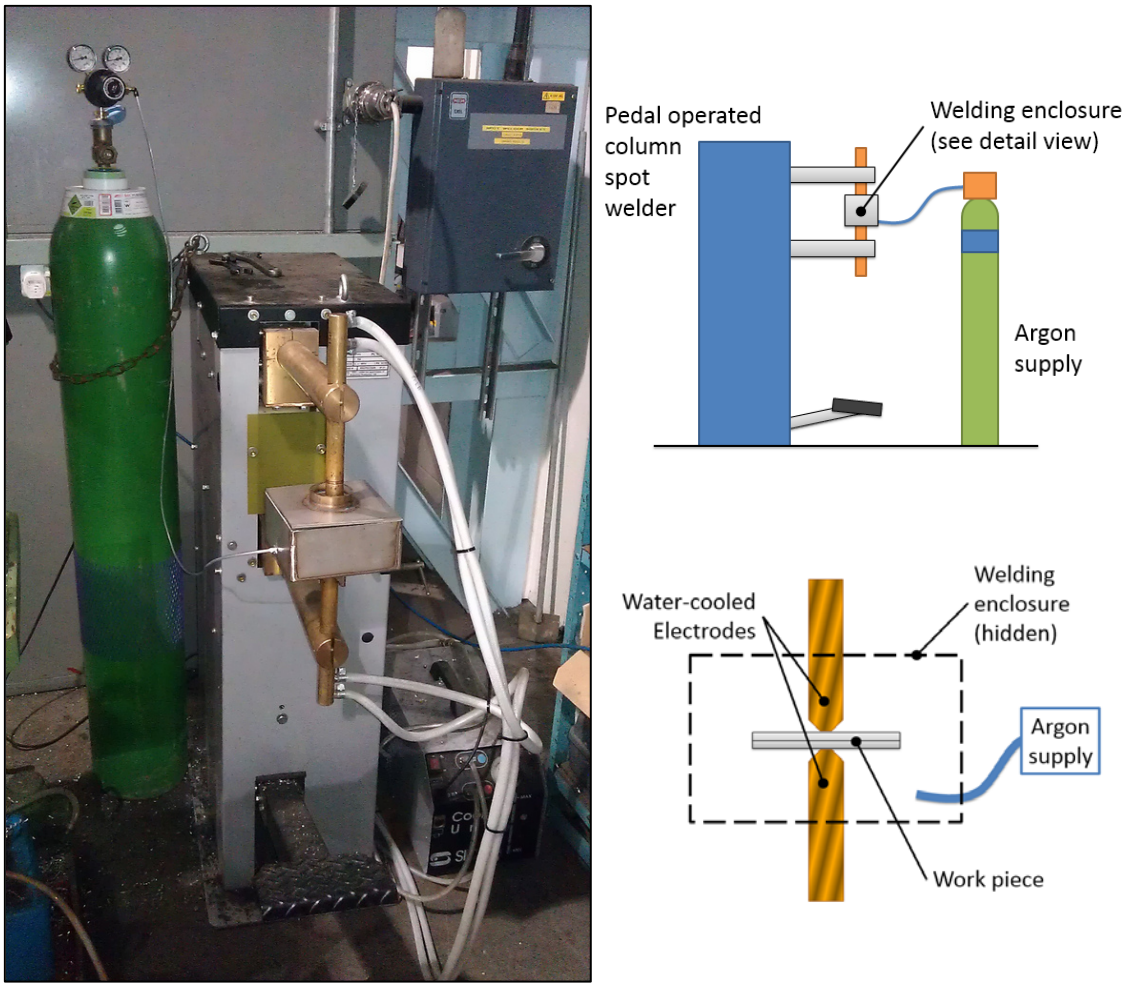

Figure 4-3 – SIP PL10 spot resistance welder with metal box gas enclosure around electrode tips, electrodes later completely enclosed in a gas tent

Figure 4-4 - Microsection of a preliminary trial of the hybrid material resistance spot weld concept

The requirement was set to achieve a cumulative total of 1mm thickness (four plys) of carbon fibre in the material stack. Further trials were undertaken to introduce sufficient metal into the material stack by interleaving with various thicknesses of metal sheet in various stacking sequences. For each interleaved stacking sequence a parametric study was conducted, as before, to identify production of the best possible resistance spot weld.

Studies 1 and 2 used a limited range of resistance welding process parameters, The third study (Study 3) of the investigation used the optimum identified stacking sequence, as identified in Study 2, in a full parametric study to understand how changing all RSW parameters affected the weld joint, and so to identify the set of parameters that result in optimum weld quality.

Study 3 of the investigation required accurate control of the electrode pinch force. To achieve this an AWL-Techniek WP63RL-K resistance spot welder was used, as shown in Figure 4-5. The electrode closure mechanism of this welder is pneumatically actuated. Varying the pressure of in the pneumatic system controls the pinch force of the electrodes. The maximum pinch force of 4.5kN was achievable with the AWL-Techniek WP63RL-K.

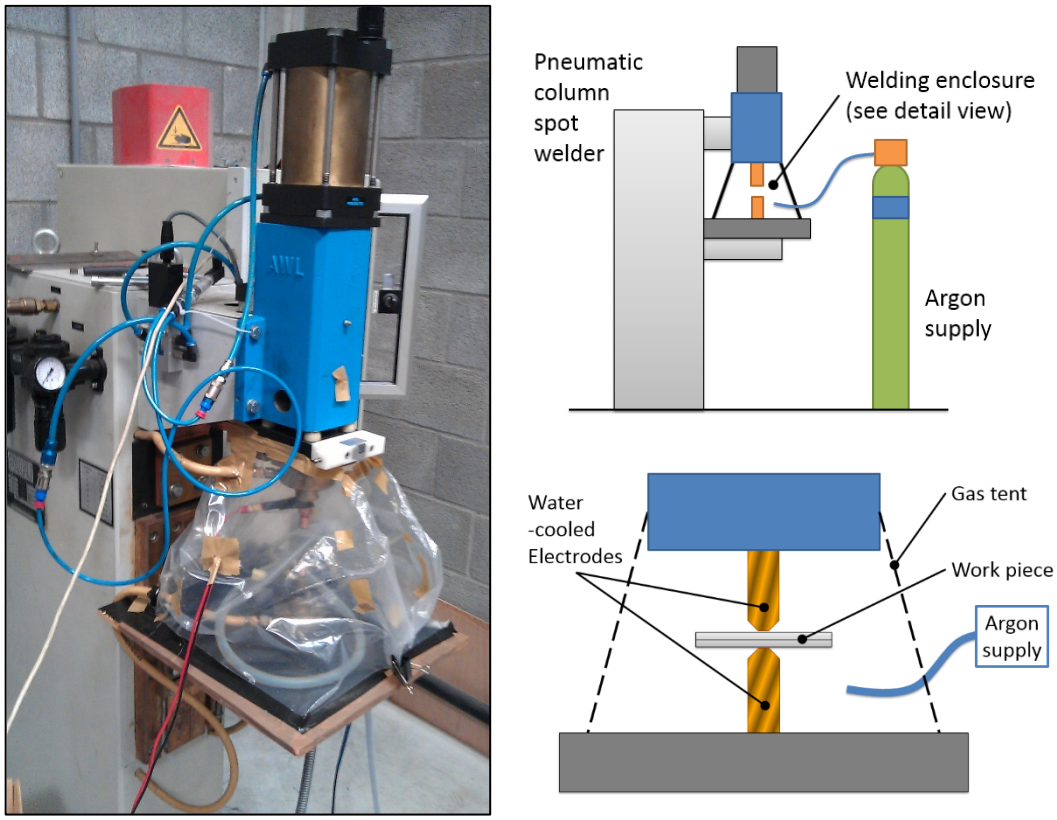

Figure 4-5 - AWL-Techniek WP63RL-K resistance spot welder, with gas enclosure tent around electrodes

Instrumentation used with AWL-Techniek:

- Calibrated inline pressure transducer
- Current probe
- Voltage probe
- Polytec CLV-1000 Laser vibrometer (to measure electrode displacement)
- Dewetron DEWE-2600 data logger

In all cases an argon filled gas enclosure tent was used to achieve an oxygen concentration below 500 ppm. This was to ensure that any reactions that occurred were between the metal and carbon fibres and not between either of these materials and elements in the atmosphere.

.

Electrodes were redressed regularly, and on any signs of tip wear or contamination, to ensure that the current density was only an effect of varying applied electrical power and clamping force, and not as a result of changes in electrode tip contact area.

In Table 4-3 there are listed the parameters of resistance spot-welding that were investigated in this study. Together with a description of how the parameters affect the welding process.

Parameter	Effect
Electrode pinch force	The pressure applied to the material stack affects the contact electric current resistance between the electrodes and the workpiece and also between the material layers (the through thickness direction) in the weld stack
Electric current	The greater the electric current, and so current density, the greater the rate of workpiece heating and welding process, and also the more energetic the reactions within the weld stack (if any occur)
Current application time	Sufficient time has to be allowed to allow the welding process to be completed

Table 4-3 - Parameters of resistance spot-welding that were investigated in this study

4.2.2 Carbon fibre fabric through thickness resistivity

The through thickness resistivity is a critical parameter in resistance spot welding, and this resistivity also changes with change of electrode pinch force. As a novel material stack is used in this RSW process a study was conducted to measure the through thickness resistivity and understand how the value

changed with changing electrode pinch force. No values were found in the literature for the through thickness resistivity of carbon fibre fabrics.

A Sensy INDI-PSD handheld force transducer indicator together with a 9QUAL 10kN load cell was used to measure pinch force and a Master Instruments D3700 micro ohmmeter was used to measure electrical resistance.

The following material stacks were investigated:

- Steel / steel
- Steel / CF / steel
- Steel / CF / steel / CF / steel

4.2.3 Test specimen manufacture and testing

Prototype joints for mechanical testing were manufactured using the optimised parameters from Stage 3; these parameters are provided in Table 4-4.

Type of weld	Pinch force		Electric current		Weld time	
	Measured pneumatic pressure	Exerted force	% of equipment maximum power	Measured peak current	Number of cycles	Actual time
Interleaved Multi-material (IMM)	5.2 bar	4.29 kN	26% (16.6 kVA)	7.68 kA	65 @ 50Hz	1.30 sec
Meta-to-metal (MTM)	5.2 bar	4.29 kN	40% (25.6 kVA)	11.8 kA	15 @ 50Hz	0.30 sec

Table 4-4 - Resistance spot welding parameters used for manufacture of mechanical test joint specimens

The design of these mechanical test joint specimens is shown in Figure 4-1 and the production stages are illustrated in Figure 4-6.

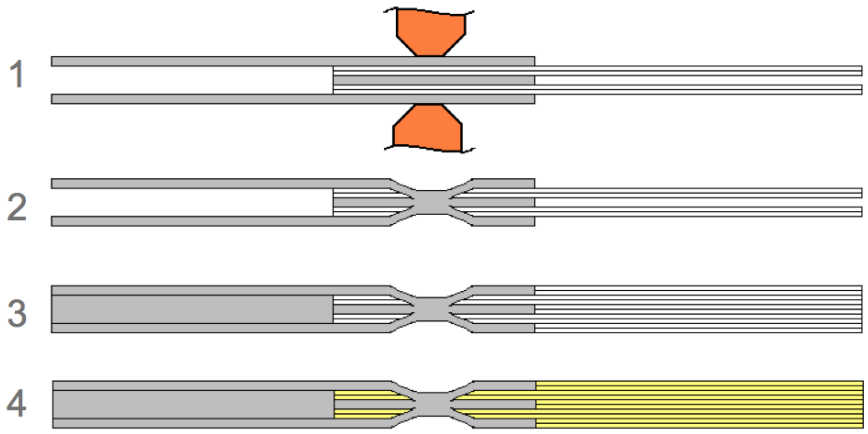

Figure 4-6 - Manufacturing steps of multi-material spot weld reinforced adhesive joint

Of the materials in the stack between the welder electrodes, metal sheet extends in one direction and carbon fibre fabric extends in the opposite direction; these form the arms of the lap-shear test specimen.

The production steps are as follows, Figure 4-6 and Figure 4-8:

Welding process

1) Stack interleaved sequence of metal sheets and carbon fibre fabric and position between resistance spot welder electrodes.
2) Apply RSW to the material stack.

Composite manufacture and adhesive bonding

3) Add additional plys of carbon fibre fabric in-between the plys that are connected to the metal sheets by the welding process, and also place inserts in-between the arms of the metal sheets (a combination of metal sheets and glass fibre fabric were used).
4) Resin infuse the carbon fibre fabric (process detailed below).

Figure 4-7 shows a photograph of a RSW being applied to a lap-shear test specimen by use of an AWL-Techniek WP63RL-K resistance spot welder.

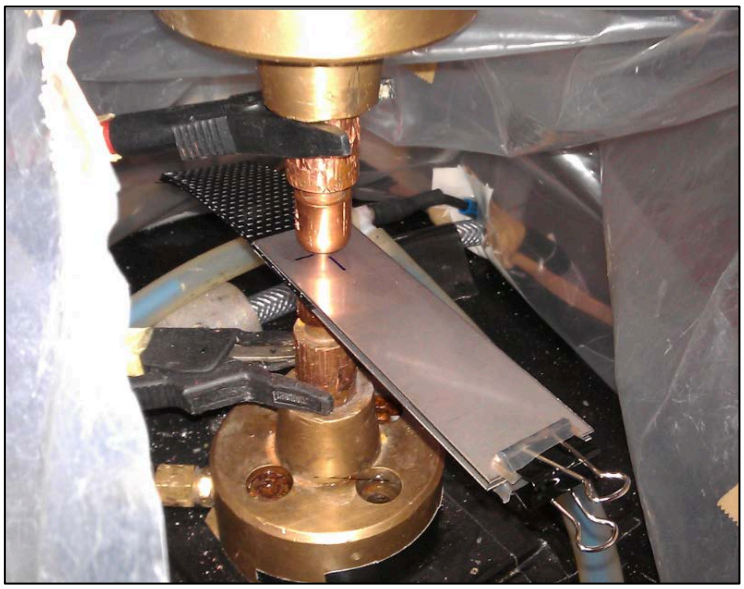

Figure 4-7 - Resistance spot welding of dissimilar material stack for the purpose of manufacturing lap-shear test specimens

To assess the strength of the multi-material spot weld, test specimens with just metal-to-metal spot welds were also manufactured. These spot weld reference joints had the same geometry and material stack as the multi-material weld test specimens, but with the difference being that holes were cut locally in the carbon fibre fabric, the holes were aligned with the location of electrode positioning, so to enable metal-to-metal welding. The manufacturing steps of these metal-to-metal resistance spot weld test specimens are illustrated in Figure 4-8. Due to the material differences at the welding site the parameters suitable for the metal-to-metal spot-weld would be different to those for multi-material spot weld, and so suitable parameters had to be determined for this arrangement of metal-to-metal spot-welding. The determination of these parameters was achieved quickly, as although there were three sheets of metal in the welding stack (rather than just two in a typical RSW), the observed

instrumentation measurements showed typical resistance welding characteristics, and so enabled rapid identification of optimum parameters, as stated in Table 4-4.

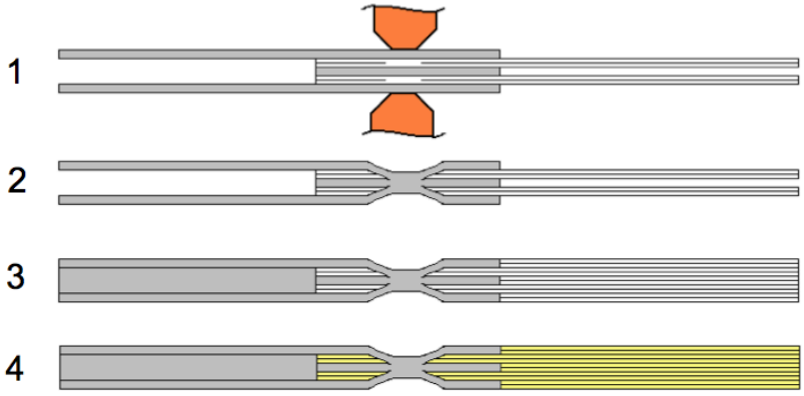

Figure 4-8 - Manufacturing steps of metal-to-metal spot weld reinforced adhesive joint

The second manufacturing process is resin infusion of the lap-shear specimens. Routine vacuum assisted resin transfer techniques were used to infuse the samples with RTM6 epoxy resin. RTM6 was chosen due to its wide use and well understood behaviour, the relatively low viscosity of RTM6 when at infusion temperatures, of 120°C, ensured that the resin would flow into the interleaved stack area, including the weld site. The temperature difference between the infusion temperature and the cure temperature of 160°C, allowed for controllability of the infusion, a dwell at 120°C gave time for the specimens to fully infuse before increasing the temperature to 160°C to speed the onset of resin gelation.

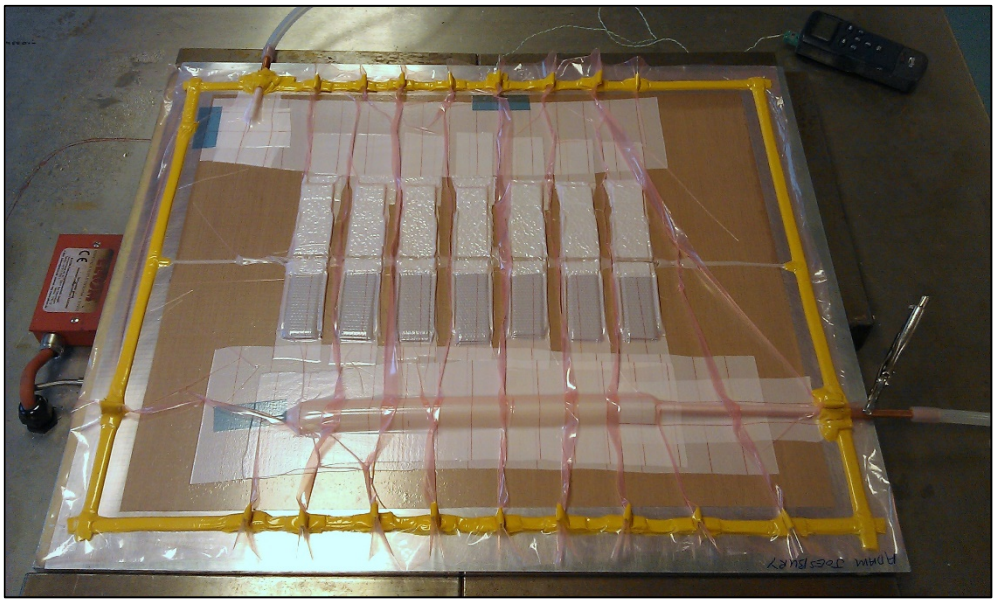

Figure 4-9 - Resin infusion assembly of seven resistance spot braze-weld reinforced adhesive lap-shear test specimens

The test specimens were infused in batches. Seven specimens were cured in each batch; with specimens of each test configuration being cured in each batch, so that any variation that might occur between one infusion batch and another would not result in a systematic error for any individual test specimen configuration. The infusion and cure schedule was as follows:

1. Heat resin infusion assembly to 120°C
2. Weigh resin into reservoir and heat to 80°C and degas in a vacuum chamber, repeating this stage three times to ensure maximum amount of gas is removed from the resin
3. Transfer resin reservoir to 80°C heated hot plate at infusion in-feed position
4. Infuse at 120°C until parts are observed to be wetted-out
5. Seal-off resin inlet and ramp infusion assembly temperature to 160°C
6. Dwell infusion assembly at 160°C for 120 minutes and then allow to cool naturally to ambient temperature

Of the first set of infusion specimens manufactured one specimen was microsectioned to confirm that resin had fully infused both the fibre fabric and also the area of spot-weld. Further detail of this investigation can be found in Section 4.4.3.

To summarise the joints constructed to test the joining concept:

An effective Double Lap Shear (DLS) joint was made between two 0.9mm thick sheets of stainless steel 304L and a combined 3.7 mm thickness laminate of composite material, which itself was comprised of Hexcel G1157 carbon fibre UD reinforcement in a RTM6 epoxy matrix. The joint is shown diagrammatically in Figure 4-1. The hybrid joining method consists of an interleaved adhesively bonded region; this region is mechanically reinforced by the pre-infusion application of a resistance spot weld-braze. The interleave technique is required to facilitate resistance spot welding through carbon fibre fabric, see Section 4.2.1. The interleaved stack is as follows, from bottom to top: 0.9mm thick steel (lower DLS arm), two plys of 0.25mm thick carbon fibre fabric, central 0.9mm thick steel interleave, two plys of 0.25mm thick carbon fibre fabric, and finally 0.9mm thick steel (upper DLS arm). Details of the mechanical test specimen are provided in Figure 4-10.

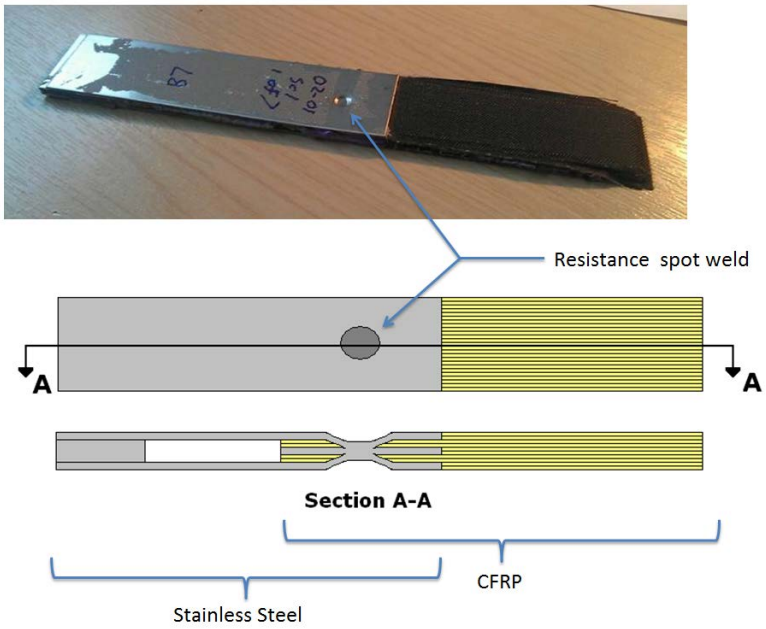

Figure 4-10 - Example of the manufactured 'resistance weld reinforced adhesive joint' test specimens

4.3 Mechanical testing

4.3.1 Tensile testing of various configurations

To evaluate the performance of this joining technique various structural configurations were tested, as detailed in Table 4-5, the variety of configurations were investigated so to understand the strength contributions provided by the various joining elements, i.e. adhesive bond and resistance spot weld, and so to give insight into the overall performance of this hybrid joining method.

Structural configuration	Adhesive bond	Weld	Fibres at weld	Comment	Test ID
Adhesive bond only 	Yes	No	NA	Adhesively bonded joint with no weld or mechanical reinforcement. To determine the adhesive strength	1
Weld (fibres) only 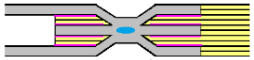	No	Yes	Yes	Release film placed between fibres and metal prior to infusion. To prevent adhesive bonding between metal and the composite; to test the strength of the resistance braze-weld, and so understand the effect on weld strength resulting from contamination by carbon fibre.	2
Weld (no fibres) only 	No	Yes	No	Release film placed between fibres and metal prior to infusion. Holes cut in fibre fabric to facilitate uncontaminated welding. To determine effect on weld strength due to carbon fibre contamination of weld.	3
Weld (fibres) and adhesive bond 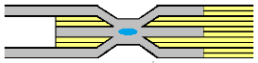	Yes	Yes	Yes	Resistance spot weld through carbon fibres, together with adhesive bonding between laminate and metal. Joint of specific interest in this study.	4

Structural configuration	Adhesive bond	Weld	Fibres at weld	Comment	Test ID
Weld (no fibres) and adhesive bond 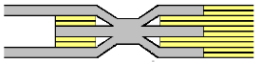	Yes	Yes	No	Holes cut in fibre fabric to facilitate uncontaminated welding, together with bonding between laminate and metal. To determine effect on the joint strength due to carbon fibre contamination of weld.	5
Adhesive bond reinforced by mechanical fastener 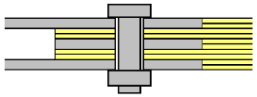	Yes	No	NA	Installation of a mechanical fastener post adhesive cure. Evaluate the performance of the resistance spot weld reinforced joint against a more typical type of mechanically reinforced joint.	6

Table 4-5 - Description of the structural configurations of the various test specimens

The test equipment and procedure used for the RSW reinforced adhesive joint mechanical tests specimens was the same as used for the micropin reinforced adhesive joint, which is described in Section 3.3.1. The test specimens were prepared by adhesive bonding aluminium tabs to the composite laminate in the area that were to be clamped in the testing machine. Laser extensometer reflective strips were applied at the boundaries of the joint interface, as described in Figure 4-1. Mechanical testing was performed using an Instron 5500 operating with a 100kN load cell at a cross-head displacement rate of 1mm/min.

4.4 Metallographic inspection

4.4.1 Microsection directions

Figure 4-11 provides an illustration of the direction of microsections made through the various specimens. The illustration is a plan view of a generic spot weld sample, in the illustration the black lines represent carbon fibre and the blue area represents metal sheet (the blue area is semi-transparent to aid visualisation of the carbon fibre sandwiched between metal sheets) with the blue circle representing the location of a spot weld. Section A-A is described as transverse, as it is transverse to the direction of the carbon fibre. Section B-B is described as longitudinal, as it is along the length of the carbon fibres.

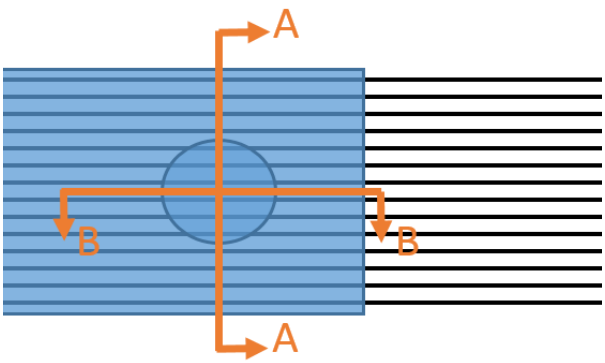

Figure 4-11 - Illustration of microsection directions; Section A-A is transverse direction and Section B-B is longitudinal direction

4.4.2 Microsection preparation

Standard sectioning and polishing procedure was used; as detailed in Section 3.4.1.

4.4.3 Extent of resin infusion

To check the extent of resin infusion a microsection was taken through an infused multi-material spot weld, as shown in Figure 4-12. This microsection was intentionally unpolished so to leave scratch marks on the section. Figure 4-12 shows an area of defect in a weld. The light grey is stainless steel, the

medium grey is carbon fibre remnants, and the dark grey is porosity in the weld. The presence of parallel scratch marks across the entire sample shows that RTM6 not only infuses the fibres but also penetrates into the weld defects.

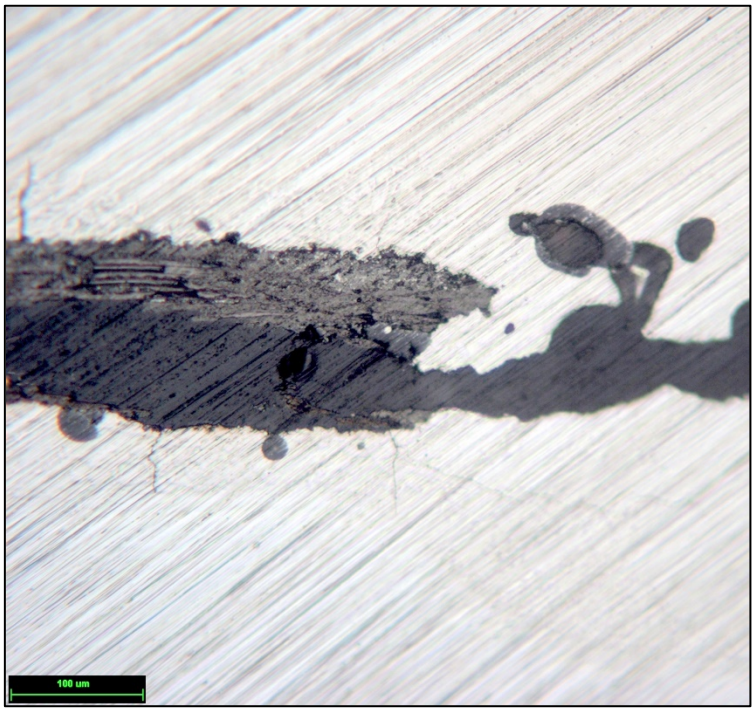

Figure 4-12 - Cross-section of infused spot braze-weld

4.4.4 Chemical etching for the identification of weld nugget composition

To observe microstructure detail of the resistance spot welds, specimens were subjected to a chemical etching procedure. Use of Kalling's No. 1 etchant was chosen due to suitability for use with stainless steel. The etchant was applied to polished surfaces using a cotton wool swab for an expose time of 10 seconds followed by rinsing in flowing water for up to 30 seconds. This relatively short etchant application time proved sufficient to reveal microstructure detail in the welds.

4.5 Results and Discussion

4.5.1 Trials of various metals

4.5.1.1 Result of trials with titanium

The following table and figure, Table 4-6 and Figure 4-13 respectively, show the results of the parameter trials using titanium, which was part of Study 1, as described in Section 4.2.1.

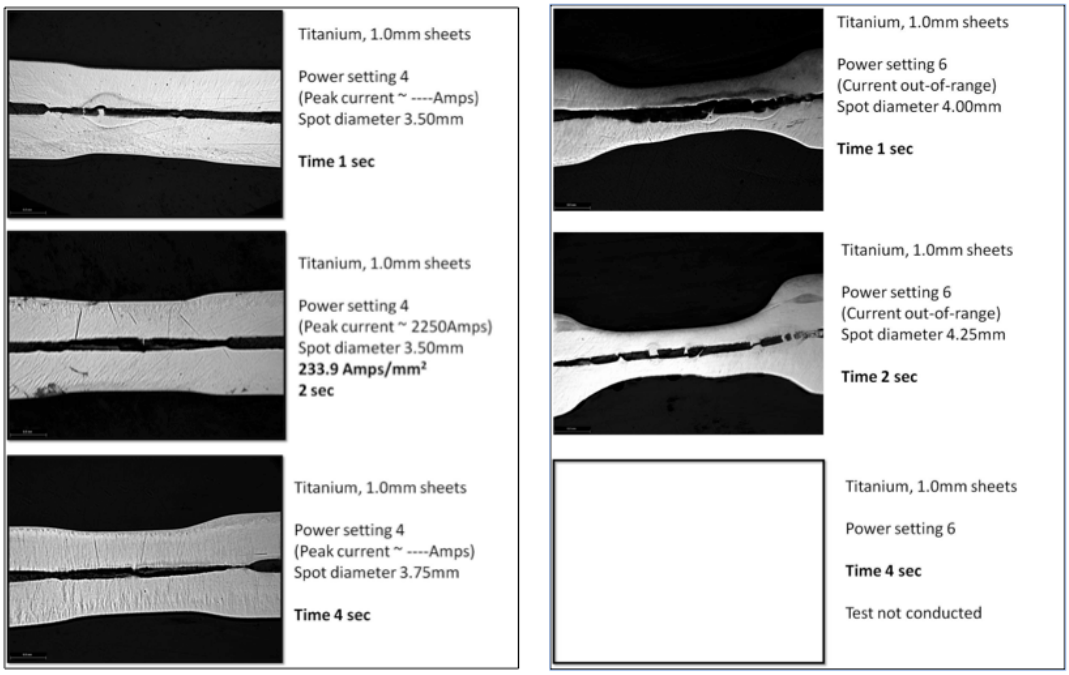

Figure 4-13 - Microsections of trials with titanium

Power setting (kW)	1 sec application	2 sec application	4 sec application
2	• Some visible effect to fibres in current application area	• As 2kW-1sec sample plus: • Material stack very slightly stuck together	• As 2kW-1sec sample
4	• Slight HAZ on external surfaces of Ti • Fibres transferred to Ti and material interface in current application area • Ti internal surface HAZ slightly elongated in fibre direction	• Material stack handleable without falling apart • Forced apart by hand • Fibres transferred to Ti and material interface in current application area • Ti internal surface HAZ elongated in fibre direction • Some surface depression at electrode contact points	• As 4kW-2sec sample plus: • Greater surface depression at electrode contact points • Larger internal HAZ
6	• Sparks expelled from within material stack, sparks expelled in fibre direction • Deep deformation at electrode contact points • Material stack cannot be separated by hand	• Not conducted due to observations of 6kW-1sec sample	• Not conducted due to observations of 6kW-1sec sample

Table 4-6 - Observations of parameter trials for titanium

Simple by-hand destructive testing at the time of specimen production showed that the parameters of: 4kW for 2sec, 4kW for 4 sec, 6kW for 1sec, and 6kw for 2sec, produced a joint that could not be separated by hand. When specimens produced using the same parameters were microsectioned it could be seen in all cases that a typical RSW weld-nuggets had not been formed. Metal [faying] surfaces in the area of an expected weld nugget were still separated by carbon fibre, the areas that are around the circumference of the expected weld nugget location are however seen to be in contact.

Figure 4-14 shows a microsection of this circumferential region. It can be seen that the bulk metal of the titanium sheets are connected by weld metal. Furthermore, carbon fibre is also present in this area, and this carbon fibre is thoroughly wetted by the titanium weld metal. An intermediate substance is observable as a medium grey colouration around individual fibres, this is expected to be titanium carbide, which has been formed by interaction of molten titanium and carbon fibre. The presence of titanium carbide is an explanation for the observed good wetting. There are also speckles of medium grey colouration throughout the weld metal region between the bulk titanium sheets. This is also expected to be titanium carbide, however, no EDX analysis was conducted to verify the presence of titanium carbide.

(a)

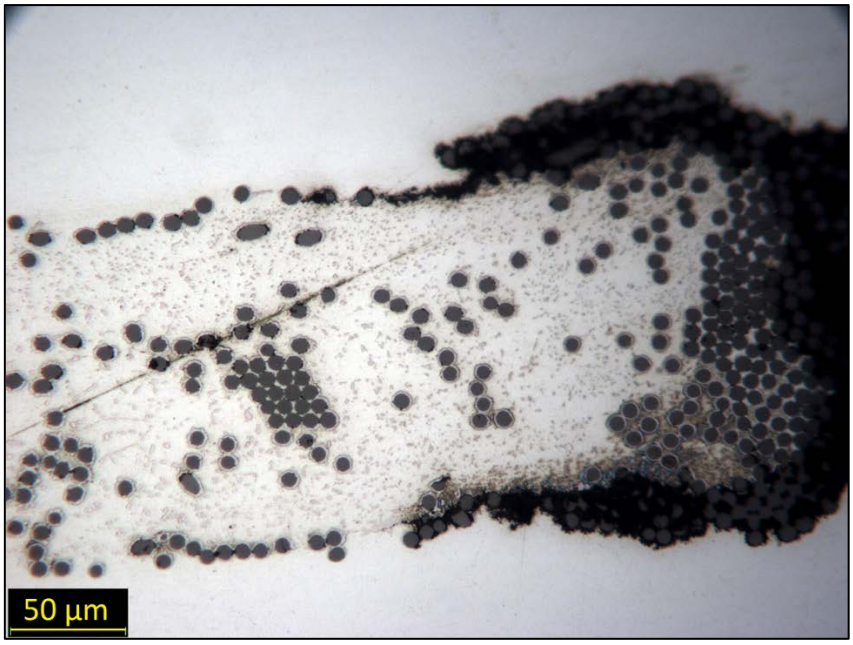

(b)

Figure 4-14 - Microsection of circumferential region around electrode application site, upper image shows location (a), lower image shows detail (b). Images of a specimen produced using parameters of '6kW for 2 sec'.

Though a typical resistance spot weld nugget was not formed, the interaction between molten titanium, the bulk titanium of the metal sheets, and carbon fibre, has produced a joint that is sufficiently strong to resist forces that can be exerted using hand tools.

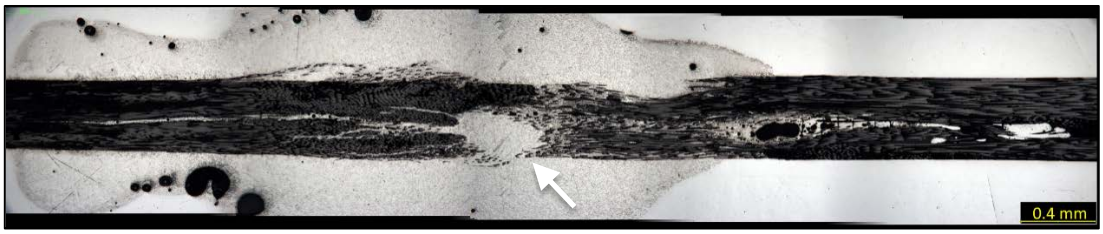

Figure 4-15 - Longitudinal microsection through titanium carbon fibre weld

Overall the weldability of titanium appears to be quite poor. This is likely due to the relatively high melting temperature and high resistivity of titanium. Also, the specific strength of titanium significantly, and rapidly, decreases with increase in temperature. This characteristic of titanium is exploited in superplastic forming manufacturing techniques. However in this through-dissimilar-material welding process this characteristic of titanium could be hindering the process by resulting in excessive flow of titanium in localised regions. This in turn forms local metal-to-metal bridges, which will enable localised high current flow, and undermines the more global Joule heating effect of the RSW process. Localised metal-to-metal bridges, which discreetly penetrate the carbon fibre fabric, can be observed in the upper image of Figure 4-14, and localised excessive flow of metal can be seen in Figure 4-15, as indicated by arrow.

4.5.1.2 Result of trials with stainless steel

The following table and figure, Table 4-7 and Figure 4-16 respectively, are the results of the parameter trials using stainless steel, which was part of Study 1, as described in Section 4.2.1.

Figure 4-16 - Microsections of trials with stainless steel

Power setting (kW)	1 sec application	2 sec application	4 sec application
2	• No observable effect	• No observable effect	• No observable effect
4	• Slight HAZ on external surfaces of SS • Slight surface depression at electrode contact points • Material stack handleable without falling apart	• As 4kW-1sec sample	• As 4kW-2sec sample plus: • Greater surface depression at points of electrode contact • Larger external HAZ
6	• HAZ on external surfaces of SS • Deep surface depression at electrode contact points • Material stack handleable without falling apart	• Sparks expelled from within material stack, sparks expelled in fibre direction • Deep deformation at electrode contact points • Metal flash expelled at points of electrode contact	• Not conducted due to observations of 6kW-2sec sample

Table 4-7 - Observations of parameter trials for stainless steel

The parameter trials using stainless steel produced several specimens that were readily handleable; 4kW for 1sec, 4kW for 2 sec, 4kw for 4sec, 6kW for 1 sec, and 6kW for 2sec. Examination of microsections of samples produced using these parameters showed that, apart from the 4kw for 1sec specimen, a recognisable resistance spot weld nugget was formed to some extent between the sheets of stainless steel.

An explanation for the readiness of weld formation when steel is used, compared to the other metals trialled in this study, is attributed to the affinity of carbon and iron. A weld nugget forms due to carbon fibres being eliminated from the weld site. This is likely to occur due to a combination of factors: the carbon of the fibres being dissolved in to the molten iron of the weld nugget, and transportation of the fibres away from the weld site by the flow of molten metal in the form of weld splash and sparks, which were observed during trials using higher power and greater current application time. The expelled weld splash can be seen in Figure 4-17, which shows a microsection along the direction of fibre orientation.

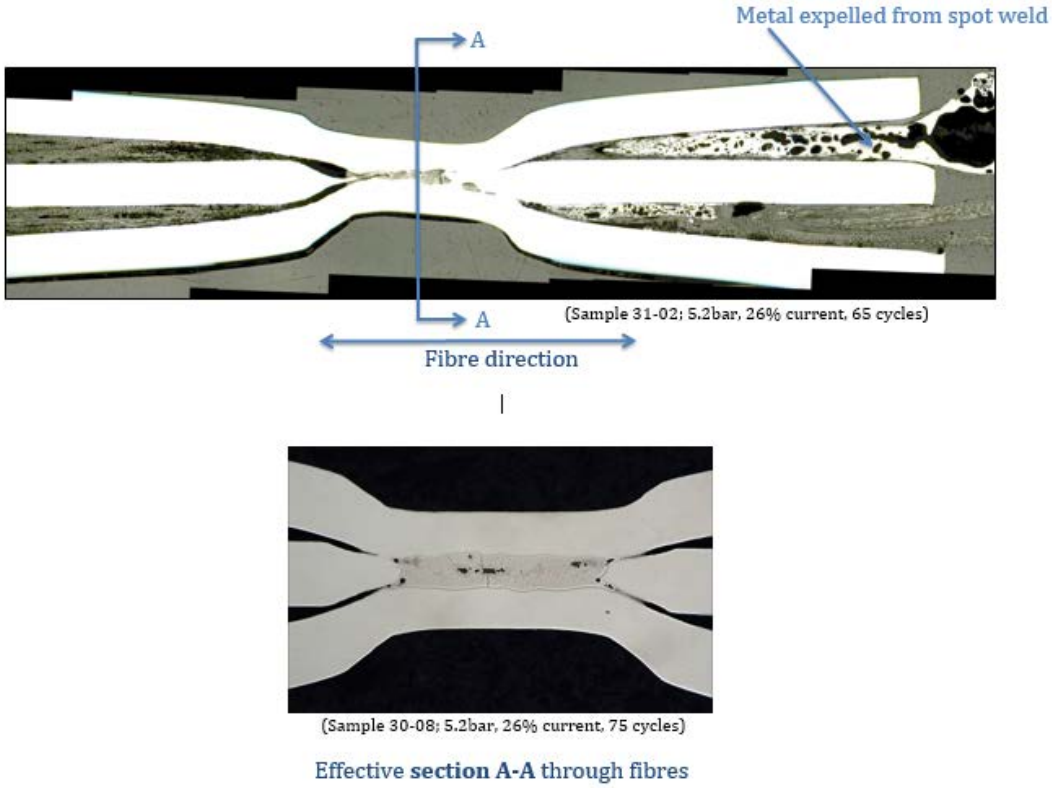

Figure 4-17 - Longitudinal microsection through stainless steel carbon fibre weld, showing an example of weld splash that has flowed away from the RSW site

4.5.1.3 Results of trials with aluminium

The following table, Table 4-8, and figure, Figure 4-18, shows the results of the parameter trials using aluminium, which were part of Study 1, as described in Section 4.2.1.

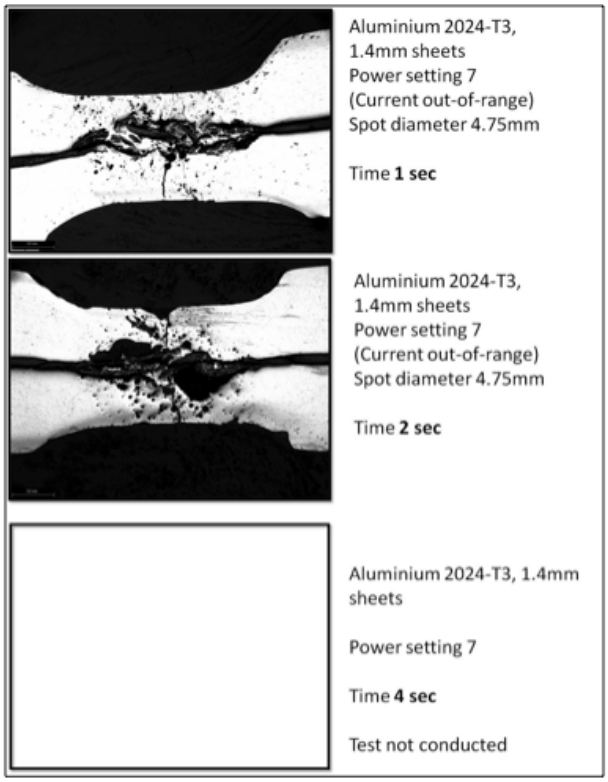

Figure 4-18 - Microsections of trials with aluminium

Power setting (kW)	1 sec application	2 sec application	4 sec application
2, 4, 6, 8, 10	• No observable effect	• No observable effect	• No observable effect
Increase externally applied force			
8	Test not conducted	• Very deep surface depression at electrode contact points • Large amount of metal flash expelled at points of electrode contact • Material stack forced apart by hand	• Not conducted due to observations of 8kW-2sec sample
7	• Surface depression at electrode contact points • Large amount of metal flash expelled at points of electrode contact • Material stack handleable without falling apart	• Large surface depression at electrode contact points • Large amount of metal flash expelled at points of electrode contact • Material stack handleable without falling apart	• Not conducted due to observations of 7kW-2sec sample

Table 4-8 - Observations of parameter trials for aluminium

It is traditionally very difficult to resistance spot weld aluminium due to the high conductivity of the metal. The high conductivity generates low Joule heating of the metal. Therefore high currents are required to generate sufficient Joule heating to enable welding. Porosity is also a common problem in fusion welding of aluminium. Contamination can result in a large amount of porosity. Hydrogen porosity that is as a result of moisture could occur due to moisture absorbed by the carbon fibre fabric. A drying procedure of the fabric prior to welding may have therefore resulted in less porosity.

As explanation of why trials using aluminium showed poor results, possible reactions between carbon and aluminium are considered. From the galvanic series, aluminium is a highly reactive metal. Therefore when it is heated during welding it reacts with the carbon of the fibres and several electrochemical reactions can occur between carbon and aluminium, and carbon and aluminium oxide, some of these reactions producing gases. For example (Madan and Prakash, 1987):

$2\ Al_2O_3 + 9\ C \rightarrow Al_4C_3 + 6\ CO$

$2\ Al_2O_3 \rightarrow 4\ Al + 3\ O_2$

Production of gases by such electrochemical reactions could explain the high levels of porosity seen in the microsections of spot-weld trials using aluminium.

There are other potential contaminants present that could result in porosity of the welds. Carbon fibres are treated with chemical sizing agents to improve processing of fibres during composites manufacture. The sizing agents are typically chemicals analogous to the composite polymer matrix intended for use, which in this case would have been an epoxy, the hydrocarbons of the polymer sizing agent could have contributed to hydrogen porosity of the aluminium welds. It was investigated whether sizing agents could be removed from fibres

by pyrolysis prior to welding. It was found that carbon fibre fabric became too difficult to handle without the sizing agents. In all welds carbon fibre with sizing agents were used. It is considered that any porosity generating contaminant from sizing agents would therefore be a systematic effect across all metals trialled, though it would be likely that some metals may be more susceptible to porosity than others.

4.5.1.4 Summary of the different metals trialled

The greatest flexibility in processing parameters was seen for the material stacks using either titanium or stainless steel. It proved difficult to achieve welding through a stack of aluminium and carbon fibres, and when it was achieved metallographic inspection showed high levels of bulk aluminium degradation. Aluminium has significantly higher electrical conductivity than the other metals investigated in this study. In resistance welding processes metal melting is a result of Joule heating generated by the flow of electric current through the material. The amount of Joule heating is dependent on the resistance of the bulk materials, and also the surface contact resistance between parts being welded (Hongyan and Senkara, 2012). In Table 4-9 the resistivity of the metals of interest is provided. As stated above, resistance welding of aluminium is difficult due to the low amount of Joule heating generated within the metal and so the majority of heating will be generated as a result of contact resistance. In this case the conduction path contact is between the metal and carbon fibre fabric. As heat energy is being generated at the point of contact between the aluminium and carbon this region is highly energetic and also the situation is suitable for the electrochemical reactions detailed above to take place.

It has also been observed that with all three metals there are regions of carbon fibre fabric that have been infused with molten metal during the resistance heating process. It has also been seen from the metallographic inspection that

carbon fibres disappear during the process when stainless steel is used but that when titanium is used this happens to far less extent.

The resistivity of the metals of interest in this section are provided in Table 4-9 (Kittel, 1996).

Metal	Specification	Conductivity / $(ohms \cdot cm)^{-1}$	Conductivity / IACS
Titanium	Ti-6AL-4V	5.62×10^3	1.00
Steel	AISI 304	13.9×10^3	2.90
Aluminium	2024-T3	172×10^3	32.0

Table 4-9 - Conductivity of metals of interest

4.5.2 Interleaved ply limit and stacking sequence trials

4.5.2.1 Limit of number of plys

Study 1 of the resistance spot weld investigation enabled the identification of stainless steel as being the metal that enabled production of the best quality joining between sheets of metal and also an interaction between the metal and carbon fibre fabric. The second study investigated how to maximise the number of carbon fabric plys that could be used in the spot weld process, as described in Section 4.2.1.

From Study 1, which used one ply of carbon fibre fabric, it was shown that a range of welding parameters produced reasonable results, these parameters were: 4kW for 1sec, 4kW for 2 sec, 4kw for 4sec, 6kW for 1 sec, and 6kW for 2sec. As the resistance of the material stack was increased by the inclusion of two carbon fibre fabric plys, the upper limit of this range of parameters were first trialled. Figure 4-19 shows a microsection of the result of using welding parameters of 6kW for 2 seconds. Due to good results being readily observed

for two plys the decision was made to not do a parametric sensitivity study but instead to increase the number of plys to three, as the aim of this work was to investigate the upper limit of ply number.

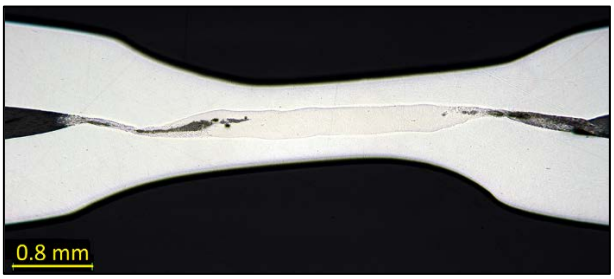

Figure 4-19 - Microsection of resistance spot weld of two plys of carbon fabric between sheets of 0.9mm thick stainless steel, welding parameters: 6kW for 2 seconds (12kJ)

On increasing the number of plys to three a wide range of parameters also appeared to produce good results; this judgment was based on the robustness of the specimens at the time of manufacture. The robustness was determined by conducting a simply destructive test on manufactured specimen using hand tools, though this approach cannot be quantified it gave an intuitive sense of whether the joint formed would be structurally significant. The parameters that produced robust specimens are as follows: 6kw for 2 seconds, 6kW for 4 Wseconds, 7kW for 1 second, 7kW for 2 seconds, and 8kW for 1 second. On sectioning specimens manufactured using these parameters it was observed that a metal-to-metal joint was not achieved in any of the cases as no weld nugget developed. Microsections of samples manufacturing using parameters 6kW of 4 seconds and 8kW for 1 second are shown in Figure 4-20.

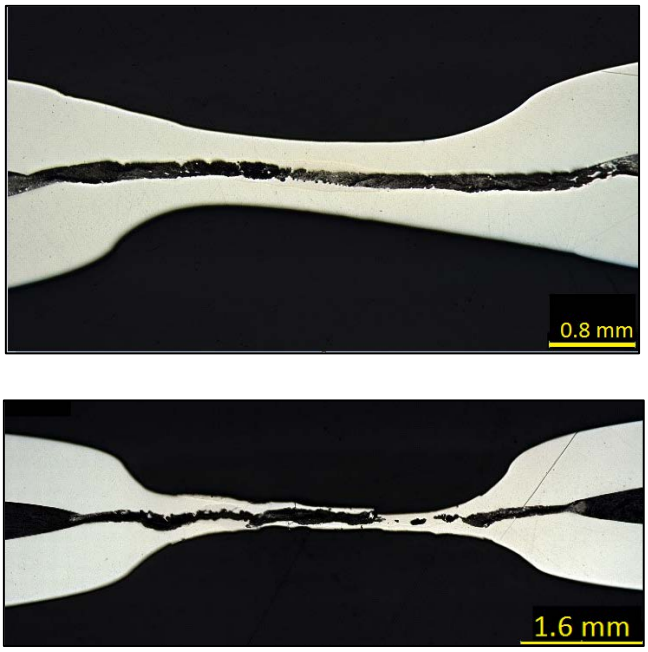

Figure 4-20 - Microsections of resistance spot weld trial of three plys of carbon fabric between sheets of 0.9mm thick stainless steel, welding parameters: 6kW for 4 seconds (24kJ), and 8kW for 1 second (8kJ), respectively

On increasing the number of plys to four only one set of trialled parameters produced a sample that was robust. The set of parameters was 9kW for 1 second, and was at the upper power setting limit of the equipment used. It can be seen from the microsection that no weld nugget is formed; Figure 4-21.

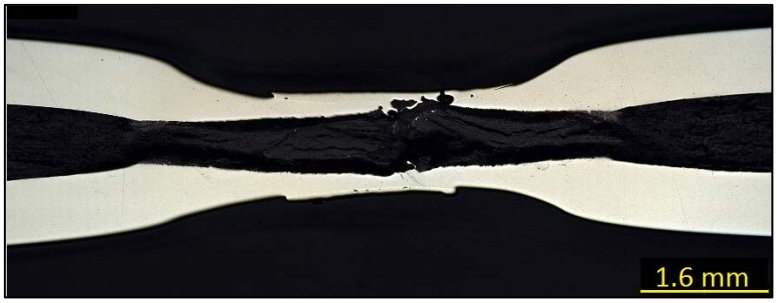

Figure 4-21 - Microsection of resistance spot weld trial of four plys of carbon fabric between sheets of 0.9mm thick stainless steel, welding parameters: 9kW for 1 seconds (9kJ)

It can be concluded from this series of trials, which was to simply increase the number of carbon fibre fabric plys between two sheets of 0.9mm thickness stainless steel, that there is a limit of two plys that can be used and still achieve a metal-to-metal weld characterised by the presents of a distinct resistance spot weld nugget. There is the trend that as the number of plys increases higher welder power settings (greater current density) are required to produce a sample that is sufficiently joined so to be considered as being robust. It can further be seen from the microsections that as the ply number and associated power input increases there is an accompanied thinning of the metal sheets at the site of welder electrode application. The thinning of sheets is a result of weld metal expulsion, in the form of molten metal splash, from the spot weld region. It was observed that when higher power settings are used considerable amounts of flash metal is observed to be expelled from between (within) the material stack, emerging at the edge of the sample, as shown in Figure 4-22 (and previously in the microsection of Figure 4-17).

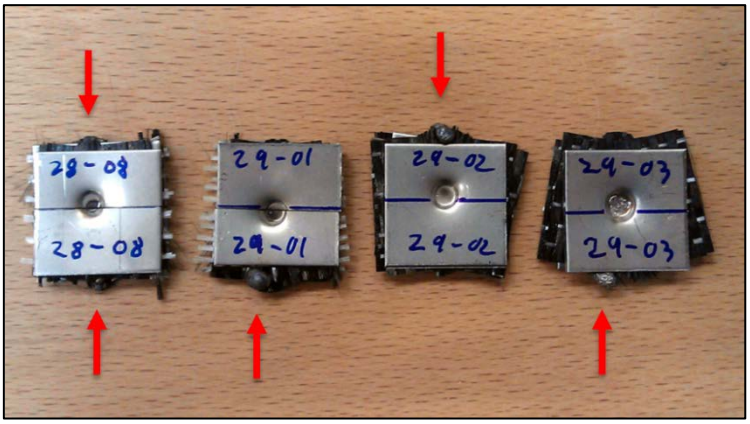

Figure 4-22 – Weld flash expelled at edge of samples; all samples manufactured using 3.7 bar electrode clamp pressure, and power settings of: 26%, 28%, 30%, and 35%, respectively. The size of the metal sheets are 20mm x 20mm.

In a traditional metal-only resistance spot weld the pinch force exerted by of the electrodes not only acts to clamp the metal parts together, this pressure in turn also restrains the position of the molten metal during the welding process and weld nugget formation, as illustrated in Figure 4-23 (a). When plys of carbon

fibre fabric are present in the welding stack, the fibres breach the region of applied pressure that would normally act to contain the molten weld metal. The molten metal can therefore flow away from the expected nugget formation region forming substantial weld splash at the edge of the workpiece, as illustrated in Figure 4-23 (b).

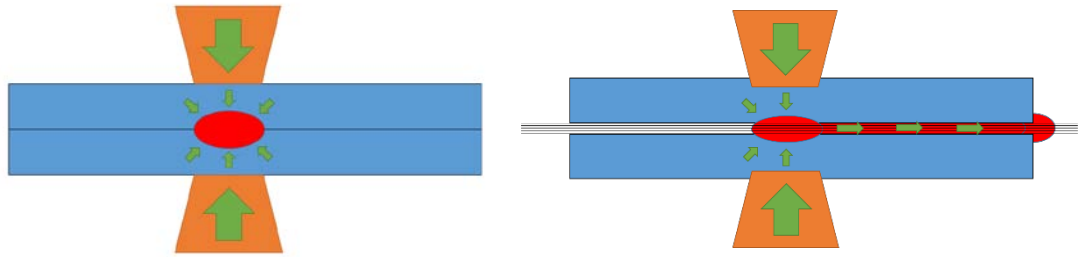

(a) (b)

Figure 4-23 - Diagram of weld nugget formation in traditional metal-only resistance spot welding (a), diagram of molten metal splash flow in multi-material resistance spot weld process (b), arrows represent applied forces

A resistance spot weld nugget, as is observed in Figure 4-19, occurs when the metal from the sheets comes into contact with one another. It was postulated that this would occur in a multi-material spot weld by molten metal permeating through the fibres. Carbon does not have a melting point, but instead sublimates at 3642°C, the temperature of this phase change is substantially higher than the 1450°C melting point of stainless steel 304. In the case of the stainless steel welding no remaining fibres are present in the region of weld nugget formation. This lack of fibres could be explained by the carbon of the carbon fibres dissolving in the iron of the stainless steel.

However the amount of carbon in the fibres could not all be dissolved at the region of the spot weld as it would be above the saturation limit for carbon in iron. Cementite iron carbide is a martensitic super-saturated solid solution of

carbon in ferrite and contains 6.67% carbon. If the volume of materials beneath the 3.5mm diameter electrode contact is considered there is 12.2 x 10^{-3}g of carbon present from four plys of the 277 GSM (Grams per Square Meter) HexForce G1157 carbon fibre fabric. Figure 4-36 shows that the depth of a spot weld nugget is approximately comparable to the thickness of one 0.9mm sheet of metal. The volume of the weld nugget can therefore be estimated to be 9.89mm^3 and the mass of this, if the material was cementite, would be 76.2 x 10^{-3}g. As cementite is 6.67% carbon content the mass of carbon in this cementite weld nugget can be approximately estimated to be 5.08 x 10^{-3} g. The quantity of carbon of the fabric (12.2 x 10^{-3} g) is therefore approximately 2.4 times the amount of carbon that could possibly be present in the weld nugget (5.08 x 10^{-3} g). Therefore the carbon fibres must have been cleared from the weld region via some kind of mechanism.

One possible clearing mechanism could be combustion of carbon fibres, however as welding is done in an inert atmosphere combustion would be minimised to a negligible amount. The act of molten metal flow and resulting edge splash, as described above, is the only mechanism present that could transport carbon fibre away from this region. This would explain the increased thinning of metal with increased number of plys. At the higher ply number trials there is an insufficient amount of metal available to provide a sufficient flow of molten material to clear fibres from the weld nugget formation region; so to enable local metal-to-metal spot weld formation.

The second image of Figure 4-20, and also Figure 4-24, show samples in which almost all metal was exhausted from the RSW site therefore preventing formation of a weld nugget. In cases where trials used greater energy input the limit of available metal was exceeded, permitting electrodes to penetrate the metal and come into direct contact with carbon fibre, this would cause contamination and damage to the electrode tips as carbon from the fibres would transfer to the copper electrodes. The electrode tips would then require dressing to restore the electrode surface condition and geometry. In extreme cases the electrodes and the workpiece would fuse together.

There is the trend of increased current being required to form spot welds as the number of plys increases. The use of elevated resistance spot welding currents is conducive to the weld splash phenomenon in traditional metal-only resistance spot welding. Therefore it could be reasoned that the greater amount of weld splash generated, by the use of higher currents, aids in the ability of this process to effectively clear fibres from the weld nugget formation region, thus enabling the formation of a metal-to-metal RSW that has penetrated the carbon fibre fabric.

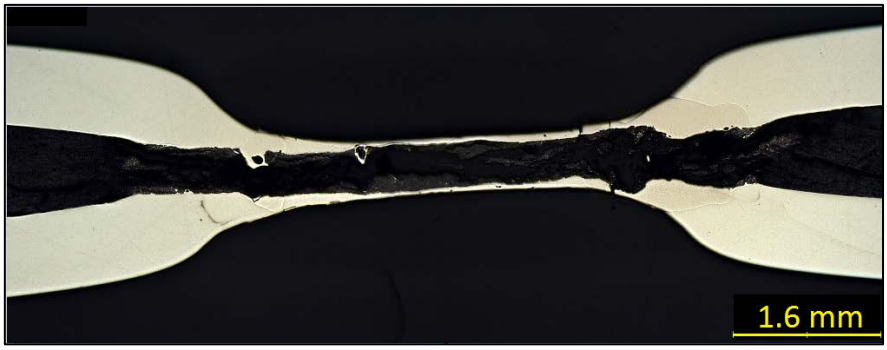

Figure 4-24 - Microsection of resistance spot weld trial of four plys of carbon fabric between sheets of 0.9mm thick stainless steel, welding parameters: 7kW for 2 second (14kJ).

4.5.2.2 Interleaved stacking sequence

The results shown in Figure 4-25 detail the various stacking sequence trialled, together with accompanying microsection, and welding parameters of the best achieved results.

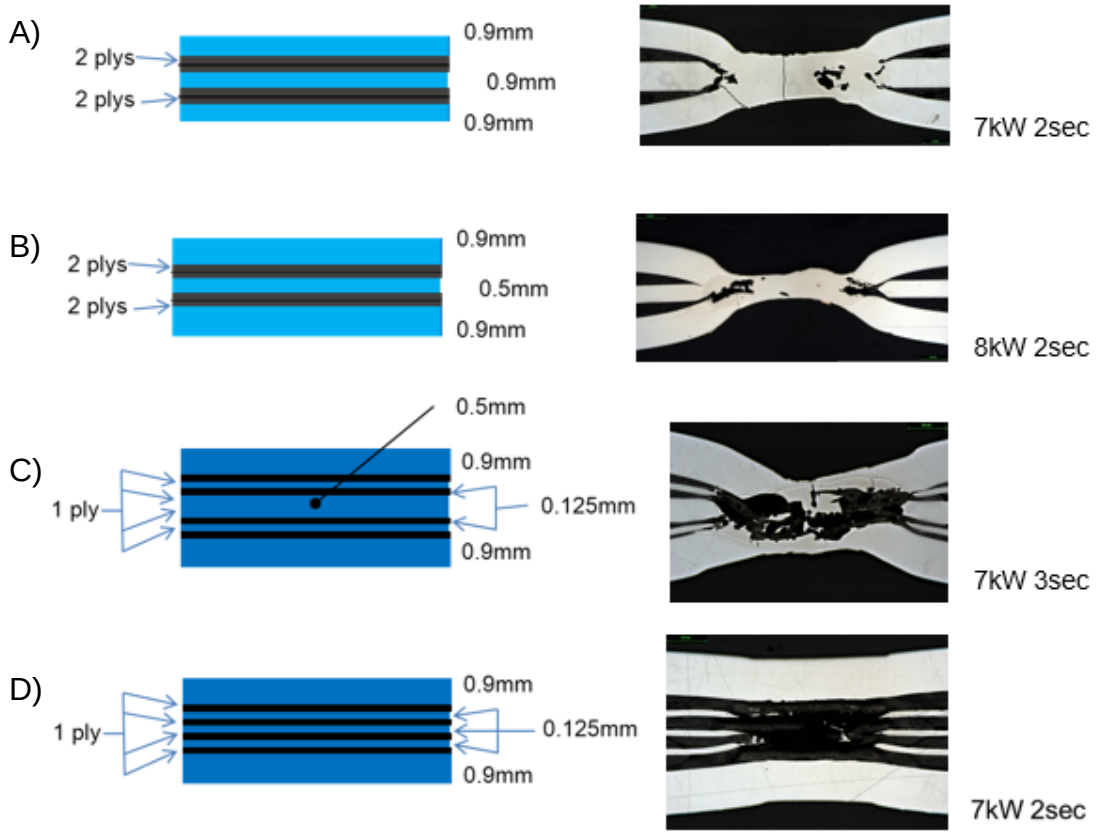

Figure 4-25 – Best achieved results for each trailed interleaved stacking sequence

It can be seen that out of the various trialled stacking sequence the best quality spot weld nugget was achieved with the stacking sequence of: 0.9mm steel, two plys, 0.9mm steel, two plys, 0.9mm steel; Figure 4-25 (A). This result is most likely due to this stacking sequence containing the greatest amount of metal, and therefore providing the greatest supply of molten metal during the welding processing to be available to flow and clear the region of carbon fibre, and therefore enabling metal to metal welding. The multiple metal sheets and foils used in the other trialled stacking sequences could have acted to impede the flow of molten weld splash metal away from the weld site, therefore restricting the clearing action of the fibre.

4.5.3 Through thickness resistance characteristic as a function of pressure

Resistance welding is reliant on the Joule heating phenomenon to raise the temperature of the metal above the melting point to enable fusion welding. In the resistance welding process there are two distinct types of resistances: the bulk material resistance, as provided in Table 4-2, and the contact resistance between the parts being welded together. For the interleaved material stack the contact is between dissimilar materials that have significantly different bulk material resistivities. Understanding of the situation is also complicated by the carbon being in the form of a fabric comprised fundamentally of 6 µm diameter carbon filaments. There was no information in the literature for the conductivity values of carbon fibre fabric in the through-the-thickness direction. Figure 4-26 shows the result of a study of direct measurement to gain understanding of the through-the-thickness resistivity of carbon fibre fabric and how the resistivity is affected by changing the pinch force of the electrodes.

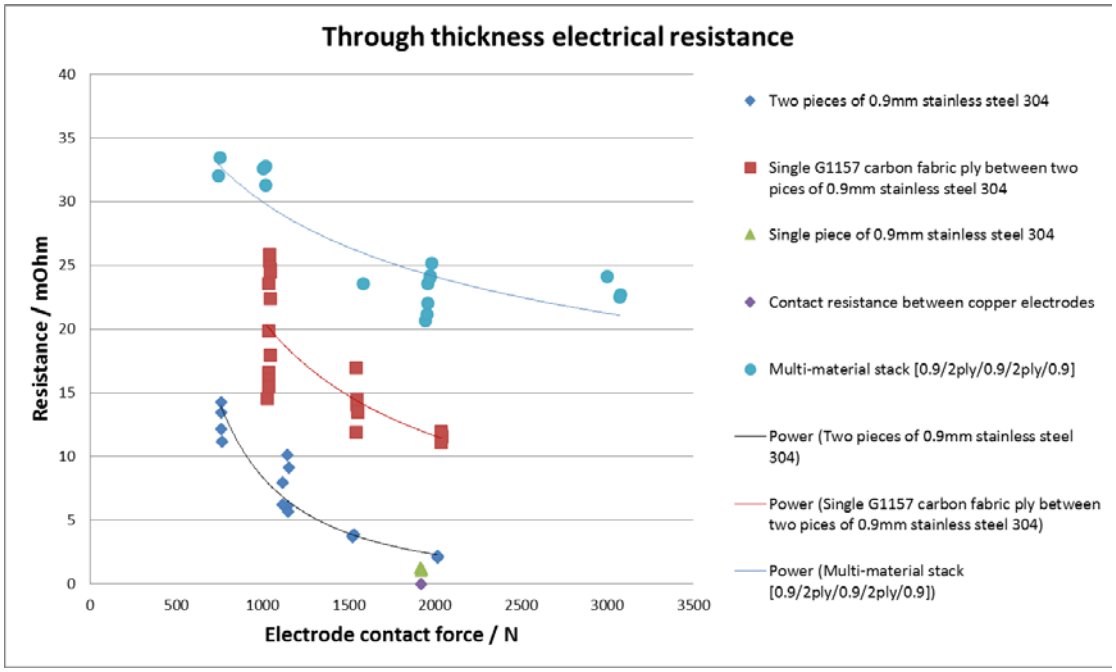

Figure 4-26 - Through thickness resistance change with change of electrode clamp force

The trend in all cases is that as the pinch force increases the resistance decreases. It can also be seen that this relationship is asymptotic. With the asymptote beginning at a pinch force of 2.1kN for the case of the optimally interleaved multi-material stacking sequence identified in Section 4.5.2. In all cases the electrode contact area was circular with a diameter of 3.5 mm, so to ensure the contact interface is the same as used in the parametric studies that will be discussed in Section 4.5.5.

In the metal-to-metal case, as the pinch force increases the contacting surfaces are compressed together, this increases the surface contact area at the microscopic scale; this effect is illustrated in Figure 4-27. The increase in contact area is an increase in the cross-sectional area of the electric current flow path therefore explaining the characteristic of decreasing resistance with increasing pinch force.

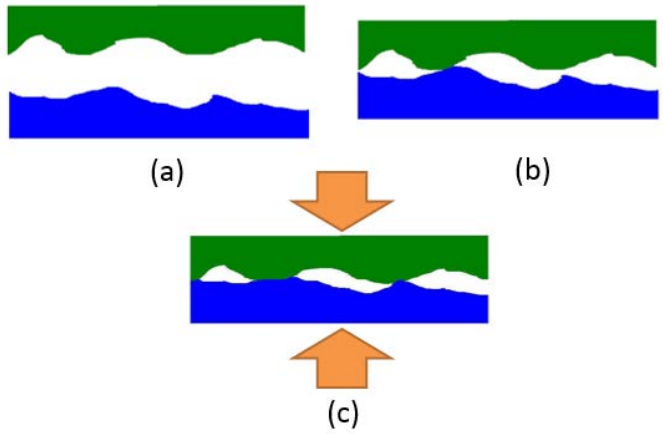

Figure 4-27 – Illustration of microscopic increase of interfacial contact area with application of pinch force. Microscopic roughness of interface surfaces (a), touch contact of interfaces (b), increased contact due to local compression (c).

The situation is however different for the multi-material interleaved stack. The fibrous form of the carbon fabric is less likely to impart the same contacting hard points as shown in the example of Figure 4-27. In this case the pinch force will

increase the nesting density of the fabric, as illustrated in Figure 4-28, which results in a greater number of contact points between the fabric and the metal and also between fibres within the fabric. This creates more current pathways through the fabric and therefore having the same effect of reducing the overall electrical resistance as seen in the metal-to-metal example.

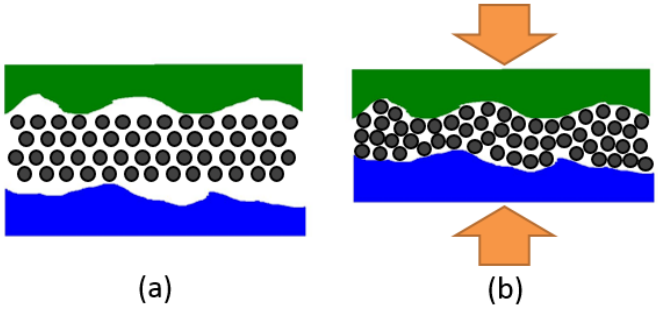

Figure 4-28 - Illustration of microscopic increase of carbon fabric nesting density. Metal-fabric-metal interface (a), increased fabric nesting density with application of pinch force (b).

The asymptotic nature, observed in Figure 4-26, is due to the physical limits of compressibility of surface contact points and nesting of fabric, in metal-to-metal and multi-material stacks, respectively. Though it can be identified that the electrical resistance asymptote begin around the 2.1kN pinch-force load level, and therefore from an electrical resistance consideration it can be said there is little reason to increase beyond this pinch force. However, the identified feature of multi-material welding is the effect of molten weld metal splash flow clearing fibre from the weld nugget formation region, as discussed in Section 4.5.2. The resulting pressure applied to the weld nugget formation zone will affect the rate at which splash is ejected. This could explain why improved quality welds were seen with pinch forces above 2.1kN. A force in the order of 4.2kN was used to manufacture the mechanical test specimens (as will be discussed in Section 4.5.5). As part of the parametric studies it was seen that a pinch force above 4.2kN was likely to produce welds that appeared to be of further improved quality, however this was beyond the limit of the equipment that was used and so placed doubts on the consistency of manufactured specimens. Therefore 4.2kN was chosen as the pinch force for specimen manufacture. The higher

splash expulsion rate generated by the higher pinch pressure would appear to more effectively clear the weld nugget formation zone of the carbon fibre remnant contamination.

Among the results displayed in the chart in Figure 4-26, the multi-material interleaved stacking sequence of metal-fabric-metal (red square data points) and metal-fabric-metal-fabric-metal (blue circle data points), the former contains two metal-to-fabric interfaces in the current flow direction and the later has four metal-to-fabric interfaces. As the number of interfaces is doubled the value measured for the resistance is doubled. The quantity of carbon fabric is doubled and the quantity of metal is 50% greater. This suggests that the carbon fabric and the metal-to-fabric interfaces generate the dominant values of resistance in the circuit, this is to be expected given the comparative resistances provided in Table 4-2, it also supports the expectation that the relationship between number of interfaces and overall resistance is linear.

4.5.4 Interleaved multi-material welding characteristics

Understanding of the novel process of welding through a multi-material interleaved stack was significantly enhanced by instrumentation of the welding equipment. This section discusses the nature of the process that was uncovered due to the measurements made. Measurements of how the current, electrode force, and electrode displacement changed during the welding events enabled identification of distinct characteristics that could be looked for to identify whether the resistance welding process was complete. The welding equipment used generated an alternating electric current therefore the traces measured are fundamentally sinusoidal in nature.

Figure 4-29 provides an example of a metal-to-metal resistance weld. Two characteristics that identify the welding process as being complete can be seen in the measured traces of the electric current and the electrode displacement.

During the welding event the peak absolute magnitude of the electric current pulses increase up to a maximum and asymptotes, which indicates the welding process is complete; as the system has reached an equilibrium state with a stable current flow that is greater than at the start of the welding event. The increase in current is because as the weld nugget forms during the welding process the cross-sectional area, in the current flow direction, increases; the larger this cross-sectional area the greater the permitted current flow. As discussed in Section 4.5.3 there is also a relationship between the current flow-path cross-sectional area and the Joule heating generated. Resistance welding equipment is based on set power output. Therefore an equilibrium condition is reached with a maximum current that can be driven by the welding equipment power setting and a corresponding amount of Joule heating, and resulting weld nugget formation, that can be generated by that maximum current. The welding event is described as a dynamic event as the current and pinch pressure change during the welding event due to metal melting and flow. The characteristics of the dynamic process affect the quality of the resulting weld. If the events are of too low energy the weld nugget will be under-formed and the weld quality will be limited. If the weld events are of too high energy then degradation of the workpiece will occur due to excessive metal melting, which is subsequently lost as weld splash, and the quality of weld will be degraded.

An example of measurements taken during the resistance spot welding of an interleaved multi-material stack is shown in Figure 4-30. This figure includes lettered annotations on the time axis (A through F) that will be referred to in the following discussion.

Significant differences can be seen between the metal-to-metal (MTM) and the interleaved multi-material (IMM) welding measurements. The first difference of note is the time taken for the welding processes. The IMM process takes a much greater time to reach a post weld equilibrium state; 1.10 seconds (from the beginning of zone A (current-on) through to the beginning of zone F (equilibrium state reached), compared to the 0.20 seconds of the MTM process. The fusion event of the IMM weld can be described as the metal melting

accompanied by local material flow; this resulting loss of material rigidity enables the electrodes to move towards each other, and is observable in the measurements (zone C). In the MTM process this takes 0.16 seconds and in the IMM process 0.6 seconds. This longer time is likely due to time required for weld splash to flow out of the nugget formation region, clearing the region of the majority of carbon fibre contamination, before metal-to-metal welding can occur.

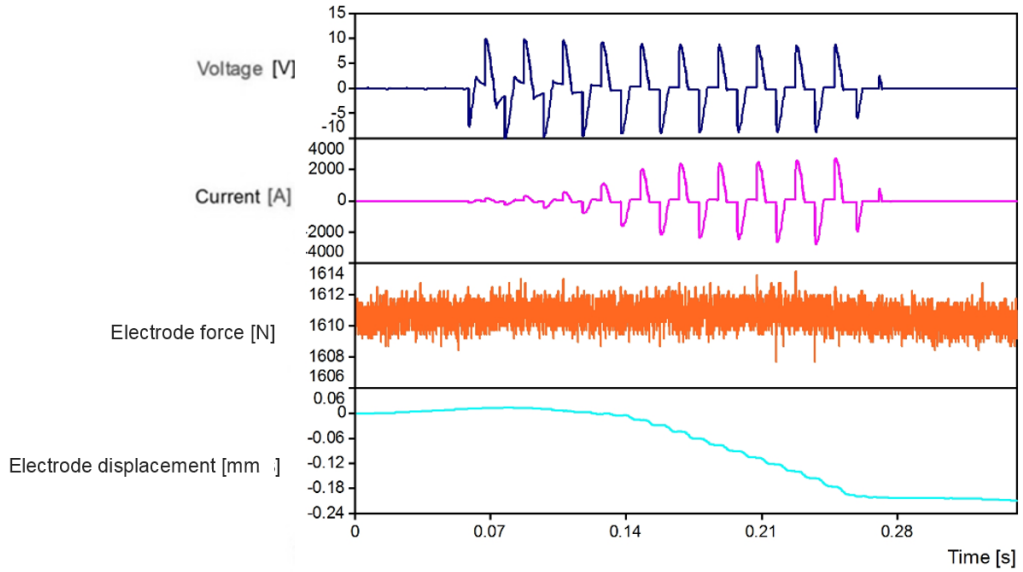

Figure 4-29 - Instrumentation readings of metal-to-metal resistance spot weld

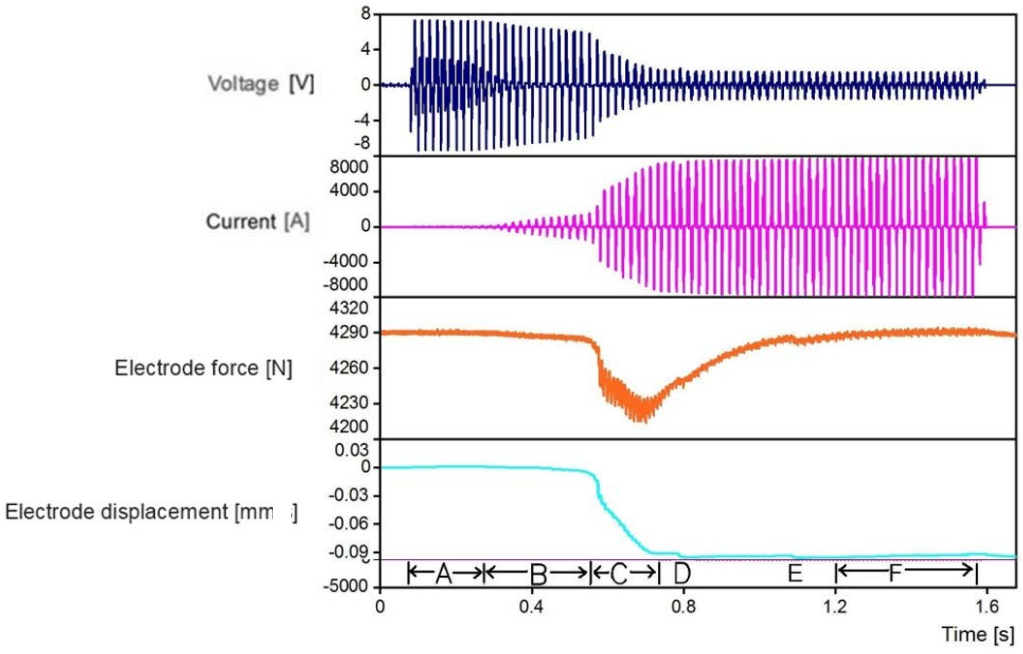

Figure 4-30 - Instrumentation readings for the multi-material resistance spot weld

In the traces shown in Figure 4-30 it can be seen that by the start of zone F the post weld event equilibrium state has been reached and that also the electrode force has recovered to the full load. The reduction in load associated with the welding event is considered to be as a result of the electrode movement during the welding event. The electrode pinch force is driven by a pneumatic system, as the electrode moves pressure in the system momentarily drops, when movement of the electrode stops the pressure in the system is able to recover and therefore so does the exerted pinch force. However, the same pressure drop and recovery is not seen in the MTM weld, Figure 4-29, even though both welding processes experience similar behaviour of electrode displacements. It is uncertain why this is the case, one explanation could be the speed of the processes; perhaps the relatively short duration of the MTM welding process does not afford the pressure change events to be observed.

In addition to the unexpected observation of no force drop and subsequent recovery of the MTM weld there is also unexpected measurements of electrode displacement. It would be expected that the electrode displacement would be greater for the IMM weld than the MTM weld due to the metal thinning of the IMM welding process due to high amounts of weld splash. The electrode displacement of the MTM weld is measured to be 0.21mm and the IMM weld is only 0.10mm. Further investigation would be required to understand whether there is great variance in electrode displacement of the two welding process and also to assess whether the vibrometer is sufficiently calibrated. Due to these uncertainties the measurements by the vibrometer were used simply as indicative of electrode movement and the subsequent identification of a post-weld process equilibrium state.

It can be seen in the electrode force and displacement traces for the IMM weld that there are discontinuity features at points D and E, Figure 4-30, these discontinuities frequently coincided with events observable by the equipment operator, such as popping and creaking noises or sparks being emitted from within the interleaved layers. They are therefore measureable features associated with the weld settling into the post-weld equilibrium condition.

4.5.5 Parametric study of multi-material resistance spot welding

This section discusses the parametric study conducted to determine optimum resistance spot welding parameters for the chosen interleaved multi-material stack; as determined by Study 2 and detailed in Section 4.5.2. The efficiency of the parametric study was greatly improved by understanding the nature of the novel IMM welding process, understanding that was gained by the use of welding equipment instrumentation. The process characteristic identified, and discussed in Section 4.5.4, where considering together with microsection evaluation of welds. This enabled a more complete understanding of the welding process to be revealed, which in turn streamlined the procedure of determining optimum welding parameters.

Section 4.5.4 discussed how instrumentation measurements can be used to identify the post weld-event equilibrium condition. This observation enabled the time parameter to be omitted from the parametric study; as during the parametric study welding duration could be set to have excessive length so to allow the equilibrium state to be reached. From examination of the instrumentation measurements it could then be identified how much time could be trimmed from the welding process; Zone F in Figure 4-30. Therefore the parametric study could be limited to: welding power, and electrode pinch pressure. The chart in Figure 4-31 summarises the series of trials that constituted the parametric study.

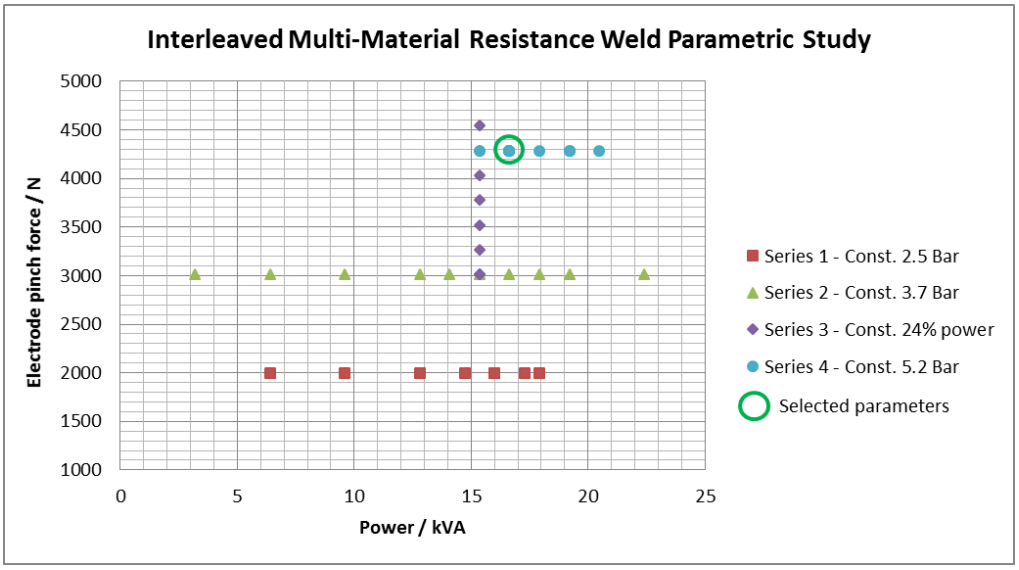

Figure 4-31 - Series of trials constituting a parametric study to determine optimum Interleaved Multi Material resistance spot-welding parameters

In the above chart, Series 1 trialled various power levels while keeping the electrode pinch pressure constant at 2.5 bar (1990 N pinch force), this series produced samples that at the lower power settings were not sufficiently welded; the samples either fell apart or could be easily separated by hand. At the higher power levels weld splash occurred at the electrode-to-workpiece contact points. This suggested that the molten metal at the welding interface was not penetrating the sandwiched fibre fabric and so no weld nugget was formed. Weld nugget formation enables electrical resistance to drop due to the substrate-to-substrate contact resistance being eliminated. The accompanying reduction in joule heating limits the increase in metal substrate melting. In the case of Series 1 the high amount of joule heating generated by the maintained relatively high electrical resistance resulted in metal substrate melting to continue up to the point at which liquid metal breached at the electrode contact interface.

For Series 2; electrode pinch pressure was increased to 3.7 bar (3010 N) and maintained for trials of various power levels. As with Series 1 no reasonable welding occurred at lower power, however when the power was increased to 15.4 kVA (with a corresponding measured maximum current of 6430 A) the

parts were sufficiently joined to prevent them being easily separated by hand. As further trials were conducted with the power level being increased further the welding event was obviously more energetic; with an increase in sparking and weld splash from between interleaved layers. At the highest trialled power settings of Series 2 weld splash breached the substrate at the electrode-to-workpiece contact points. Specimens of the Series 2 samples were evaluated by microsectioning to investigate the extent of welding; these results are presented in Figure 4-32.

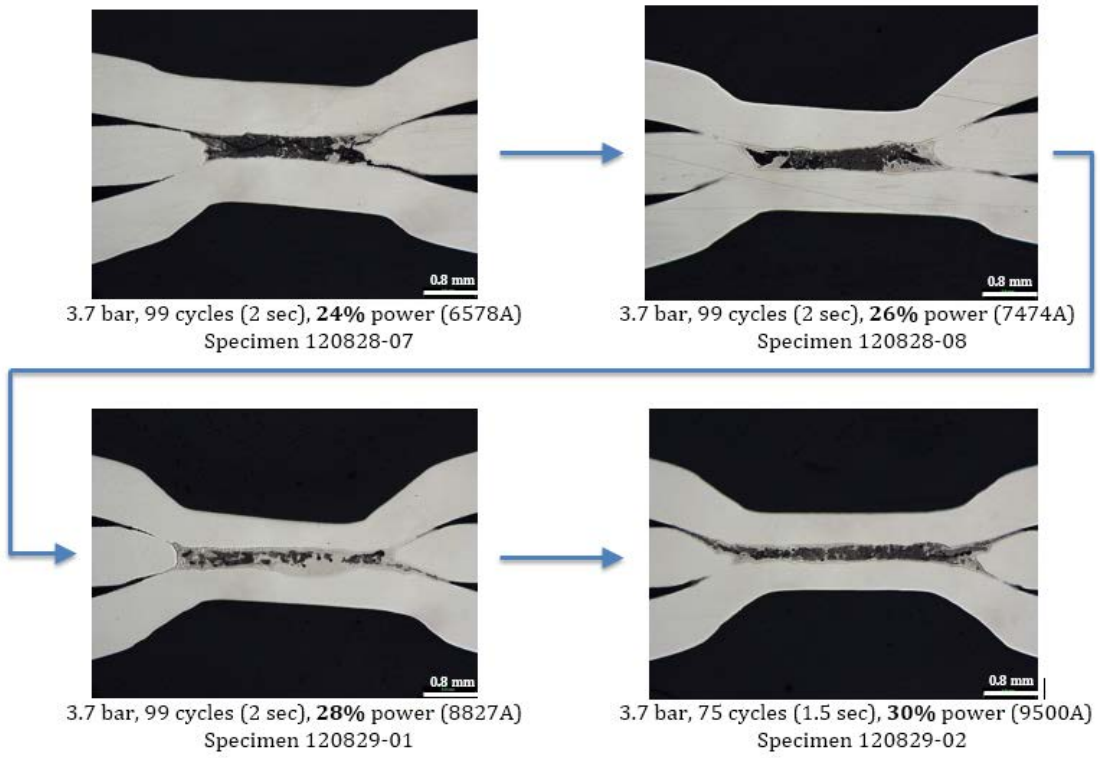

Figure 4-32 – Microsections of parametric study Series 2; constant electrode pinch pressure (3.7 bar) and increasing welding electrical power (driven current)

From the above figure it can be seen that as the power level is increased there is little improvement in weld nugget formation. Two effects that can be seen are thinning of the metal substrate under the electrode contact points and elongation of the weld nugget formation zone. This effect is not time dependant, as in all cases a post-weld equilibrium state was achieved, therefore these variations in the form of the weld interface zone are resultant characteristics of

the weld-event generated by the power and pressure parameters. The increase in power will result in an increase in molten metal generated by the greater Joule heating. The greater quantity of molten metal enables the nugget formation zone to flow into the broader and narrower shape. As the metal substrate has thinned, and during the manufacturing of samples sparks and weld splash were observed, the molten metal must have travelled away from the nugget formation zone. With the increase in molten metal travel the shape of the nugget formation zone has changed into the higher aspect ratio elongated shape.

For Series 3; the power setting was kept constant at 24% (15.7 kVA) and increasing electrode pinch pressures were trialled. At the time of manufacture all the trial samples produced were perceived to be reasonably well joined; parts required significant manual effort using hand tools to separate. Specimens of the Series 3 samples were also evaluated by microsectioning to investigate the extent of welding; these results are presented in Figure 4-33.

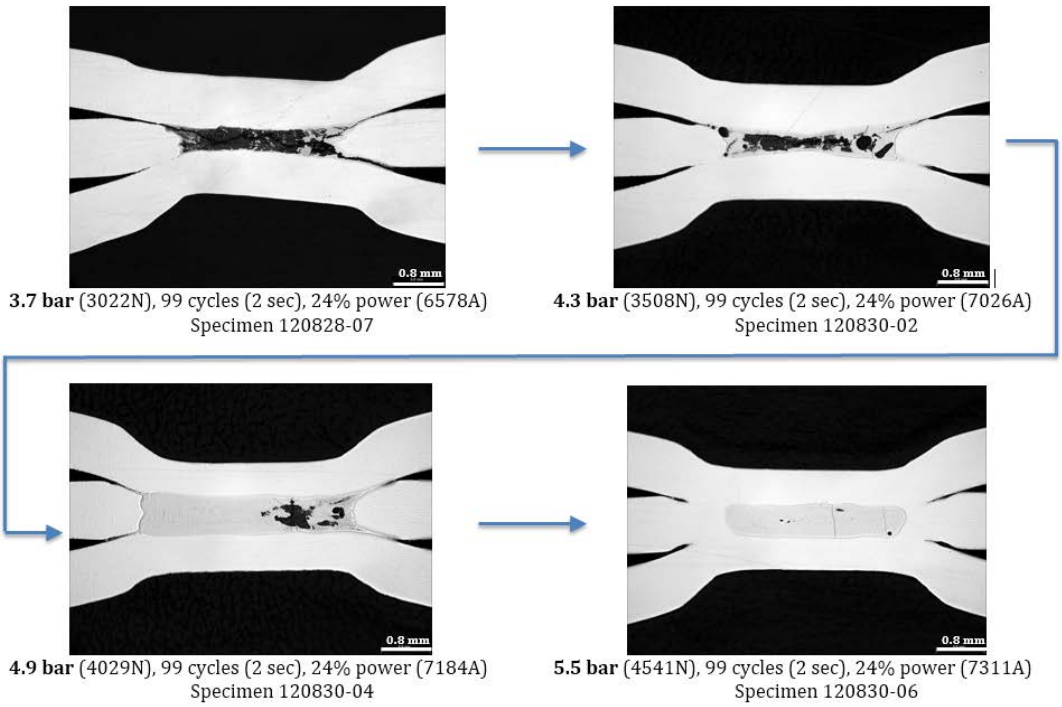

Figure 4-33 - Microsections of parametric study Series 3; constant welding electrical power of 24% of welding equipment capacity (15.4 kVA) and increasing electrode pinch pressure

From the above figure the improvement in weld nugget formation with higher electrode pinch pressures can clearly be seen. A high quality resistance spot weld was formed when a pressure of 5.5 bar (4540 N pinch force) was used. However, this pressure was at the extreme capacity of the welding equipment used and significant load on the pneumatic system was observable as high system leakages. A system pressure of 5.2 bar (4290 N pinch force) was deemed to be the maximum that could be used. This below maximum-capacity pressure was chosen so to not overstress the equipment and also to avoid instability issues that can arise when equipment is operated at the very extremes of capacity.

The importance of the electrode pinch force has clearly been demonstrated in this study. In Section 4.5.3 the effect pinch force has on the onset of a welding process was discussed. This can be summarised as the pinch force determining both the magnitude and variation of the electrical contact resistance (see

Section 4.5.3). Here in the Series 3 trials the effect of the pinch force on the finished quality of the weld is demonstrated. The force applied is significantly above the threshold at which contact resistance is affected by further increase in force, however a second threshold is observed where the containment force is capable of overcoming expulsion of liquid metal even with the factor of a low resistance expulsion flow path that is provided by fibres breaching the weld nugget formation zone.

Series 4 was conducted at the established maximum pressure to investigate whether further weld formation improvements could be achieved with higher power levels, the microsectional evaluation is presented in Figure 4-34.

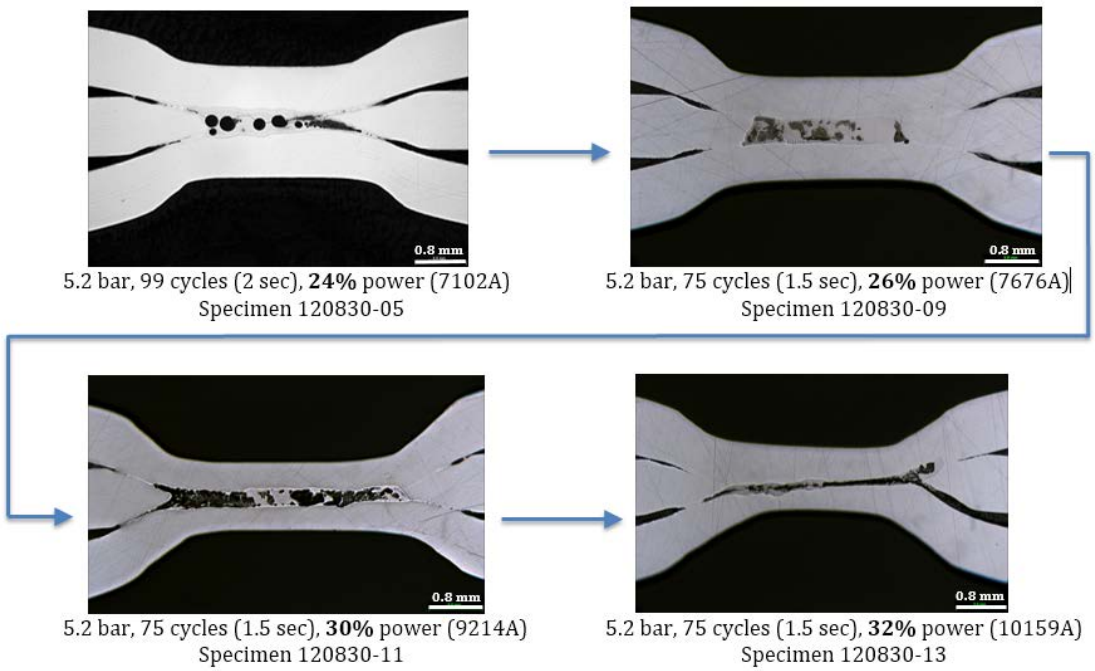

Figure 4-34 - Microsections of parametric study Series 4; constant electrode pinch pressure (5.2 bar) and increasing welding electrical power (driven current)

It can be seen from the microsections of Series 4 that as current is increased there is little improvement in weld nugget formation only an elongation of shape and thinning of metal substrate, as also observed for Series 2 and in the studies that were discussed in Sections 4.5.1 and 4.5.2. There is significant porosity in the specimen that was manufactured at 24% power and it is uncertain why this

is, as of all the trials conducted, high levels of porosity were only observed when an aluminium substrate was used (see Section 4.5.1.3). Therefore the porosity could be a result of contamination of the weld surface that could have resulted from insufficient cleaning of the faying surfaces or possibly an insufficiently inert atmosphere due to a possible failure of argon supply. The sample manufactured using a power setting of 26% was deemed to be the best balance of weld nugget formation and substrate thinning. Examination of the instrumentation measurements showed that the post weld equilibrium state was achieved within 65 AC cycles.

The details of the identified welding schedule for the IMM joint is as follows:

- AWL-Techniek WP63RL-K resistance spot welder
- Copper electrodes with a conical shape and 3.5 mm diameter contact
- Inert atmosphere; with oxygen levels below 500 ppm, by use of argon
- 5.2 bar pneumatic pressure generating a pinch force of 4290 N
- Power setting of 26%; producing 16.6 kVA, and driving a maximum current of approximately 7.68 kA
- Current application time for 65 AC 50 Hz cycles; equating to 1.30 seconds

This information was also summarised in Table 4-4.

For the purposes of evaluating the mechanical strength performance of composite to metal joints that use an IMM weld it was required to benchmark against traditional MTM welds. To ensure maximum commonality between the IMM and the MTM welds (the single difference being the presence of fibres in-between metal faying surfaces) the MTM weld was also not a traditional welding configuration as there would be two faying interfaces in series in the current flow direction. It was therefore required to define a suitable welding schedule for the serial resistance welding technique. This activity was straightforward compared to defining a welding schedule for the IMM weld and the efficiency of determining adequate welding parameters was enhanced by the use of welding equipment instrumentation. For commonality the same electrode pinch force was used for the MTM as was determined for the IMM weld. A short trial series

quickly established a suitable welding power setting, which was confirmed by instrumentation measurements, and the measurements also identified the required time for the welding process.

The details of the identified welding schedule for the MTM joint is as follows:

- AWL-Techniek WP63RL-K resistance spot welder
- Copper electrodes with a conical shape and 3.5 mm diameter contact
- Inert atmosphere; with oxygen levels below 500 ppm, by use of argon
- 5.2 bar pneumatic pressure generating a pinch force of 4290 N
- Power setting of 40%; producing 25.6 kVA, and driving a maximum current of approximately 11.8 kA
- Current application time for 15 AC 50 Hz cycles; equating to 0.30 seconds

This information was also summarised in Table 4-4.

A specimen of the MTM weld produced using the above welding scheduled was microsectioned to assess the quality of the weld, and is shown in Figure 4-35. The same microsection preparation method was used for this MTM weld as for all IMM welds. It can clearly be seen that a weld is produced without weld nugget contamination from carbon fibres, due to the fibres being clear of the faying surfaces before welding. Microstructure changes associated with melting and solidification of the weld nugget and heat effected zone around the weld are not seen as no etching procedure was applied to the microsection.

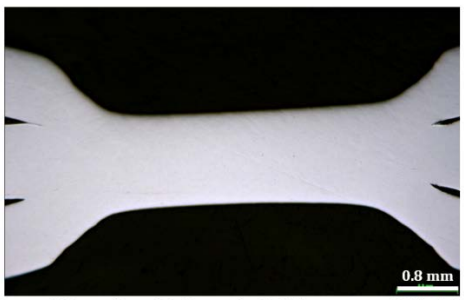

5.2 bar, 15 cycles (0.3 sec), 40% power (25.6 kVA)
Specimen 120803-16

Figure 4-35 – Microsection of Metal-to-metal weld showing that there is no carbon fibre remnant or contaminant of the weld due to the fibres being cleared of the faying surfaces prior to welding.

4.5.6 Weld nugget formation and microstructure

To investigate the microstructure of the IMM weld polished microsections were subject to acid etching. Figure 4-36 shows micrographs of an etched specimen that was manufactured using the optimal electrode pinch force and welding power setting identified by the parametric study discussed in Section 4.5.5.

5.2 bar, 75 cycles (1.5 sec), 26% power (16.6 kVA)
Specimen 120830-08

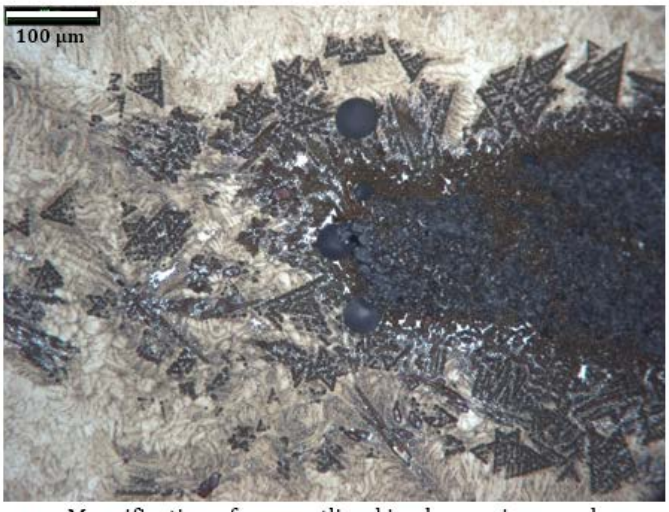

Magnification of area outlined in above micrograph

Figure 4-36 – Microstructure of Interleaved Multi Material (IMM) weld, specimen 120830-08

The top picture of Figure 4-36 shows the cross-sectional shape of the weld nugget (brown colouration) the shape is not the typical oval of a traditional metal to metal resistance spot weld. This is both due to the presence of carbon fibre

between the faying surfaces and the arrangement of having two faying interfaces in series. As the welding event occurs and the nugget formation region becomes fluid, the position of the carbon fibres are susceptible to movement due to flow of the molten metal, and also degradation of the fibres due to reactions and solution of the fibres with the molten metal. As the position of the fibres change the local electrical resistance and corresponding Joule heating changes, the result is the uneven and non-symmetric weld nugget shape, as seen in the micrograph. Remnants of carbon fibre can also be seen; this is the black substance within the weld nugget.

The arrangement of having two faying interfaces in series affects the shape of the weld nugget. The greatest contributor to the Joule heating is the contact resistance between faying surfaces. Therefore the weld nugget grows in width along the faying interface. In this case there are two faying interfaces to stimulate weld nugget growth and so a ‘double-lobed’ weld nugget is produced. This effect is illustrated in Figure 4-37.

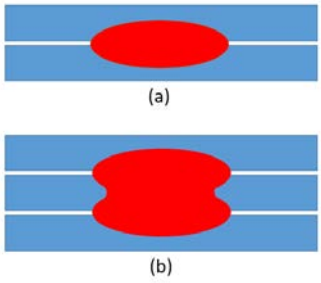

Figure 4-37 – Comparison of the single-lobed weld nugget shape of a traditional resistance spot weld (a) with the double-lobed weld nugget shape generated due to two faying interfaces stacked (b).

Further magnification of the weld-nugget / fibre-remnant boundary, lower image of Figure 4-36, shows the presence of tetrahedral shaped formations within the weld nugget. It is uncertain as to what these structures are. Due to the high quantity of carbon present during the welding process the molten metal (iron) could become saturated with dissolved carbon and as the metal solidifies

carbon could then precipitate forming the tetrahedral shaped formations observed. Of the possible substances present in the weld; silicon carbide can also form tetrahedral structures. Silicon is an alloy element of 304 stainless steel, at less than 1% content, due to the large number of the tetrahedral shaped formations seen it is unlikely that the tetrahedral formations are silicon carbide crystals. Only carbon is present in great enough quantities to account for the number of formations seen, however the temperatures and pressures generated in the resistance weld are likely to be significantly lower than those required to form the carbon tetrahedral crystal formation of diamond.

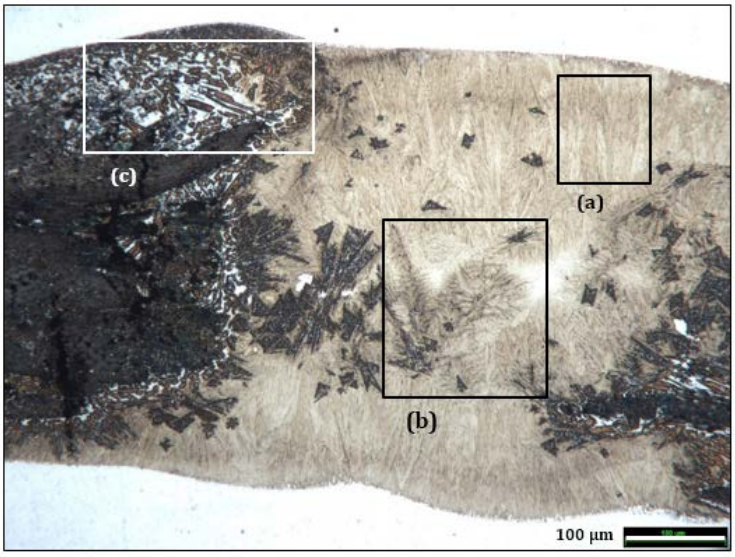

Figure 4-38 - Microstructure of Interleaved Multi Material (IMM) weld, sample 120831-02

Figure 4-38 shows a high magnification etched microsection of an IMM specimen that was produced using the welding parameters identified for manufacturing mechanical test specimens. As with the specimen of Figure 4-36, carbon fibre remnant and the tetrahedral-shaped formations can again be seen. Other microstructures that can be seen are: columnar crystal grains (a) that are typical of weld solidification, dendritic crystal structures (b) that tend to nucleate

from isolated carbon fibre remnant, and local high concentrations of iron carbide (c) occurring adjacent to high concentrations of carbon fibre remnant. Such observations are evidence of the chemical interactions occurring between carbon fibre and molten stainless steel due to the affinity between the carbon and iron. Although the reactants produced tend to [in isolation] not have desirable mechanical properties for structural joining, for example iron carbide has low ductility, the evidence that chemical reaction driven microstructure changes are occurring shows that a joining mechanism is occurring between the carbon fibres and the metal, which is neither adhesive bonding nor mechanical interlocking.

4.5.7 Joining performance

This section discusses the mechanical test results of the six structural configurations that are detailed in Table 4-5. The combination of three fundamental joining mechanisms were investigated, these being: the adhesive strength of the interleaved double-lap-shear analogous joint arrangement (Figure 4-39), the strength of the baseline MTM weld (Figure 4-40), and the strength of the IMM weld, which penetrates in situ carbon fibre fabric (Figure 4-41). All graphs are plotted on the same axis ranges to allow clear comparison between strength and strain performances. Where a dashed line style is used the result has been considered as anomalous and omitted from any averaged values. The results for all the various structural configurations are summarised in Figure 4-46 which can be found towards the end of this section on page 165.

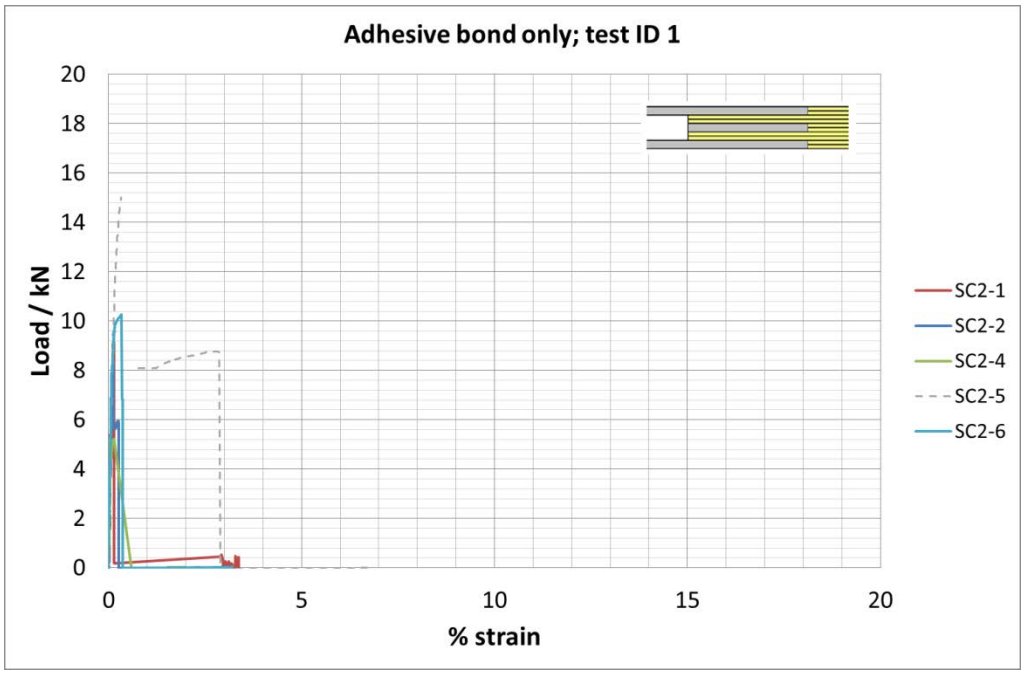

Figure 4-39 – Adhesively bonded strength of the interleaved DLS joint

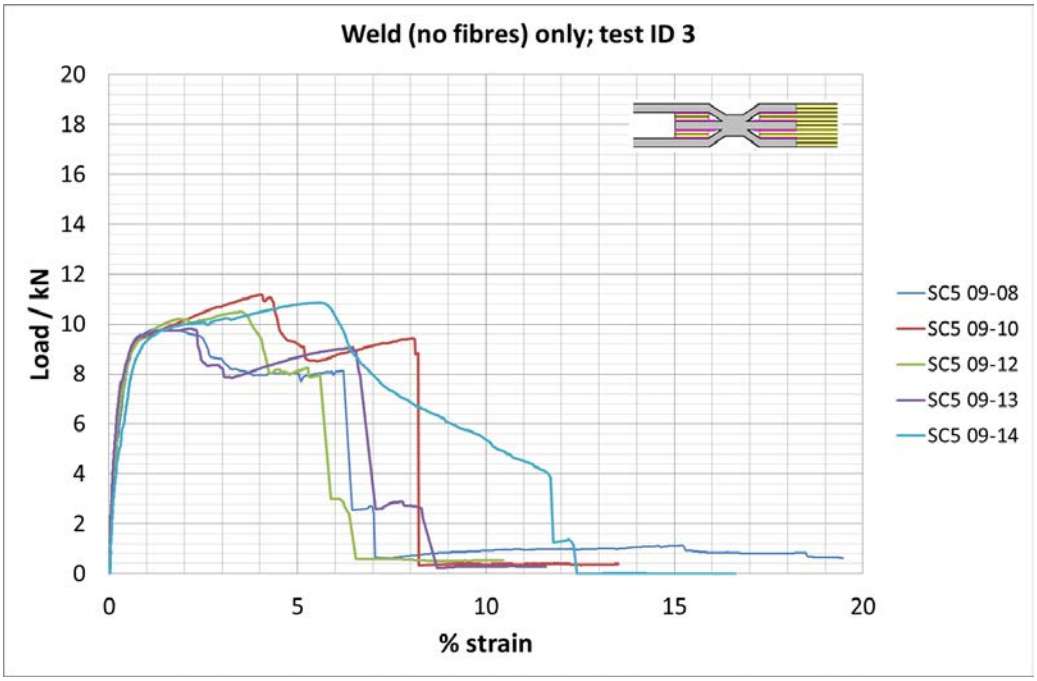

Figure 4-40 – Strength of the MTM weld; baseline weld of same joint configuration as the IMM resistance spot weld

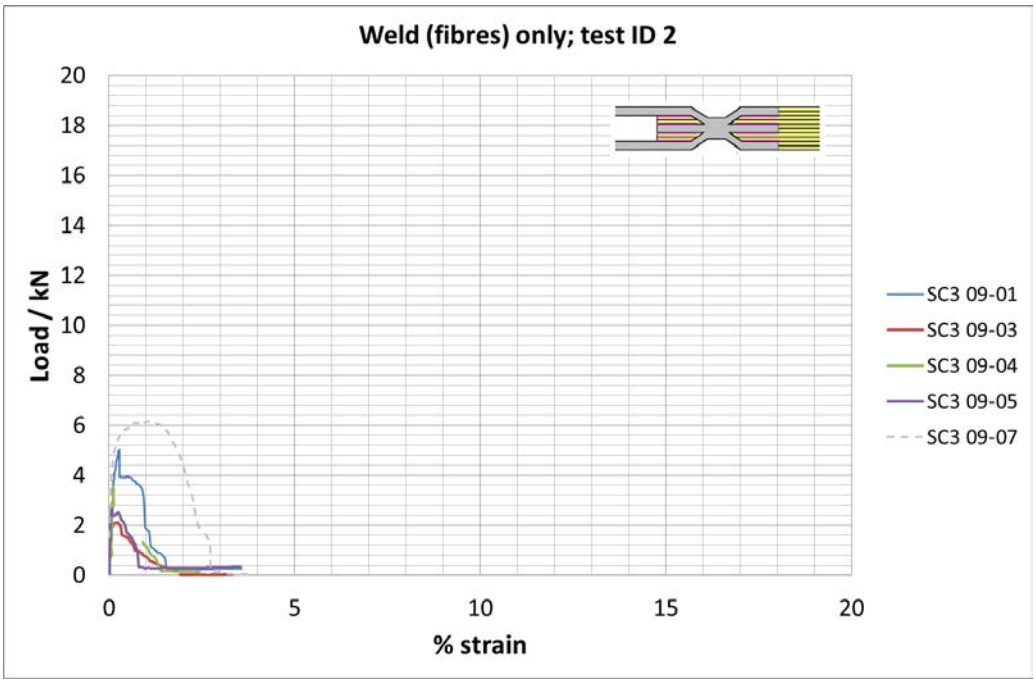

Figure 4-41 – Strength of the IMM resistance spot weld; which penetrates in situ fibres

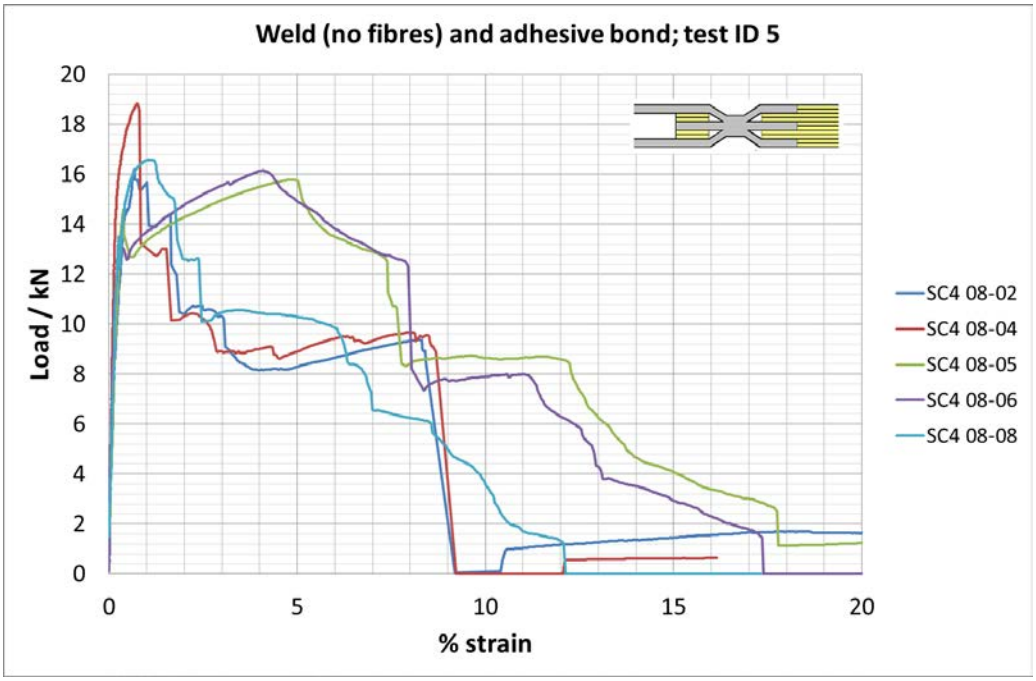

Figure 4-42 - Strength of adhesive joint reinforced with MTM baseline resistance spot weld

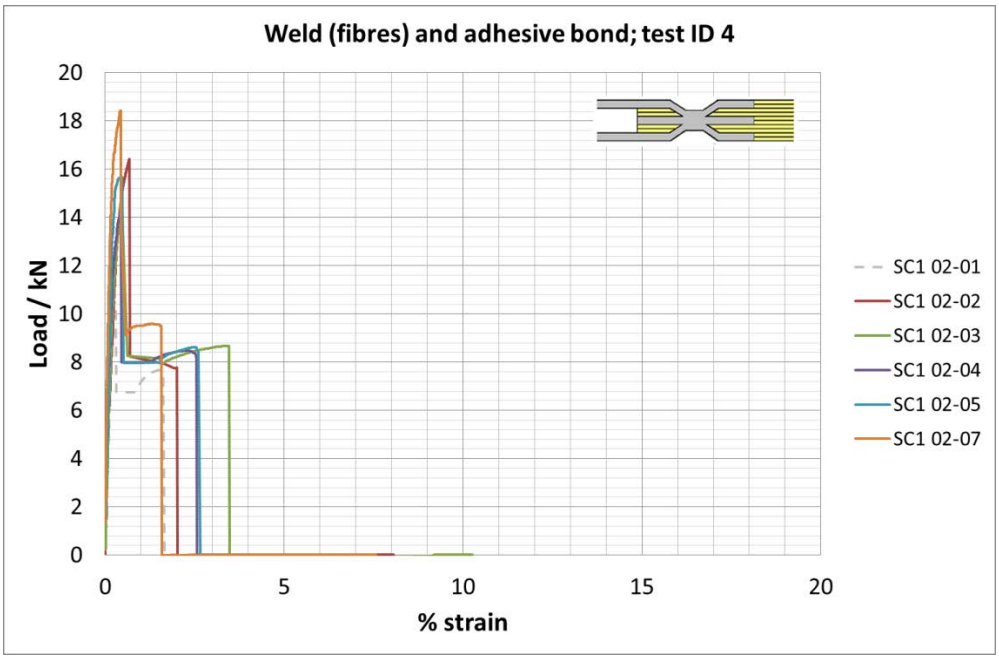

Figure 4-43 - Strength of adhesive joint reinforced with IMM resistance spot weld

When comparing the strength performance of the IMM resistance spot weld against that of the MTM resistance spot weld, Figure 4-41 and Figure 4-40, respectively, the IMM is significantly weaker. This is attributed to two observations: the contamination of the weld by the chemical reaction between the carbon fibres and the molten metal, and the reduction in the amount of metal present at the weld due to molten metal escaping from the weld nugget region as weld splash flowed along the directions of fibres as they breach the weld nugget formation region.

The strength performance of an adhesive bond reinforced with the baseline MTM resistance spot weld is provided in Figure 4-42 and an adhesive joint reinforced with an IMM resistance spot weld is provided in Figure 4-43. The initial failures of these two joint types are associated with failure of the adhesive bond; as the strains at the point of initial load drop is comparable to the strain at failure of the adhesive bond, this value being 0.16%, as seen in Figure 4-39. The load is then reasoned to be transferred to the weld, therefore the welds are considered to provide residual strength to the joints.

For the MTM weld, Figure 4-40, the maximum load is 10.4 kN and the residual load for the MTM weld reinforced adhesive joint is slightly less, but comparable, 8.29 kN, Figure 4-42. There are two distinct behaviours observable in the test results for the MTM weld reinforced adhesive joint. Specimens SC4 08-02, SC4 08-04, and SC4 08-08, fit very well with the above description, i.e. the peak load is the maximum load and occurs at very low strain. However for specimens SC4 08-05 and SC4 08-06, after a slight load drop at very low strain the load carried by the specimens continued to increase, before dropping to a load comparable to the strength of the MTM weld in isolation. It is believed that in this second observed behaviour the distribution of the load between the adhesive bond and the weld is somehow more evenly shared, enabling the peak load to occur at higher strain. This could be due to a comparatively smaller area of the adhesive disbonding during the initial failure allowing the load to be more progressively transferred to the weld. This effect could be a result of lower energy release rate of the initial failure but further investigation would be required. This shows that

the MTM weld reinforced adhesive joint geometry could potentially be further optimised if it was desired for the peak load to be at a higher strain.

The lower strength of the IMM weld compared to the MTM weld is also evident when comparing the results of the MTM reinforced and the IMM reinforced adhesive joints. The maximum strength of the IMM weld was 3.85 kN. The residual strength of the IMM reinforced adhesive joint is measured to be greater than this; 8.58 kN, and is closer to the residual load strength of the MTM reinforced adhesive joint; 8.26 kN, although it occurs at a much lower strain; 2.40% compared to 9.45%, respectively. This apparent increased strength performance of the IMM weld when it is applied to reinforcing an adhesive joint is unclear. For all the reinforced adhesive joints further understanding of the failure mechanisms could be gained by partially testing samples to just beyond the initial load drop and then inspecting the samples by metallographic or X-ray CT to observe the physical state of the partially failed joints to see which joining mechanisms have failed and where material has strained.

In both the MTM weld and IMM weld reinforced adhesive joints the load at initial failure (which is attributed to adhesive bond strength) is significantly increased; from 10.3 kN to 16.1 kN and 15.8 kN, respectively. This increase in apparent adhesive strength performance is likely a result of the welds acting to resist induced out-of-plane loads. There could also be an element of joint ‘self-jigging’ during manufacture. As the welds are applied to the joints prior to application of adhesive (infusion of fibres) the relative position of the adherends, the metal and the fibres, is controlled.

From the results presented in Figure 4-46, it can be seen that when a RSW reinforcement is applied to an adhesive joint, in addition to an effective strength increase being achieved in the region of the load-strain response attributed to adhesive joining (the maximum strength of the joints) there is also a reduction in the measured variance of the maximum strength. This effect is seen whether the reinforcing resistance weld used is a MTM or IMM weld. The residual strength (load at ultimate failure) of the MTM and IMM reinforced adhesive

joints is also similar, with the advantage of the MTM being that the ultimate failure occurs at a significantly greater strain; of 9.45% compared to 2.40% for the IMM reinforced joint.

A traditional method of reinforcing adhesive joints is to install mechanical fasteners. To make a comparison with the resistance weld reinforced adhesive joints and adhesive-only joints, of the same geometry and stacking sequence as used throughout this study, M3 bolts were installed in the same position and were of comparable size to the resistance welds. Figure 4-44 shows a photograph of the adhesive joint with a mechanical fastener installed and Figure 4-45 shows the strength performance of this joint.

Figure 4-44 - Traditional reinforced adhesive joint; bolt of similar diameter as resistance welds installed on cured adhesive joints

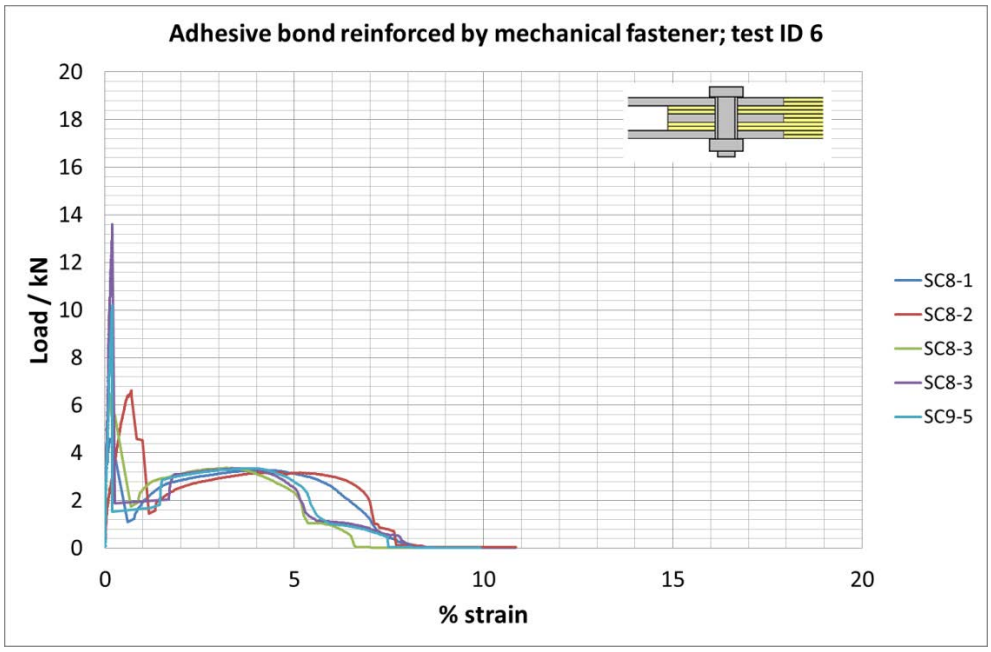

Figure 4-45 - Strength of adhesive joint reinforced with traditional mechanical fastener

As is the case with the resistance weld reinforced adhesive joints, when a traditional mechanical fastener is used the joints display the characteristic of an initial failure associated with adhesive failure and a residual load carrying capacity that is attributed to the mechanical reinforcement.

With regards to the bolt reinforced adhesive joint, compared to the adhesive only joint, there is a reduction in both maximum strength and the strength at ultimate failure, however the advantage is that the ultimate failure occurs at a significantly higher strain 4.14% compared to 0.90%. The strain at ultimate failure of the bolt reinforced adhesive joint is ranked in-between those of the IMM and MTM weld reinforced adhesive joints, 4.14% compared to 2.40% and 9.45%, respectively. However the load at ultimate failure of the bolt reinforced adhesive joint is significantly less than both the IMM and MTM weld reinforced adhesive joints, 3.30 kN compared to 8.58 kN and 8.29 kN, respectively.

The reduced strength of the bolt reinforced adhesive joint compared to the adhesive only joint is attributed to the reduction in bonding area caused by drilling through the cured adhesive bond, and also that the drilling operation will

induce damage to the adhesive bond around the drilling location. The bolt reinforced adhesive joint may have a lower ultimate failure load than either of the weld reinforced adhesive joints due to lower strength of the bolt compared to the welds, particularly the MTM weld. Also a M3 bolt was used, which has slightly smaller cross-sectional area than the 3.5mm of the welds (the value of 3.5 is based on the welder electrode contact tip interface area of 3.5 mm). Figure 4-46 provides a summary of the resistance weld reinforced adhesive joints and the associated comparison joints investigated as part of this study.

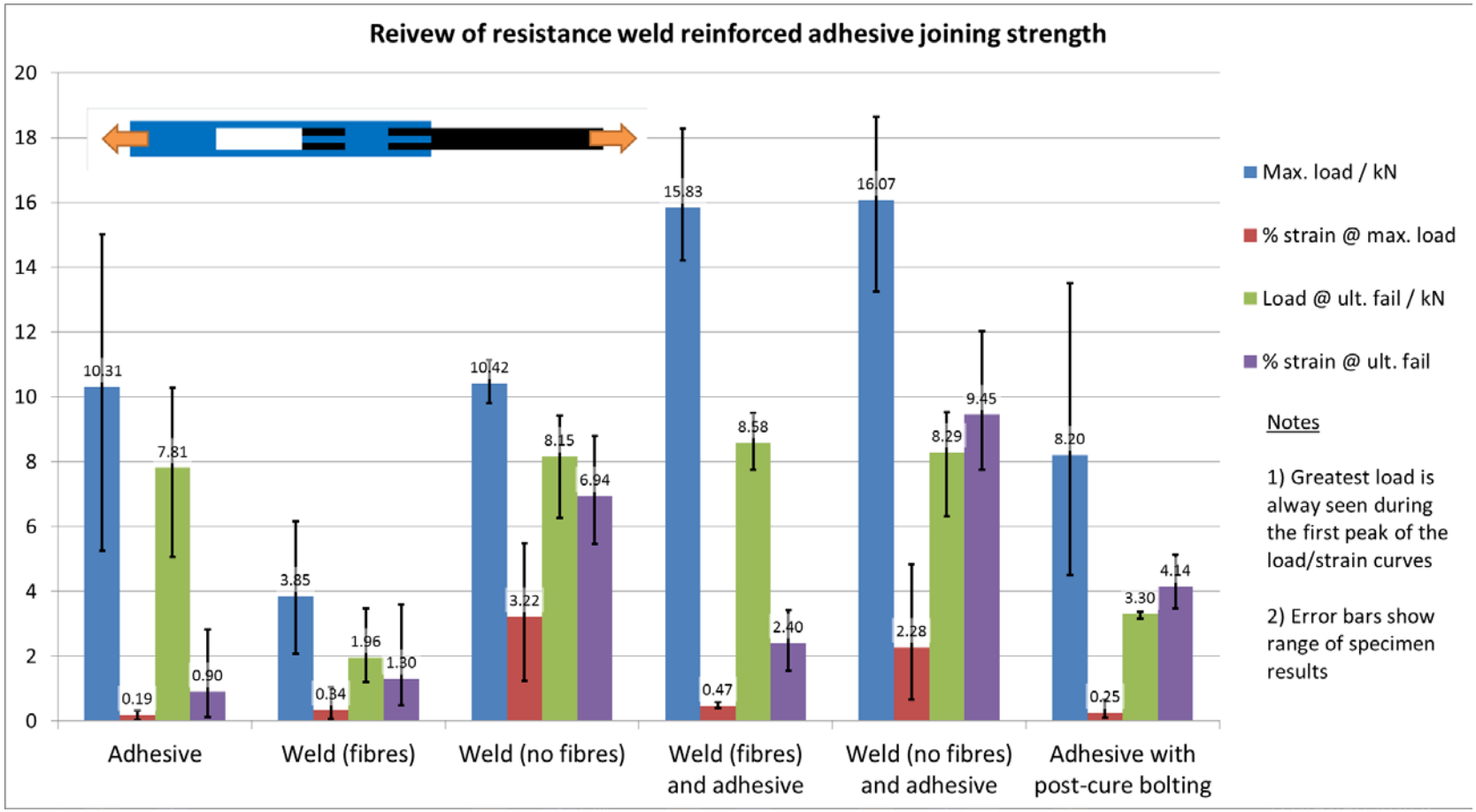

Figure 4-46 – Summary of strength performance of resistance weld reinforced adhesive joints, resistance welds, and comparative joints investigated in this study

Overall the joint with the greatest mechanical performance is the MTM reinforced adhesive joint. However, the IMM weld reinforced adhesive joint also performs well. There appears to be a cumulative, even synergistic, effect of reinforcing adhesive joints with resistance welds. This effect is most apparent with the IMM weld reinforced adhesive joint, which performs significantly better than either the adhesive bond or IMM weld in isolation. The cumulative/synergistic effect is likely a result of the intimate way in which the weld reinforced adhesive joints are formed. As the welds are performed before adhesive bonding there is a greater interaction between the composite reinforcement fibres and the metallic adherend.

In summary, it can be seen from these results that the structural performance of an adhesively bonded joint can be improved by mechanical reinforcement by the application of a resistance spot weld. The strength of the joint is increased and also the reliability, as less variance is observed in the measured maximum loads.

4.6 Discussion and Conclusions

4.6.1 Concluding message

The application of a resistance spot weld as mechanical reinforcement of an adhesively bonded joint is a technique that has been extensively used in the automotive industry for metal-to-metal joining (Bartczak, Mucha and Trzepieciński, 2013; Darwish and Al-Samhan, 2004). It is reported in the literature that a modification of this technique has been investigated for composite to metal joining, for cases where the composite laminate has been cured and holes drilled through the laminate in a post-processing operation to enable metal-to-metal RSW that sandwiches the laminate (Shah et al., 2010). The technique of applying a RSW through carbon fibre fabric before manufacturing the composite laminate; and so forming a joint directly between carbon fibre and metal, is wholly new and has been demonstrated in this work

to result in improved structural joining performance between the two dissimilar materials of carbon fibre reinforced plastic and metal.

4.6.2 How this chapter supports this message

The concept of using a resistance spot weld that penetrates carbon fibre fabric required development of the technique to an adequate technology readiness level that enabled the manufacture of representative joints suitable for mechanical testing. Stainless steel was identified as an appropriate metal for use. Equipment instrumentation and microsection evaluation was used to determine an interleaved stacking sequence, together with suitable processing parameters, that resulted in a interleaved multi-material RSW that was reasonably well formed; considering the effects of weld contamination by the presence of carbon fibre. It was identified that as well as contamination of the weld metal, the presence of carbon fibre facilitated loss of molten metal from the nugget formation zone.

The necessity to use an interleaved stack of carbon fibre fabric and sheets of metal in order to achieve a fibre penetrating RSW required a non-standard adhesive joint configuration. A series of joint configurations were devised to enable the fibre penetrating RSW reinforced adhesive joint to be baselined against an adhesive-only joint, and also quantify the strength of the fibre penetrating RSW against an uncontaminated metal-to-metal RSW weld, both in terms of direct comparison of the two types of weld in isolation and their effect when used to reinforce an adhesive joint.

The results of the series of mechanical tests showed that an improvement in strength performance is achieved when a fibre penetrating RSW is used to reinforce an adhesive joint. The strength of the adhesive bond is effectively improved due to induced out-of-plane loads being resisted by the RSW. A reduction in variance of joint strength is attributed to the consistent jigging of the carbon fibre and metal sheet adherends that is achieved by applying the RSW

before the adhesive. Further joining improvement is observed when a metal-to-metal RSW is used as reinforcement of an adhesive joint. This is attributed to increased strain to failure when an RSW is not contaminated by carbon fibre in the weld.

4.6.3 Points that remain open to interpretation

It is anticipated that direct joining of carbon fibre and metal, which is observed to occur in the [IMM] fibre penetrating RSW, contributes to the overall performance of the reinforced adhesive joint. In the fibre penetrating RSW case there is a significant amount of weld splash that escapes from the weld nugget formation zone and flows along the fibres. It could be considered that interaction between the weld splash and both the carbon fibres and the metal substrate acts as a braze joint between carbon fibre and metal substrate outside of the RSW region. It is shown in the literature that braze joining is an effective means of joining metals and ceramic matrix composites (Singh et al., 2005; Singh, Asthana and Shpargel, 2007). Further investigation of this supposed braze-joining, which may be occurring in the fibre penetrating RSW joints, could be quantified by fibre pull-out tests. If braze-joining were proven to be of an advantage to the overall joining mechanism the manufacturing method could be developed to generate a greater quantity of weld splash to fibre interaction. This development could involve using a seam-welding technique as a replacement to spot-welding.

4.6.4 Further work that could be done

It was demonstrated in both the literature and work presented in Chapter 3 that the position of mechanical reinforcements along an adhesive joint affects the load carrying capability of the joint. The study discussed in this chapter concerns the development of a new type of technique for mechanical reinforcement. The joints manufactured consisted of a single mechanical

reinforcement placed centrally within an adhesive bond. A continuation step in developing the RSW reinforced adhesive joining technique would be to investigate what effect a RSW reinforcements has depending on the position along an adhesive bondline. The effects could be in terms of achieved joining strength and failure characteristics. It would be expected that the greatest advantage would be seen when applying the RSW to bondline runout areas. However, distortion to the shape of the metal substrate can occur in resistance welding, with significant distortion observed in this study, which is attributed to the offset distance between metal sheets due to the carbon fibre fabric being interleaved between the metal sheets. This distortion of substrate could impact the effective bondline thickness between the carbon fibre fabric and metal adherend. Therefore there could be an advantage of regularly spaced RSW to maintain the bondline thickness. This would support the argument that application of RSW before composite manufacture controls the bondline and so results in improvements of adhesive bond performance.

In the similar concept of using RSW to join cured composite laminates to metal sheets by a weld-bonding method, discussed in Section 2.3.3, a joint geometry termed ‘Super-lap-shear’ (SuLS) (Shah et al., 2010) was devised. The SuLS joint tested a line of three RSW in parallel to the loading direction. It is expected that mechanical reinforcement of an adhesive joint is more effective when applied in series to the loading direction. However the SuLS joint arrangement presents a loading case that is more representative of a real-world structural application. A similar SuLS joint could be replicated using the RSW reinforced adhesive joining technique developed in this study.

In this study a unidirectional fibre orientation was used. When composites are joined by mechanical fastening it is recommend to use a lay-up sequence that is predominantly n[+45/-45]s in the dominant loading direction, or at least quasi-isotropic, so that the architecture of the laminate is resilient to induced bearing loads around the fastener shank. The interleaved stacking sequence used in this joining concept could therefore be modified, as is illustrated in Figure 4-47 with the aim of increasing the bearing resistance of the laminate and so

potentially improving the performance of the joining technique. The improvement will likely manifest in the ultimate-failure/residual strength performance of the joint. However the change of fibre orientation at the laminate to metal adherend interface may also effect the adhesive performance of the joint, which is associated with the initial failure.

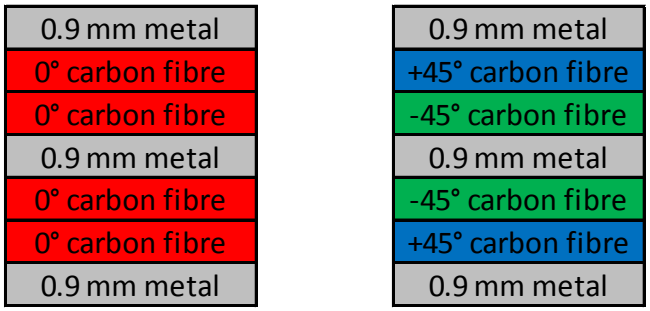

Figure 4-47 - Suggestion for modification to interleaved stacking sequence from (a), as used in this study, to (b), for potentially improved mechanical fastening bearing resistance of the laminate

The change to the carbon fabric stacking sequence will change the way in which the fibres nest when a compressive force is applied. This change in the way fibres contact each other will affect the through-the-thickness electrical resistance of the material stack. Which in turn will impact on the required resistance spot welding parameters required to manufacture a fibre penetrating RSW. With a change in fabric ply stacking sequence, as a minimum the study to determine RSW parameters (Study 3, as described in Section 4.2.1) will require repeating. The change in ply stacking sequence as described in Figure 4-47 is expected to result in less fibre nesting, particularly at the interfaces between plys. This reduced nesting, and so reduction in number of fibre-to-fibre contact points, is expected to increase the through-the-thickness resistance and therefore a reduced power input may be required to generate adequate Joule heating for the welding process.

The metal used in this study was stainless steel 304. This metal was identified in Stage 1 of the study as having the best potential for forming carbon fibre fabric penetrating spot welds compared to the other metals trialled. Structural applications that would require stainless steel and carbon fibre reinforced thermosetting plastics are relatively limited, the sector in which these materials may find use within a single structure is likely to be off-shore and marine. Although glass fibre reinforced composites are most commonly used for off-shore applications carbon fibre composites are beginning to be used in the blade structure of the latest generation large wind turbines. The automotive and defence land-systems sectors could have potential uptake of this joining technology if it could be developed for use with the type of high strength steels typically used in conjunction with CFRP in vehicles. Therefore an argument exists to trial other metals through Stages 2 and 3 of the study. Of the metals trialled in Stage 1 titanium also showed some potential for use in this joining technique. Titanium was eliminated from further study due to the lack of formation of a consolidated metal-to-metal resistance weld nugget. However it was observed that when titanium is used there are discreet areas where metal flowed and encapsulated carbon fibre. If it were proved that a braze joining process, which can withstand structural loading, could be achieved between resistance heating generated metal flow (weld splash) and carbon fibres, then further investigations using titanium would be worthwhile. If the RSW reinforced adhesively bonded joining concept could be demonstrated to work with titanium and CFRP then there would be significant application opportunity within the aerospace sector. The combined use of titanium and CFRP in weight critical aerospace structures is well established due to the high specific strength of the two materials and also thermal expansion and galvanic corrosion compatibility.

The methodology of this study was to determine RSW parameters that produced a weld that when examined microscopically appeared to have reasonable quality. The developed RSW was then applied to representative joints for mechanical characterisation. The main aim of this study was to investigate the joining performance of the concept. Therefore it could be argued

that the parametric study could be extended to include mechanical characterisation of adhesive joints that were reinforced by RSWs that were produced using various welding parameters. This would enable a direct comparison between welding parameters and joining performance.

It was identified, as discussed in Section 4.5.5, that the welding parameters may not have been fully optimised due to lack of pinch force capacity of the welding equipment. A pinch force of 4290 N was used to manufacture specimens however the equipment limit force of 4540 N appeared to produce higher quality welds. The approach of correlating joining performance against welding parameters could reveal greater insight of the characteristics of the novel joining method. By understanding whether a RSW optimised for weld quality does result in optimum overall joint performance or if other mechanisms, such as interaction between weld flash and carbon fibre, play a significant role in the overall performance of the joint.

4.6.5 Chapter closing comments

The work reported in this chapter describes the process of developing a new joining concept to the stage where the structural performance can be assessed and this enabled structural joining advantages to be identified. In addition to structural joining performance benefits, it has also been briefly discussed in this work that there is potential for manufacturing efficiency advantages to be gained by this joining technique, which includes: adherend self-jigging and reduced pre-processing of composite fabric. As a mechanical joint is formed between the metal and fabric prior to application of resin the adherends are inherently held in relative position to each other, which reduces the extent of jigging required during fabric infusion. This could potentially result in improved manufacturing efficiency, as if it is proved possible to reduce the adherend jigging equipment needed, to hold parts in place while the resin cures. This could present a significant time and equipment cost saving.

With regards to pre-processing of fabric, it has been demonstrated in this work that if local holes are prepared in the fabric, to enable direct metal-to-metal resistance welding, there is improved adhesive bond strength performance and post adhesive failure residual joint strength to high strains. However, when no fabric holes are prepared and the RSW has to penetrate layers of fabric the same improvement of adhesive performance is achieved. Improvements are both in terms of increased strength and reduced variance, although post adhesive failure residual strength is not effective to as high a strain. Therefore if the adhesive performance is the prime concern for the structural application then there is no need to perform the pre-processing operation of cutting holes in fabric for resistance spot welding, by eliminating this production step a manufacturing cost saving will be achieved. As the joining concept is further developed to higher TRLs it would be beneficial to quantify the manufacturing processes to enable structure designers to choose which type of RSW reinforced adhesive bond is most suitable for their application and manufacturing capabilities.

5 THERMOPLASTIC INFUSED METAL FOAM – AN INTERMEDIARY MATERIAL IN A COMPOSITE TO METAL JOINT

5.1 Introduction

This CFRP to metal joining concept uses an intermediary joining hybrid material between the two dissimilar materials. The intermediary material is structurally compatible with both dissimilar materials and so enables load transfer between the CFRP and metal, while accommodating the difference in physical properties between the two dissimilar materials, such as thermal expansion coefficient, which makes traditional structural joining methods directly between metals and composites problematic. The intermediary material used is a thermoplastic Polymer Infused Metal Foam (PIMF), and it is this material that enables the manufacture of the Metal Foam Intermediary (MFI) joint.

The use of a polymer infused metal foam can accommodated established joining techniques between both the foam and CFRP and also between the foam and the metal sheet. Braze joining techniques between porous metal foams to sheet metals and also ceramics have been investigated and reported in the literature by Shirzadi et al and Longerich et al (Longerich et al., 2007; Shirzadi, Kocak and Wallach, 2004; Shirzadi, Zhu and Bhadeshia, 2008). There was scope for widening the investigations of braze joining metal foams and also a method of joining the PIMF to CFRP needed to be devised.

A proof of concept joint was built in which 2mm stainless steel 304 plate was joined to a 2mm thick laminate of unidirectional CFRP APC-2 (APC-2 is a trade name for carbon fibre reinforced PEEK) by the means of a 6mm thick PIMF material, which was a PEEK infused RECEMAT 1116 nickel metal foam. The nickel metal foam is first joined to the steel plate by brazing. The heat required to form the braze joint is provided by laser energy applied indirectly; on the opposing side of the metal plate from the braze joint interface. The metal foam is then infused with melted PEEK thermoplastic, and a thermoplastic weld joint is simultaneously formed between the infused PEEK and the PEEK matrix

system of the APC-2. Figure 5-1 shows a diagram of the joining concept. This joining concept brings together variations of established joining techniques to form a new method of joining metal to composite.

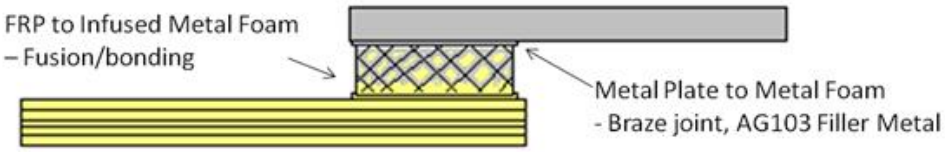

Figure 5-1 - Diagram of Metal Foam Intermediary (MFI) joining concept

Microsectioning of the materials and joints is used to evaluate the quality achieved by the processes. Differential Scanning Calorimetry is used to evaluate the condition of the thermoplastic after the infusion process. The prototype joint manufactured was subjected to quasi-static mechanical testing to evaluate the strength of the joining concept and understand failure mechanisms.

5.2 Methodology

5.2.1 Manufacture of MFI joint

5.2.1.1 Braze joining of nickel metal foam to stainless steel by use of laser induced heating applied away from joining interface

The first production step when manufacturing this joint was to braze join the metal foam to the metal plate by laser induced conduction heating, as illustrated in Figure 5-2. Laser brazing was used because of the potential of the process to produce high quality joints in large structures on an industrial scale.

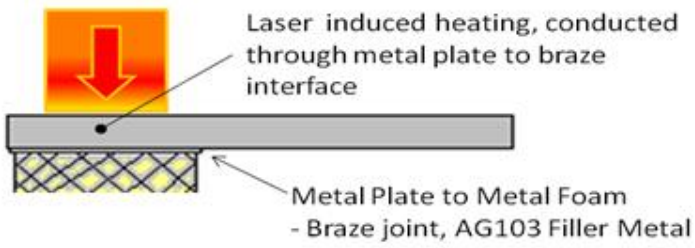

Figure 5-2 - Laser induced conduction brazing. Metal foam not yet infused with thermoplastic

The laser used was an 8 kW fibre laser, with the delivery head mounted on a 6-axis robot, this was used in conjunction with a 1-axis moving work bed. Laser power was set to 1.5 kW, which was the lowest setting that could be used by this laser while maintaining a stable energy delivery rate. To protect the laser from a reflected beam re-entering the delivery fibre the beam was inclined to an angle of 10 degree from normal to the work piece incident surface. A laser spot size of 15mm diameter was used, which was achieved by positioning the laser at an 809.5mm standoff distance from the work piece surface. The laser and work piece arrangement are shown in Figure 5-3.

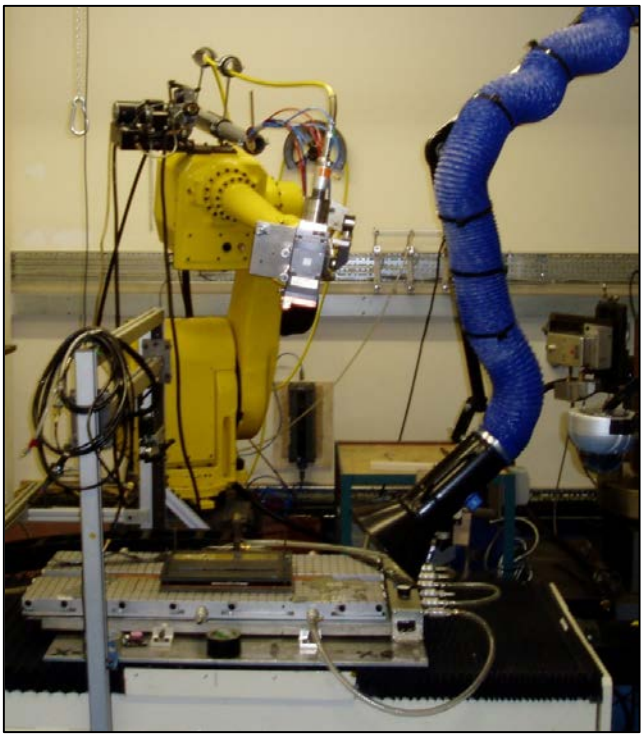

Figure 5-3 - 8 kW fibre laser, delivery head mounted on a 6-axis robot (yellow), together with a 1-axis moving work bed

Laser brazing parameters were identified by a series of trials that used the laser set-up as described above, and altered the laser travel speed in order to vary the energy input into the work piece. Using an identical equipment set-up and joint configuration as would be used for manufacturing the brazed joints of the MFI concept test specimen, thermocouples were placed within the joint at the braze interface so to directly measure the resulting interface temperatures as a result of the set parameters.

A laser spot size of 15mm was used, however the joint interface area was 25mm by 40mm. Therefore the laser spot was scanned across the interface twice, with a lateral offset between passes. The laser was scanned along the 40mm width of the specimen, Figure 5-4 (a), and then offset by 10mm lateral to the beam travel direction, and then scanned again along the 40mm width, Figure 5-4 (b).

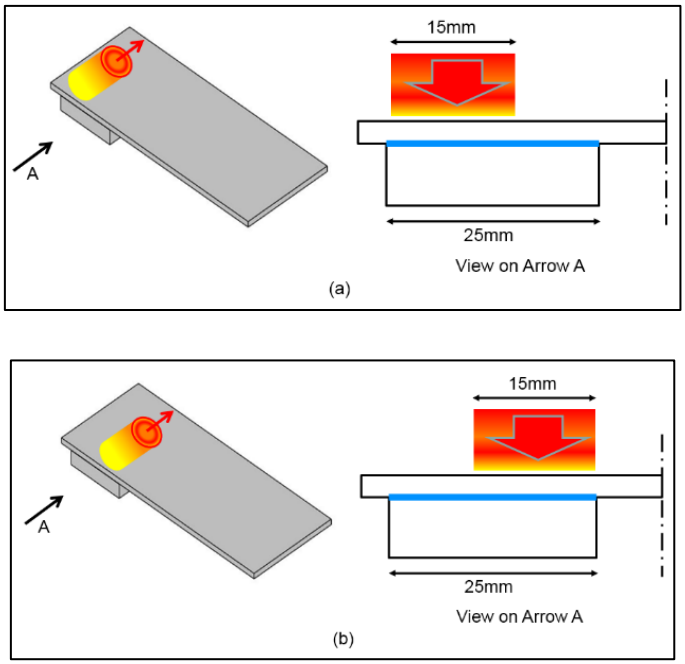

Figure 5-4 - Laser scanning positions, first scan (a) and second scan (b)

The use of multiple laser scan passes was to ensure that the entire interface area had been scanned by the laser in an effort to maximise the area of the interface that was exposed to ideal brazing temperatures. An array of thermocouples were placed at the braze joining interface to measure the temperatures generated. Figure 5-5 shows the measured peak temperatures and gradients resulting from the laser parameters chosen from the trials.

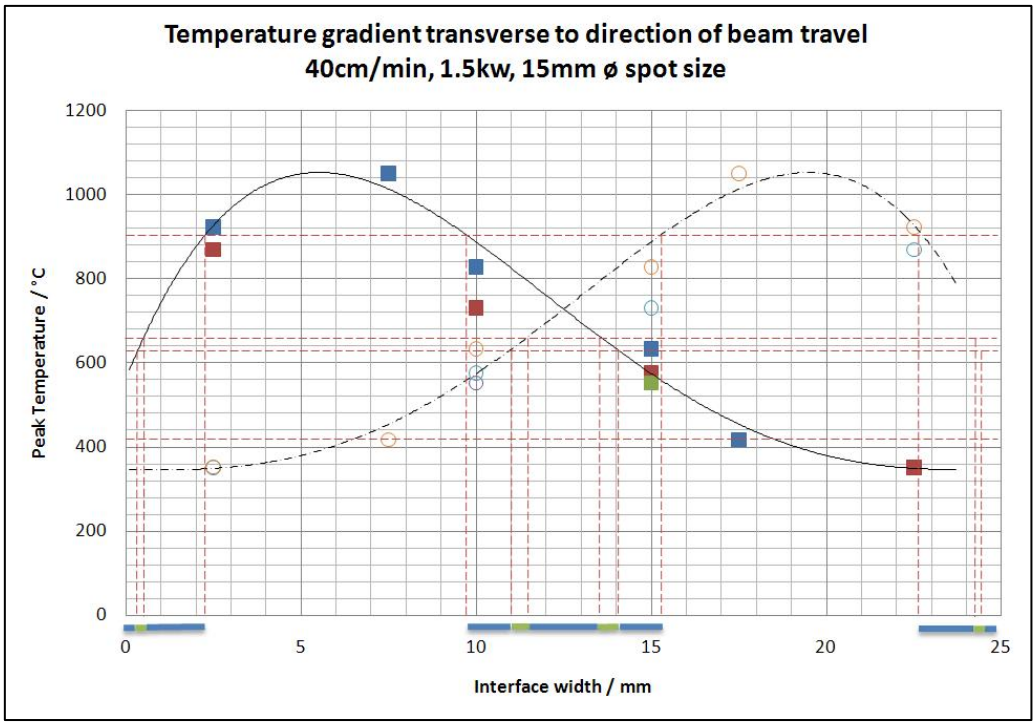

Figure 5-5 - Graph of peak temperature gradient at braze joining interface used for the MFI concept joint manufacturing process. The solid trend line represents the peak temperature profile resulting from the first laser pass, and the dashed trend line represents the temperature profile resulting from the second laser pass.

The braze filler metal used was BS EN 1044:1999 AG103, of which the constituent components are silver (55%), copper (21%), zinc (22%), and tin (2%). The choice of braze filler metal was guided by the British Standards on choice of filler metals and application of brazed joints, and also by the Welding Handbook (BSI, 2004, 2010; Kearns, 1978). The filler metal AG103 was chosen due to the alloy's compatibility with both stainless steel and the chromium treated nickel metal foam.

The optimum brazing temperature range for AG103 is 630°C-660°C, this is illustrated in Figure 5-5 by the green bars shown along the horizontal axis. The regions of the interface that is subjected to this ideal temperature range can be estimated as approximately 1%. It can also be noted that the second laser pass

is likely to have degraded the braze joint at 13.5-14mm, which was formed under ideal temperature conditions during the first laser pass.

It is estimated that approximately 1% of the interface surface is exposed to ideal brazing temperatures for AG103 alloy. However some amount of non-ideal brazing may have been achieved outside of this temperature range. A phase diagram was unavailable for the chosen alloy, therefore based on the phase change temperatures of the alloy constituent elements an estimation was made of a non-ideal brazing temperature range. This range is 420°C - 907°C; 420°C being the melting temperature of zinc (the highest melting temperature of any of the constituent metals) and 907°C being the vaporisation temperature of zinc (lowest vaporisation temperature of any of the constituent metals). This temperature range is shown as the blue bars in Figure 5-5.

An example specimen of the manufactured laser-braze metal foam to metal plate joint is presented in Figure 5-6.

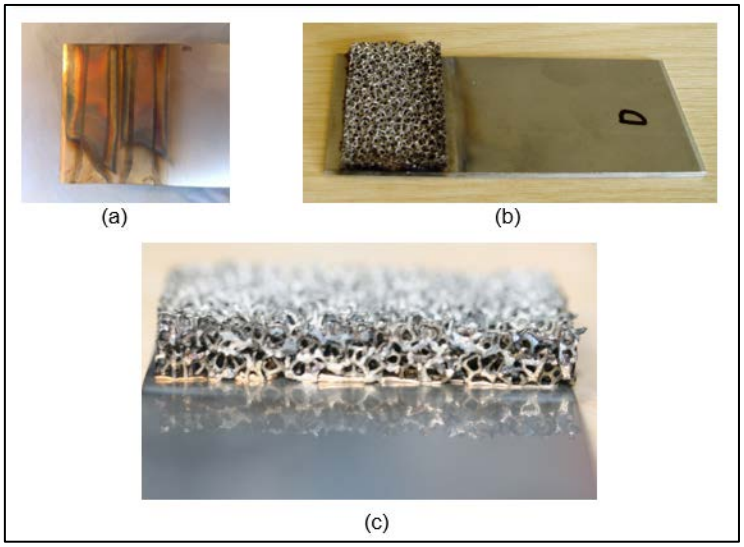

Figure 5-6 - Metal foam joined to metal plate by laser brazing, laser heating induced discoloration of metal plate (a), joined arrangement of plate and foam (b), and detail of braze filler metal between plate and foam (c)

5.2.1.2 Infusion of nickel metal foam with PEEK and fusion welding to APC-2 CFRP

Following the braze joining of metal foam to metal plate, the next production step was to form the PIMF intermediate joining material by infusing the metal foam with PEEK thermoplastic. A mould cavity with matching dimensions to that of the metal foam was positioned above a piece of APC-2 CFRP. The mould cavity was completely filled with a stack of three 2mm thickness sheets of PEEK. The metal foam was then positioned on top of this, see Figure 5-7. The whole assembly was placed in a [JBT Engineering 40 Tonne Press] heated platen press, as shown in Figure 5-8, the platens were heated to the onset melting temperature of the thermoplastic, which was observed to be 360°C, and the press then closed with a load of 3 tonne to force the molten thermoplastic into the metal foam, as also shown in Figure 5-7. As the APC-2 CFRP was positioned in the mould in contact with the PEEK; as well as infusing the metal foam with PEEK this production step also achieved thermoplastic welding of the infused PEEK (constituent of the PIMF material) to the APC-2 composite material matrix.

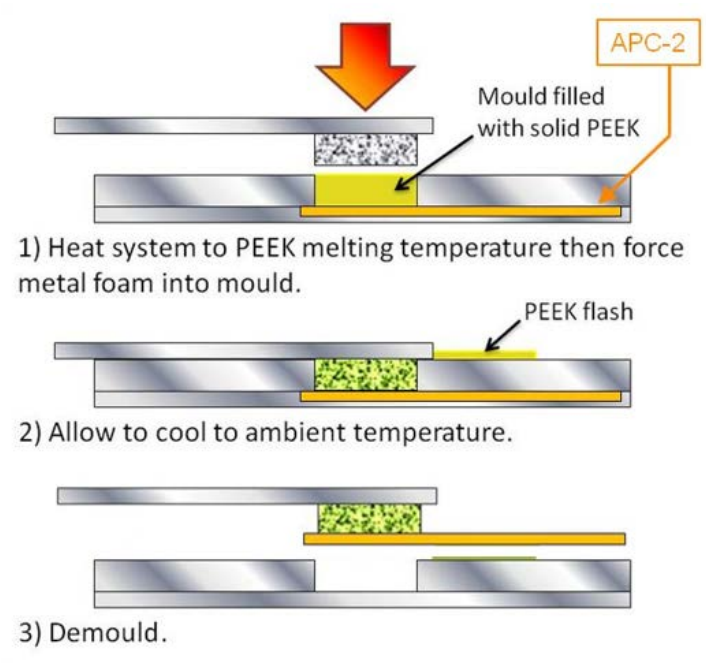

Figure 5-7 - Metal foam infusion process

Figure 5-8 - JBT Engineering 40 tonne heated platen press

Figure 5-9 shows a photograph of the manufactured joint specimen.

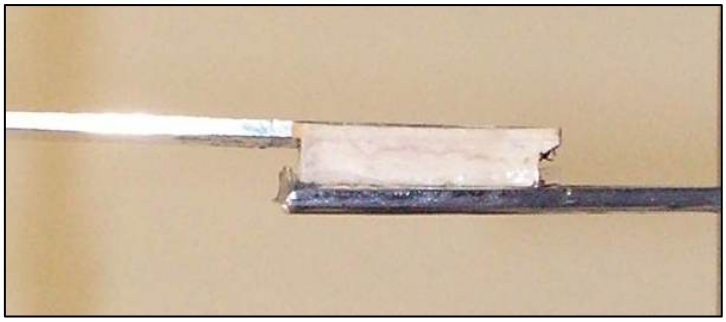

Figure 5-9 - MFI joint specimen

5.2.2 MFI joint testing and inspection

5.2.2.1 Mechanical testing Single-lap-shear joint arrangement

The MFI joint was tested in a single-lap-shear configuration, using an Instron 5500R Electro-mechanical testing machine operating with a 100kN load cell. The test was conducted with a cross-head displacement speed of 0.5mm/min. Figure 5-10 shows a diagram of the mechanical test specimen and Figure 5-11 provides an illustration of the specimen test arrangement. Aluminium tabs were adhesively bonded to the CFRP composite, which was to enable grips to clamp the composite without causing damage to the test specimen. The metal was drilled to enable loading via a pin. This arrangement was chosen so to accommodate the large SLS offset that resulted from the 6mm thick PIMF intermediate material, and also to accommodate any geometry distortions (as a result of manufacturing or testing) of the test specimen.

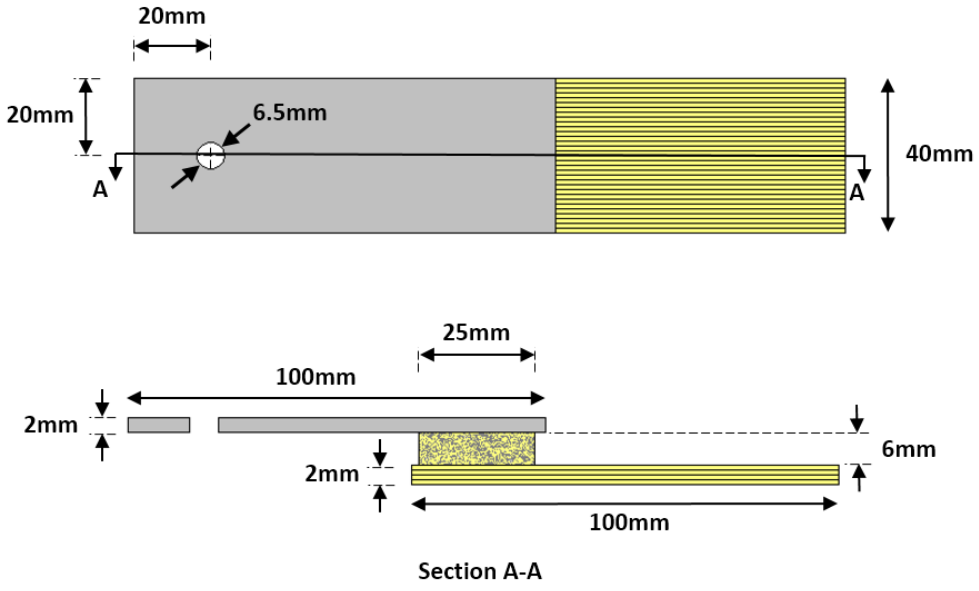

Figure 5-10 - Diagram of MFI joint mechanical test specimen

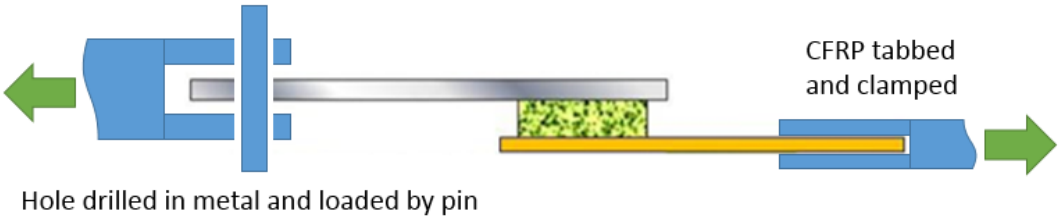

Figure 5-11 - Illustration of MFI joint mechanical test arrangement

5.2.2.2 Metallographic inspection of MFI joint

A standard sectioning and polishing procedure was used, as detailed in Section 3.4.1, for the purpose of Metallographic inspection of the various interfaces that make up the MFI joint. These are illustrated diagrammatically in Figure 5-12, and are: the brazed joint between plate and foam (A), the PIMF intermediary material (B), and the thermoplastic fusion weld between the PIMF and the composite materials (C).

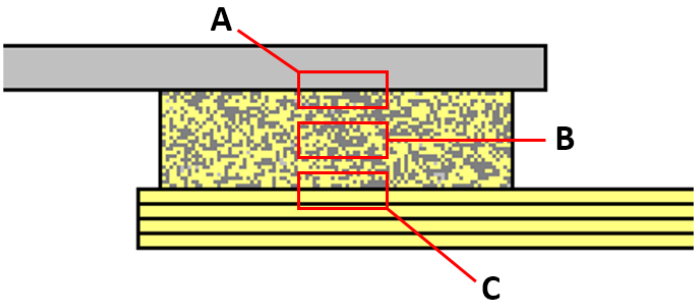

Figure 5-12 - Regions of metallographic interest of the MFI joint

5.2.2.3 Measurement of infused PEEK crystallinity

Infused PEEK extracted from the PIMF intermediary material of a MFI joint specimen was analysed by Differential Scanning Calorimetry (DSC) to determine the condition of the PEEK as a result of processing. The equipment used for this investigation was a TA Instruments Q200 Differential Scanning Calorimeter together with TRIOS software. The DSC method ran from room temperature up to 400°C at a heating rate of 20°C/min. To understand the DSC results of the PEEK extracted from the PIMF material, specimens of PEEK that were quench cooled and slowly cooled through polymer solidification temperatures were also analysed by DSC.

5.3 Results and Discussion

5.3.1 Comparison of the measured lap-shear strength of the joint with the strength of constituent structural elements

The result of the FMI joint single-lap-shear tensile mechanical test is shown in Figure 5-13. The load-extension (based on cross-head displacement) mechanical behaviour of the FMI joining technique indicates a linear modulus followed by a sudden failure with a slight step.

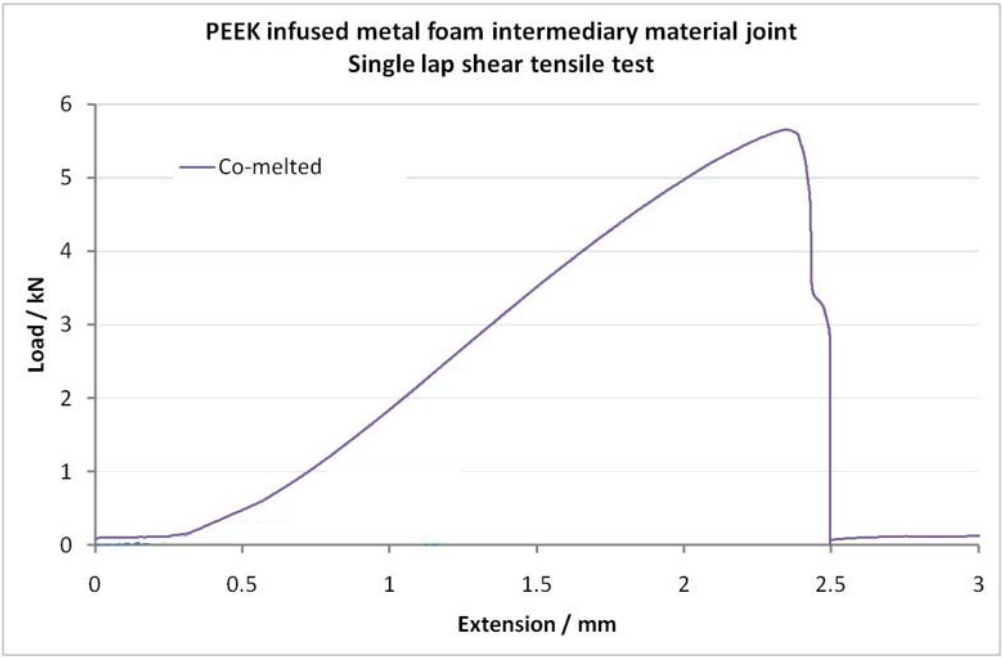

Figure 5-13 - PEEK infused metal foam intermediary material joint, single lap shear tensile test

Mechanical Property	Value for MFI joint
Max Load (Ultimate Failure)	5.65 kN
Extension at Max Load	2.35 mm
Max Stiffness	3.25 kN/mm
Max Shear Stress	5.64 MPa

Table 5-1 - Mechanical performance of MFI joint

A summary of the measured FMI joint mechanical properties are stated in Table 5-1. The MFI joint specimen failed at a shear load of 5.64 MPa. Table 5-2 gives the ultimate strengths of the constituent materials used to construct the MFI joint specimen. It can be seen that the weakest material is the nickel metal foam, which has an ultimate flexural strength of 5.77±1.35 MPa, the observation can be made that the MFI joint failure shear strength is within the range of the metal foam flexural strength.

Material	Tensile strength (MPa)	Shear strength[†] (MPa)
APC-2	2070	1035
PEEK	86.9 - 150	43.5 – 75.0
Nickel	45.0	22.5
Nickel foam	5.77±1.35[‡]	2.89±0.68
Silver*	140	70.0
Copper*	210	105
Zinc*	37.0	18.5

Tin*	220	11.0
Stainless steel 304	505	253

†Based on stated tensile strength value, ‡Flexural strength of RECEMAT 1116, *Braze metal constituents.

Table 5-2 - Ultimate strength of MFI joint constituent materials

Figure 5-14 shows a photograph of the MFI joint specimen braze joint interface after failure. It can be seen that some of the braze metal has smoothly peeled away from the stainless steel plate (a), which shows that full braze joining between the filler metal and the stainless steel plate was not achieved. In areas where the braze metal has not peeled away from the substrate, pieces of nickel metal foam can be seen to still be imbedded within the braze metal (b). No evidence was observed of polymer melt adhesion between PEEK and the braze metal. This observation and the above noted order of magnitude similarity between the MFI joint failure strength and nickel foam ultimate flexural strength suggest that the performance of the MFI joining concept is limited by the strength of the metal foam. These observations also indicate that the MFI joint is behaving as, and has the failure characteristics of, a structure rather than simply being analogous of a classical adhesive joint. This conclusion is reasonable given the various elements within the joining system and the geometry of the joint. By having an intermediary material that has a thickness greater than either the metal or the composite substrates, the resulting offset between substrates is excessively greater than the bondline thickness in a typical adhesive joint.

(a)

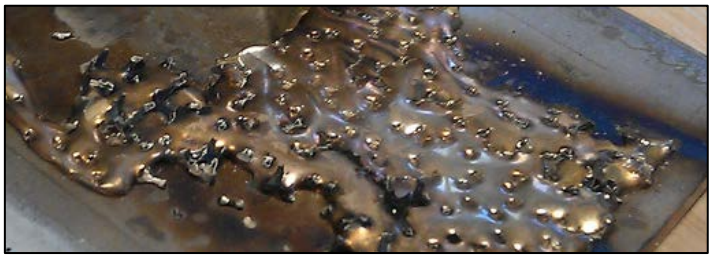

(b)

Figure 5-14 – Photographic detail of mechanical test specimen failed interface

In an associated piece of work conducted by colleagues at Cranfield University a similar polymer infused metal foam (PIMF) intermediary material joint between metal plate and FRP was manufactured and tested. A diagram and photograph of this alternative MFI joint are shown in Figure 5-15. The differences of this MFI joint from the laser-brazed/thermoplastic MFI joint were: the metal foam was vacuum brazed to the metal plate, the metal foam was infused with thermosetting epoxy resin, and the joint had a double-lap-shear configuration. The failure interface of this associated joint was also in the region of metal foam to metal plate braze joint interface. Due to this vacuum-brazed/thermoset MFI joint being resin infused with epoxy the metal foam to metal plate joining

interface is a combination of braze joining and adhesive bonding. This joint failed at a shear stress of 8.83 MPa, which is 56% higher than the failure load of the laser-brazed/thermoplastic MFI joint and this is attributed to: the improved joining performance due to vacuum brazing compared to laser-brazing, and also the DLS joint configuration.

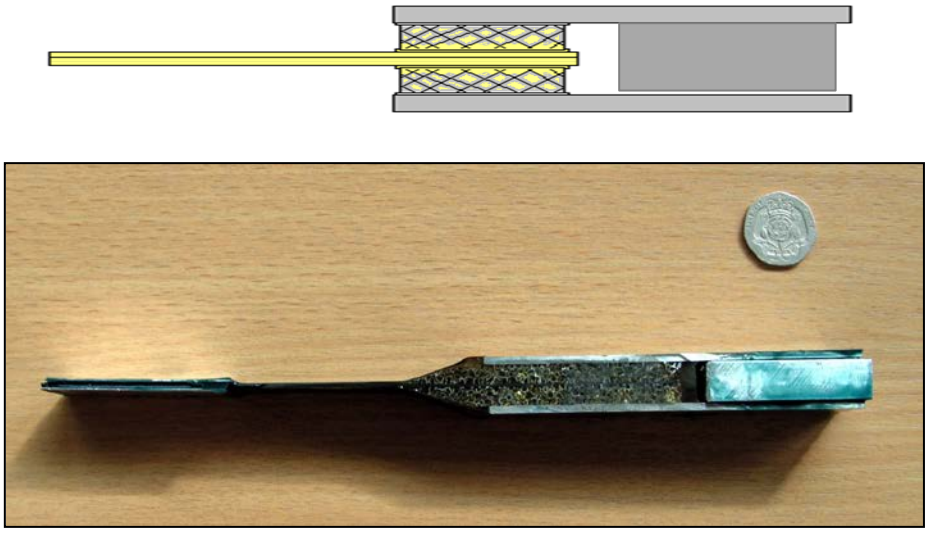

Figure 5-15 – Diagram and photograph of an alternative MFI joint that was manufactured by vacuum brazing and thermosetting resin infused processes

5.3.2 Physicality of joint as a result of processing/manufacture

5.3.2.1 Metallographic inspection of braze joining

A section through the laser-brazed joint, perpendicular to laser travel direction, are shown in Figure 5-16, the detail view (on the right) shows an area of good wetting of the braze filler metal on to both the nickel metal foam and the stainless steel plate. From the overview image in Figure 5-16 (left lower image) it can be seen that braze joining between the metal foam and the steel plate occurs in discrete areas along the interface surface between the two materials. These discrete areas of braze joining occur when a node of the highly porous metal foam comes into sufficient proximity to the solid plate.

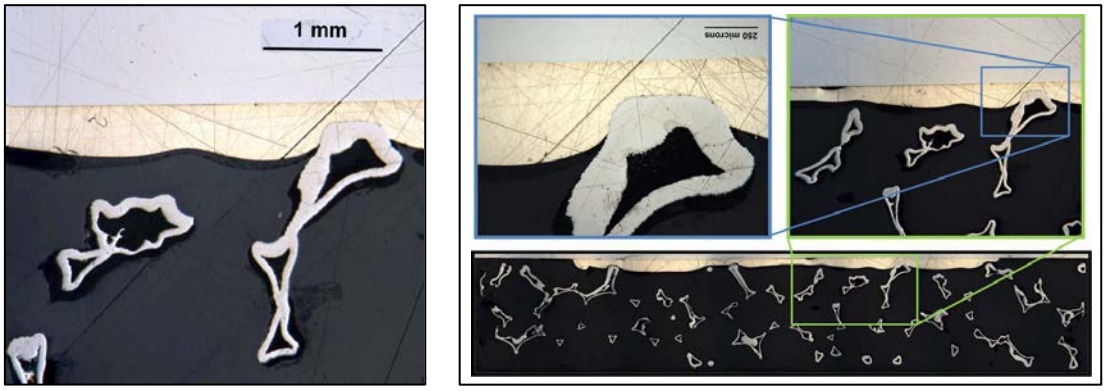

Figure 5-16 - Microsection through the laser-brazed joint (perpendicular to laser travel direction)

5.3.2.2 Metallographic inspection of Polymer Infused Metal Foam and thermoplastic weld

Microsections showing detail of the PEEK infusion and thermoplastic welding of infused PEEK to APC-2 are shown in Figure 5-17, it can be seen from Images 1, 2, and 4 that a good quality and consistent thermoplastic weld has been achieved between the APC-2 laminate and the PEEK that has infused the metal foam. Further observations that can be made from Figure 5-17 are: high porosity in the infused PEEK (Image 6), poor adhesion between the PEEK and the metal foam (Image 5), and voids present in the APC-2 laminate (Image 3).

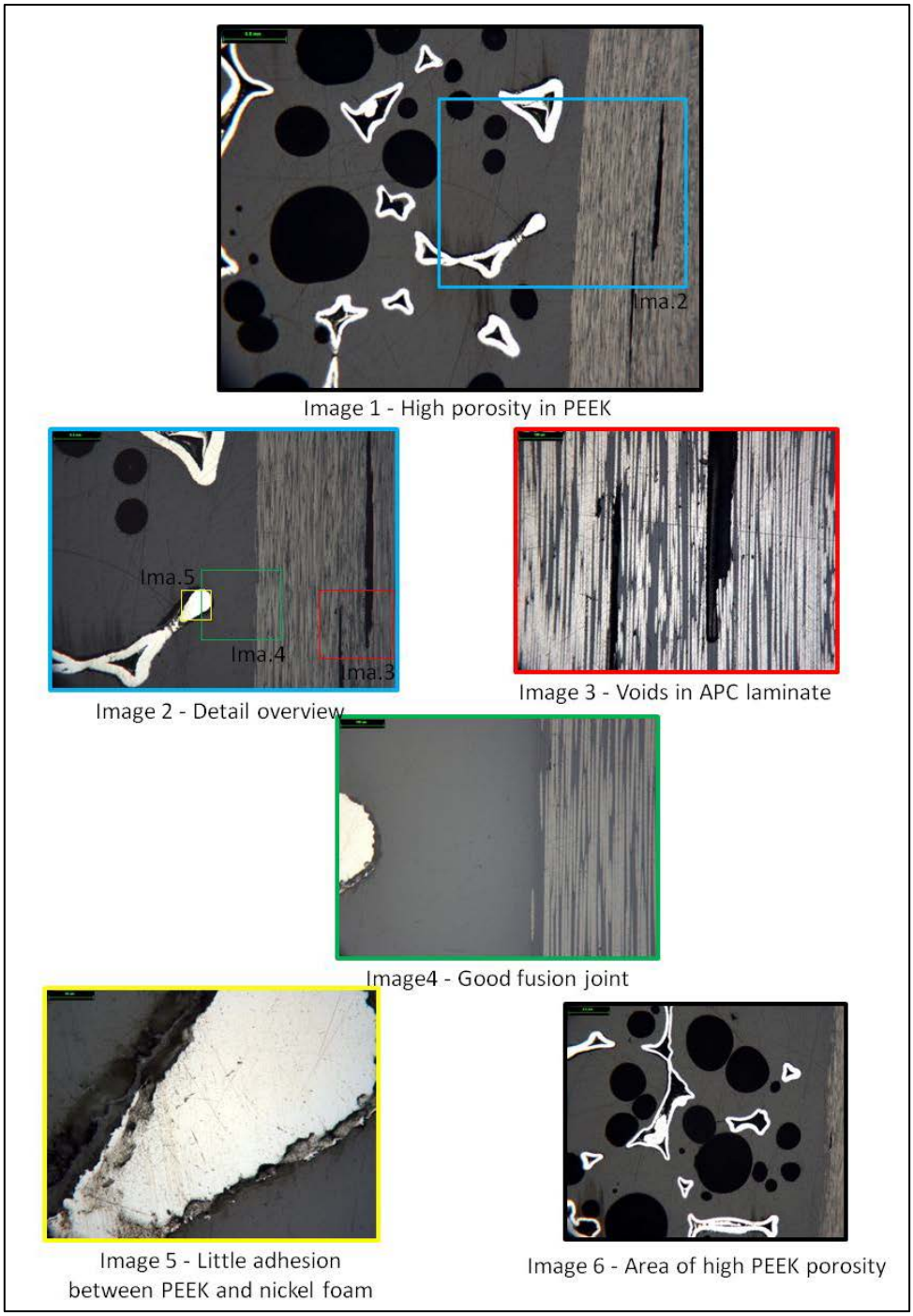

Figure 5-17 - PEEK infusion of metal foam and thermoplastic welded join to APC2 composite

5.3.2.3 Crystallinity of PEEK within the PIMF intermediate material

The DSC trace of PEEK extracted from the PIMF intermediary material is shown in Figure 5-18, and DSC traces of specimens of PEEK that were quench cooled and slowly cooled through polymer solidification temperatures are shown in Figure 5-19 and Figure 5-20, respectively.

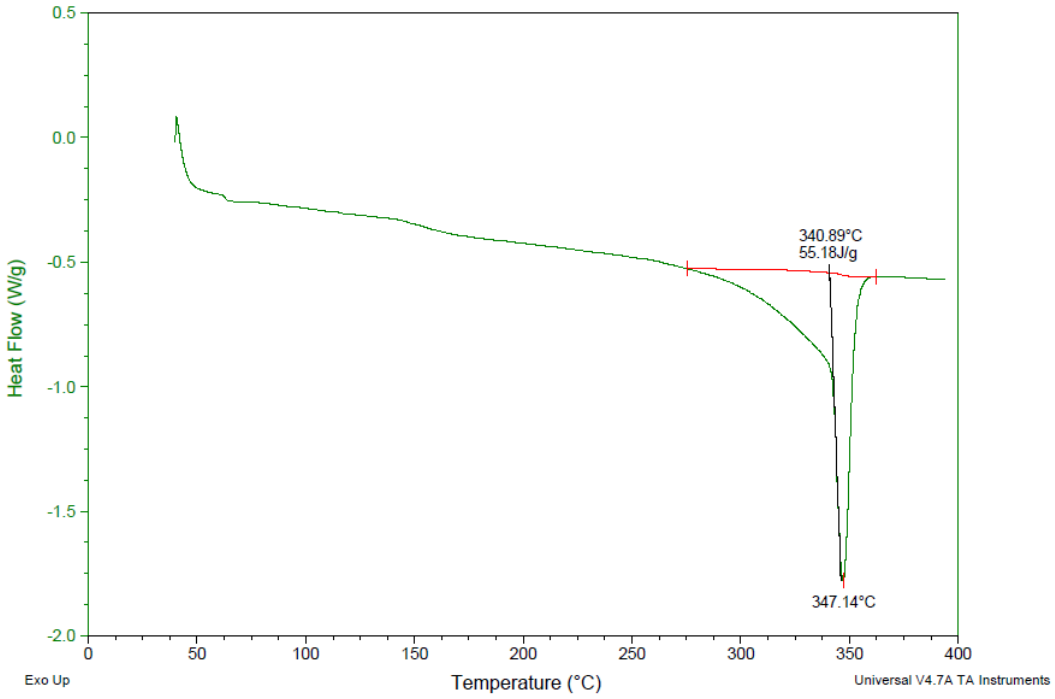

Figure 5-18 - Result of DSC with temperature ramp rate of 20°C/min, sample was 10.09mg of PEEK extracted from PIMF material

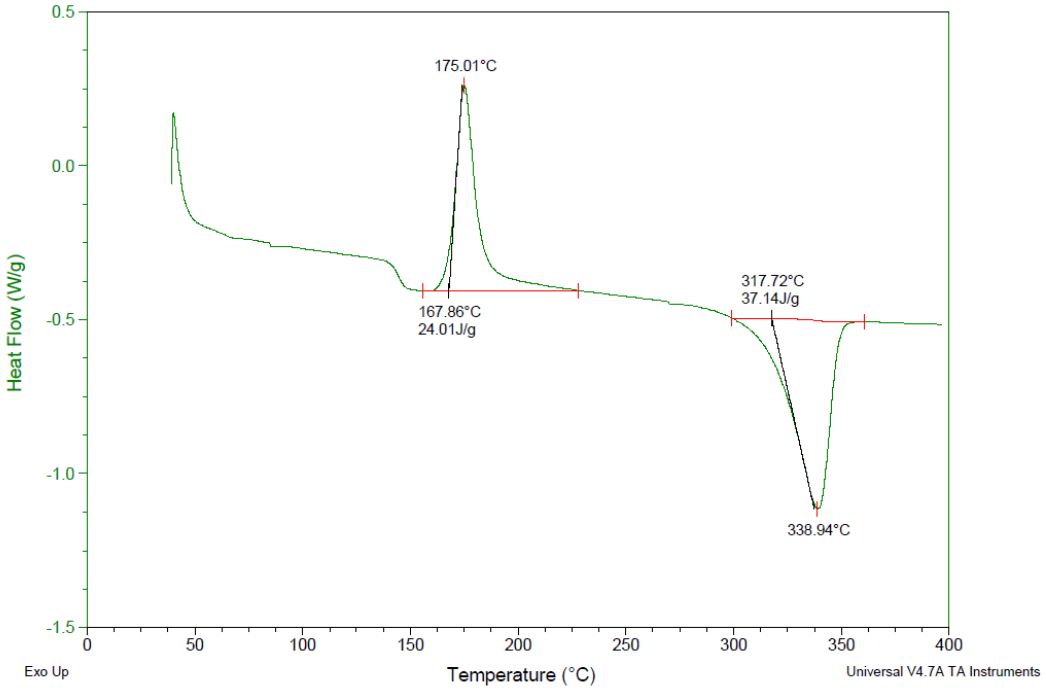

Figure 5-19 – Result of DSC with temperature ramp rate of 20°C/min, sample was 10.09mg of PEEK that was quench cooled from molten to solid

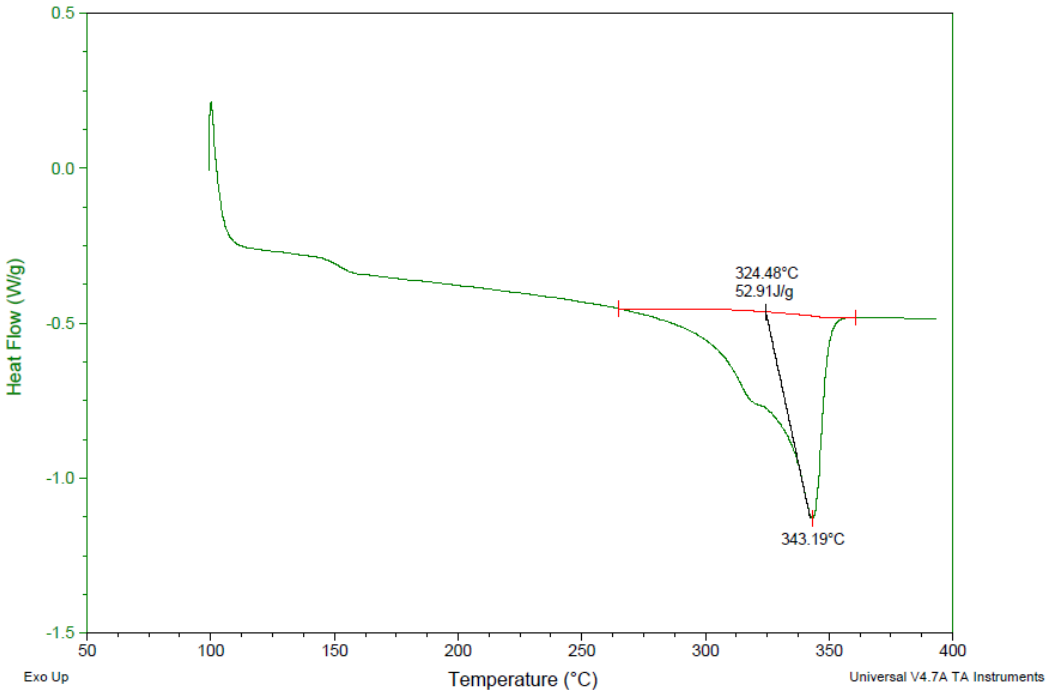

Figure 5-20 - DSC with temperature ramp rate of 20°C/min plot, sample was 10.09mg of PEEK that was cooled from molten to solid at a rate of 1°C/min

From the DSC trace of the PEEK specimen extracted from the PIMF material, shown in Figure 5-18, it can be seen that there is no exothermic peak in the 150-200°C range. Such an exothermic peak is associated with energy release as molecules move to a lower energy state as the polymer structure changes from amorphous to crystalline. An example of PEEK crystallisation can be seen in the DSC trace of the quench-cooled amorphous PEEK sample, shown in Figure 5-19. The DSC trace of the PEEK extracted from the PIMF material more closely resembles the DSC trace shown in Figure 5-20, which is of a PEEK sample that was cooled sufficiently slowly to have maximum crystallinity. The conclusions can therefore be drawn that the PEEK, which is infused into the metal foam (i.e. the PEEK of the PIMF material), has the maximum crystallinity that is possible when allowing the material to cool slowly in a controlled manner. The slow cooling was a result of the surrounding polymer processing equipment cooling unassisted to ambient conditions over a 12 hour period. This maximum value of PEEK crystallinity is approximately 35% (Kumar, Anderson and Adams, 1986). It is seen in the literature that this maximum percentage of PEEK crystallinity corresponds to maximum tensile strength, tensile modulus, shear strength, and shear modulus but minimum fracture toughness (Jones, Leach and Moore, 1985). Also observable in all the DSC traces are: the expected glass transition discontinuity at 140-150°C, and the endothermic melting peak at 340-360°C. These finding indicate that the process of melt press infusion of PEEK into chromium treated nickel metal foam is not causing degradation of the PEEK.

5.4 Discussion and Conclusions

5.4.1 Concluding message

It has been demonstrated that a polymer infused metal foam can be used as an intermediary material for joining metal sheets and fibre reinforced polymer. The novelty of this joining technique is structural joints can be achieved between the two dissimilar materials without the necessity of using either of the traditional joining techniques of adhesive bonding or the use of mechanical fasteners.

5.4.2 How this chapter supports this message

This chapter has detailed a method of manufacturing a prototype joint in order to evaluate the concept of using a polymer infused metal foam as an intermediary joining material. Limited mechanical testing showed that the joining technique was capable of withstanding loads that could be useful for structural applications. Evaluation of the joint failure characteristics together with metallographic inspection of the various joining elements indicate that the joint is best considered as a structure with the three distinct joining elements of: metal-plate to metal-foam braze joining, dissimilar material interlocking by polymer infusion of metal foam, and thermoplastic welding of polymer infusion to composite laminate matrix system.

5.4.3 Points that remain open to interpretation

5.4.3.1 Strength of metal foam and effect on FMI joint performance

The metal foam strength value considered in this work was the flexural strength, however the joint ultimate failure appears to be by local tensile/shear failure of the metal foam, therefore an accurate method of quantifying the strength of the metal foam in combination tension and shear loading would lead to a better understanding of the MFI joining behaviour. Overall, from examination of post mechanical test failed specimens, the joint strength is expected to be limited by the strength of the metal foam. Strength improvement could therefore be achieved by varying the density of the metal foam to attain a strength increase of the foam at the braze-joining interface, as shown diagrammatically in Figure 5-21. A higher foam density at the brazing interface would also provide a greater number of metal foam nodes that are within optimum braze joining proximity to the metal plate. The foam density could be locally increased by crushing, however this would result in damage to the foam that may degrade the materials properties further. Alternatively, a desired metal micro-architecture could be formed by additive manufacturing (Li, 2015).

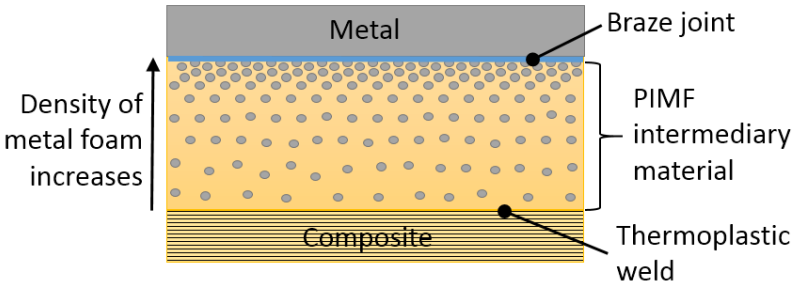

Figure 5-21 – Cross-section illustration of the concept of a density gradient metal foam to potentially improve foam to metal joining

5.4.3.2 Porosity of infused PEEK within the PIMF intermediate material

High PEEK porosity was observed in the specimen shown in Figure 5-17. This may be due to the following two reasons: the formation of a good fusion bond between the PEEK and APC-2 prevented gas escaping from the molten PEEK as it was press infused into the metal foam, and/or, as the APC-2 (which was essentially one wall of the mould from the point of view of PEEK infusion into the metal foam) was in a semi-fluid state at the time of press infusion there was not sufficient pressure to squeeze all air out of the molten PEEK. The degradation temperature of PEEK is 538°C and the processing temperature used in the manufacture of this specimen was 360°C. Insignificant levels of out-gassing are expected when PEEK is processed at temperatures below the degradation temperature (Victrex plc, 2015). Therefore the only likely cause of porosity is trapped air as a result of processing.

It has been identified in Section 5.3.1 that the weakest part of the MFI joint structure is the metal foam. Porosity in the PEEK that occurs in the region of the metal foam to metal plate joining interface (i.e. where the metal foam is exposed to greatest stress concentration) would result in in the metal foam not being fully supported by infused PEEK. This could have resulted in the foam being further exposed to loading, and therefore contributed to the failure of the metal foam being the site of ultimate MFI joint failure.

5.4.4 Further work that could be done

5.4.4.1 Improved brazing method

Of the two methods of braze joining discussed in Section 5.3.1 the greater joint performance is achieved by the vacuum brazing process. Therefore it is expected that if further development was done to improve the joining performance of the laser-brazed joint, and applied to a laser-brazed/thermoplastic MFI joint, the strength of the overall joint would not exceed the value of 8.83 MPa, even if the inherent SLS to DLS strength differences

were accounted for. This is because of the optimum brazing quality that is achieved by the vacuum brazing process, and also due to the combined braze and adhesive joint of the vacuum-brazed/thermoset joint. In the laser-brazed/thermoplastic joint no adhesion is observed between metal and thermoplastic. Observations of the lack of metal/thermoplastic adhesion can be seen in Figure 5-16 as gaps between the infused thermoplastic and both the metal foam and the braze metal. Also from examination of the failed mechanical test specimen, as shown in Figure 5-14, no polymer residue is seen on the interface surface, which further indicates a lack of adhesion between thermoplastic and metal. In the laser-brazed/thermoplastic joint, joining between metal foam and metal plate is exclusively by brazing.

5.4.4.2 Joint production efficiency improvements

The laser-brazing process can be further optimised, for example in this work two laser passes were used to ensure that the entire braze joining interface area was exposed to sufficient brazing temperatures; resulting from the laser induced heating. The resulting temperature measurements show that this particular multiple pass approach resulted in very limited areas of the braze interface that had been exposed to ideal brazing temperatures. And also that the areas heated to ideal brazing temperatures by the first laser pass were subsequently exposed to excessive temperatures by the second laser pass. The laser heating process could be modified to use a lower power laser beam and a high beam-travel speed, which follows a raster scan pattern that is repeated over the surface of the metal. The aim of this modified laser scanning method would be to heat up the whole area of metal more progressively, to achieve a more uniform distribution of heating at the braze joining interface, which would enable the whole area to be exposed to ideal brazing temperatures without subsequent overheating.

Also, in this laser heating approach used in this work it was not taken into account that the laser brazing was performed at the edge of the metal plate

(because of the SLS test configuration). Due to bulk material being available on one side of the heating location there was an asymmetric heating distribution, as illustrated by Figure 5-22. Understanding of this could be furthered by a numerical simulation study.

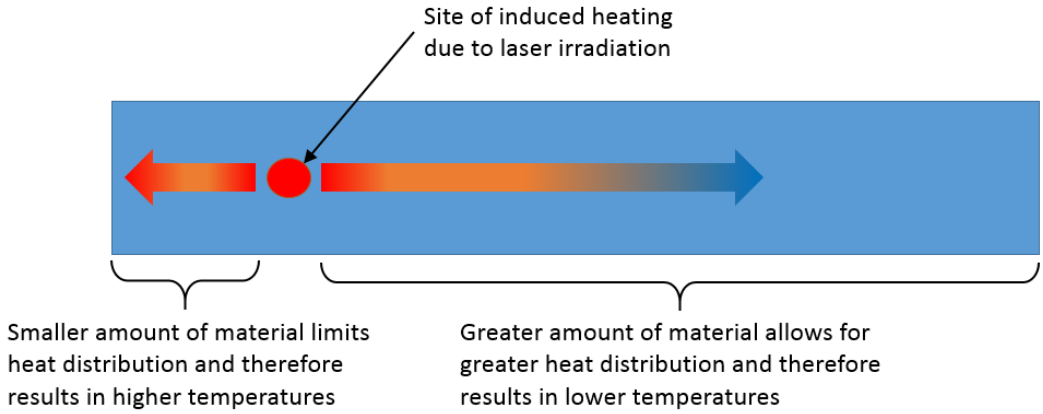

Figure 5-22 – Asymmetric heating distribution due to edge-of-plate induced heating

The heated press-moulding method of simultaneously infusing metal foam with PEEK and fusion welding PEEK to composite laminate had a slow cycle time and required complex tooling and demoulding procedures. In a manufacturing production environment a more time efficient alternative could be to use an injection moulding process. In all cases the tooling would be a significant expense and would also require a manufacturing concept similar to an injection over-moulding; as the composite and metal parts would have to be accommodated in the mould tool in the required relative positions of the final structure.

It could also be possible to improve joining between PEEK and metal. In the work reported here no evidence is seen of adhesion between the infused PEEK of the PIMF material and either: the metal plate, the braze filler metal, or the metal foam. This is considered as one reason for exploiting the metal-polymer interlocking nature of the PIMF material for the purpose of dissimilar material

joining. However, by also achieving an adhesion bond between PEEK and metal, particularly at the braze-joining interface, the MFI joint should achieve greater mechanical performance. From polymer processing reference literature (Plastics Design Library, 1997) it is reported to be possible to form a structural joint between PEEK and aluminium of approaching 20MPa, by melt bonding techniques. Metal surface pre-treatment has a significant effect on the performance of the joining technique. Further investigation could be undertaken to establish whether melt bonding could provide an additional joining mechanise in a FMI joining technique.

5.4.5 Chapter closing comments

The use of a polymer infused metal foam as an intermediate material for joining composite to metal is a wholly new method of joining that does not rely on either traditional joining methods of adhesive bonding or the use of mechanical fasteners. The investigations of the MFI joining concept described in this work, thought relatively limited, were sufficient to understand that the joining concept is capable of transferring structural loads from metal to composites. The work also identified further areas of investigation and manufacturing process development that could improve the joining technique.

6 OVERALL DISCUSSION AND CONCLUSIONS

6.1 Discussion Introduction

Engineers are increasingly turning towards fibre reinforced polymer composites material options where weight, environmental resistance, and complex geometry are critical requirements for structural applications. Key growing industries that are incorporating ever greater quantities of composites include: aerospace, automotive, and renewable energy generation. However, composites have limitations that mean they are not always the most suitable material for all structural applications. Metals have properties that are preferable for structural applications where complex loading states and durability are prime requirements. If advances in overall structural effectiveness are to be made the most suitable material for the varying application requirements should be chosen, and where this may require the dissimilar materials of composites and metals to be used within a single structure, effective, robust, and process efficient methods of joining need to be developed.

This study took several conceptual ideas of novel methods of forming structural joints between composites and metals, manufacturing methods were then devised so to enable the production of specimens that could be used to enable comparable strength and joint failure characterisation.

There are specific challenges of joining composites due to the anisotropic nature of the material architecture. The strength of long fibre laminar composites, especially where the matrix material is polymeric, is predominantly in the planar directions. The out-of-plane, often also referred to as through-the-thickness, direction is dominated by the [comparative to reinforcement fibre strength] low strength polymer matrix. Discrete joining methods, such as mechanical fastening or limited area adhesive bonding, have the tendency to either introduce or [through secondary bending] induce out of plane loads at the location of the joint. The joining process can also result in localised knock-downs in strength, the most common example of this is hole drilling for the installation of fasteners.

Of the two principle joining methods for composites; mechanical fastening and adhesive bonding, adhesive bonding is preferable as the composite laminate damaging processes of hole drilling and fastener installation are not required, also the load introduction is more uniformly distributed in adhesive bonding. However, there are three significant drawbacks of adhesive bonding:

- Induced secondary bending due to joint geometry, which results in out-of-plane peel loads that have the effect of diminishing the bonded joint strength to below that of the idealised adhesive bond strength. Fastening is routinely employed as a method of providing reinforcement at the extremities of a bondline. The fastening elements work to resist the out-of-plane peel loads
- There is often low confidence in adhesive bonding due to the difficulty of inspecting bondline quality, fastening elements are frequently incorporated as a way of providing a fail-safe joint
- Complex and costly adherend jigging is often required to hold parts in the correct position while the adhesive system cures. Mechanical fastening can be utilised to provide jigging.

These three factors steered this study towards investigating novel methods of mechanically reinforcing adhesive joints.

The challenge of this study was to investigate the dissimilar material structural joining between composites and metals. There are added complexities of combining these two dissimilar materials due to the differences in properties between the two: thermal response, chemical affinity, and the processing temperatures required for the efficient metal joining techniques. A highly effective and efficient method of joining metals is by fusion welding. The temperatures required for fusion welding are above the degradation temperatures of polymer matrixes of composites. This places limitations on the order (manufacture schedule) of constructing specimens of the concept joints in this study. It was identified however that there was an opportunity to exploit metal-to-metal joining techniques to manufacture novel metal-to-composite

joints that have a greater robustness than traditional metal-to-composite joining techniques, this increased robustness can then be considered to offset some of the issues associated with joining the dissimilar materials:

- Stronger joints negate the inherently higher localised loading that occurs due to the differing mechanical properties of the materials being joined, for example, significantly different values of thermal expansion and [specific] stiffness
- A more efficient joining process results in a Life-Cycle Analysis (LCA) cost saving in one area that can offset additional LCA costs incurred due to additional production steps.

6.2 Novel mechanical reinforcement of adhesive joints for residual strength, pseudo-ductility, and increased energy absorption during failure

Ductile failure is a desirable engineered characteristic for structural joints. Ductility of a joint enables failure to be progressive, this enables load-elevation of highly loaded structural elements without complete loss of structural integrity, and also provides the opportunity for damage to be identified and repaired before catastrophic failure occurs. It is well known that adhesive joints exhibit low strain-to-failure, brittle failure characteristic, and that such behaviour is also typically for fibre reinforced plastic composites.

Both the micropin and RSW reinforced joints are predominantly an adhesive bonded joint; with the resin system of the composite being exploited as an adhesive between laminate and metal adherends. Due to the differences in properties between the adhesive bond (polymer driven and so comparatively brittle; lower strain-to-failure) and the shear/tension loaded micropins (metallic driven and so comparatively ductile; higher strain to failure). The adhesive bond will initially react the entire joining load, the micropins only pick-up load once the adhesive bond is in a failing state. The same situation exists for the RSW reinforced adhesive joint. This is why both joining techniques are described as

mechanically reinforced adhesive joint and not an adhesive reinforced mechanical joint.

In comparison with previous investigations of micropin reinforced joints: TWI Comeld (Smith, 2005), CMT-Pin hybrid joining (Ucsnik et al., 2010), and more recently Airbus Group Innovations HYPER joint, (Parkes et al., 2014), the strength improvements seen in these joining methods have also been seen in the investigations report in this work. The discovery made here is that the same shear-loaded joining strength improvements can be achieved with micropins that do not have mechanical locking head shapes. Further understanding of how joining performance is enhanced has been gained through examination of the behaviour of the joint's micro-architecture; both of the composite laminate and the surface structured metal adherend, by inspection of partially failed specimens, this made it possible to ascertain the reasons for the joining performance advantages of micropin reinforced adhesive joints.

The locally resin-rich area around the micropins; due to eyelet formation as a result from micropin insertion, creates a locally soft region of the composite laminate adjacent to the micropins. These soft areas permit localised micro-failure of the laminate at lower stresses than the bulk laminate. The localised damage enables the micropins to deform from a purely shear loaded geometry into a combination shear and tension loaded state. These localised micro-failures of joining elements contribute to the overall pseudo-ductile failure characteristic of this joining technique.

The reported strength values are the ultimate strength of the joints. In all cases the ultimate failure is beyond the linear region of the stress strain curve and the linear region appears to be unaffected by the inclusion of reinforcing micropins. The use of micropin reinforcement enable the joints, during failure, to progress further into the yield region of the stress strain curve before ultimate failure occurs. The yield region is a combination of reduced bond area, as the joint disbonds during failure, and localised yielding of the metal substrate and micropins. As the disbond area grows a greater amount of the metal substrate

is exposed to the loading. This exposed area of the metal substrate can be considered to have been deprived of being reinforced by the laminate to which it was bonded, this therefore results in greatly increased stress (60% increase for 6mm substrate samples and 75% for the 3mm), which in turn drives the metal that is newly exposed to the higher stress-state, to undergo substrate yielding. This is most apparent in the samples that that use 3mm metal substrate. [Within the joining region, during failure, residual joint strength is greater than the yield strength of the exposed metal adherend, enabling ductility within the joint as it fails.]

The increase in joint strain at ultimate failure with use of reinforcing micropins is greater than the corresponding increase in ultimate strength for the same samples; this demonstrates the increased ductility of the micropin reinforced adhesive joining system.

The RSW reinforced joints do not exhibit quite the same behaviour, in the majority of cases there was an initial brittle-like failure that is attributed to adhesive failure, there is a more clear transfer of loading onto the RSW attributed joining mechanism compared to the load transfer to micropins. One key difference between the micropin and RSW reinforcement techniques is that the use of micropins is observed to degrade the adhesive bond performance whereas the application of a RSW enhances the adhesive bond performance. The micropins effectively reduce the adhesive bond area because of the physical presence of micropins at the bonding interface. The micropins also disrupt the bondline by locally increasing the bondline thickness as the weld fillets of the micropins force reinforcement fibres away from the planar faying surface of the metal adherend. Whereas the application of the RSW acts to pinch the fibres and the metal adhered surface closer together so ensuring the bondline is not excessively thick around the site of mechanical reinforcement by the RSW. For adhesive bonding it is usually considered that there is an optimum thickness for a bondline, and in this work what this value may be is not specifically considered, however as a typically guideline a thin bondline is usually preferable to a thick bondline.

As the greatest improvements in the strain-to-failure capability of the micropin reinforced joint is within the yielding region of the stress-strain curve, which in engineering terms is considered as a failure state of the structure, the strength improvement cannot be considered as useful for repetitive operational loading conditions. Where this feature of the joining system can be considered as useful is in the situation of extreme loading conditions, as it both increase the ultimate failure load of the joint and also provides residual strength to partially failed adhesive joints. Therefore the micropin reinforced adhesive joint can be considered as a damage tolerant adhesive joint. This provides a valuable non-separation feature of the joint, which can be utilised for ‘get-me-home’ loads and so increase engineering confidence in adhesive joining for aerospace applications. The same can be said of the exhibited residual strength characteristic of the RSW reinforced joint but with the added advantage that the [adhesive bond attributed] maximum load is increased by the application of the RSW.

In civil aeronautics there is a requirement that bonded joints must be failsafe by means of mechanical fastening, the micropin reinforced adhesive joint is therefore a novel way of addressing this requirement in a more structurally and manufacturing efficient way than the use of mechanical fasteners. The exhibited joint pseudo-ductility of micropin reinforced adhesive joints, in addition to progressive failure and residual load carrying capability, also absorb a comparative greater amount of energy during failure. This characteristic of the joining technique will also be of benefit in real-world applications such as crash loading in automotive applications. The RSW reinforced adhesive joint cannot be strictly classified as fail-safe, as the RSW does not withstand equal or greater load than the adhesive, however it can be described as damage tolerant. This is an advantage over adhesive-only joining and so is also a step towards increasing the confidence of employing adhesive bonding for structural applications. Further confidence in adhesive bonding can be gained for the RSW reinforced joint as the technique results in a reduced variance of ultimate load.

6.3 Joining performance enhanced by increased interaction of metal and composites

The principle load carrying elements in a composite material are the reinforcement fibres with the polymer matrix having the functions of controlling fibre orientation and transferring load between the fibres. When joining metals to composites by adhesive bonding the load path of the joint is therefore from the fibres, into the composite polymer matrix, from the surface of the polymer matrix into the polymer system of the adhesive, and then from the adhesive into the surface of the metal structure. Polymers are considerably weaker than either the reinforcement fibres or structural metals. Therefore the weak link in an adhesive joining system is either the polymer matrix of the composite or the polymer system of the adhesive, depending on the polymers chosen.

In mechanical fastened joints, when a fastener is loaded in shear, the load path is different from an adhesive bond. Load is transferred from the composite laminate via the fastener into the metal structure. Load is transferred from laminate to fastener shank by bearing load. This is a local compressive load of a portion of the inside surface of the bolt hole. When considering the interaction between fastener shank and laminate there is a more direct interaction between fibres and bolt shank when compared to adhesive bonding; as the fibres (end-on) and fastener shank are in direct contact. However, the compressive strength of a composite is significantly less than the tensile strength, typically the compressive strength is between 25% and 50% of the tensile strength. When loaded in compression a composite is usually considered to be dominated by the properties of the polymer matrix. Therefore once again the polymer system can be considered as the weak link in the joining system.

Both the above descriptions of joining load paths are simplified, as other features of the joints contribute to load transfer, for example in a fastened joint loaded in shear the clamping force between joined parts, which is introduced by tightened the fastener, increases the friction force between faying surfaces.

Such load transfer mechanisms can prove to be significant to the performance of a joint but must be considered as secondary to the primary load transfer mechanisms, this is particularly the case during joint failure as secondary load transfer mechanisms can be greatly diminished. In the above example, during the failure of a mechanically fastened joint, once the tightness of the fastener is lost, which could be due to local deformation, the high friction between faying surfaces will be lost.

The load transfer mechanisms of the concept joints of this study have significant differences to those of traditional adhesive or mechanical fastened joints. It is these differences that contribute to the observed joining improvements. The nature of the interaction between metal and reinforcement fibres being the most significant difference. In the micropin reinforced adhesive joint the micropins penetrate into the laminate, and due to the use of arrays of many micropins, when compared to numbers of fasteners in a mechanically fastened joint, there is much higher density of interaction between the mechanical joining elements and fibres. The size of a micropin is also closer to the size of the reinforcement fibres than is the size of a traditional mechanical fastener, this comparative scale may also play a significant factor in the joining performance. In the RSW reinforced adhesive joint the fibres interact directly with the metal, the fibres and metal adherend are crimped tightly together at the RSW and when a fibre penetrating IMM weld is used the fibres pass into the weld itself. There is also interaction between fibre and weld splash that is expelled from the IMM RSW.

When considering metal and reinforcement fibre interaction of the Metal Foam Intermediary joining technique; there is no interaction between the metal and composite being joined, this was a criteria of the joining concept. If the three concept joints were to be ranked in terms of the observed joining improvement over baseline joints, the RSW Reinforced Adhesive Joint would be greatest, followed by the Micropin Reinforced Adhesive Joint, and then the Metal Foam Intermediary Joint. Therefore it can be ascertained that by increasing interaction between metal and the composite reinforcement fibres the joining performance of metal and composites is improved.

6.4 Manufacturing process improvement by use of novel mechanical reinforcement of adhesive joints

The joining concepts investigated demonstrate potential manufacturing process improvements and represent a progressive step forward from similar techniques previously investigated and which are reported in the literature. The following paragraphs discuss the manufacturing advantages of the joining techniques investigated in this work.

The micropin reinforced joint demonstrates that the joining technique can be used with prepreg composite materials, which has manufacturing process advantages over the dry-fibre preform and resin infusion methods (Smith, 2005; Ucsnik et al., 2010). In the previous studies the greatest improvement in joining performance was achieved when micropins with a ball-headed shape were used. The high performance was attributed to the geometry of the micropins acting to restrain themselves within the composite laminate and preventing them from simply being pulled-out of the laminate. There was a significant manufacturing limitation of using ball-headed micropins which was the labour-intensive manufacturing method of inserting micropins into dry fibre fabric with a subsequent resin transfer infusion manufacturing process.

The investigation in this study showed that the same type of joining advantages can be achieved when high aspect ratio sharply pointed pins are inserted into laminates of uncured CFRP prepreg. The pointed shape is required to enable ultrasonically assisted penetration of the pins into an already laid-up but uncured prepreg laminate. The micropins used in this study resist pull-out due to a combined effects of: the depth of laminate penetration, the large adhesively bonded surface area of the pins, and local laminate softness around the pins that enable them to deform during failure loading into shapes that withstand higher loading states. This demonstrates that the same joining performance advantages can be achieved when a prepreg composite manufacturing method is used.

As a composite manufacturing method, prepreg has advantages over dry-fibre infusion in that the fibre to resin ratio, laminar placement, and materials quality assurance can all be controlled to a higher standard. These are the reasons why prepreg is the preferred composite manufacturing method for critical aerospace applications. And so the possible use of prepregs for the micropin reinforced adhesive joint enables the benefits of prepreg to still be exploited when using the micropin reinforced adhesive structural joining technique.

Combination adhesive and RSW joining techniques are extensively used in the automotive sector for metal-to-metal joining. Recent investigations have demonstrated that similar methods can be used for joining composites to metals (Shah et al., 2010), provided post laminate manufacture preparations are made, preparations that are akin to those required for mechanical fastener installation, specifically: machining of holes. The RSW reinforced joint investigated in the work presented here demonstrates that mechanical reinforcement can be achieved without the need to make holes in the composite material to accommodate metal-to-metal resistance spot welding, as is required by the contemporary Super-Lap-Shear RSW composite to metal joining technique (Shah et al., 2010). As a result of these investigations it is now understood that the molten metal generated in the RSW process can be exploited to penetrate carbon fibre fabric, this penetration of fabric by molten metal is a process that can replace the necessity of preparing holes in a composite laminate.

The observed interaction between welding process generated molten metal and carbon fibre is also is a step towards demonstrating that the metal to ceramic braze joining technique discussed and investigated by Messler, Chen et al, and Singh et al, (Chen et al., 2010; Messler, 2004; Singh et al., 2005; Singh, Asthana and Shpargel, 2007) could be applied as a technique for joining metal to ceramic fibres; such as carbon fibre used in CFRP.

Common to both the micropin and RSW reinforced joints, it is demonstrate that epoxy resins matrix systems can be utilised for adhesive bonding of composite laminate to stainless steel adherends. This shows that it is not always

necessary to include an additional specific adhesive material in order to form an adhesive joint; the composite polymer matrix system can be sufficient, particularly when increased joint strength is provided by mechanical reinforcement of the adhesive bond.

The metal foam intermediary joining concept demonstrates how a single material, the open-cell metal foam, can be utilised to accommodate effective metal-to-metal and polymer-to-polymer joining techniques. The infusion of the metal foam with a thermoplastic forms an interconnecting mechanically-interlocking network between the metal foam and the infused polymer that overcomes the issues of poor adhesion between the two materials. This intermediary material enables the application of proven joining methods; a thermoplastic welded joint to a composite laminate and also a braze joint to a metal. It can be said that this novel mechanical joint between a composite and a metal is a method of mitigating bonding issues between thermoplastic matrix composites and metals.

6.5 Elimination of traditional mechanical fastening of composites

The three joining concepts investigated in this work all contain mechanical fastening elements that do not require the use of traditional mechanical fasteners such as bolts or rivets. It is demonstrated that the mechanical fastening elements of the micropin reinforced and RSW reinforced adhesive joints outperform benchmark adhesive-only joints. This is in-part attributed for the same reasons as do adhesive joints reinforced by mechanical fasteners; principally, the mechanical reinforcements react out-of-plain peel loads. The metal-polymer interlocking network of the MFI joining concept achieves a mechanical connection between thermoplastic matrix composite and metal, in the same philosophy as does the use of a traditional fastener would enable a mechanical joint between these two materials that are difficult to adhesively bond. The novel methods that are employed in these three concept joints of

forming mechanical connections have advantages over the use of traditional mechanical fasteners.

The installation of mechanical fasteners requires damage inducing post-processing of the parts being joined due to the necessity of drilling holes. This is of particular concern for composite laminates that have greater damage sensitivity than metals. The mechanical joining methods of the three concept joints do not require such post manufacture processing of composite laminates and therefore eliminate this cause of material degradation. There is still a directly attributed material degrading effect on the quality of composite laminates that is a result of the joining techniques of the three concept joints. For the micropin and RSW reinforced adhesive joints the mechanical reinforcement methods cause disruption to the fibre architecture of the composite laminate, however these disruptions are caused prior to curing of the thermosetting resin and so no damage is introduced into the laminate polymer matrix system post cure. For the MFI joining technique, a thermoplastic welding technique is used to join the thermoplastic that is infused into the metal foam to the thermoplastic matrix system of the composite laminate. As the thermoplastic matrix system is melted there is the possibility for fibre movement that could result in a degradation of the reinforcement fibre architecture. Degradation of the polymer system due to the melting and solidification process is less of a concern as DSC measurements indicated that a high level of polymer crystallinity was present in the polymers after the welding process. It is considered that polymer properties of toughness and chemical resistance improve with increased crystallinity. Overall it is considered that although for all three of the concept joints the composite laminate has some aspect of degradation induced, compared to an ideally manufactured composite laminate, but that the damage is less detrimental than post manufacture process hole drilling. This is considered as a contributing factor to the improved joining performances observed.

The use of mechanical fasteners as either a primary joining method or as reinforcement of adhesive joints adds weight to the overall structure due to the

weight of the actual fasteners. For this reason, when low weight is a critical design criteria adhesive bonding is preferential over mechanical fasteners. As the weight of the adhesive and the structural overlaps required for adequate bonding area will be less than the weight of a joining solution that is reliant primarily of the use of fasteners. However, civil airworthiness requirements stipulate the use of mechanical fasteners as a failsafe feature for bonded joints due to the low confidence in adhesive bonding owing to complicated assembly methods and difficulty of bondline inspection. It has been stated previously that the novel methods of mechanically reinforcing adhesive joints, which are investigated in this work, could be considered as a step towards meeting such criteria by providing alternative mechanical reinforcement methods to the use of fasteners. This potentially represents a lower weight solution to the use of mechanical fasteners. The novel methods investigated in this work require additional structure compared to an adhesive-only joint: these being the micropins accompanied by an adequately thick composite to permit insertion of the pins, and an interleaved stack of metal sheets and carbon fibre fabric for the RSW joint. To ascertain whether there is a weight saving potential of the novel joining methods structural joints would need to be designed, using the various methods, which are capable of withstanding equivalent loads. By weighting the prototype joints, and validating by mechanical testing that the joints have equivalent strength, it could be understood whether there is any weight saving advantage with the novel joining methods.

By eliminating the use of mechanical fasteners, the fastener installation manufacturing stages are also eliminated. It could be argued that this would save time and cost of the overall manufacturing of structures, however the joint concepts do require additional operations in early manufacturing stages (for example micropin welding and insertion, and IMM resistance spot welding). A dedicated study, supported by LCA techniques, would therefore be required to understand whether the novel joining techniques present a manufacturing efficiency improvement compared to traditional joining methods.

It is however worth acknowledging that there are disadvantages of the novel joining techniques investigated in this work when compared to traditional mechanical fastened joints. This first concerns the joining process, the use of mechanical fasteners is relatively straightforward and can be achieved by flexible and well understood procedures. The process can accommodate either part-to-part assembly with pre-prepared fastener holes or in-situ drilling, where assembly tolerance control is more critical. Joining by fasteners is also convenient when a structural assembly is formed from parts provided by various suppliers or when parts are particularly large or complex in shape or function. Even though the mechanical fastening scheme is methodically considered during structural design the consideration of the joining process requirements of these novel techniques will be of greater emphasis due to the reduced process flexibility compared to mechanical fastening. It is argued by R. W. Messler that as materials and applications become ever more sophisticated that so should the joining process become more sophisticated also, and that the joining methodology be equally considered along with the material and structural design (Messler Jr., 2004).

Another real-world consideration is inspection of a joint. Fasteners are relatively simple to inspect; as to whether they have been installed correctly and likewise during in-service inspections whether there is loss of structural integrity due to, for example, fastener torque loss or corrosion. If rework or repair is required straight-forward techniques are available, which will typically involve the fastener being replaced either like-for-like or with an oversized fastener installation process. The novel joining methods investigated in this work are prone to the same inspection difficulties as adhesive joints. Non-Destructive Evaluation methods may be further complicated due to greater interaction of metal and composite materials. The feature of these joints are that they include reinforcement and multiple load paths and so are more robust than adhesive-only joints and should mitigate the difficulties of inspection.

It can be required for structures to be disassembled for such activities as maintenance, inspection, or repair. Mechanical fasteners provide a convenient

method of assembling an essentially temporary joint. The novel joints are again subject to the same limitation as an adhesive joint, in that they cannot be easily disassembled. Methods are available for breaking-down adhesive joints in some situations. However due to the level of interaction between metal and composite in the novel joints such disassembly is unlikely without the destruction of at least one part of the joined structure; most likely the composite laminate. It could be possible for pyrolysis or acid digestion processes to be used to salvage the metallic components of the Micropin Reinforced Adhesive and the Metal Foam Intermediary joints, which could then be reused in a new structural assembly.

Where a non-permeant assembly is required the new joining concepts may provide a benefit by enabling an effectual structural transition from composite to metal within a single part for the purpose of providing distinct sections of the part that have high structural efficiency (composite) and are robust for the use of mechanical fasteners (metal). Figure 6-1 provides an illustration of a possible application of a removable access panel. This application exploits the improved composite to metal joining properties of one of the novel joining concepts, in this example it is the RSW reinforced adhesive joint, while still accommodating the design requirement for structural disassembly; which in this example is by the use of mechanical fasteners.

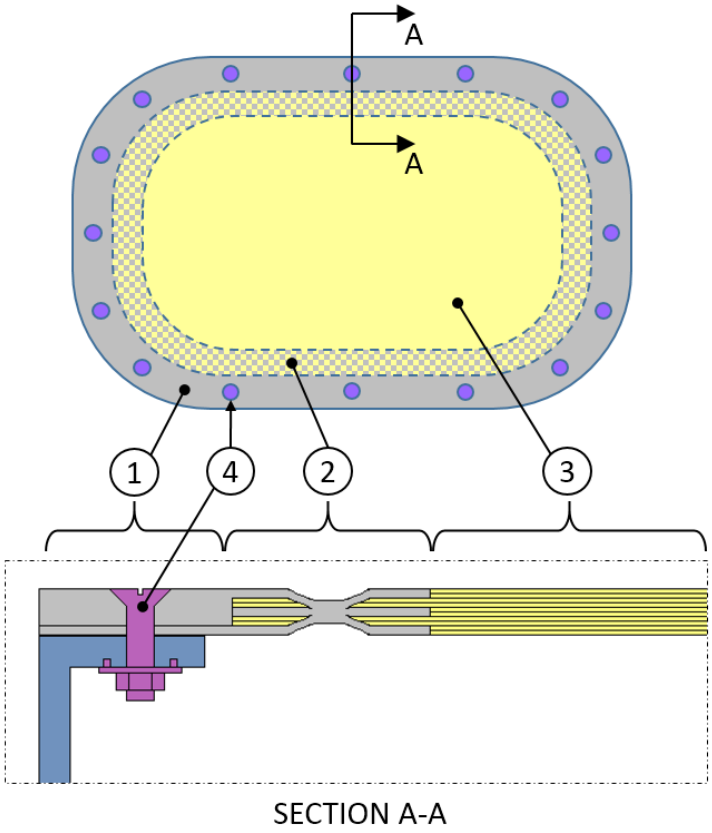

Figure 6-1 - Application concept of a novel joining method where disassembly is a design requirement

In Figure 6-1 (1) is a robust metal to metal interface that accommodates the use of mechanical fasteners (4), (2) is the transition zone from metal to composite that exploits a novel joining technique, and (3) is the structurally efficient main body of the part formed from composite material.

6.6 Further work

6.6.1 Refine and develop the concept joining methods to establish design guidelines

The three novel joining methods that have been investigated in this work have exhibited benefits when considered against traditional methods of joining metals to composites. The work here can be considered as preliminary investigations that were conducted principally to understand and characterise the nature of the

novel joining methods. In order to progress through the TRLs to become viable in application it would be necessary to further the understanding of the novel joining methods so that adequate design guidelines can be established that would enable the structural joints to be used with confidence.

The micropin reinforced adhesive joint can be further investigated in a number of ways. The arrays of micropins were shown to be most effective when concentrated in the bondline runout regions of the adhesive bond. This was contrary to the prediction of FEM simulation, which suggested that the arrangement pattern of the micropins had negligible effect and that it was simply the total number of micropins that influenced joint strength. The knowledge that micropin arrangement does affect joint strength could be used to improve FEM simulation of the micropin reinforced joint, which conversely may prove useful in developing an improved accuracy FEM simulation sensitivity study, to determine optimum micropin array pattern. Alternatively, Design of Experiments (DoE) methods could be used to define a series of experimental tests to understand optimal micropin array patterns. The overall joint and adherend geometries could likewise be investigated to determine optimums for various loading conditions and real-word application driven structural geometry limitations, which for example may be a Single-Lap-Shear scarf joint rather than the Double-Lap-Shear geometry investigated in this study.

The same methodologies as described in the previous paragraph; FEM simulation and DoE driven optimisation studies, could also be used to define reinforcement patterns and joint geometry of the RSW Reinforced Adhesive and the Metal Foam Intermediary joints. Also applicable to development of all three novel joining methods is the case that only one set of materials were ultimately investigated for each joining concept. In practical application this would place a significant limitation on the usefulness of the joining methods. Changing materials, particularly the metal, is likely to have the greatest impact on the micropin and RSW reinforced adhesive joints. As the CMT-Pin welding and the Interleaved Multi-Material resistance spot welding processes are technologically sophisticated it would require significant investigative work to achieve

implementation of these techniques for alternative metals. The Metal Foam Intermediary joint is relatively flexible to changes of metals provided an adequate braze filler metal is chosen that is compatible with both the metal foam and the solid metal part.

When choosing the various materials, including the choice of adhesives, it could also be investigated how joining performance is affected due to comparative strain to failure properties of the dissimilar materials. For example, if metals and composite materials with more similar stiffness properties were used together it may facilitated a more progressive failure owing to a more gradual exposure of joining elements to the changing loading states that occur during material and structural failure. Indication that ‘failure characteristic optimisation’ could be achieved with the RSW reinforced adhesive joint has been observed (variations in such behaviour can be seen in Figure 4-42).

The investigation of this method of joining proved that the micropins behaved as mechanical reinforcements of the adhesive joint in the same way as traditional mechanical fasteners do. And also that the positioning of the reinforcements had an effect on the joint strength, this was something that is again analogous to what would be traditionally expected. Although in the supporting FEM numerical simulation study it was stated that position of micropins had negligible effect, the micropins did in fact have greatest effect when positioned in bond run-out regions that experience the greatest out-of-plane loading. Such similarities between the behaviour of the novel joining concepts and traditional well-understood joining methods, will help steer the choice of investigations required to establish design guidelines for the novel joining concepts.

6.6.2 Investigation of observed unique features for further exploitation as joining mechanisms

6.6.2.1 Pseudo-ductility and biomimetic characteristics of micropin shapes and joint geometry

Inspection of failed and partially failed micropin reinforced adhesive joints showed that the high aspect ratio pins do not pull out of the composite laminate. Micropin pull-out might have been expected due to the lack of any pin-head fastening mechanism such as is present with the use of the ball-headed pins of other studies. The micropins used in this study resist pull-out due to a combined effect of: (1) depth of laminate penetration and the high surface area of the embedded pins that is adhesively bonded within the laminate, and (2) the symmetric DLS geometry of the joint being resistant to relative-rotation of the composite and metallic adherends into a deflected shape that would otherwise favour pull-out of micropins. These two aspects of the joint configuration permit local deformation of the micropins close to the metal-substrate attachment points.

The micropin deformation is also considered to be enabled due to local softness of the laminate that is a result of the localised resin richness of the laminate around the pins, which results because of eyelet formation that occurs as fibres are separated by micropin insertion. The localised softness coincides with load intensification that is caused by the pin (Liu and Hou, 2003; Liu, Raju and You, 1999). The localised micropin deflected shape has the effect that the pins carry load as a combination of shear and tension of the pin shank rather than purely shear as may be expected by the joint geometry This behaviour of micropins deflecting into a shape that better resist loading is analogous to structural properties being specifically engineered into composite material architecture and joint design as part of contemporary studies that are inspired by biomimicry (Burns et al., 2012a, 2012b). The work by Burns et al was to develop structures and joints of composite laminates that inherently exhibit load relieving features and tailoring of material micro-architecture to resist specific loading conditions. The characteristic of micropin reinforced adhesive joints to naturally conform to

higher load resisting configurations, and the analogies of this to biomimicry, suggests that further investigations into joining of composites to metals could benefit if biomimetics were considered as one of the core aspects of the studies.

The characterisation of the joints to withstanding localised non-critical damage can be considered as pseudo-ductility of the joining method. This observed composite joint pseudo-ductility is complementary to investigations currently underway to develop FRP composites that are themselves pseudo-ductile (Czél and Wisnom, 2013; Czél, Jalalvand and Wisnom, 2015).

6.6.2.2 In-situ casting of Metal Matrix Composite for direct fibre to metal braze joining

It was observed during the investigations of RSW reinforced adhesive joints that in the Interleaved Multi-Material spot welding process the molten metal, generated in the nugget formation zone, readily escapes as weld splash and flows along the carbon fibres that breach the welding location. It was considered that the relatively high joining performance of the IMM reinforced joints could be a result of a braze joining process between carbon fibre fabric and metal substrate, with the molten weld splash being in effect a braze filler metal. It is discussed in this work that if this were shown to be the case, the braze joining process could be improved by use of a seam welding technique; which could be used to both generate weld splash and encourage flow of the molten metal to increase wetting of carbon fibres. Further work could aim towards exploiting such a technique to a stage where the result could be effectively in-situ casting of a Metal Matrix Composite along a selective length of an interleaved stack of carbon fibre fabric and metal sheets.

In addition to such a process being useful for the purpose of forming structural joints, directly between metals and composites, the technique may also be capable of manufacturing MMCs. Established MMC manufacturing methods are batch processes that require significant energy input, in the form of both heat

and pressure, and are therefore expensive. Recent developments have progressed towards continuous manufacturing line processes but so far have been limited to the use of silicon carbide reinforcement fibres (Kong and Soar, 2005; Testani and Ferraro, 2010). Silicon carbide fibres are significantly more expensive compared to mass produced carbon fibre. A continuous process of manufacturing carbon fibre reinforced MMCs, by Joule heating driven in-situ casting, could therefore have significant cost benefits.

In this study investigations focused on the use of stainless steel due to the relatively wide processing window of the IMM welding technique compared to trials with titanium and aluminium. However from a lightweight applications point of view the combination of carbon fibre and titanium would be more desirable than carbon fibre and stainless steel. Some limited success was observed with trials using titanium that in part is attributed to superplastic flow of titanium at elevated temperature. Therefore work to further develop IMM resistance spot welding using titanium, and progression via resistance seam welding towards a continuous in-situ casting process for manufacturing of carbon fibre reinforced titanium MMC, could result in significant advantages in terms of both MMC manufacturability and ultimately achievable materials properties and structural application capabilities.

6.6.2.3 Gradual transition from metal to composite by use of variable density metal foam

It was identified that the weakest structural element in the Metal Foam Intermediary joining concept was the metal foam; and that failure of the metal foam lead to failure of the joint. The metal foam failed close to the brazed joining interface to the metal plate, which is a region of the foam that is relatively unsupported by infused polymer. It has been suggested in this work that a variable density metal foam could be used to improve performance of the joint. The density would be required to vary through the foam thickness; varying from lower density at the composite laminate interfacing side of the foam through to a

greater density at the metal sheet (braze) interfacing side. The greater density foam would have greater strength and so would be expected to increase the overall strength of the joint.

By arranging locally lower density metal foam at the laminate interface the joint could be further developed so that composite material reinforcement fibres pass into the metal foam. This could be achieved by infusing the metal foam with a short-fibre reinforced thermoplastic or by incorporating low areal weight chopped fibre matt into the process of infusing the metal foam with thermoplastic. It was shown in the micropin and RSW reinforced adhesive joints that joining performance improves with greater interaction between composite reinforcement fibres and metal. Therefore it is anticipated that by enabling interaction between reinforcement fibres and metal foam in this way could result in improved joining performance of the MFI concept.

6.7 Key novelties, innovation, and new data

- Demonstration of micropins resisting laminate pull-out, even without mechanical locking micropin geometry; such as CMT-Pin ball-head
- Measurement of carbon fibre fabric through-thickness electrical resistance and identification of asymptotic behaviour of resistance decrease with increase electrode pinch force
- Fist development of a technique to penetrate carbon fibre fabric with a metallic resistance spot weld
- Application of carbon fibre fabric penetrating resistance spot weld for enhanced structural joining of composites to metals; improved adhesive bond strength and provision of residual strength to partially failed joints
- Use of laser irradiation to provide indirect heating for the purpose of braze-joining metal foam to metal plate
- First development of a technique to use a thermoplastic infused metal foam intermediary material for structural joining of composites to metal.

6.8 Conclusions

The following summarises conclusions that are drawn from these investigations of new approaches to metal composite joining. These conclusions are organised with regards to the three joining concepts specifically and to composite metal joining in general.

6.8.1 Micropin reinforced adhesive joint

- There is a minimum areal density of anchored metallic micropins required to improve composite to metal joining performance, below this limit the disruption caused to the bondline by the presence of the micropins negates the reinforcement advantage they provide
- Bondline reinforcing micropins are most effective when located at bondline runout areas, where they react out-of-plane peel loads, and this finding is contrary to those of FEA studies (Bianchi)
- The joining enhancement provided by mechanically reinforcing an adhesive bond with anchored micropins is manifest in the characteristic of a pseudo-ductile joint failure.

6.8.2 RSW reinforced adhesive joint

- The application of a resistance spot weld prior to adhesive bonding improves joining performance; both in terms of an increase in strength of the adhesive bond and also a reduction in the variability of achieved strengths
- When forming a carbon fabric penetrating metallic resistance spot weld the electrode pinch force is the parameter of greatest effect; influencing both the through-thickness electrical resistance and also the quality of subsequent weld nugget formation
- The flow of molten metal as weld splash has the effect of clearing carbon fibre contaminant from the weld nugget formation region and so enabling metal to metal resistance spot welding

- An apparently robust carbon fibre penetrating metallic resistance spot weld can be achieved even without the formation of a typical weld nugget, this is attributed to direct interaction between welding process generated molten metal and carbon fibre.

6.8.3 Intermediary material joining

- Use of a polymer infused metal foam as an intermediary joining material enables the joining of composites to metals without application of either of the traditional joining methods of adhesive bonding or mechanical fastening
- Braze joining of delicate structures can be achieved by laser induced heating; the heating is induced remote from the braze joining interface and is delivered to the interface by conduction
- The use of a polymer infused metal foam intermediary material can negate the difficulties of bonding thermoplastics to metals.

6.8.4 General conclusion of metal composite joining

- The metal-to-metal joining techniques of arc micro-welding, resistance spot welding, and metal filler brazing can be exploited to form novel micro-architecture metal adherends that can be used for enhanced composite to metal joining.
- Mechanical reinforcement of an adhesive joint by either micropins or resistance spot welding are methods of providing residual strength performance of primarily adhesive joints
- The performance enhancements of the three joining concepts are ranked as: 1) RSW reinforced adhesive joint, 2) Micropin reinforced adhesive joint, 3) Intermediary material joining
- Composite to metal joining is enhanced by increased direct interaction between the reinforcement fibres of a composite material and the metal structure.

Appendix A - Preliminary Study of micropin reinforced adhesive joint

A.1 Introduction to appendix

This appendix reports a preliminary study that was conducted to investigate the micropin reinforced adhesive joining concept. This study involved testing of an adhesive joint reinforced with a regular array pattern of 5x7 micropins applied to the adhered interface of a 3mm thickness metal substrate, and also the baseline adhesive strength of the M21 epoxy matrix system. These results were then compared against comparative studied from the literature. The learning from this study, both in terms of the testing results and the methodology chosen, were used to inform the definition of the main micropin reinforced adhesive joint study, which is reported in Chapter 3. The only methodology differences, between this preliminary study and the main study, were the positioning of crack starter PTFE films, all manufacturing stages were the same.

A.2 Micropin reinforced adhesive joining concept

In this joint concept the interface surface of a 304 stainless steel plate was structured with a regular array of stainless steel micropins. An array of 35 micropins were CMT-Pin welded on both sides of the 3mm thick metal plate, the micropins were arranged in a regular paten of 5x7 on an interface area of 25mm (width) x 30mm (length; in the DLS loading direction). The plate was then embedded into an uncured quasi-isotropic lay-up of M21/T700 prepreg by use of ultrasonic horn, forming a double-lap-shear (DLS) joint. The laminate was then cured in an autoclave in accordance with the prepreg manufactures stipulated cure cycle. A diagram of this joining concept is shown in Figure A-1.

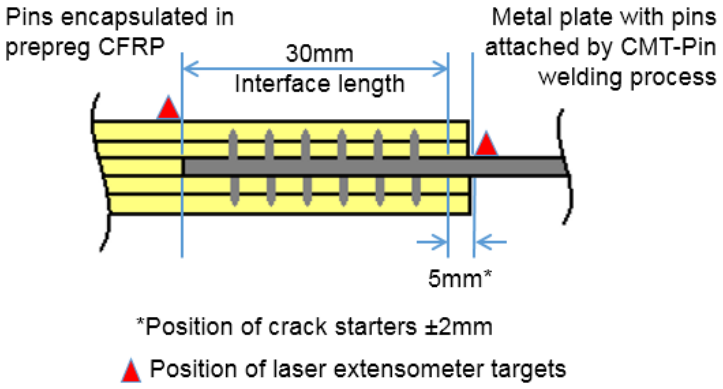

Figure A-1 - Diagram of the DLS micropin reinforced adhesive joining concept

A.3 Double-lap-shear joint testing

A series of mechanical tests were made of DLS micropin reinforced adhesive joint specimens using an Instron 5500R Electro-mechanical testing machine operating with a 100kN load cell. The test was conducted with a cross-head displacement of 1mm/min. Strain in the direction of load application was measured across the joint overlap area using a laser extensometer. Figure A-2 shows a graph of the results obtained from these tests, also plotted on the graph is the test data from a DLS specimen of identical geometry, materials, and surface preparation as the micropin reinforced adhesive joint samples, but which did not have the metal surface structured with arrays of micropins and so was a purely adhesive joint.

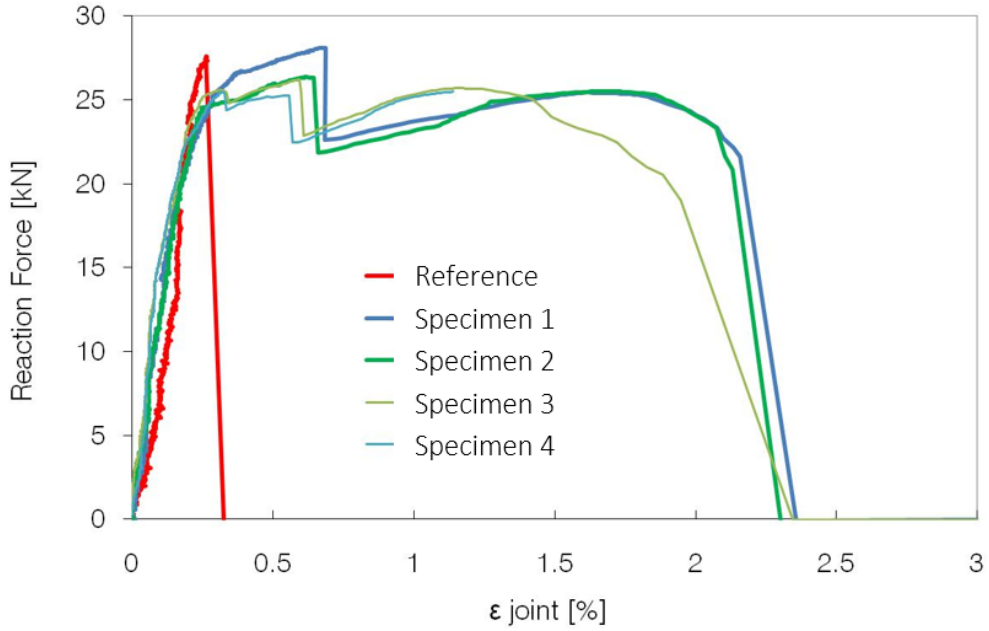

Figure A-2 - Results of micropin reinforced adhesive joint DLS mechanical tests

It can be seen from Figure A-2 that there is no significant change in the maximum load that can be carried by the micropin reinforced adhesive joints, when compared to the equivalent adhesively bonded only (reference) joint, however the strain at ultimate failure is approximately nine times greater. It can also be seen that despite modes of failure being present in the micropin reinforced adhesive joint a load of no less than 80% of maximum is carried up until a strain of approximately 85% of maximum. This micropin reinforced adhesive joint exhibits post-failure residual load carrying capability. Whereas in the purely adhesively bonded joint complete failure abruptly occurs shortly after initial failure. The energy absorbed in failure of the micropin reinforced adhesive joint is approximately eight times greater than that of the purely adhesively bonded joint.

A.4 Comparison with other dissimilar-material joining concepts

Work has been conducted by Ucsnik et al. (Ucsnik et al., 2010), at the Vienna University of Technology, to investigate similar micropin reinforced adhesive joints. The differences between the Ucsnik work and the work being reported here is in the method of manufacturing joints and also the geometry of micropins. The method of composite manufacturing - and simultaneous composite to metal joining – used by Ucsnik was to lay-up dry carbon fibre non-crimp fabric over CMT-Pin formed micropins and then use an epoxy resin infusion manufacturing method. The micropin geometries used in the Ucsnik investigation were plain cylinders and ball-headed cylinders, whereas in the work reported here the micropins were pike shaped (to aid insertion into uncured prepreg laminate). Similarities between the Ucsnik work and the work being reported here are: metal substrate and micropin material (304 stainless steel) and the method of welding micropins to substrate, planar interface area, micropin number and array pattern, and DLS joint configuration. Figure A-3 shows the mechanical testing results obtained in the work conducted by Ucsnik et al. and Figure A-4 is an overlay of the data presented in Figure A-2.

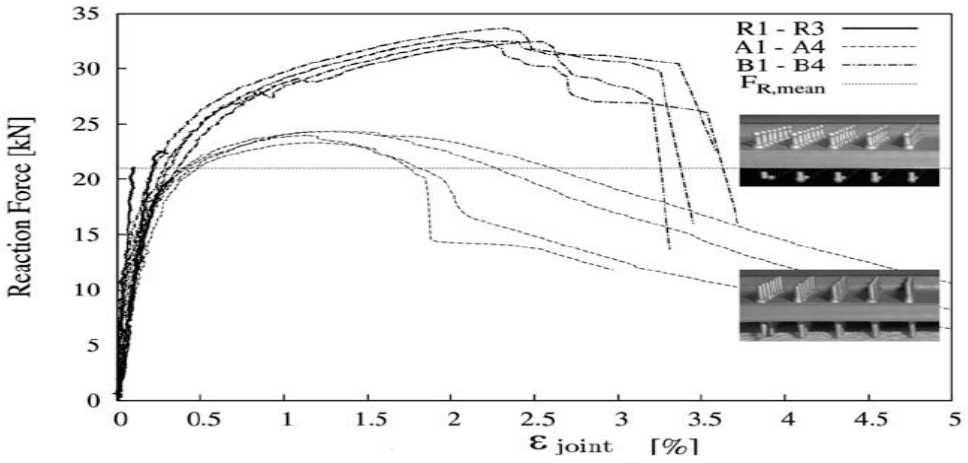

Figure A-3 - Results of 'Hybrid metal-composite joining' investigation conducted by Ucsnik et al. (Ucsnik et al., 2010). 'A' samples use cylinder micropins, 'B' samples use ball-headed cylinder micropins, and 'R' samples are reference samples that have no pins and are therefore only adhesively bonded. Test conducted at a cross head displacement of 1 mm/min.

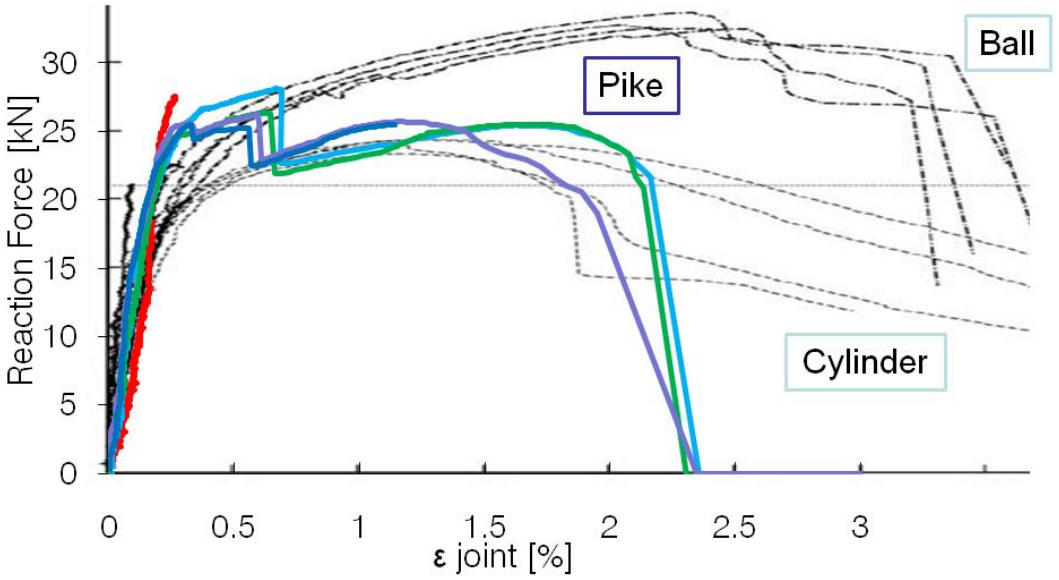

Figure A-4 - Overlay of results reported from this preliminary study (Figure A-2) and those obtained by the Ucsnik et al. (Figure A-3).

It can be seen that the joints which use pike shaped micropins initially exhibit a load-strain response that resembles the performance of joints with ball-headed micropins up until a joint strain of 0.60 ± 0.05 %, at which point there is a step change of the behaviour to one that more closely resembles joints that use cylinder shaped micropins, this is followed by a sudden complete failure at a joint strain in the region of 1.8 - 2.1 %. This final sudden failure of the joints with pike micropins resembles the final sudden failure of the ball-headed micropins. This combination of ball-headed and cylinder micropin joint failure modes is further evident when inspecting sections through failed joints. Figure A-5 shows a section through a failed joint that uses pike shaped micropins and Figure A-6 is an extract from the Ucsnik et al. work that shows sections through failed joints that use cylinder and ball-headed micropins.

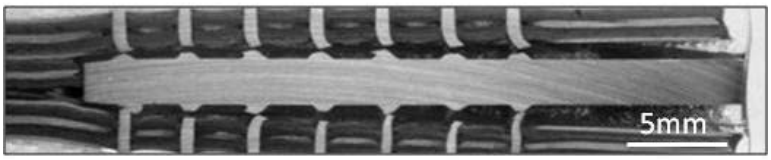

Figure A-5 - Section through a failed micropin reinforced adhesive joint that uses pike shaped micropins

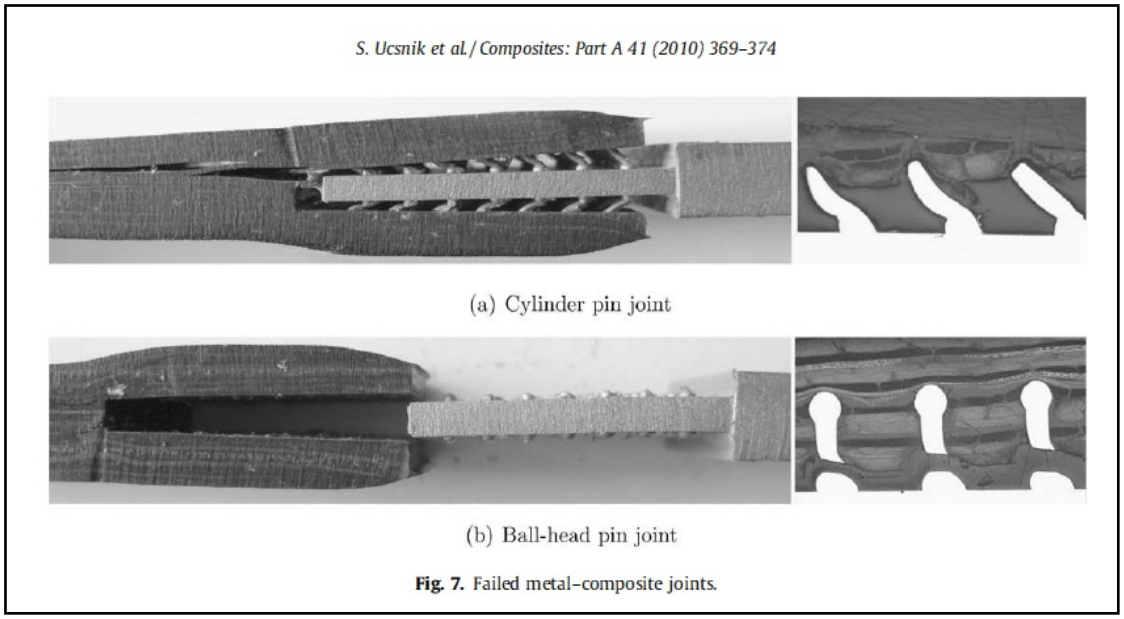

Figure A-6 - An extract from the work conducted by Ucsnil et al. (Ucsnik et al., 2010), which shows sections though failed joints that use cylinder and ball-headed shaped micropins

When comparing the failed joints in Figure A-5 and Figure A-6 it can be observed that the failed joints that use pike shaped micropins (Figure A-5) has similarities with both the joints that use cylinder and ball-head shaped micropins (Figure A-6); there is significant deformation in the shank of the pike micropins, as seen with the cylinder micropins, and also shear fracture above the weld fillet of the pike micropins, as seen with the ball-head micropins.

A.5 Failure mechanisms

Work conducted by Sugiman et al. (Sugiman, Crocombe and Katnam, 2011), at the University of Surrey, on GLARE panels reinforced with adhesively bonded aluminium stiffeners have failure characteristic similarities with the micropin reinforced adhesive joints reported here. Though the metal-composite interfaces of the micropin reinforced adhesive joints and the reinforced GLARE panels are dissimilar both structures use similar materials combinations: continuous fibre reinforced epoxy composites, and toughened epoxy bonded joints between metal components of various thickness. With some metal thicknesses being in the order of magnitude of 1mm (i.e. micropin diameter in micropin reinforced adhesive joints and GLARE aluminium laminae thickness in the reinforced GLARE structure) and also several millimetres (i.e. steel substrate in micropin reinforced adhesive joints and stiffener thickness in the reinforced GLARE structure).

The work by Sugiman et al. included identification of the failure mechanisms that result in features seen on a load displacement trace, which was obtained from a reinforced GLARE structure loaded in tension, the results are shown in Figure A-7.

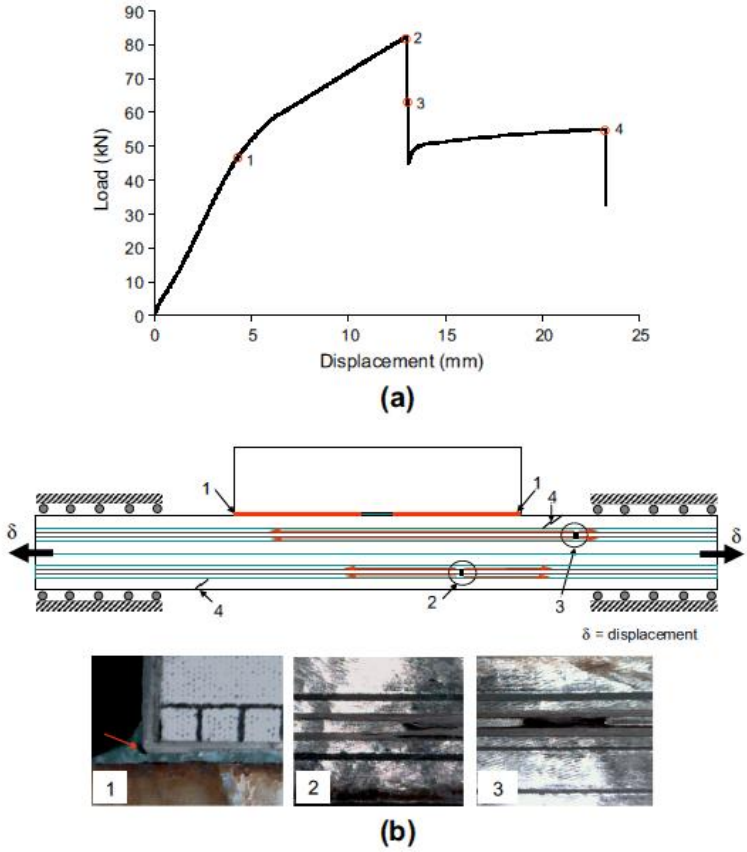

Fig. 4. (a) Showing load level when the failure observed and (b) schematic of failure process of SP specimen under static tension.

Figure A-7 - Extract from Sugiman et al. (Sugiman, Crocombe and Katnam, 2011), load displacement response of a reinforced GLARE structure loaded in tension with observed failures

In Figure A-7 at point 1 a crack is initiated at the extremity of the adhesive bond between the GLARE panel and the aluminium stiffener, this results in a knee in the trace line that corresponds to a change of stiffness of the structure as the crack runs along the bondline, this continues up until sufficient load has been transferred into the GLARE panel to initiate modes of failure within the panel. Initial GLARE panel failure is seen at point 2, and shortly after point 3, these two points correspond to the through thickness fracture of thin internal aluminium laminae (and interfacing GFRP laminae). The remaining load is then carried

predominantly by the thicker aluminium face sheets of the GLARE panes, up until complete failure at points 3 and 4.

When comparing this to the load-strain response trace lines obtained from tests of micropin reinforced adhesive joints, shown in Figure A-2, it is reasonable to say that the first knee seen in the trace lines is a result of disbond crack initiation thus changing the stiffness of the joint as the crack runs along a bondline.

In an effort to understand what failure mechanism results in the load drop at a strain of 0.60 ± 0.05 % (as shown in Figure A-2) a DLS joint specimen was loaded to a joint strain of approximately 0.75% and then unloaded. This specimen was sectioned and can be seen in the upper image of Figure A-8.

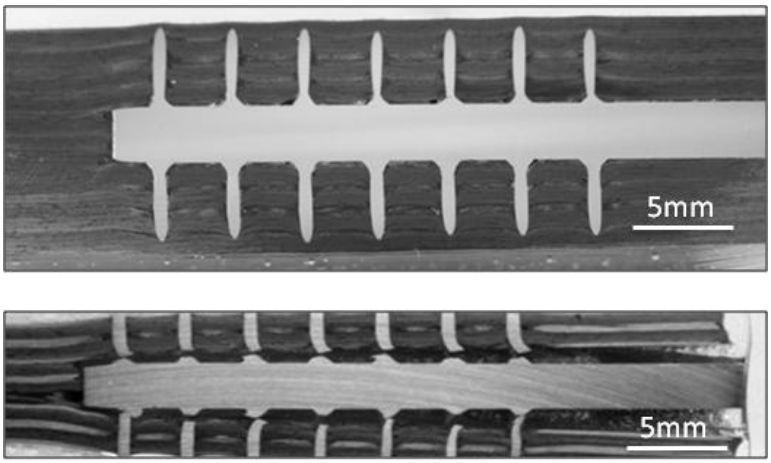

Figure A-8 - Partially failed (~0.75% joint strain), upper image, and completely failed (2.75% joint strain), lower image. DLS micropin reinforced adhesive joint samples.

No damage is immediately obvious in the partially failed sample, but it can be seen that the micropins have not broken; therefore it is likely that the load drop is associated with a complete bondline failure occurring.

A.6 Discussion

In the investigations reported here it has been found that double-lap-shear micropin reinforced adhesive joints are not able to carry a greater maximum load than an equivalent, purely adhesively bonded, reference joint. However, the micropin reinforced adhesive joints do carry significant load up to a far greater joint strain, and so absorb greater energy during joint failure.

When making comparisons between the load-strain response trace lines of the pike micropin joints reported here and those obtained by Ucsnik et al. - for cylinder and ball-headed micropins - it can be seen that the joints with pike micropins first carry a load that is similar to the ball-headed micropins. This is followed by a partial failure that results in the pike micropin joints then carrying a load more similar to the joints with cylinder micropins. This behaviour could be explained when considering the micropin geometry; especially the height and surface area, of the various micropin types Table A-1 details micropin geometries.

Micropin type	**Ball-headed**	**Cylinder**	**Pike**
Shank Ø	0.8	0.8	0.8
Base Ø	1.5	1.5	1.5
Ball-head Ø	1.2	-	-
Total height	3.0	3.0	4.0
Surface area	9.6	8.6	10.0

Table A-1 - Micropin nominal geometries

It is shown in Figure A-6 that cylinder micropins deform and pull-out of the laminate and that ball-headed micropins resist pulling-out from the laminate,

due to the mechanical locking action of the ball-heads, and then shear above the weld fillet of the micropin. Pike micropins show a final failure which more closely resembles ball headed micropins than cylinder micropins. The greater height of the pike micropins compared to the cylinder micropins could be the reason for this, as the greater interface length (and area) could be acting to generate greater frictional resistance to the micropins pulling out of the laminate.

It is identified by the comparison of images in Figure A-8 that bondline failure is likely to occur before the fracture of micropins. The surface area of the different micropin shapes could have an influence on the force required to grow a crack along the bondline, as using micropins with a greater surface area effectively equates to a greater bondline area.

REFERENCES

Adams, R.D. and Mallick, V. (1993) 'The effect of temperature on the strength of adhesively-bonded composite-aluminium joints.', *The Journal of Adhesion*, 43(1 and 2), pp. 17–33.

Aerospace Growth Partnership (2013) *Industrial Strategy: government and industry in partnership* HM Government, London

Ashby, M.F. (1999) *Materials selection in mechanical design*. Oxford: Butterworth-Heinemann.

Astashev, V.K. and Babitsky, V.I. (1998) 'Ultrasonic cutting as a nonlinear (vibro-impact) process', *Ultrasonics International 1997*, 36(1-5), pp. 89–96.

Baker, A., Dutton, S. and Kelly, D. (2004) 'Joining of Composite Structures', in *Composite Materials for Aircraft Structures*. Reston, VA: American Institute of Aeronautics and Astronautics, p. 289.

Bartczak, B., Mucha, J. and Trzepieciński, T. (2013) 'Stress distribution in adhesively-bonded joints and the loading capacity of hybrid joints of car body steels for the automotive industry', *International Journal of Adhesion and Adhesives*, 45, pp. 42–52.

Berger, L. (2010) 'Design and fabrication of a structural composite automotive underbody', *Society of Plastics Engineers - 10th Annual Automotive Composites Conference and Exhibition 2010, ACCE 2010*., pp. 494–503.

Bianchi, F. (2012) *Numerical modelling of through-thickness reinforced structural joints*. Cranfield University.

Boyes, R. (1998) *Adhesive bonding of stainless steel: strength and durability* . Sheffield Hallam University Research Archive: Sheffield Hallam University.

BSI (2004) *BS EN 14324:2004 Brazing — Guidance on the application of brazed joints* British Standards Institute, London

BSI (2010) *BS EN ISO 17672:2010 Brazing - Filler metals* British Standards Institute, London

Burns, L. a., Mouritz, a. P., Pook, D. and Feih, S. (2012a) 'Bio-inspired design of aerospace composite joints for improved damage tolerance', *Composite Structures*, 94(3) Elsevier Ltd, pp. 995–1004.

Burns, L.A., Mouritz, A.P., Pook, D. and Feih, S. (2012b) ‘Strength improvement to composite T-joints under bending through bio-inspired design’, *Composites Part A: Applied Science and Manufacturing*, 43(11), pp. 1971–1980.

Camanho, P.P., Fink, A., Obst, A. and Pimenta, S. (2009) ‘Hybrid titanium-CFRP laminates for high-performance bolted joints’, *Composites Part A: Applied Science and Manufacturing*, 40(12), pp. 1826–1837.

Cashman, J., Rayani, A. and Nuruddin, I. (2009) *Joining Metal Foams to Stainless Steel.* Unpublished: Cranfield University.

De Castro, J. and Keller, T. (2008) ‘Ductile double-lap joints from brittle GFRP laminates and ductile adhesives, Part I: Experimental investigation’, *Composites Part B: Engineering*, 39(2), pp. 271–281.

Chen, B., Xiong, H., Mao, W. and Cheng, Y. (2010) ‘Wettability and interfacial reactions of PdNi-based brazing fillers on C-C composite’, *Transactions of Nonferrous Metals Society of China*, 20(2), pp. 223–226.

Czél, G., Jalalvand, M. and Wisnom, M.R. (2015) ‘Demonstration of pseudo-ductility in unidirectional hybrid composites made of discontinuous carbon/epoxy and continuous glass/epoxy plies’, *Composites Part A: Applied Science and Manufacturing*, 72, pp. 75–84. Available at: 10.1016/j.compositesa.2015.01.019 (Accessed: 22 November 2015).

Czél, G. and Wisnom, M.R. (2013) ‘Demonstration of pseudo-ductility in high performance glass/epoxy composites by hybridisation with thin-ply carbon prepreg’, *Composites Part A: Applied Science and Manufacturing*, 52, pp. 23–30. Available at: 10.1016/j.compositesa.2013.04.006 (Accessed: 22 November 2015).

Dance, B., Irvine, G., Kellar, E. and Crawford, J. (2004) *Workpiece structure modification.* (WO 2004/028731 A1).

Darwish, S.M. and Al-Samhan, A. (2004) ‘Design rationale of weld-bonded joints’, *International Journal of Adhesion and Adhesives*, 24(5), pp. 367–377.

Darwish, S.M.H. and Ghanya, A. (2000) ‘Critical assessment of weld-bonded technologies’, *Journal of Materials Processing Technology*, 105(3), pp. 221–229.

Fink, A., Camanho, P.P., Andrés, J.M., Pfeiffer, E. and Obst, A. (2010) ‘Hybrid CFRP/titanium bolted joints: Performance assessment and application to a spacecraft payload adaptor’, *Composites Science and Technology*, 70(2), pp. 305–317.

Fink, A. and Kolesnikov, B. (2005) ‘Hybrid titanium composite material improving composite structure coupling’, *European conference on spacecraft structures, materials and mechanical testing*

Friel, R.J. and Harris, R.A. (2010) ‘A nanometre-scale fibre-to-matrix interface characterization of an ultrasonically consolidated metal matrix composite’, *Proceedings of the Institution of Mechanical Engineers, Part L: Journal of Materials: Design and Applications*, 224(1), pp. 31–40.

Fronius International GmbH (2009) *If it can’t be welded, pin it - Fronius International GmbH - Press releases*.

Furukawa, K. (2006) ‘New CMT arc welding process - welding of steel to aluminium dissimilar metals and welding of super-thin aluminium sheets’, *Welding International*, 20(6) Aichi Sangyo Corporation: Woodhead Publishing Limited, pp. 440–445.

Hart-Smith, L.J. (1982) *Design Methodology for Bonded-Bolted Composite Joints. Volume I. Analysis Derivations and Illustrative Solutions*. Long Beach, CA: McDonnell Douglas Corp.

Hart-Smith, L.J. (1973) *Adhesive-bonded double-lap joints*. Langley Research Centre, USA: National Aeronautics and Space Administration.

Hart-Smith, L.J. (1983) *Designing to minimize peel stresses in adhesive-bonded joints*. ASTM Symposium on delamination and debonding of materials, USA: Douglas Aircraft Company, McDonnell Douglas Corporation.

Hexcel Corporation (2010) *HexPly M21 Product Data* Hexcel Corporation,

Hongyan, Z. and Senkara, J. (2012) *Resistance welding : fundamentals and applications*. Boca Raton, FL: CRC Press.

Hooker, J.A. and Doorbar, P.J. (2004) ‘Metal matrix composites for aeroengines’, in Cantor, B., dunne, F. and Stone, I. (eds.) *Metal and ceramic matrix composites*. Bristol and Philadelphia: Institute of Physics, pp. 3–17.

Jones, D.P., Leach, D.C. and Moore, D.R. (1985) ‘Mechanical properties of poly(ether-ether-ketone) for engineering applications’, *Speciality Polymers 84*, 26(9), pp. 1385–1393.

Karpov, Y.S. (2006) ‘Jointing of high-loaded composite structural components. Part 1. Design and engineering solutions and performance assessment’, *Strength of Materials*, 38(3), pp. 234–240.

Kearns, W.H. (1978) *Welding Handbook; welding processes - arc and gas welding and cutting, brazing, and soldering*. 2501 Northwest 7th Street, Miami, Florida 33125: American Welding Society.

Kinlock, A.J. (1987) *Adhesion and Adhesives: Science and Technology*. London: Chapman and Hall.

Kittel, C. (1996) *Introduction to Solid State Physics*. New York: Wiley.

Kolesnikov, B., Herbeck, L. and Fink, A. (2008) 'CFRP/titanium hybrid material for improving composite bolted joints', *Composite Structures*, 83(4) Institute of Composite Structures and Adaptive Systems, Lilienthalplatz 7, 38108 Braunschweig, Germany, [mailto:boris.kolesnikov@dlr.de]: Elsevier Science, pp. 368–380.

Kong, C.Y. and Soar, R.C. (2005) 'Fabrication of metal-matrix composites and adaptive composites using ultrasonic consolidation process', *Materials Science and Engineering A*, 412(1-2), pp. 12–18.

Kong, C.Y., Soar, R.C. and Dickens, P.M. (2004) 'Optimum process parameters for ultrasonic consolidation of 3003 aluminium', *Journal of Materials Processing Technology*, 146(2), pp. 181–187.

Kumar, S., Anderson, D.P. and Adams, W.W. (1986) 'Crystallization and morphology of poly(aryl-ether-ether-ketone)', *Polymer*, 27(3), pp. 329–336.

Li, P. (2015) 'Constitutive and failure behaviour in selective laser melted stainless steel for microlattice structures', *Materials Science and Engineering: A*, 622, pp. 114–120. Available at: 10.1016/j.msea.2014.11.028 (Accessed: 13 October 2015).

Liu, D. and Hou, L. (2003) 'Three-dimensional size effects in composite pin joints', *Experimental Mechanics*, 43(2), pp. 115–123.

Liu, D., Raju, B.B. and You, J. (1999) 'Thickness effects on pinned joints for composites', *Journal of Composite Materials*, 33(1), pp. 2–21.

Longerich, S., Piontek, D., Ohse, P., Harms, A., Dilthey, U., Angel, S. and Bleck, W. (2007) 'Joining Strategies for Open Porous Metallic Foams on Iron and Nickel Base Materials', *Advanced Engineering Materials*, 9(8) Welding and Joining Institute (ISF), Aachen University (RWTH), Pontstr. 49, 52062 Aachen, Germany; [mailto:Stefanie.angel@iehk.rwth-aachen.de]: Wiley-VCH Verlag GmbH, pp. 670–678.

Madan, R.D. and Prakash, S. (1987) 'Chapter 27 Carbides', in *Modern Inorganic Chemistry*. New Delhi: S. Chand, p. 984.

Malkin, R., Yasaee, M., Trask, R.S. and Bond, I.P. (2013) ‘Bio-inspired laminate design exhibiting pseudo-ductile (graceful) failure during flexural loading’, *Composites Part A: Applied Science and Manufacturing*, 54(0), pp. 107–116.

Matthews, F.L. and Tester, T.T. (1985) ‘The influence of stacking sequence on the strength of bonded CFRP single lap joints’, *International Journal of Adhesion and Adhesives*, 5(1), pp. 13–18.

MatWeb (2015) *Material property data*.

Messler Jr., R.W. (2004) ‘Joining composite materials and structures: Some thought-provoking possibilities’, *Journal of Thermoplastic Composite Materials*, 17(1), pp. 51–75.

Messler, R.W. (2004) *Joining of materials and structures: from pragmatic process to enabling technology*. Burlington, MA: Elsevier Butterworth-Heinemann.

Messler, R.W. (1993) *Joining of advanced materials*. Boston: Butterworth Heinemann.

Montabone, M., Nebiolo, M. and Vigada, C. (1997) ‘An Investigation on a Bolted-Cold Bonded Joint for Large Diameter Structures’, *Bolted/Bonded Joints in Polymeric Composites*. Florence, Italy: AGARD-CP-590, pp. 11–18.

Niu, M. (1992) *Composite Airframe Structures - Practical Design Information and Data*. Hong Kong: AD Adaso/Adastra Engineering LLC.

Parkes, P.N., Butler, R., Meyer, J. and de Oliveira, A. (2014) ‘Static strength of metal-composite joints with penetrative reinforcement’, *Composite Structures*, 118, pp. 250–256. Available at: 10.1016/j.compstruct.2014.07.019 (Accessed: 7 April 2015).

Paulshus, B., Carlsen, T., Storhaug, T. and Johnsen, J.M. (2006) *Composite Pipe Having at least one metal end piece and method of manufacturing such a pipe.* WO 2006/03.

Plastics Design Library (1997) Handbook of plastics joining *Plastics Design Library*. Plastics Design Library, Norwich, N.Y.

Rathi, N.J. (2009) *Processing metal foams into hybrid composite.* Cranfield University: Cranfield University.

Rolls-Royce plc (1998) ‘Titanium MMCs key option for jet compressor design’, *Metallurgia (UK)*, 65(12) Queensway House, 2 Queensway, Redhill, Surrey, RH1 1QS, UK, [URL:http://www.dmgworldmedia.com]: FMJ International Publications Ltd, pp. 361–362.

Santos, I.O., Zhang, W., Gonçalves, V.M., Bay, N. and Martins, P.A.F. (2004) 'Weld bonding of stainless steel', *International Journal of Machine Tools and Manufacture*, 44(14), pp. 1431–1439.

Semmes, E. (2009) Improved Joining of Metal Components to Composite Structures *NASA Tech Briefs*. Marshal Space Flight Center

Shah, B., Frame, B., Dove, C. and Fuchs, H. (2010) 'Structural performance evaluation of composite-to-steel weld bonded joint', *Society of Plastics Engineers - 10th Annual Automotive Composites Conference and Exhibition 2010, ACCE 2010*., pp. 545–561.

Shirzadi, A.A., Kocak, M. and Wallach, E.R. (2004) 'Joining stainless steel metal foams', *Science and Technology of Welding & Joining*, 9(3) Department of Materials Science and Metallurgy, University of Cambridge, Pembroke Street, Cambridge CB2 3QZ, UK; [mailto:as10043@cam.ac.uk]: Maney Publishing, pp. 277–279.

Shirzadi, A.A., Zhu, Y. and Bhadeshia, H. (2008) 'Joining ceramics to metals using metallic foam', *Austenitic stainless steels*, 496(1-2) Department of Materials Science and Metallurgy, University of Cambridge, Pembroke Street, Cambridge CB2 3QZ, UK; [mailto:hkdb@cam.ac.uk]: Elsevier Science SA, pp. 501–506.

Singh, M., Asthana, R. and Shpargel, T.P. (2007) 'Brazing of carbon–carbon composites to Cu-clad molybdenum for thermal management applications', *Materials Science and Engineering: A*, 452-453, pp. 699–704.

Singh, M., Shpargel, T.P., Morscher, G.N. and Asthana, R. (2005) 'Active metal brazing and characterization of brazed joints in titanium to carbon–carbon composites', *International Conference on Recent Advances in Composite Materials*, 412(1-2), pp. 123–128.

Smith, F. (2005) *Changes on the surface, radical advances have been made in composite to metal joining - Bulletin July 2005*.

Stieglbauer, W. and Kazmaier, J. (2009) 'Innovative, multifunctional, form-locked joining technology for dissimilar material combinations', *Welding in the World*, 53(SPECIAL ISSUE), pp. 453–456.

Sugiman, S., Crocombe, A.D. and Katnam, K.B. (2011) 'Investigating the static response of hybrid fibre–metal laminate doublers loaded in tension', *Composites Part B: Engineering*, 42(7), pp. 1867–1884.

Testani, C. and Ferraro, F. (2010) 'Development of a low-cost process for manufacturing of Ti-metal matrix composite by roll-diffusion bonding', *Journal of Materials Engineering and Performance*, 19(4), pp. 521–526.

Tu, W., Guild, F. and Hogg, P. (2009) ‘Comeld TM Joints: A novel technique for bonding composites and metal’, *ICCM17*. Edinburgh, UK.

Ucsnik, S., Scheerer, M., Zaremba, S. and Pahr, D.H. (2010) ‘Experimental investigation of a novel hybrid metal-composite joining technology.’, *Composites Part A: Applied Science and Manufacturing*, 41(3), pp. 369–374.

United States Department of Defence (1976) *MIL-STD-889B Military Standard Dissimilar Metals* United States Department of Defence, USA

Victrex plc (2015) *Properties guide*

Weber, F. (2010) *DG Flugzeugbau GmbH - How a High-Performance Sailplane is Manufactured*., *Composites Part A: Applied Science and Manufacturing*

Weiland, F., Weimer, C. and Mitschang, P. (2011) ‘Ultrasonic welding of carbon fiber preforms: Process and mechanisms’, *International SAMPE Technical Conference*.

Wenzelburger, M., Silber, M. and Gadow, R. (2010) Manufacturing of light metal matrix composites by combined thermal spray and semisolid forming processes - Summary of the current state of technology *Key Engineering Materials*.